ADVERTIMENT. La consulta d’aquesta tesi queda condicionada a l’acceptació de les següents condicions d'ús: La difusió d’aquesta tesi per mitjà del servei TDX (www.tesisenxarxa.net) ha estat autoritzada pels titulars dels drets de propietat intel·lectual únicament per a usos privats emmarcats en activitats d’investigació i docència. No s’autoritza la seva reproducció amb finalitats de lucre ni la seva difusió i posada a disposició des d’un lloc aliè al servei TDX. No s’autoritza la presentació del seu contingut en una finestra o marc aliè a TDX (framing). Aquesta reserva de drets afecta tant al resum de presentació de la tesi com als seus continguts. En la utilització o cita de parts de la tesi és obligat indicar el nom de la persona autora.

ADVERTENCIA. La consulta de esta tesis queda condicionada a la aceptación de las siguientes condiciones de uso: La difusión de esta tesis por medio del servicio TDR (www.tesisenred.net) ha sido autorizada por los titulares de los derechos de propiedad intelectual únicamente para usos privados enmarcados en actividades de investigación y docencia. No se autoriza su reproducción con finalidades de lucro ni su difusión y puesta a disposición desde un sitio ajeno al servicio TDR. No se autoriza la presentación de su contenido en una ventana o marco ajeno a TDR (framing). Esta reserva de derechos afecta tanto al resumen de presentación de la tesis como a sus contenidos. En la utilización o cita de partes de la tesis es obligado indicar el nombre de la persona autora.

WARNING. On having consulted this thesis you’re accepting the following use conditions: Spreading this thesis by the TDX (www.tesisenxarxa.net) service has been authorized by the titular of the intellectual property rights only for private uses placed in investigation and teaching activities. Reproduction with lucrative aims is not authorized neither its spreading and availability from a site foreign to the TDX service. Introducing its content in a window or frame foreign to the TDX service is not authorized (framing). This rights affect to the presentation summary of the thesis as well as to its contents. In the using or citation of parts of the thesis it’s obliged to indicate the name of the author

COMPLEXATION OF Th(IV) AND U(VI) BY POLYHYDROXY AND POLYAMINO CARBOXYLIC ACIDS

Elisenda Colàs Anguita

Barcelona, 2014

UNIVERSITAT POLITÈCNICA DE CATALUNYA

Departament d'Enginyeria Química

Programa de doctorat: Enginyeria de Processos Químics

COMPLEXATION OF Th(IV) AND U(VI) BY POLYHYDROXY AND POLYAMINO CARBOXYLIC ACIDS

Memòria de tesis presentada per Elisenda Colàs Anguita per a l'obtenció del títol de Doctor per la Universitat Politècnica de Catalunya dins del programa d'Enginyeria de Processos Químics.

Barcelona, 2014

Supervisors:

Dr. Mireia Grivé i Solé

Dr. Isabel Rojo Cort

Tutor:

Prof. Joan de Pablo Ribas

Acknowledgements

Hi ha moltíssimes persones a qui donar les gràcies... espero no deixar-me ningú... perquè tots han estat importants per a mi.

En primer lloc, és clar, gràcies a les meves directores de tesi, Mireia Grivé i Isabel Rojo, gràcies de tot cor. Mireia, gràcies per els ànims, el suport, l'empenta, i per no rendir-te mai. Isabel, gràcies per tot el camí que hem fet al laboratori. I, és clar, a les dues per totes les discussions, correccions, seny, experiència, paciència i hores que hi heu posat. Moltes gràcies també a la Lara Duro, coautora, juntament amb la Mireia i la Isabel, dels articles que formen l'ànima d'aquesta tesi. Sense vosaltres res de tot això hauria estat possible.

Moltes gràcies també al Jordi Bruno, pels ànims i les idees, i al Joan de Pablo, tutor d'aquesta tesi; gràcies per tots els "i que et semblaria provar amb...".

Merci également à Eric Giffaut, pour me donner cette opportunité et spécialement pour les commentaires et les discussions scientifiques.

Aquí no pot faltar tota, absolutament tota la gent de Amphos. Especialment el David, l'Alba, l'Olga i la Maria Rosa, però també la Teresa, la Maita, l'Isaac, amb qui hem compartit el vaixell tant en tempestes com en calmes. Xavi, Joan, Vane, Cris, també hi sou ben presents!!! Roser, Vicenç, Tere i Carola, gràcies pel suport. Salvador, Luis Manuel, Hugo, un gràcies especial per ensenyar-me els altres punts de vista. I tota la resta de gent, es clar, si fes tota la llista aquests agraïments no s'acabarien mai...

Als companys del CTM, una abraçada i un "gràcies" molt gran, tant als companys de despatx com de laboratori (no faig la llista però ja sabeu qui sou!!!), i al Miquel Rovira i al Vicenç Martí. Gràcies per tot el suport, però sobretot per fer-me sentir com a casa.

Many thanks to Andreas Scheinost and Christoph Henning for their help in using ROBL beamline, and specially for all the time they spent trying to explain me some of the secrets and mysteries beyond the EXAFS spectra.

Gràcies al Josep Elvira, de l'Institut de Ciències de la Terra Jaume Almera, per els anàlisis de XRD, i a la Clara Viñas per els anàlisis de NMR. També vull donar les gràcies a tota la gent del Departament d'Enginyeria Química de l'UPC, especialment a la Irene.

Un petó molt gran a tota la meva família. I sobretot, gràcies, Peter, per ser-hi sempre i per la paciència i la comprensió en aquest llarg, llarg camí que ja sabíem que no seria planer... i per esperar només un xic de sort. I a l'Arnau; toutes les grandes personnes ont d'abord été des enfants.

Al meu pare

“Cheshire Puss,” she began, rather timidly,
as she did not at all know whether it would like the name:
however, it only grinned a little wider.
“Come, it's pleased so far,” thought Alice, and she went on.
“Would you tell me, please, which way I ought to go from here?”
“That depends a good deal on where you want to get to,” said the Cat.

Lewis Carroll, “Alice's Adventures in Wonderland”

This PhD has received the following financial support:

1) Main funds for experimental and desktop studies have been received from the French National Agency for Radioactive Waste Management (ANDRA) through the ThermoChimie project.

2) The European Synchrotron Radiation Facility (ESRF) is acknowledged for provision of synchrotron radiation facilities to perform EXAFS measurements in the Rossendorf Beamline (ROBL, BM20).

3) A mobility grant from "Departament d'Enginyeria Química" (Universitat Politècnica de Catalunya) allowed a 2-week stage at the Rossendorf Beamline at ESRF, to work on interpretation of EXAFS data measurements.

The support from Amphos 21 is specially acknowledged.

ABSTRACT

Radioactive wastes arise from almost all activities (nuclear and non-nuclear industry, research, military activities, medical applications) involving the handling of radioactive materials. There exists a clear necessity to dispose those wastes in order to avoid the radionuclides contained in the wastes being released to the biosphere in concentrations that could represent an unacceptable hazard to humans or to the environment.

Some of the materials present among radioactive wastes are made of organic polymers; other organic substances (e.g. organic chemicals used in construction, buffer, and sealing materials) can also be present. Those organic substances may influence the behaviour of the radionuclides contained in the wastes. It is then necessary to assess the reactions that are likely to occur between radionuclides and those complexing agents, in order to estimate the quantities of radionuclides that can be transported out of the confinement. In order to do that, it is essential to know the relative stabilities of the compounds and complexes that may form under the relevant conditions, an information that is often provided by speciation calculations using chemical thermodynamic data.

The main goal of this PhD thesis is to obtain thermodynamic data that can be used to quantitatively predict the reactions between some organic ligands that may be present in a repository and radionuclides. Gluconate, isosaccharinate and EDTA have been studied, because they represent three different types of organic substances (cement additives, cellulose degradation products and decontamination agents) relevant for nuclear wastes. The experimental work has been conducted using natural Th(IV) and natural U(VI). The attention has been focused mainly on the alkaline pH range, taking into account the key role of cement in conditioning matrices, engineered barriers and construction materials of waste repositories.

Two different type of experiments have been used to fulfil this objective: macroscopic solubility experiments and spectroscopic analyses

The results obtained have allowed to:

- obtain thermodynamic data (stability constants) in the thorium-gluconate system;

- obtain experimental data in the thorium-isosaccharinate system. Taking into account the similarities between the chemical structure of gluconate and isosaccharinate, the analogy between both ligands has also been investigated;

- increase the knowledge regarding the role of calcium in the thorium-gluconate and thorium-EDTA systems under the alkaline range; and

- obtain data in the U(VI)-gluconate and U(VI)-EDTA systems.

RESUM

Els residus radioactius procedeixen de gairebé totes les activitats (indústria nuclear i no nuclear, investigació, activitats militars, aplicacions mèdiques) que impliquen la manipulació de materials radioactius. Existeix doncs una clara necessitat de gestionar i confinar aquests residus, de forma que s'eviti que els radionúclids continguts en ells s'alliberin a la biosfera en concentracions que puguin representar un risc inacceptable per als éssers humans o el medi ambient.

Alguns materials presents entre els residus radioactius són polímers orgànics; altres substàncies orgàniques (per exemple, productes químics orgànics utilitzats a la construcció, materials sellants, tampons) també poden ser-hi presents. És doncs necessari avaluar les reaccions que poden donar-se entre aquests lligands orgànics i els radionúclids, per tal d'estimar les quantitats de radionúclids que poden ser transportats fora del confinament. En aquest sentit, és fonamental conèixer les estabilitats relatives dels compostos i complexos que es poden formar, una informació que sovint s'obté a través de càlculs d'especiació utilitzant dades termodinàmiques.

L'objectiu principal d'aquesta tesi doctoral és obtenir dades termodinàmiques que es puguin aplicar en la predicció quantitativa de les reaccions entre alguns lligands orgànics i radionúclids. S'han estudiat els lligands gluconat, isosacarinat i EDTA, que representen tres tipus diferents de substàncies orgàniques (additius per a ciment, productes de degradació de cel·lulosa i agents de descontaminació) rellevants en el context dels residus nuclears. El treball experimental s'ha realitzat utilitzant tori (Th(IV)) i urani (U(IV)) naturals. L'estudi s'ha centrat principalment en medis de pH alcalí, tenint en compte el paper clau del ciment tant en matrius de condicionament dels residus com en els materials de construcció i barreres d'enginyeria dels dipòsits de residus.

Per assolir aquest objectiu s'han utilitzat dos tipus diferents d'experiments: experiments de solubilitat i anàlisis espectroscòpiques.

Els resultats obtinguts han permès:

- obtenir dades termodinàmiques (constants d'estabilitat) en el sistema tori-gluconat;

- obtenir dades experimentals en el sistema tori-isosacarinat. Tenint en compte les similituds entre les estructures químiques del gluconat i l'isosacarinat, l'analogia entre els dos lligans també s'ha estudiat;

- augmentar el coneixement sobre el paper del calci en els sistemes de tori-gluconat i tori-EDTA en el rang de pH alcalí, i

- obtenir dades termodinàmiques en els sistemes d'U(VI)-gluconat i U(VI)-EDTA.

PREFACE

The present manuscript is organized in different sections:

- *Introduction and objectives* (sections 1 and 2);
- *Experimental setup* (section 3);
- *Results* (sections 4 to 10);
- *Summary and further work* (section 11);
- *Articles* (Papers I to IV)
- *Appendixes* (sections 13 to 16);

The main goal of this PhD thesis is to obtain thermodynamic data for the reactions between organic ligands (gluconate, isosaccharinate and EDTA) and radionuclides (thorium and uranium) under alkaline conditions. The specific objectives set out in present work are linked to the four articles (Papers I to IV) included in the manuscript, as described in the figure below.

-Paper I (published) is devoted to the quantification of the influence of gluconate on thorium solubility, especially in the alkaline pH range characteristic of cementitious environments;

-Paper II (under preparation) provides experimental data on the complexation strength of isosacharinate towards thorium and on the potential aqueous species formed in this system. A comparison between data for gluconate and isosaccharinate is also provided.

-Paper III (published) provides information on the role of calcium in the thorium-gluconate and thorium-EDTA systems;

-Paper IV (published) is related to the study of the U(VI)-gluconate and U(VI)-EDTA systems.

In order to facilitate the comprehension of the information included in the text, the reader is suggested to read first the information included in the four *Papers* described above and, if necessary, the *Introduction* and the *Objectives* sections. The papers contain the most relevant findings in the present PhD.

The *Results* sections contain basically the same information as the Papers, although more extensive explanations are provided.

Finally, the *Appendixes* contain an extensive description on the thermodynamic database used in the calculations, the analytical techniques applied and solid synthesis and characterization procedures.

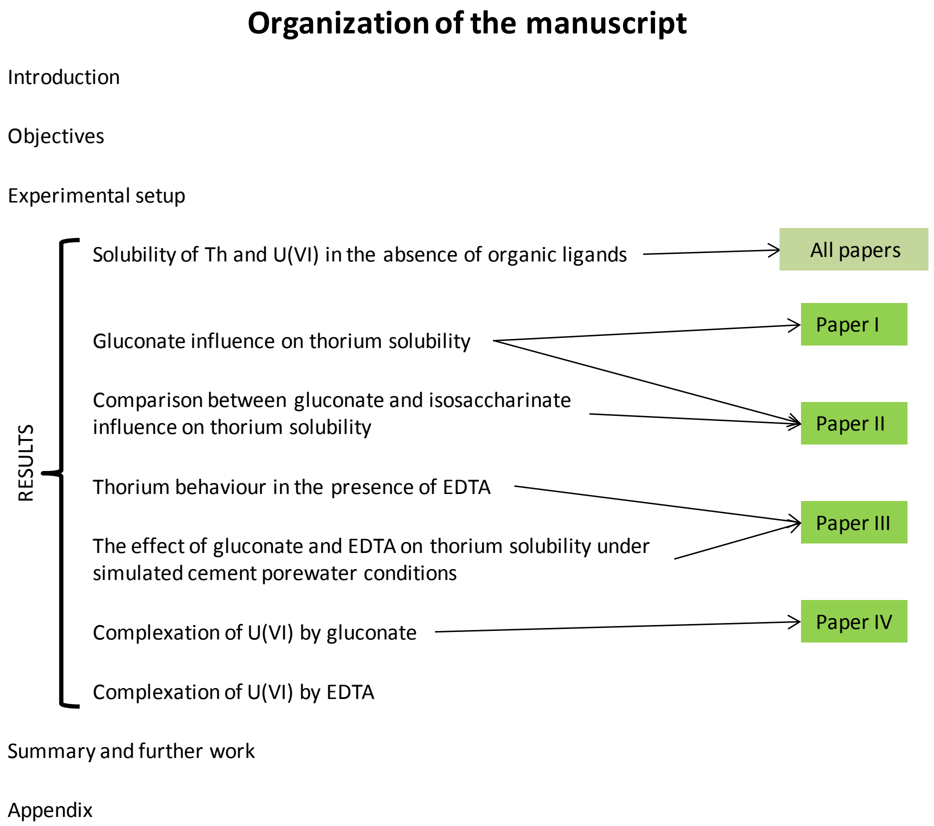

Organization of the manuscript

Introduction
Objectives
Experimental setup
RESULTS
Solubility of Th and U(VI) in the absence of organic ligands
All papers
Gluconate influence on thorium solubility
Paper I
Comparison between gluconate and isosaccharinate influence on thorium solubility
Paper II
Thorium behaviour in the presence of EDTA
Paper III
The effect of gluconate and EDTA on thorium solubility under simulated cement porewater conditions
Complexation of U(VI) by gluconate
Paper IV
Complexation of U(VI) by EDTA
Summary and further work
Appendix

Index

COMPLEXATION OF TH(IV) AND U(VI) I

ABSTRACT III

RESUM V

PREFACE VII

INDEX IX

1 INTRODUCTION 1

1.1 GENERAL INTRODUCTION 1
1.2 THE INFLUENCE OF ORGANIC LIGANDS ON RADIONUCLIDE MIGRATION 4
1.2.1 Gluconate 5
1.2.2 Isosaccharinate 8
1.2.3 Ethylenediaminetetraacetic acid 8

2 OBJECTIVES 11

3 EXPERIMENTAL SETUP 13

3.1 REAGENTS, MATERIALS AND SOLUTIONS 13
3.2 PHASE SEPARATION AND ANALYTICAL TECHNIQUES 14
3.2.1 Filtration 14
3.2.2 pH measurements 15
3.2.3 ICP-MS and TOC measurements 15
3.3 SOLUBILITY EXPERIMENTS 15
3.4 EXAFS EXPERIMENTS 18
3.5 UV-VIS EXPERIMENTS 19
3.6 OTHER EXPERIMENTAL METHODS 20

4 SOLUBILITY OF TH AND U(VI) IN THE ABSENCE OF ORGANIC LIGANDS (PAPER I TO IV) 21

4.1 TH AND U(VI) CHEMISTRY IN ALKALINE CONDITIONS 21
4.1.1 Thorium 21
4.1.2 Uranium 22
4.2 TH SOLUBILITY IN THE ABSENCE OF ORGANIC LIGANDS (PAPER I) 23
4.3 U(VI) SOLUBILITY IN THE ABSENCE OF ORGANIC LIGANDS 27
4.4 SUMMARY AND CONCLUSIONS 30

5 GLUCONATE INFLUENCE ON THORIUM SOLUBILITY (PAPER I AND PAPER II) 31

5.1 INTRODUCTION 31

5.2 OBJECTIVES 31
5.3 THORIUM HYDROXIDE SOLUBILITY IN THE PRESENCE OF GLUCONATE (PAPER I).......................32
5.4 DETERMINATION OF THORIUM-GLUCONATE STABILITY CONSTANTS (PAPER I) 39
5.4.1 Discussion on the obtained results...41
5.5 STRUCTURE OF THE THORIUM-GLUCONATE COMPLEX (PAPER II)...43
5.5.1 Discussion on the obtained results...47
5.6 SUMMARY AND CONCLUSIONS 48

6 COMPARISON BETWEEN GLUCONATE AND ISOSACCHARINATE INFLUENCE ON THORIUM SOLUBILITY (PAPER II) 51

6.1 INTRODUCTION 51
6.2 OBJECTIVES 52
6.3 THORIUM HYDROXIDE SOLUBILITY IN THE PRESENCE OF ISOSACCHARINATE (PAPER II) 53
6.3.1 Determination of the thorium-isosaccharinate stability constants (Paper II)......................53
6.4 STRUCTURE OF THE THORIUM-ISOSACCHARINATE COMPLEX...56
6.4.1 EXAFS experiments...57
6.5 COMPARISON BETWEEN GLUCONATE AND ISOSACCHARINATE 58
6.6 COMPARISON WITH LITERATURE VALUES...60
6.7 SUMMARY AND CONCLUSIONS...66

7 THORIUM BEHAVIOUR IN THE PRESENCE OF EDTA (PAPER III)...............................69

7.1 INTRODUCTION 69
7.2 OBJECTIVES 69
7.3 SOLUBILITY EXPERIMENTS 69
7.4 SUMMARY AND CONCLUSIONS...71

8 THE EFFECT OF GLUCONATE AND EDTA ON THORIUM SOLUBILITY UNDER SIMULATED CEMENT POREWATER CONDITIONS (PAPER III)..73

8.1 INTRODUCTION 73
8.2 OBJECTIVES 77
8.3 THORIUM BEHAVIOUR IN THE PRESENCE OF GLUCONATE AND CALCIUM..................................78
8.3.1 Solubility experiments 78
8.3.2 Calcium analysis...80
8.3.3 EXAFS experiments...82
8.4 THORIUM BEHAVIOUR IN THE PRESENCE OF EDTA AND CALCIUM 83
8.5 SUMMARY AND CONCLUSIONS...84

9 COMPLEXATION OF U(VI) BY GLUCONATE (PAPER IV)..87

9.1 INTRODUCTION 87
9.2 OBJECTIVES 88

9.3 SOLUBILITY EXPERIMENTS 89

9.4 UV-VIS EXPERIMENTS 91

9.5 DISCUSSION OF THE OBTAINED RESULTS 95

9.6 SUMMARY AND CONCLUSIONS 100

10 COMPLEXATION OF U(VI) BY EDTA (UNPUBLISHED RESULTS) 103

10.1 INTRODUCTION 103

10.2 OBJECTIVES 104

10.3 SOLUBILITY EXPERIMENTS 104

10.4 SUMMARY AND CONCLUSIONS 105

11 SUMMARY AND FURTHER WORK 107

11.1 SUMMARY 107

11.2 FURTHER WORK 109

PAPER I 111

PAPER II 119

PAPER III 131

PAPER IV 149

12 APPENDIX A: APPLICATION ON PERFORMANCE ASSESSMENT CALCULATIONS169

13 APPENDIX B: THERMODYNAMIC DATABASE 173

13.1 THORIUM 173

13.2 URANIUM 174

13.3 ORGANIC LIGANDS 175

13.4 IONIC STRENGTH CALCULATIONS 176

13.4.1 SIT approach 176

13.4.2 Comparison with Davies corrections 179

14 APPENDIX C: ANALYTICAL TECHNIQUES 181

14.1 PH DETERMINATION 181

14.2 ICP-MS AND ICP-OES 183

14.3 TOC 184

14.4 EXAFS 184

14.5 XRD 185

14.6 NMR 185

14.7 SEM-EDX 186

14.8 ESI-MS 186

15 APPENDIX D: SOLID SYNTHESIS AND CHARACTERIZATION 189

15.1 THORIUM HYDROXIDE 189
15.2 SODIUM URANATE 190
15.3 SODIUM ISOSACCHARINATE 191

16 REFERENCES 195

Figure 1-1. The phases representative of cement degradation, as a function of lixiviation cycles. Adapted from (ANDRA 2005b). 3
Figure 1-2. Basic structure of a polycarboxylate ether superplasticizer (Andersson et al. 2008). 6
Figure 1-3. Gluconate chemical structure. In the text, “H_4” in GH_4^- refers to the hydrogen of the secondary alcohols in the molecule (Sawyer 1964). 7
Figure 1-4. Different coordination modes for polyhydroxycarboxylic acids. I) Bidentate coordination through the carboxylic function. II) and III) Examples of coordination modes involving ionized diol functions 7
Figure 1-5. Isosaccharinate chemical structure. In the text, “H_2” in $ISAH_2^-$ refers to the hydrogen of the secondary alcohols in the molecule. 8
Figure 1-6. Ethylenediaminetetraacetic acid ($EDTAH_4$) structure 9
Figure 3-1. Scheme of the experimental set-up for solubility experiments from undersaturation direction. 17
Figure 3-2. Procedure for EXAFS experimental data acquisition (1), theorethical structure (2) and spectra fitting (3), adapted from (Scheinost 2010) 19
Figure 4-1. Calculated amorphous thorium hydroxide solubility (black solid line) and underlying thorium aqueous speciation (dotted lines) as a function of pH, using thermodynamic data from (Rand et al. 2009). I=0. 22
Figure 4-2. Uranium aqueous speciation as a function of pH and Eh in the absence of complexing agents other than OH^-; only aqueous species are shown. Green dashed lines stand for Eh limits for water oxidation and reduction. Calculations performed using the thermodynamic database reported in section 13.2, I=0, $[U]_T=1\cdot10^{-9}$ M. 23
Figure 4-3. Solubility of thorium oxyhydroxide (I=0.5M, $NaClO_4$), after 1 kD (triangles) or 300 kD (diamonds) filtration. Blue symbols: from undersaturation direction, >40 days of experiment. Red symbol: oversaturation direction, 5 days of experiment. The grey circle indicates the measured samples at alkaline pH values ($pH_c\approx12$). Solid line stands for solubility calculated in present work, as described in the text (with uncertainty, dashed lines). 25
Figure 4-4. Solubility of thorium oxyhydroxide (I=0.5M, $NaClO_4$) obtained in present work (colour symbols) and comparison with literature data (open symbols). 27
Figure 4-5. Solubility of sodium uranate (left: I=0.5M, $NaClO_4$; right: I=0.1M, $NaClO_4$) from undersaturation direction, after >34 days. Solid line stands for calculated $Na_2U_2O_7(s)$ solubility (with uncertainty, dashed lines). 28
Figure 4-6. Solubility of sodium uranate in I=0.5M KCl media from undersaturation direction, after >27 days. Solid red line stands for calculated $Na_2U_2O_7(s)$ solubility. Solid black line stands for calculated $K_2U_2O_7(s)$ solubility (with uncertainty, dashed lines). 30
Figure 5-1. Solubility of thorium hydroxide in I=0.5M $NaClO_4$ media at $pH_c=12$ as a function of measured gluconate concentration, after 1 kD filtration. Triangles: oversaturation direction (15 or 149 days). Circles: undersaturation direction (>39 days). Only solid symbols were used in the calculations (see text). Solid black line is calculated thorium hydroxide solubility taking into account 1:1 Th:gluconate formation (with uncertainty, dashed line). Dotted line is calculated solubility in the absence of organic ligands. 33
Figure 5-2. Solubility of thorium hydroxide in I=0.5M $NaClO_4$ media, $pH_c=12$, from undersaturation direction, as a function of measured gluconate concentrations in solution. Blue circles: after 1kD filtration. Open triangles: after 300 kD filtration. Stars: After ultracentrifugation at 149000g, without filtration. Dashed black line stands for

thorium hydroxide solubility in the absence of organic ligands determined in present work. Error bars omitted for clarity in this graph. 34
Figure 5-3. Added versus measured gluconate concentrations in the system. 36
Figure 5-4. Measured gluconate concentrations in solution (grey circles) *vs.* grams of solid thorium hydroxide. Dashed line indicates initial gluconate concentration in solution. Detection limit of measured gluconate is $1\cdot10^{-4}$M. I=0.5M $NaClO_4$, pH_c=12. 37
Figure 5-5. Comparison between results from oversaturation experiments in the thorium-gluconate system, after 1kD filtration. Black triangles: after 15 days. Red triangles: after 141 days. 38
Figure 5-6. Solubility of thorium hydroxide as a function of pH_c and initial gluconate concentration $4.5\cdot10^{-3}$ M after 1 kD filtration (I = 0.5 M, $NaClO_4$). Dashed line is thorium hydroxide solubility in the absence of gluconate. 39
Figure 5-7. A) Solubility of thorium hydroxide in I=0.5M $NaClO_4$ media at pH_c=12 as a function of measured gluconate concentration, after 1 kD filtration. Triangles: oversaturation direction. Circles: undersaturation direction. Solid grey line is calculated thorium hydroxide solubility taking into account 1:1 and 1:2 Th:gluconate formation (with uncertainty, dashed lines). Dotted line is calculated solubility in the absence of organic ligands. B) Th-gluconate speciation in agreement with the results obtained in present work. 41
Figure 5-8. Stability constants of metal complexes with gluconate, versus $g_1(z/r^2+g_2)$ (Brown et al. 1985). Blue symbols are stability constants reported by (Sawyer 1964). Red symbol stands for thorium-gluconate stability constant obtained in present work. 42
Figure 5-9. Relationship between the stability constants of An(IV)-gluconate complexes with $\Delta_f G(An^{4+})$, adapted from (Rojo et al. 2013). Red triangle stands for thorium-gluconate stability constant obtained in present work. Blue cross: from (Rojo et al. 2013). Black symbols: values recalculated from (Cross et al. 1989, Felmy 2004, Moreton 1993, Warwick et al. 2004). 43
Figure 5-10. Structure of $Th(CO_3)_5^{6-}$ complex, from (Rand et al. 2009). 44
Figure 5-11. Experimental data of EXAFS fourier transforms of Th L_{III} edge for Th-gluconate and Th-carbonate solutions. The solid lines are the experimental data, and dashed lines correspond to preliminary theoretical fits. 45
Figure 5-12. Comparison between thorium coordination to carbonate (A) and theoretical thorium coordination to gluconate through the carboxylic function (B). As seen in the figure, Th-O_{dist} distance would be expected to be shorter than the Th-C_{dist} distance..... 46
Figure 5-13. Fourier-filtered peak at an uncorrected distance of ca. 3.5 Å.................... 47
Figure 5-14. Coordination-ionization scheme of metal-polyhydroxycarboxylic complexes as a function of increasing pH, from (Van Duin et al. 1989). 47
Figure 6-1. Comparison between isosaccharinate ($ISAH_2^-$, left) and gluconate (GH_4^-, right) chemical structure. 52
Figure 6-2. Solubility of thorium hydroxide in I=0.5M $NaClO_4$ media, pH_c=12, as a function of measured isosaccharinate concentrations in solution, after 1 kD filtration. Blue circles: from undersaturation direction. Red triangles: from oversaturation direction. 54
Figure 6-3. Solubility of thorium hydroxide in I=0.5M $NaClO_4$ media as a function of measured isosaccharinate concentrations in solution, after 1 kD filtration. Circles: from undersaturation direction. Triangles: from oversaturation direction. Only solid symbols were used in the calculations (see text). Grey solid line: calculated solubility taking into account the formation of both 1:1 and 1:2 Th:ISA complexes (with uncertainty, dashed

lines). Dotted black lines indicate thorium hydroxide solubility in the absence of organic ligands.. 55
Figure 6-4. Calculated thorium aqueous speciation in Figure 6-3 (thorium hydroxide solubility in the presence of isosaccharinate), in agreement with the stability constants determined in present work. 56
Figure 6-5. Experimental data of EXAFS fourier transforms of Th L_{III}-edge for Th-isosaccharinate, Th-gluconate and Th-carbonate solutions. The exact composition of each sample are described in the text. 58
Figure 6-6. Solubility of thorium oxyhydroxide from undersaturation (circles) and oversaturation (triangles) direction as a function of the concentration of organic ligand, at fixed pH_c=12 (I=0.5M, $NaClO_4$). Black symbols: in the presence of isosaccharinate. Green symbols: In the presence of gluconate. Black solid line: calculated solubility taking into account the formation of a 1:1 and 1:2 Th-ISA complex. Green line: calculated solubility taking into account the formation of a 1:1 and 1:2 Th-gluconate complex. Dashed line: calculated solubility in the absence of organic ligands. 59
Figure 6-7. Symbols: Solubility of thorium hydroxide as a function of total isosaccharinate concentrations in solution at pH=12, from (Rai et al. 2009). Black solid line: calculated solubility taking into account the formation of both 1:1 and 1:2 Th:ISA complexes calculated in present work (with uncertainty, dotted lines)......................... 62
Figure 6-8. Symbols: Influence of ISA on the sorption of thorium on a polyallomer tube wall at pH=12, from (Vercammen 2000). Black solid line: calculated K_d values taking into account the formation of both 1:1 and 1:2 Th:ISA complexes obtained in present work (with uncertainty, dotted lines).. 63
Figure 6-9. Symbols: Measured distribution coefficients for liquid-liquid extraction data at 25ºC and pH≈8, at total acetylacetone concentrations of $8.72\cdot10^{-4}$M (left) or $1.12\cdot10^{-3}$M (right), from (Allard & Ekberg 2006a, Allard & Ekberg 2006b). Solid lines: Calculated distribution coefficients using Th-ISA complexes obtained in present work. For the meaning of dotted lines, see text.. 65
Figure 7-1. Solubility of $ThO_2\cdot xH_2O$ as a function of EDTA concentration, at fixed pH_c=12 (I=0.5M, $NaClO_4$). Blue diamonds: experiments at solid-to-liquid ratios =0.4 g/l, 300kD filtration. Green diamonds: experiments at solid-to-liquid ratios =2.5 g/l, 300kD filtration. Grey circles: experiments at solid-to-liquid ratios =2.5 g/l, 1kD filtration. Solid line is calculated solubility by considering the formation of $Th(OH)_2(EDTA)^{2-}$ complex (with uncertainty, dotted line). Dashed line is thorium hydroxide solubility in the absence of organic ligands. 70
Figure 8-1. Gluconate (left) and EDTA (right) speciation in I=0.5M $NaClO_4$ media as a function of total calcium concentration in the system. $[L]_T=1\cdot10^{-2}$M, pH=12.............. 74
Figure 8-2. Amorphous thorium hydroxide solubility (black solid line) and underlying thorium aqueous speciation (dashed lines) and calcium aqueous speciation (dotted lines) as a function of calcium concentration in the system. pH=12, I=0.5 M $NaClO_4$........... 75
Figure 8-3. Representation of a 2:2:1 Ca-Al(III)-glucarate complex, from (Venema 1992).. 76
Figure 8-4. Influence of ISA on the sorption of Th on a polyallomer tube wall at pH 12.0 in the absence of calcium (empty circles) in the presence of 0.7mM Ca (blue diamonds) and in the presence of 10mM Ca (green triangles). Experimental data from (Vercammen 2000, Vercammen et al. 2001).. 77
Figure 8-5. Solubility of thorium oxyhydroxide from undersaturation direction as a function of measured gluconate concentration at fixed pH_c=12 (I=0.5M, $NaClO_4$), time>39 days. Open circles: in the absence of calcium. Blue squares: $[Ca]=5\cdot10^{-4}$ M.

Green triangles: $[Ca]=2\cdot10^{-2}$ M. Solid line is calculated thorium hydroxide solubility taking into account $Th(OH)_2(GH_2)^-$ formation (with uncertainty, dashed line) as reported in section 5.4. Dotted line is calculated solubility in the absence of organic ligands. 79

Figure 8-6. Measured vs. initial calcium concentrations in thorium hydroxide solubility experiments at $pH_c=12$ in the presence of both calcium and gluconate. Black dotted line indicates $Ca]_{measured}=[Ca]_{initial.}$ 80

Figure 8-7. SEM images for amorphous thorium oxyhydroxide after contact with 0.5 M $NaClO_4$ solution at $pH_c=12$ for >70 days. A) $[GH_4^-]=1.0\cdot10^{-2}$ M, no calcium B) $[GH_4^-]=1.7\cdot10^{-3}$ M, $[Ca]=2.2\cdot10^{-2}$ M. 81

Figure 8-8. EDX results for amorphous thorium oxyhydroxide after contact with $[GH_4^-]=1.7\cdot10^{-3}$ M, $[Ca]=2.2\cdot10^{-2}$ M, 0.5M $NaClO_4$ solution at pH=12 for >190 days. 82

Figure 8-9. Experimental data of EXAFS Fourier transforms of Th L_{III}-edge for Th-gluconate solutions, $[Th]_0=1\cdot10^{-3}$ M and $[GH_4^-]=0.1$ M at pH≈11.8. Solid line: in the absence of calcium. Dashed line: $[Ca]_0=1\cdot10^{-2}$ M. 83

Figure 8-10. Solubility of thorium oxyhydroxide from undersaturation direction as a function of measured EDTA concentration at fixed $pH_c=12$ (I=0.5M, $NaClO_4$), time>19 days. Open circles: in the absence of calcium. Yellow circle: $[Ca]=5\cdot10^{-4}$ M. Blue cross: $[Ca]=9\cdot10^{-4}$ M. Red triangle: $[Ca]=2\cdot10^{-3}$ M. Solid line is thorium hydroxide solubility taking into account $Th(OH)_2(EDTA)^{2-}$ formation (with uncertainty, dashed line). Dotted line is calculated solubility in the absence of organic ligands. 84

Figure 9-1. Results from solubility (oversaturation) experiments. Triangles: Measured uranium concentrations in solution as a function of gluconate concentration at fixed $pH_c=12$ (I=1 M $NaClO_4$), after filtration. Dashed line: total uranium concentration added ($1\cdot10^{-4}$ M). Grey zone: expected $Na_2U_2O_7$ solubility under those conditions in the absence of organic ligands. 90

Figure 9-2. Results from solubility (undersaturation) experiments. Diamonds: Measured uranium concentrations in solution as a function of gluconate concentration at fixed $pH_c=12$ (I=0.5 M KCl), after filtration. Grey zone: expected $K_2U_2O_7$ solubility under those conditions in the absence of organic ligands. 91

Figure 9-3. Spectra for solutions with a constant uranium concentration ($5\cdot10^{-3}$ M) and increasing gluconate concentrations (from $2\cdot10^{-4}$ to $4\cdot10^{-3}$ M) at pH=12. Dashed red line indicates the absorbance in the absence of organic ligand. 92

Figure 9-4. UV-VIS results in the continuous variation method for uranium-gluconate samples at pH≈12; $[U]+[L]=1\cdot10^{-2}$ M. The plot shows absorbance at λ=435nm vs. the mole fraction for uranium. Open symbols indicate the samples where a yellow precipitate was observed. 93

Figure 9-5. UV-VIS results in the molar variation method for uranium-gluconate samples at pH≈12; $[U]_{total}=1\cdot10^{-3}$ M. The graph shows absorbance at λ=435nm vs. the ratio [L]/[U], after sample filtration. Open symbols: samples were precipitation was observed before filtration. 94

Figure 9-6. Results from solubility (oversaturation) experiments. Triangles: Measured uranium concentrations in solution as a function of gluconate concentration at fixed $pH_c=12$ (I=1 M $NaClO_4$), after filtration. Dashed line: total uranium concentration added ($1\cdot10^{-4}$ M). Grey zone: expected $Na_2U_2O_7$ solubility under those conditions in the absence of organic ligands. Black solid line: calculated solubility taking into account the formation of the 1:1 U(VI):gluconate complex. 96

Figure 9-7. Results from solubility (undersaturation) experiments. Diamonds: Measured uranium concentrations in solution as a function of gluconate concentration at fixed pH_c=12 (I=0.5 M KCl), after filtration. Grey zone: expected $K_2U_2O_7$ solubility under those conditions in the absence of organic ligands. Black solid line: calculated solubility taking into account the formation of a 1:1 U(VI):gluconate complex, with uncertainty (dotted lines). 97
Figure 9-8. U(VI) speciation in the presence of gluconate, taking into account the results obtained in present work (reaction 9-4). $[U(VI)]_T=1\cdot10^{-9}$M, $[GH_4^-]_T=1\cdot10^{-4}$M. The possible precipitation of solids has not been taken into account in the calculations. 98
Figure 9-9. Reevaluation of the results from solubility (undersaturation) experiments. Diamonds: Measured uranium concentrations in solution as a function of gluconate concentration at fixed pH_c=12 (I=0.5 M KCl), after filtration. Grey zone: expected $K_2U_2O_7$ solubility under those conditions in the absence of organic ligands. Black solid line: calculated solubility taking into account reaction 9-4. Red dotted line: calculated solubility taking into account reaction 9-5. 99
Figure 9-10. U(VI) speciation in the presence of gluconate, taking into account the results in reaction 9-5. $[U(VI)]_T=1\cdot10^{-9}$M, $[GH_4^-]_T=1\cdot10^{-4}$M. The possible precipitation of solids has not been taken into account in the calculations. 100
Figure 9-11. Summary of the experiments for the study of U(VI) complexation with gluconate........ 101
Figure 10-1. Suggested speciation scheme for the U(VI)-EDTA system, according to the stability constants in Table 10-1. $[U]=1\cdot10^{-7}$ M, $[EDTA]=1\cdot10^{-4}$ M. 104
Figure 10-2. Blue diamonds: Sodium uranate solubility (undersaturation direction) in I=0.5M $NaClO_4$ media at pH=11.8 and different EDTA concentrations (>26 days). Grey zone: Sodium uranate solubility in the absence of organic ligands. Solid red line: calculated sodium uranate solubility using U(VI)-EDTA stability constants highlighted in grey in Table 10-1. 105
Figure 14-1. Electrode calibration titration plot. The graph shows the potential measured *vs*. the volume of NaOH added (V_i). 182
Figure 14-2. Plot of the Gran function in front of the total volume of solution. 183
Figure 14-3. Example of an ICP-MS calibration for thorium. 184
Figure 15-1. X-ray powder diffractogram for the $ThO_2\cdot xH_2O$ solid. Blue and green lines indicate characteristic patterns of thorium oxide. Red lines are due to minor $NaNO_3$ impurities. 189
Figure 15-2. X-ray powder diffractogram for sodium uranate. 190
Figure 15-3. Scheme for the synthesis of the sodium isosaccharinate salt. 191
Figure 15-4. X-ray powder diffractogram for solid calcium isosaccharinate (black) and comparison with the spectra reported in (Rai et al. 1998) (blue lines). 192
Figure 15-5. $^{13}C\{^1H\}$ NMR spectra of solid sodium isosaccharinate. 193

Table 6-1. Summary of stability constants for the formation of Th-ISA complexes (in the near-neutral to alkaline pH range). 61
Table 10-1. Stability constants available in the literature for U(VI)-EDTA complexation. 103
Table 13-1. Summary of stability constants for thorium used in present work............ 174
Table 13-2. Summary of stability constants for U(VI) used in present work. 175
Table 13-3. Summary of stability constants for acid/base, sodium and calcium complexes with organic ligands used in present work. 176
Table 13-4. Ion interaction coefficients used in present work. 178
Table 13-5. Ion interaction coefficients used in present work in order to perform analogies. 179
Table 13-6. Comparison of Th-gluconate and Th-isosaccharinate constants obtained in present work (I=0.5) and after correction to I=0 with SIT or Davies approaches. Two significant figures are provided for the values at log K° in order to facilitate the comparison.. 180

1 Introduction

1.1 General introduction

Radioactive wastes arise from almost all activities (nuclear and non-nuclear industry, research, military activities, medical applications) involving the handling of radioactive materials. These wastes are characterised by an enhanced radioactivity (compared to natural backgrounds), which decreases with time. A wide variety of materials and elements have this enhanced radioactivity and should be handled as radioactive wastes, for example (ANDRA 2009, Chapman & McKinley 1987):

-the spent fuel (material that has already been used in a nuclear reactor to obtain energy);

-the metal cladding of the fuel elements;

-steel, concrete and other structural materials from dismantled nuclear reactors;

-radioactive liquids and solids from the treatment and reprocessing of wastes;

-ion exchange resins used in the reprocessing of spent fuel or in the filtration systems of nuclear power plants;

-miscellaneous contaminated laboratory material, such as paper tissues, gloves…

-lightning conductors containing radium;

-wastes generated in the uranium mining and extraction

The most appropriate management solution for each waste type depends on the legal frame of the country where the waste is produced and is linked to its physical and chemical properties. Transition radioactive wastes (very short lived) are disintegrated during temporary storage; after this period, the wastes can be stored as non-radioactive. Very low level radioactive wastes, as well as short-lived wastes (with a half life ≤ 31 years), can be stored in surface disposal facilities. Low level long-lived wastes are planned to be stored in near surface disposal facilities. Intermediate level long-lived wastes, as well as high level wastes, may be stored in deep disposal facilities.

Independently of the origin of the wastes and the type of management solution, it is necessary to confine them in order to avoid the radionuclides contained in the wastes being released to the biosphere in concentrations that could represent an unacceptable hazard to humans or to the environment (Miller et al. 2000). The nuclear waste facilities are then designed to retain and confine the wastes until its radioactivity level decreases below legislated radiation levels. In order to guarantee this confinement, the disposal facilities are provided of several engineered barriers, following a multi-barrier concept. Three different types of engineered barriers can usually be distinguished:

-The first barrier is related to the treatment of the wastes itself. Some wastes[1] are poured in containers and confined in a matrix such as bitumen, cement, sand or glass, creating both a chemical and a physical barrier that avoids radionuclide mobilization.

-The second barrier (engineered barrier) is formed by the materials used to build the facility infrastructure.

-The third barrier, especially relevant in deep geological disposal, is the geological formation around the facility.

In those engineered barriers, cement and concrete play a crucial role. They may be used as matrix to immobilise some types of radioactive wastes (first confinement barrier). They will also be present in the second confinement barrier, as they will be used in repository construction, both for creating the repository infrastructure (in surface and deep disposal) and for supporting the repository host rock (in the case of deep geological disposal).

Cement materials are formed by different solid phases such as portlandite, calcium silicate hydrates or ettringite. In contact with groundwaters, those phases will suffer dissolution and precipitation process, and will evolve with time. Different phases can be considered as representative of the chemical evolution of the porewaters in contact with cement, and different pH values are characteristic of each one of these phases (see Figure 1-1).

The evolution initially generates a high-pH water (pH > 13) rich in K^+ and Na^+ ions, due to the lixiviation of Na_2O and K_2O oxides (state I). This first period is followed by a period in which the pH is dominated by equilibrium with portlandite, $Ca(OH)_2$ giving a pH of 12.2 (state II). Calcium concentrations at this degradation state are in the order of 10^{-2} M (Ochs et al. 1998, Ochs et al. 2002). After this state, hydrated calcium silicates (CSH) control the porewater chemistry, leading to porewaters with pH ranging from 12.5 to 10.5, depending on the calcium to silica ratio in the CSH minerals (state III).

---

[1] It must be noticed that not all the wastes are confined in such type of matrices; some of them, when appropriate, are just compacted or poured in containers without any additional confinement matrix.

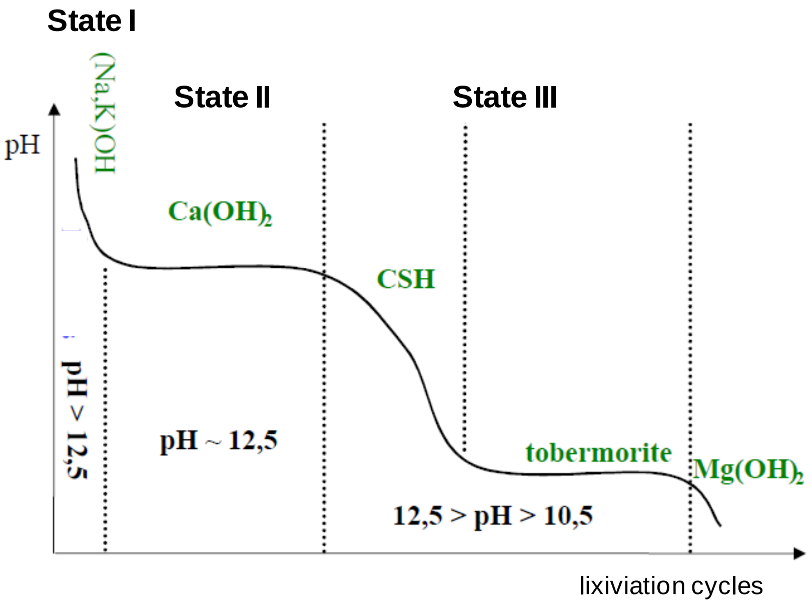

Figure 1-1. The phases representative of cement degradation, as a function of lixiviation cycles. Adapted from (ANDRA 2005b).

Cement and concrete provide not only a physical barrier to the radionuclide mobility, but also a chemical barrier (Nirex 2001). The first component of chemical containment is due to solubility limitations. The high pH conditions created by cement and concrete materials will cause a radionuclide chemistry dominated by hydroxyl ion, forming radionuclide insoluble oxides and hydroxides. The second component is sorption, that is, the binding of otherwise mobile chemical species to the cement surface. Sorption produces additional retardation of radionuclides, so that a higher proportion of them may decay before reaching the geological barrier or the biosphere.

There is a clear need of assessing the reactions that are likely to occur between radionuclides and the complexing agents present in or near the waste, in order to estimate the quantities of radionuclides that can be transported out of the confinement barriers. In order to do that, it is essential to know the relative stabilities of the compounds and complexes that may form under the relevant conditions, an information that is often provided by speciation calculations using chemical thermodynamic data (Hummel et al. 2005).

One of the points which is relatively poor understood is radionuclide solubilisation due to complexation by organic ligands (Keith-Roach 2008).

1.2 The influence of organic ligands on radionuclide migration

Some of the materials present among radioactive wastes are made of organic polymers. Examples of these materials are packaging plastics, clothes, paper, gloves, or ion-exchange resins. These materials are usually found in radioactive wastes classified in low and intermediate level categories. The wastes could also be affected by organic substances present in the geological media of the repository, by organic chemicals used in construction, buffer, and sealing materials, or by organic substances left behind from human activities before the closure of the repository (Hallbeck 2010).

The role of organic complexing agents in enhancing radionuclide migration is undisputed (Keith-Roach 2008). Organics influence both, solubility and sorption, two of the main chemical phenomena that control the migration of radionuclides through the environment. Different organic substances in the waste or in degradation products emanating from the waste, and chemical substances added during the building of cementitious barriers in the repository, may exhibit complexing properties towards radionuclides (ANDRA 2005b, Chapman & McKinley 1987, Fanger et al. 2001, Glaus & Van Loon 2008, Hakanen & Ervanne 2006). Some examples are:

- cement additives such as water reducers, retarders, and superplasticizers;
- products from degradation of cellulose, as isosaccharinic acid;
- chemicals used for decontamination and cleaning of radioactive waste material, such as EDTA (ethylene diamine tetraacetic acid), NTA (nitroltriacetate), or citric acid.
- soluble substances formed when ion exchange resins, plastics or similar products degrade, as oxalic acid;

- fulvic acids or other organic molecules naturally present in groundwaters that can infiltrate the repository.

Gluconate, isosaccharinate and EDTA have been selected in this work as representatives of three different types of organic substances (cement additives, cellulose degradation products and decontamination agents respectively) present in repositories.

The amount of available thermodynamic information for gluconate complexation with transition metals is reasonable (Sawyer 1964); the situation is worse regarding the stability constants of gluconate-radionuclide complexes (Keith-Roach 2008). In the case of isosaccharinate the number of experimental studies is very limited (Hummel et al. 2005). Finally, EDTA has been well studied regarding its complexation with radionuclides, although the available stability constants can vary within orders of magnitude (Cartwright et al. 2007), and data under alkaline pH values are very scarce. Gaps in current knowledge are then important and additional experimental data are necessary.

1.2.1 Gluconate

A large number of different types of organic compounds can be added to cement in order to influence its properties. Examples of cement additives are polycarboxylate ethers (PCEs) superplasticizers. PCEs are a family of products with significantly different chemical structures; a typical PCE is shown in Figure 1-2. PCEs are expected to “open up and progressively release” additional polymer chains when mixed with cement. As a consequence, the exact composition of the additive, as well as the structure of the products derived from it, are not completely known.

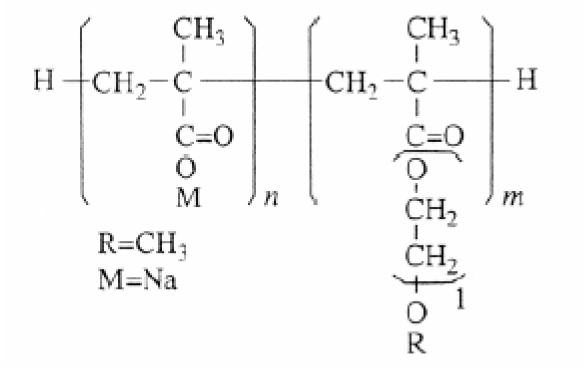

Figure 1-2. Basic structure of a polycarboxylate ether superplasticizer (Andersson et al. 2008).

From a PCEs structure, the following information can be extracted:

- PCEs contain carboxylic groups,
- when the ether groups in the molecule contact with an alkaline media they may hydrolyze, releasing polymeric chains that contain alcohol groups.

For this reason, simple polyhydroxy carboxylic acids (such as gluconate, Figure 1-3) have been used in some cases as a surrogate of the PCEs additives (ANDRA 2005b, Bradbury & Van Loon 1998). As a matter of fact, gluconate may represent the upper limit effect that a carboxylic ether superplasticizer could have on radionuclide mobilization, thus being a very conservative estimate.

On the other hand, PCEs also typically contain a range of minor components to improve the performance of the intended application. Among these minor components, gluconate may be added to PCE in order to prevent an excessive rapid sorption of the superplasticizer onto the cement (Hayes et al. 2012).

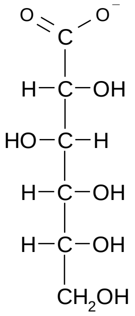

Figure 1-3. Gluconate chemical structure. In the text, "H_4" in GH_4^- refers to the hydrogen of the secondary alcohols in the molecule (Sawyer 1964).

For polyhydroxycarboxylic acids, complexation with metals may occur through carboxylate groups, ionized hydroxyl groups or a combination of different coordination modes (Van Duin et al. 1989), depending on several factors such as pH, acidity of the coordinated metal cation and steric effects, among others. An example is provided in Figure 1-4.

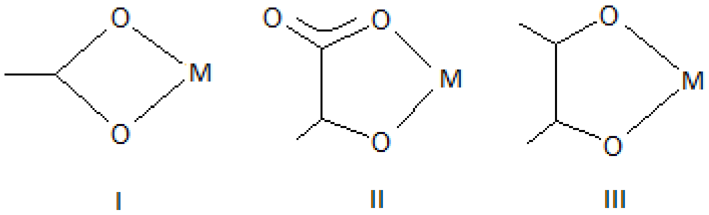

Figure 1-4. Different coordination modes for polyhydroxycarboxylic acids. I) Bidentate coordination through the carboxylic function. II) and III) Examples of coordination modes involving ionized diol functions.

Different formulas (options a) b) and c) below) have been used to represent the same molecules in the literature. This is due to the fact that, in some cases, the experimental information gathered does not allow to differentiate if the pH dependence of the complexes formed is caused by the gluconate coordination through diol functions or to the presence of hydroxyls (OH^-) in the metal coordination sphere.

$$M(OH)_xGH_y^{n-} \qquad a)$$

$$M(OH)_xG_{-zH}^{n-} \qquad b)$$
$$MG_{-yH}^{n-} \qquad c)$$

1.2.2 Isosaccharinate

Isosaccharinate (ISA, Figure 1-5) is a polyhydroxy carboxylic acid similar to gluconate. It is the most important product of alkaline degradation of cellulose in cement pore waters (Glaus & Van Loon 2008, Pavasars et al. 2003, Van Loon & Glaus 1997); thus, it is of major concern in performance assessments of radioactive waste repositories where cement materials are present (Hummel et al. 2005).

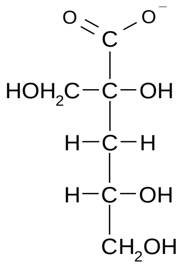

Figure 1-5. Isosaccharinate chemical structure. In the text, "H_2" in $ISAH_2^-$ refers to the hydrogen of the secondary alcohols in the molecule.

ISA is not commercially available and to obtain it requires a time-consuming synthesis in the laboratory. On the contrary, gluconate is cheap and commercially available. Given the chemical similarities between both ligands and the differences between their commercial availability, experimental studies involving ISA are scarce, and gluconate has been used as an analogue for isosaccharinate in some experimental works.

1.2.3 Ethylenediaminetetraacetic acid

Ethylenediaminetetraacetic acid (EDTA) is present in radioactive wastes as it is used in cleaning and decontamination procedures (Hummel et al. 2005). EDTA (Figure 1-6) may release up to four protons, but it may also act as a base, accepting up to two H^+ ions in the acidic pH range. Owing to its ability to form chelate rings, the ethylenediaminetetraacetate ligand is a strong complexing agent, especially in acid to mildly alkaline pH values (Fanger et al. 2001).

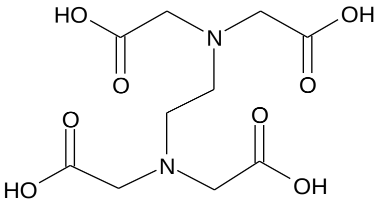

Figure 1-6. Ethylenediaminetetraacetic acid ($EDTAH_4$) structure.

In alkaline to strongly alkaline conditions, few studies on EDTA complexation capacity are available. The knowledge of the behaviour of this ligand in cementitious environments should then be increased to assess the mobility of radionuclides in radioactive disposal environments.

2 Objectives

The main goal of this PhD thesis is to obtain thermodynamic data to quantitatively predict the role of small organic ligands (gluconate, isosaccharinate and EDTA) on radionuclide mobility. Special attention has been paid to the behaviour of radionuclides under alkaline conditions, taking into account the key role of cement in both conditioning matrices and engineered repository barriers.

The experimental work has been conducted using natural Th(IV) and natural U(VI). The use of these radionuclides avoids the hazards of working with high levels of radioactivity in the laboratory. In addition, the use of a non-redox sensitive element avoids the experimental difficulties of controlling the oxidation state of a redox-radioactive radionuclide, especially at high pH values. Furthermore, Th(IV) and U(VI) can be used as analogues of other tetravalent and hexavalent actinides, respectively.

The specific objectives set out in present work, focused in the alkaline pH range, are fourfold:

1. to obtain reliable thermodynamic data (stability constants) in the thorium-gluconate system;
2. fill in the gaps of experimental data in both gluconate and isosaccharinate system, and to compare the data obtained in order to check if gluconate is a good analogue for isosaccharinate chemical behaviour;
3. to study the role of calcium in the thorium-gluconate and thorium-EDTA systems;
4. and to study the U(VI)-gluconate and U(VI)-EDTA systems.

3 Experimental setup

The experimental work has been done under conditions thought to obtain the information needed to fulfil the objectives of this work. Experimental conditions must be well controlled, and the total number of variables has to be reduced as much as possible in order to decrease the complexity of the system and to focus on the particular aspects of interest in the study (Grenthe et al. 1997).

In present work, results have been obtained mainly from two different types of experiments: macroscopic solubility experiments (section 3.3) and spectroscopic analyses (section 3.4 and 3.5). Reagents, materials and solutions and the main analytical techniques used are also briefly described in sections 3.1 and 3.2. Section 3.6 summarizes additional experimental approaches used.

3.1 Reagents, materials and solutions

Bidemineralised water (prepared by ultrafiltration with a MilliQ water purification system) was used in the experiments. All chemicals were reagent grade and were purchased from Sigma Aldrich, Scharlau and Panreac. Thorium nitrate solution (1% w/v) was obtained from J.T. Baker. Except when noted, chemicals were used without further purification.

Gluconate and EDTA are commercially available; sodium isosaccharinate was prepared in the laboratory, following the procedure reported by Whistler and co-workers (Whistler & BeMiller 1961) with some modifications (Evans 2003, Vercammen 2000). The procedure is described in detail in section 15.3.

The stabilities of An(IV) with carbonate are high and are one of the most important reactions for tetravalent radionuclides in aqueous systems. Avoiding the presence of CO_2 in the system was then important in order to prevent incorrect interpretations of the results obtained. Reagents and solutions were CO_2-free and were prepared and stored inside a nitrogen glove box. Ultrapure water was degassed by boiling and cooling in a N_2(g) atmosphere prior to its use. Concentrated NaOH was prepared following the indications in the literature (Sillen 1959) in order to obtain a free-CO_2 solution. The experiments were done inside the glove box with N_2(g) atmosphere. All these solutions were prepared on a regular basis.

Glass materials were used for the preparation of the solutions. Plastic materials (polyethylene and/or polypropylene) were used to perform the experiments, as their size and shape were useful to maintain the solutions under constant stirring. Prior to use, all material was cleaned with HNO_3 acid and extensively rinsed with deionized and ultrapure water, in order to avoid the presence of impurities. The possible sorption of thorium or organic ligands onto the materials was tested by leaching them with 2% HNO_3 after their use; the analysis of the solutions with ICP-MS or TOC did not show significant sorption within detection limits.

Except when noticed, the experiments were done at 25±2ºC.

3.2 Phase separation and analytical techniques

3.2.1 Filtration

One of the most important drawbacks in thorium analysis is insufficient phase separation, resulting in too high measurements of thorium in solution due to the contributions from polymeric or colloidal thorium species (Rand et al. 2009). Special care was devoted to separate colloids and solid particles in present work. In most experiments, Pall Microsep 300 kD (pore size ≈20nm) and 1 kD (pore size ≈1.2nm) filters with modified polyethersulfone Omega membrane were used; those have been reported to lead to a successful separation of colloids (Altmaier et al. 2005a). Prior to filtration, an aliquot (<1 ml) of the solution was passed through the filters before definitive filtration of the sample, in order to saturate any possible sorption sites of the membrane. The thorium concentrations in the sample measured after successive filtrations remained constant, showing the efficiency of the filtration method.

Ultracentrifugation[2] tests were also performed in order to check the effectiveness of the filters. Ultracentrifugation presented some disadvantages compared to filtration using Pall Microsep devices. Thus, filtration with 1 kD and 300 kD was preferred. Results of those tests are described in section 5.3.

3.2.2 pH measurements

pH_c was determined using an alkaline resistant combined glass electrode (Crison 52.22) where the reference electrolyte had been replaced by the background electrolyte used in the experiments (0.5 M $NaClO_4$) (Kitamura & Kohara 2004). The electrode was calibrated using a Gran titration procedure (Gran 1952), where 50 ml of $NaClO_4$ 0.5M were titrated with a 0.06M $HClO_4$ solution. This procedure allows determining the molal H^+ concentration (Altmaier et al. 2003). An example of a calibration is provided in section 14.1.

3.2.3 ICP-MS and TOC measurements

Inductively coupled plasma mass spectrometry (ICP-MS) was used for the measurement of metal concentration, mainly thorium and uranium. Total organic carbon analysis (TOC) was used for the measurement of organic ligand concentrations. A description of these analytical techniques is provided in section 14.2 and 14.3 respectively.

3.3 Solubility experiments

The measurement of the aqueous solubility of a sparingly soluble solid from undersaturation direction in the presence of a complexing agent (L) is one of the most common methods for the determination of stability constants of metal ion complexes (M-L) (Rossotti & Rossotti 1961). In these studies, equilibration between a well characterized solid and a solution with a known pH and ligand concentration is achieved by shacking both together in a closed vessel. In order to obtain quantitative information on metal-ligand complexation, the following information is required (Grenthe et al. 1997):

---

[2] In ultracentrifugation, high velocity rotations are used to separate colloids or submicroscopic particles. No filters are used.

-the composition of the solid phase determining the metal solubility and its solubility product (see section 4);

-all the possible complexes of the cation concerned, as well as the possible complexes formed by the organic ligand, and their stability (see section 13);

-and the concentrations of the various metals and ligands in solution (which is basically an analytical problem).

In present work, solubility experiments were usually done in polypropylene tubes (20-50 ml), which were kept under constant stirring for different time intervals at 25±2 ºC. The solid/liquid ratio to be used was determined in preliminary tests (see section 5.3). Most undersaturation experiments were performed by contacting 0.06g of solid with 20 ml of solution containing a given organic ligand concentration at the desired pH value.

Solubility reactions are affected by the ionic strength (I) of the system. Solubility experiments have to be performed at constant ionic strength values in order to be able to determine the corresponding constant at zero ionic strength (Grenthe et al. 1997). Most (but not all) of the solubility experiments undertaken in this work were performed at $I=0.50\pm0.05$ M ($NaClO_4$).

All the experiments were conducted inside a glove box, under $N_2(g)$ atmosphere to avoid the presence of $CO_2(g)$. Previous to inflow the gas into the glove box, it was flushed through a column containing a $CO_2(g)$ trap and a flask with the ionic medium (Figure 3-1).

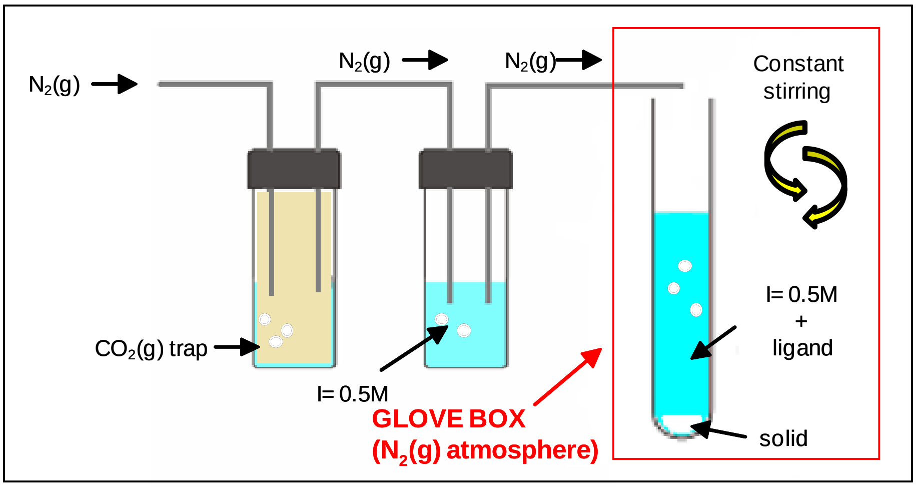

Figure 3-1. Scheme of the experimental set-up for solubility experiments from undersaturation direction.

The solubility method from undersaturation direction has some drawbacks:

-Sorption of the ligand onto the solid surface is possible. As an example, sorption of EDTA on thorium hydroxide was described by Xia et al. (Xia et al. 2003).

-In some cases, kinetics may play an important role, since equilibrium is often attained slowly (Rossotti & Rossotti 1961). Experimental factors such as the order of addition of reagents (metal+ligand or ligand+metal) can also influence the kinetics of reaction (Hummel et al. 2005). It is then necessary to check that the same concentration of metal in solution is attained after different time intervals. In present work, equilibrium was assumed when metal concentrations did not vary more than 5% within 48 hours or more.

-The temperature, preparation method, pre-treatment and storage of a solid can alter its water content and particle size. Those alterations result in differences in their corresponding solubility products; for example, they may explain differences among solubility data for amorphous thorium oxide reported in the literature (Rand et al. 2009). In present work, different fractions of the same solid were used all through the experimental work. Preparation and characterization of the solids is described in section 15.

Solubility experiments were performed not only from undersaturation direction, but also from oversaturation direction, in order to confirm the results obtained.

Most oversaturation experiments were done by preparing 20 ml of a solution containing a given organic ligand concentration at the desired pH value. Afterwards, a spike of acidic concentrated thorium or uranium solution was added to the system.

In the experiments from oversaturation direction, kinetic factors must also be taken into account. However, due to the small amounts of solid that usually precipitate in those systems, sorption of the ligand on the solid might be negligible. On the other hand, characterization of the solid precipitated in the system is very difficult or impossible for the same reason (low amounts of solid phase formed).

As in the case of experiments from undersaturation direction, those were also performed inside a glove box under N_2(g) atmosphere.

3.4 EXAFS experiments

XAFS (X-ray absorption fine structure) is a spectroscopic technique that uses X-rays to probe the physical and chemical structure of matter at an atomic scale. It requires an intense and energy-tunable source of X-rays, which in practice means the use of synchrotrons (Newville 2004).

It is a powerful tool for the determination of molecular-level information on the speciation of elements, including actinides, in solids and solutions (Reich et al. 2000). The technique not only describes the type of the element and its concentration, but also its oxidation state and coordination sphere. The structural parameters of the radionuclide surrounding, i.e., bond distances, coordination numbers, and type of neighbouring atoms, can be determined by extended X-ray absorption fine structure (EXAFS) spectroscopy (Reich et al. 2000).

The properties of EXAFS that make it so useful are (Koningsberger & Prins 1988):

-Long-range order is not required, so non-crystalline solids and aqueous samples can be analysed.

-The local atomic environment can be determined separately for each type of atom.

-Structural information is obtained by a measurement that is relative easy, rapid and non-destructive.

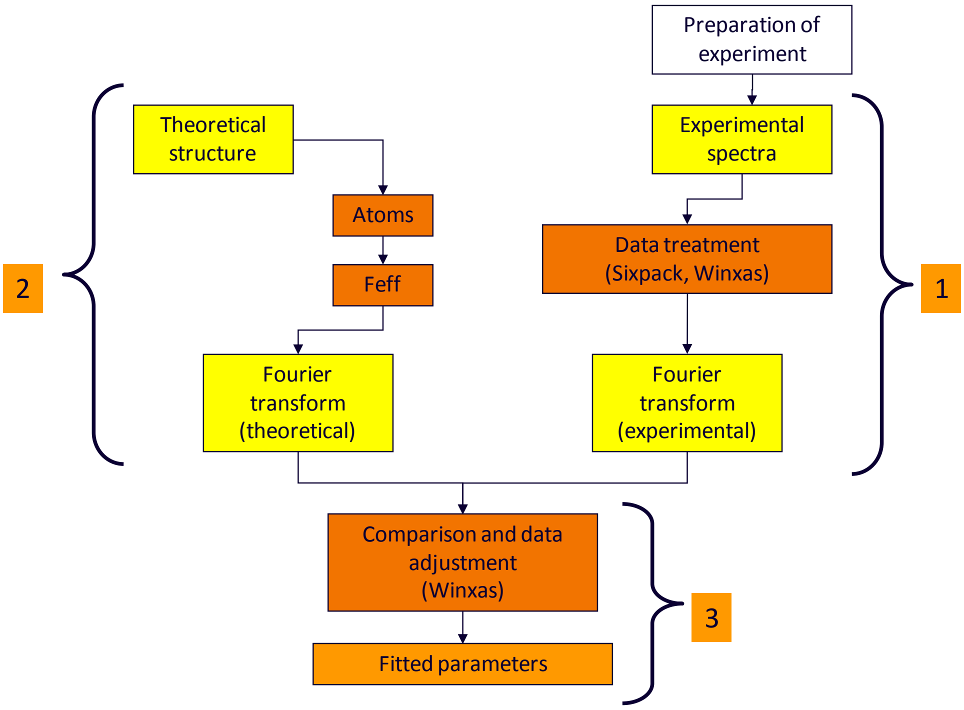
Preparation of experiment
Theoretical structure
Experimental spectra
Atoms
Data treatment (Sixpack, Winxas)
Feff
2
1
Fourier transform (theoretical)
Fourier transform (experimental)
Comparison and data adjustment (Winxas)
3
Fitted parameters

Figure 3-2. Procedure for EXAFS experimental data acquisition (1), theorethical structure (2) and spectra fitting (3), adapted from (Scheinost 2010).

In present work, thorium L_{III}-edge EXAFS spectra were collected at the ROssendorf Beam Line (ROBL) at the European Synchrotron Radiation Facility (ESRF) located in Grenoble (France). A summary of data acquisition, treatment and fitting is provided in Figure 3-2; details are provided in the corresponding results section. Additional information is provided in section 14.4.

3.5 UV-VIS experiments

Spectroscopy is widely recognized as a valuable tool to provide information on metal species in aqueous solutions (Meinrath 1998b), including actinides. Uranyl(VI) shows a characteristic UV-Vis spectra in the range 500 to 370nm, due to the electronic structure of O=U=O (Meinrath 1998b). Although UV-Vis spectroscopy is probably not sensitive enough to detect uranium(VI) in the majority of environmental samples (Meinrath 1997), those absorption properties have long been used to obtain information about uranium equilibrium in solution.

In present work, UV-Vis was used to study U(VI)-L complexation in the alkaline range. Two different methods were used:

-The continuous variation method, where the sum of metal and ligand concentrations ([M]+[L]) in solution is constant in all the samples (Rossotti & Rossotti 1961).

-The molar variation method, where the metal concentration is constant and the concentration of the ligand is increased in each sample (Rossotti & Rossotti 1961, Sawyer & Kula 1962).

The optical absorbance of a solution is governed by both a characteristic intensive factor (the molar absorptivity or the molar extinction coefficient) as well as by the concentration of each absorbing species (Rossotti & Rossotti 1961). The interpretation of the measurements mentioned above may thus be complicated if several absorbing species are present in solution. Because of this, the U(VI)-L system was studied not only with UV-VIS techniques but also with the solubility experiments described in section 3.3.

3.6 Other experimental methods

Additional methods as sorption experiments, as well as electrospray ionization mass spectrometry (ESI-MS), scanning electron microscopy (SEM) and nuclear magnetic resonance (NMR) techniques were also used in order to complement the information obtained with the techniques described above. These complementary techniques are described in section 14.

4 Solubility of Th and U(VI) in the absence of organic ligands (Paper I to IV)

The solubility of a solid in the *presence* of a ligand can be used to obtain quantitative information on metal-ligand stability. To achieve this objective, it is mandatory to know the solubility product of the solid and all the possible complexes formed in solution by the metal cation in the *absence* of the ligand under study.

The determined solubility products of thorium and uranium solids used in this work is described below.

4.1 Th and U(VI) chemistry in alkaline conditions

Present work focuses the attention on the alkaline pH values generated by the use of cement in engineering barriers and conditioning materials in a nuclear waste repository. It is then advisable to understand the chemistry of the studied radionuclides under alkaline conditions prior to assess the effect of organic ligands on its mobility.

4.1.1 Thorium

Th(IV) is a non-redox sensitive element. Its chemistry is dominated by its strong tendency to hydrolyze and to form colloids (Rand et al. 2009). Amorphous thorium hydroxide solubility is low in the alkaline range, and its main hydrolysis species at pH>7 is $Th(OH)_4(aq)$. Figure 4-1 shows thorium hydroxide solubility and thorium underlying speciation, calculated with MEDUSA code (Puigdomènech 2009) using data from the NEA review on thorium thermodynamics (Rand et al. 2009) as summarized in section 13.1.

In the presence of carbonates, thorium hydroxide solubility increases significantly at near-neutral to alkaline pH values (Altmaier et al. 2006, Altmaier et al. 2005a, Rand et al. 2009). It is thus important to avoid the presence of $CO_2(g)$ in the system, as explained in section 3.1.

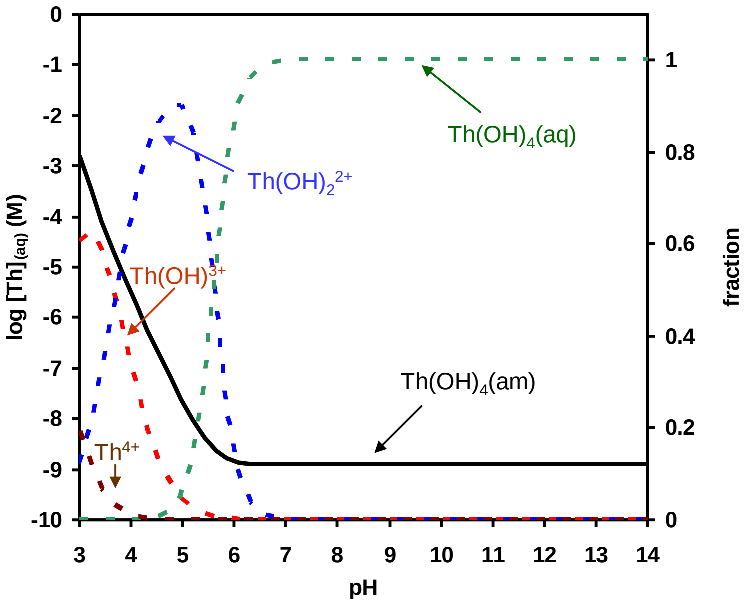

Figure 4-1. Calculated amorphous thorium hydroxide solubility (black solid line) and underlying thorium aqueous speciation (dotted lines) as a function of pH, using thermodynamic data from (Rand et al. 2009). I=0.

The role of calcium on thorium speciation has been studied by Altmaier and co-workers (Altmaier et al. 2008, Brendebach et al. 2007). Those authors suggested the formation of ternary Ca-Th-OH complexes that caused unexpectedly high solubilities of thorium hydroxide in alkaline concentrated $CaCl_2$ solutions (pH 11-12 and [$CaCl_2$] > 0.5 M). Those studies are of particular interest for the storage of nuclear waste in underground salt mines, as the corrosion of cementitious waste packages in those formations lead to the presence of such high calcium concentrations. The dominant aqueous species identified by the authors in these solutions was $Ca_4[Th(OH)_8]^{4+}$.

4.1.2 Uranium

Uranium is a redox sensitive element. In the alkaline pH range its aqueous chemistry is dominated by U(VI); strong reducing conditions are needed to avoid U(IV) oxidation. (Guillaumont et al. 2003).

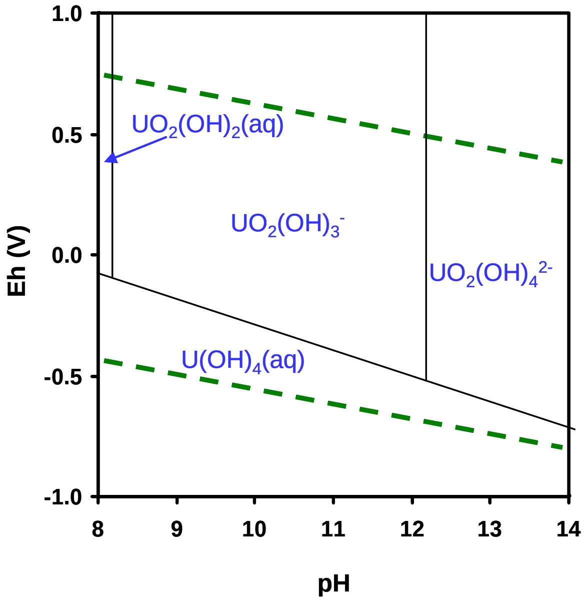

Figure 4-2. Uranium aqueous speciation as a function of pH and Eh in the absence of complexing agents other than OH^-; only aqueous species are shown. Green dashed lines stand for Eh limits for water oxidation and reduction. Calculations performed using the thermodynamic database reported in section 13.2, I=0, $[U]_T=1\cdot10^{-9}$ M.

Several solid species can limit U(VI) solubility under alkaline conditions, depending on the composition of the contacting water. In the absence of any complexing agent, schoepite ($UO_2(OH)_2(s)$) may precipitate (Guillaumont et al. 2003). In the presence of sodium or calcium, the formation of uranates ($Na_2U_2O_7\cdot xH_2O$, $CaU_2O_7\cdot xH_2O$) is expected (Altmaier et al. 2005b, Yamamura et al. 1998).

4.2 Th solubility in the absence of organic ligands (Paper I)

In the absence of other ligands than OH^-, Th(IV) may precipitate as X-ray amorphous hydrous oxides, which are not well-defined compounds. Although they are commonly called "$Th(OH)_4(am)$", "$ThO_2\cdot H_2O(am)$" or "$ThO_2(am, hyd)$", their structure would probably be better represented by the formula of an hydrated oxyhydroxide

“$ThO_n(OH)_{4-2n}·xH_2O$” (Rand et al. 2009). Their chemical composition, water content and crystallite size depend on the temperature, preparation method, pre-treatment and storage conditions (Rand et al. 2009), leading to different thermodynamic properties and different solubility values. For example, solubility data of a precipitate dried at room temperature (Neck et al. 2002, Osthols et al. 1994) are lower than values obtained in studies where the precipitate has only been washed with water, without drying (Neck et al. 2002). Then, although solubility values for amorphous thorium oxyhydroxides are available in the literature, it is necessary to obtain the solubility value for the particular solid used in present work in the absence of organic ligands.

Thorium oxyhydroxide used in the experiments was prepared and characterized as described in section 15.1. Using this solid, solubility experiments from undersaturation were performed as described in section 3.3. The results obtained are shown in Figure 4-3 (blue symbols). At $pH_c<7$ thorium concentration in solution shows a step decrease with increasing pH, while at $pH_c>7$ the thorium concentration remains at a constant level due to the formation of $Th(OH)_4(aq)$, in agreement with thorium aqueous speciation shown in Figure 4-1.

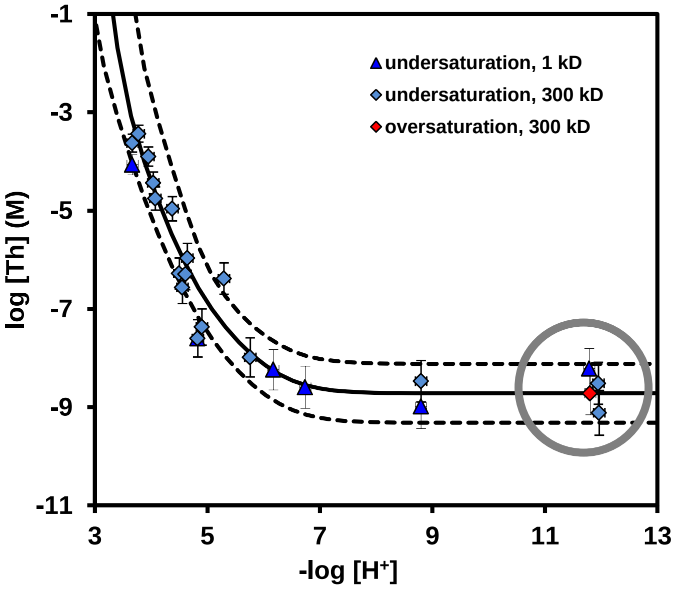

Figure 4-3. Solubility of thorium oxyhydroxide (I=0.5M, $NaClO_4$), after 1 kD (triangles) or 300 kD (diamonds) filtration. Blue symbols: from undersaturation direction, >40 days of experiment. Red symbol: oversaturation direction, 5 days of experiment. The grey circle indicates the measured samples at alkaline pH values ($pH_c \approx 12$). Solid line stands for solubility calculated in present work, as described in the text (with uncertainty, dashed lines).

One of the key points when dealing with experimental solubility data for amorphous thorium oxyhydroxides are phase separation procedures. Insufficient removal of colloids or the use of inappropriate filter material may lead to the determination of erroneous solubility values that include contributions from large polymeric or colloidal thorium species. This subject was extensively discussed in different literature publications (Altmaier et al. 2004, Altmaier et al. 2005a, Neck et al. 2002, Rand et al. 2009).

In present work samples were filtered with 300 kD (pore size ≈20nm) and 1 kD (pore size ≈1.2nm) polyethersulfone filters, which have been reported to lead to a successful separation of thorium colloids (Altmaier et al. 2005a). As seen in Figure 4-3, the results obtained for 1kD filtration (triangles) and the results for 300kD filtration (diamonds) are in agreement.

Samples from undersaturation direction were taken at different time intervals between 30 and 113 days. Furthermore, one sample form oversaturation direction (red diamond in Figure 4-3) was measured. Although the sample was obtained after only 5 days of equilibration, results are in good agreement with the measurements of the samples from undersaturation direction after 51 and 113 days obtained in the same pH range (see grey circle in the figure).

The solubility constant corresponding to this thorium hydroxide solid was calculated using FITEQL, a computer program for determination of chemical equilibrium constants from experimental data (Herbelin & Westall 1999). In FITEQL, every component (protons, thorium, etc...) has one material balance equation with two variables: the free concentration X and the total concentration T. A set of thermodynamic data (equation reactions and its corresponding stability constants, as described in section 13) must also be included in the calculations by the user. The FITEQL code iteratively optimizes the desired parameter (either stability constants or total or free concentrations, depending on the case) by minimizing the differences between calculated and experimental values using a nonlinear least squares optimization routine.

The solubility constant calculated with FITEQL (r. 4-1) is able to explain the experimental values obtained (black solid line in Figure 4-3). Uncertainty (dotted lines in the figure) was calculated taking into account the dispersion of the experimental data.

$$ThO_2 \cdot xH_2O + 4H^+ = Th^{4+} + (2+x)H_2O \quad \log K_s(I=0.5)=10.8\pm0.6 \quad \text{r. 4-1}$$

This value was corrected to I=0 using Specific Interaction Theory (SIT, see section 13.4) (Grenthe et al. 1997), using the interaction coefficients reported in the NEA review for thorium (Rand et al. 2009). The solubility constant after correction to I=0 is shown in r. 4-2.

$$ThO_2 \cdot xH_2O + 4H^+ = Th^{4+} + (2+x)H_2O \quad \log K^{\circ}_s=8.8\pm0.6 \quad \text{r. 4-2}$$

The log K^{o}_{s} value determined in present work (r. 4-2) is in agreement with the logK^{o}_{s}=8.5±0.9 value reported in the NEA review (Rand et al. 2009) for an amorphous thorium hydroxide solid dried at room temperature (ThO_2(am,aged,hyd). A comparison with literature values is also shown in Figure 4-4.

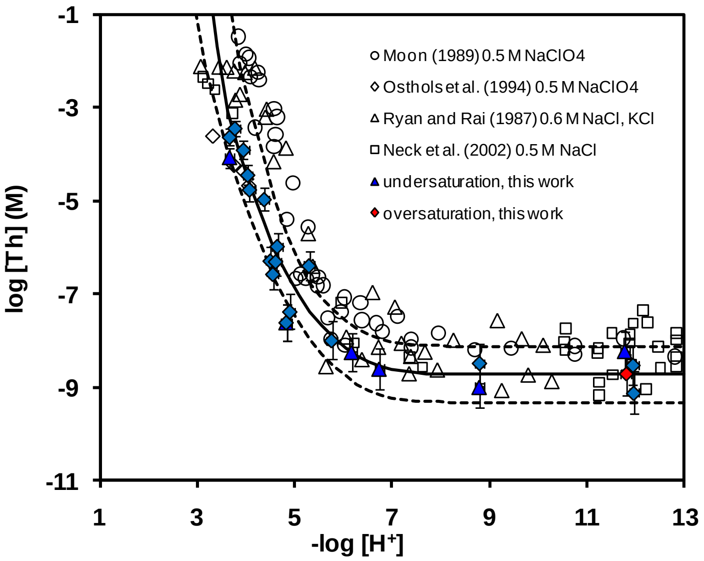

Figure 4-4. Solubility of thorium oxyhydroxide (I=0.5M, $NaClO_4$) obtained in present work (colour symbols) and comparison with literature data (open symbols).

4.3 U(VI) solubility in the absence of organic ligands

U(VI) solubility is limited by the presence of uranates (such as $Na_2U_2O_7$(s)) at alkaline pH values. The orange solid $Na_2U_2O_7$(s) can be obtained by mixing solutions of U(VI) and sodium hydroxide (Sutton 1955, Yamamura et al. 1998), as described in section 15.2.

The solubility of sodium uranate in the absence of organic ligands was measured from undersaturation direction in $NaClO_4$ media at two different ionic strength values, I=0.5M and I=0.1M. Uranium concentrations were measured after filtration using 300 kD or 1 kD polyethersulphone membrane filters; results are shown in Figure 4-5. Samples were taken at different time intervals, between 34 and 118 days; no dependence of the measured uranium concentrations with time were observed.

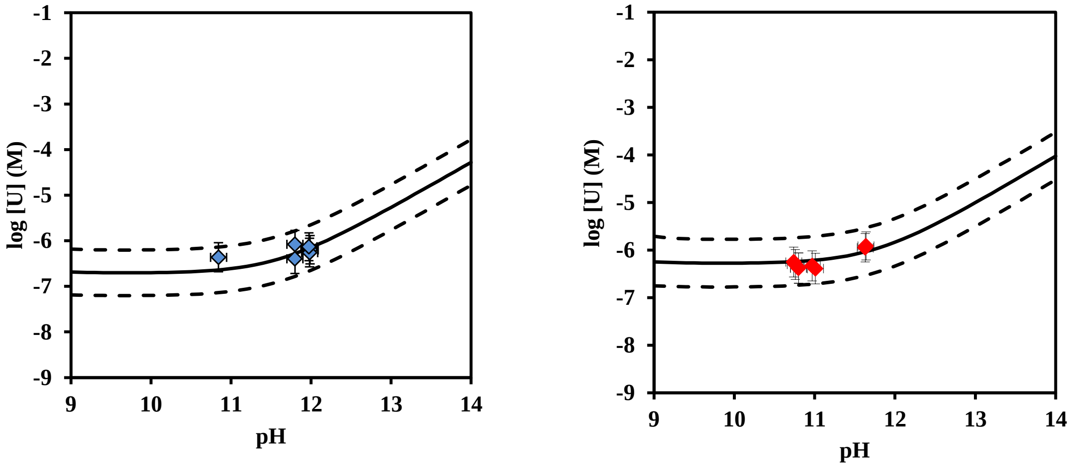

Figure 4-5. Solubility of sodium uranate (left: I=0.5M, $NaClO_4$; right: I=0.1M, $NaClO_4$) from undersaturation direction, after >34 days. Solid line stands for calculated $Na_2U_2O_7(s)$ solubility (with uncertainty, dashed lines).

The solubility (black solid line in Figure 4-5) was calculated using FITEQL (r. 4-3 and r. 4-4). Uncertainty (dotted lines in the figure) was calculated taking into account the dispersion of the experimental data.

$$Na_2U_2O_7(s) + 6H^+ = 2Na^+ + 2UO_2^{2+} + 3H_2O \qquad \log K_s(I=0.5)=27.0\pm1.0 \quad \text{r. 4-3}$$

$$\log K_s(I=0.1)=26.6\pm1.0 \quad \text{r. 4-4}$$

This value was corrected to I=0 using Specific Interaction Theory (SIT), with the interaction coefficients reported in the NEA review for uranium (Grenthe et al. 1992, Guillaumont et al. 2003), as summarized in section 13.4. The correction results in the solubility constants reported in r. 4-5 (calculated from data at I=0.5) and r. 4-6 (calculated from data at I=0.1). Average value is shown in r. 4-7.

$$Na_2U_2O_7(s) + 6H^+ = 2Na^+ + 2UO_2^{2+} + 3H_2O \qquad \log K^o_s=26.3\pm1.0 \quad \text{r. 4-5}$$

$$\log K^o_s=26.1\pm1.0 \quad \text{r. 4-6}$$

Average value: $\log K^o_s=26.2\pm1.0$ *r. 4-7*

The average value obtained (log K^o_s=26.2±1.0) is in agreement with available literature data for $Na_2U_2O_7$(s) solubility[3]:

Log K^o_s = 25.1±1.04 (Yamamura et al. 1998)

Log K^o_s = 26.5 (Warwick et al. 2006)

$Na_2U_2O_7$(s) solubility was also measured from undersaturation direction in a potassium-containing media (KCl, I=0.5M). As shown in Figure 4-6, under those conditions measured uranium concentrations (grey circles) are much lower than the solubility expected for $Na_2U_2O_7$(s) in this medium (red line in the figure).

In the case of a solution containing K^+, and according to Sutton and co-workers (Sutton et al. 1999), $K_2U_2O_7$(s) can be expected to form at pH>11. It could then be assumed that, following the dissolution of sodium uranate, and due to the presence of K^+ in the system, U(VI) will reprecipitate in the system in the form of potassium uranate, lowering uranium concentrations in solution.

The measured uranium concentrations were then modelled assuming the formation of $K_2U_2O_7$(s). The solubility of $K_2U_2O_7$(s) was calculated using FITEQL; results are shown in r. 4-8 and as the black solid line in Figure 4-6. Uncertainty (dotted lines in the figure) was calculated taking into account the dispersion of the experimental data. Correction to I=0 using SIT resulted in the value shown in r. 4-9.

$$K_2U_2O_7(s) + 6H^+ = 2K^+ + 2UO_2^{2+} + 3H_2O \qquad \begin{array}{ll} \log K_s(I=0.5)=27.2\pm1.0 & \text{r. 4-8} \\ \log K^o_s=26.3\pm1.0 & \text{r. 4-9} \end{array}$$

The calculated value (r. 4-9) is in agreement with data for $K_2U_2O_7$(s) solubility reported by Sutton and co-workers:

Log K^o_s = 25.8 (Sutton et al. 1999)

---

[3] The Log K^o_s for $Na_2U_2O_7$(s) reported in the NEA review for uranium (Grenthe et al. 1992), which is 22.6, corresponds to a more crystalline solid and was not taken into account in the comparison.

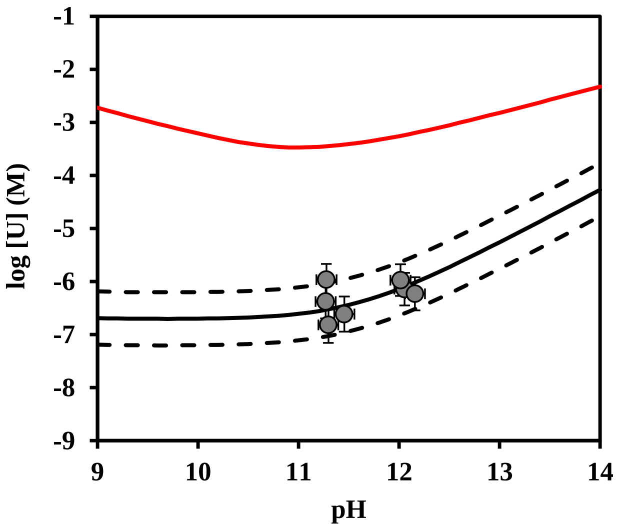

Figure 4-6. Solubility of sodium uranate in I=0.5M KCl media from undersaturation direction, after >27 days. Solid red line stands for calculated $Na_2U_2O_7(s)$ solubility. Solid black line stands for calculated $K_2U_2O_7(s)$ solubility (with uncertainty, dashed lines).

4.4 Summary and conclusions

- The solubility products of the solids studied have been determined in the absence of any organic ligands.
- The solubility constants for thorium hydroxide, sodium uranate and potassium uranate in the absence of organic ligands were determined by means of solubility experiments and calculated using FITEQL. The values were corrected to I=0 using Specific Interaction Theory (SIT) and are summarized below.

$ThO_2 \cdot xH_2O + 4H^+ = Th^{4+} + (2+x)H_2O$	$\log K^o_s = 8.8 \pm 0.6$	r. 4-2
$Na_2U_2O_7(s) + 6H^+ = 2Na^+ + 2UO_2^{2+} + 3H_2O$	$\log K^o_s = 26.2 \pm 1.0$	r. 4-7
$K_2U_2O_7(s) + 6H^+ = 2K^+ + 2UO_2^{2+} + 3H_2O$	$\log K^o_s = 26.3 \pm 1.0$	r. 4-9

- Results obtained for the solids studied are in good agreement with previous literature values (Rand et al. 2009, Sutton et al. 1999, Warwick et al. 2006, Yamamura et al. 1998).

5 Gluconate influence on thorium solubility (Paper I and Paper II)

5.1 Introduction

Gluconate ion forms soluble chelates with a variety of different metals, including actinides, transition metals, rare-earth metals and alkaline-earth metals (Rendleman 1978). The stoichiometry of these complexes may vary greatly depending on the specific metal, the molar ratio of metal to gluconate in the reaction mixture and the pH of the solution (Rendleman 1978, Sawyer 1964).

Sawyer (Sawyer 1964) undertook the first extensive review on the complexes formed by gluconic acid, covering the physical properties and chemistry of gluconic acid, its salts, its metal complexes, and their corresponding structures. Data for thorium-gluconate complexes were not mentioned, probably because no thermodynamic data for this system were available in 1964. The only experimental study for the thorium-gluconate system in the absence of calcium and in the alkaline pH range seems to be the one of Felmy (Felmy 2004). The authors performed solubility (undersaturation) experiments of $Th(OH)_4(am)$ in the presence of gluconate concentrations at 0.01M at pH range 4-13. The experimental data obtained were not modelled neither published in a peer-reviewed journal.

5.2 Objectives

The first objective of this work was to obtain thermodynamic data (stability constants) in the thorium-gluconate system in the alkaline pH range, given the lack of these data in the open literature. The procedure followed is summarized below:

1-Study of the thorium hydroxide solubility in the presence of gluconate, by taking into account parameters affecting it (filtration techniques, pH values, etc.) (section 5.3 and Paper I).

2-Determination of the stability constants for the thorium-gluconate complexes by using the results obtained in the solubility experiments (section 5.4 and Paper I)

3-Study of the structure of the complexes by EXAFS (section 5.5 and Paper II)

5.3 Thorium hydroxide solubility in the presence of gluconate (Paper I)

In order to study the formation of thorium-gluconate complexes, thorium hydroxide solubility experiments in the alkaline pH range were carried out, using the experimental set-up described in section 3. Main results are shown in Figure 5-1; a whole description is also available in Paper I. The solubility of thorium hydroxide at pH_c=12 increases significantly in the presence of gluconate, in comparison with its solubility under the same conditions in the absence of organic ligands. This suggests the formation of aqueous thorium-gluconate complexes.

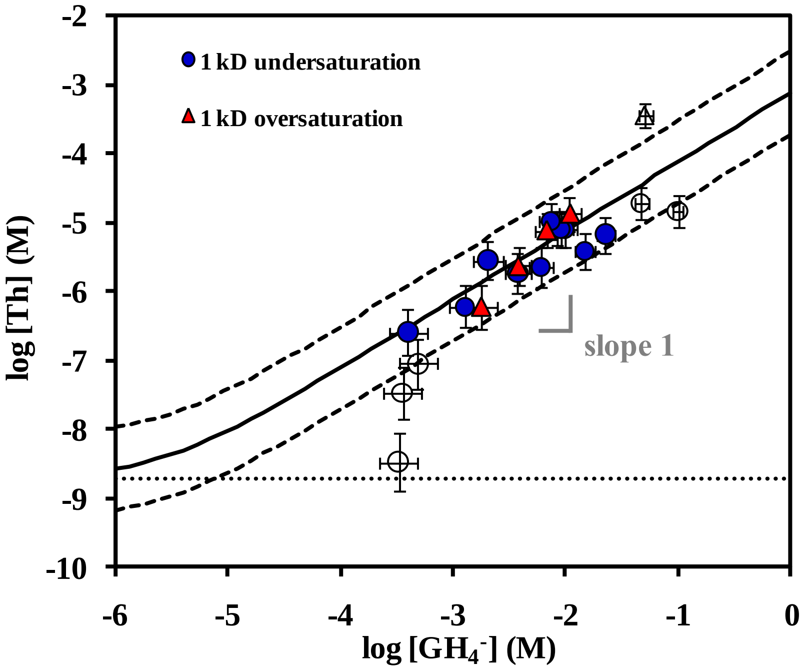

Figure 5-1. Solubility of thorium hydroxide in I=0.5M $NaClO_4$ media at pH_c=12 as a function of measured gluconate concentration, after 1 kD filtration. Triangles: oversaturation direction (15 or 149 days). Circles: undersaturation direction (>39 days). Only solid symbols were used in the calculations (see text). Solid black line is calculated thorium hydroxide solubility taking into account 1:1 Th:gluconate formation (with uncertainty, dashed line). Dotted line is calculated solubility in the absence of organic ligands.

Several parameters (such as filtration techniques, sorption, supersaturation or undersaturation of the initial system and pH) may affect the solubility of the element and are important to be well controlled in the experiments (see section 3.2 and 3.3). Those parameters were investigated in present work before the stability constants for thorium-gluconate complexes were determined.

- *Influence of filtration techniques*

Three different filtration techniques (filtration with 300 kD and 1 kD filters, and ultracentrifugation) were used in present work to investigate the influence of polymeric or colloidal thorium species in the measured thorium concentrations. Results of those tests indicate that similar thorium concentrations are measured with both 1 kD filtration and ultracentrifugation (see Figure 5-2). On the contrary, Microsept 300 kD filters led to higher thorium concentrations.

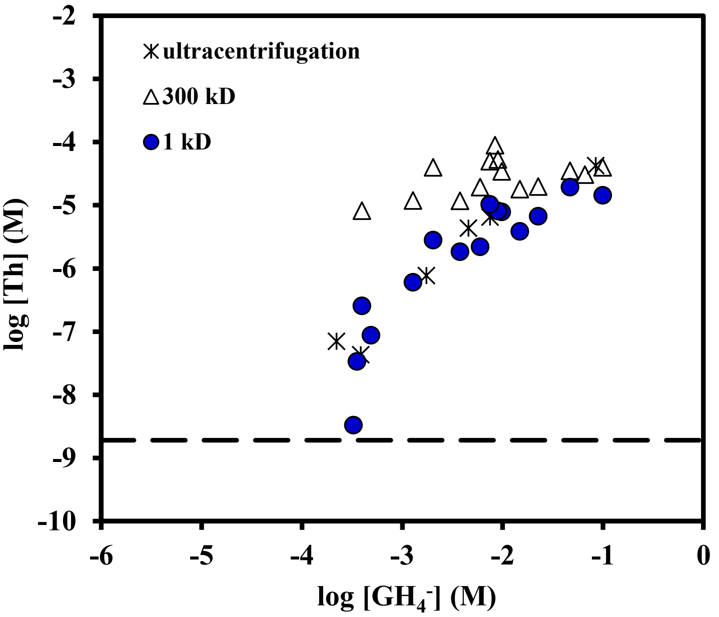

Figure 5-2. Solubility of thorium hydroxide in I=0.5M $NaClO_4$ media, pH_c=12, from undersaturation direction, as a function of measured gluconate concentrations in solution. Blue circles: after 1kD filtration. Open triangles: after 300 kD filtration. Stars: After ultracentrifugation at 149000g, without filtration. Dashed black line stands for thorium hydroxide solubility in the absence of organic ligands determined in present work. Error bars omitted for clarity in this graph.

One possibility to explain the observed differences may be the formation of gluconate-bridged colloids, especially in the alkaline pH range above pH 9. Gluconate contains carboxyl and hydroxyl groups that may act as bridges for Th. If some of these groups are not directly linked to one Th atom (for instance, as a consequence of steric hindrance) they have the possibility to be linked to a neighbouring one, specially at high thorium aqueous concentrations. These larger species may not pass through the 1kD filter.

Some examples of similar situations may be found in the literature:

-Altmaier et al. (Altmaier et al. 2005a) measured higher thorium solubilities after 220 nm filtration than after 1.2 nm filtration in a thorium-carbonate system. These differences were suggested to be caused by the formation of carbonate bridged thorium colloids (Altmaier et al. 2005a).

-Polynuclear species have been reported in metal-citrate systems (Hummel et al. 2005). Depending on the size and charge density of the metal ion, only two carboxylates and the hydroxyl group of citrate can bind to the same metal ion. The nonbonded functional group(s) can then be used as a bridge to a second metal ion.

If formed, gluconate-bridged colloids would only be relevant at high thorium aqueous concentrations (above thorium concentration limits expected for colloid formation).

- *Sorption of the organic ligand on the solid surface*

Thorium hydroxide solubility increases about one order of magnitude when increasing one order of magnitude the gluconate concentration (see Figure 5-1).

-At low gluconate concentrations, measured thorium concentrations in solution were observed to deviate from the general trend (see Figure 5-1 and Paper I), and a decrease of measured gluconate concentrations in solution was observed in comparison with the initial gluconate concentrations in the system (see Figure 5-3 and Paper I).

-At higher gluconate concentrations this deviation was not observed (see Figure 5-3). If occurring, it was not possible to quantify it.

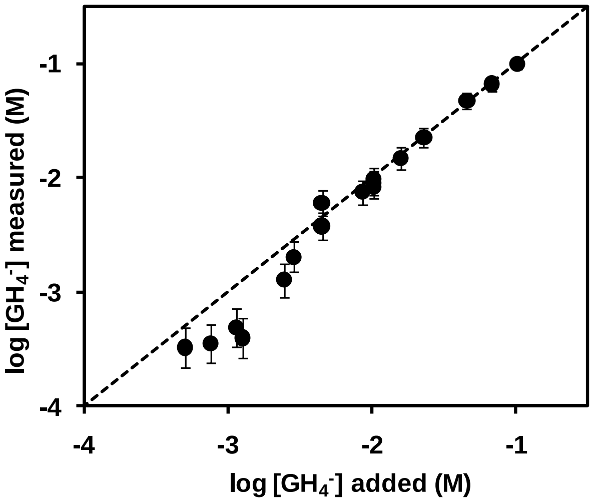

Figure 5-3. Added versus measured gluconate concentrations in the system.

The deviation was attributed to the sorption of gluconate onto the surface of the thorium hydroxide solid. In order to test this hypothesis, additional experiments with the same initial gluconate concentration ($1\cdot10^{-2}$ M) and the same total volume of solution (20 ml) but different amounts of thorium hydroxide solid (from 0.01 to 0.1 grams) were done. Figure 5-4 shows that measured gluconate concentrations decrease as the amount of solid in the samples increases; this behaviour is also consistent with sorption of the organic ligand onto the solid surface.

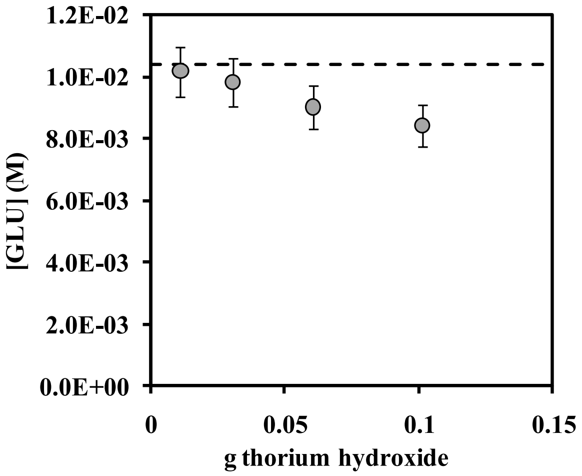

Figure 5-4. Measured gluconate concentrations in solution (grey circles) *vs.* grams of solid thorium hydroxide. Dashed line indicates initial gluconate concentration in solution. Detection limit of measured gluconate is $1 \cdot 10^{-4}$M. I=0.5M $NaClO_4$, pH_c=12.

Sorption of an organic ligand (EDTA) on thorium hydroxide was also described by Xia et al. (Xia et al. 2003).

As a consequence, the possibility of sorption of organic ligands on the thorium hydroxide solid may be considered. It was then necessary to choose a total gluconate concentration and a solid/liquid ratio in the experiments that could minimize the effect of sorption on the quantification and measurements performed.

- *Comparison of undersaturation and oversaturation results*

In order know if there was an effect of gluconate sorption onto the solid surface, additional solubility experiments from oversaturation direction were performed. The comparison between the results from both oversaturation and undersaturation direction indicated that measured thorium concentrations were not in agreement at high gluconate concentrations ($>10^{-2}$ M), as seen in Figure 5-1 and Paper I.

Thorium aqueous concentrations measured in oversaturation experiments show the same results after 15 or 141 days, as demonstrated in Paper I and Figure 5-5. Thus, equilibrium was reached in both experiments so that we can conclude that the observed disagreement is not related to kinetic factors.

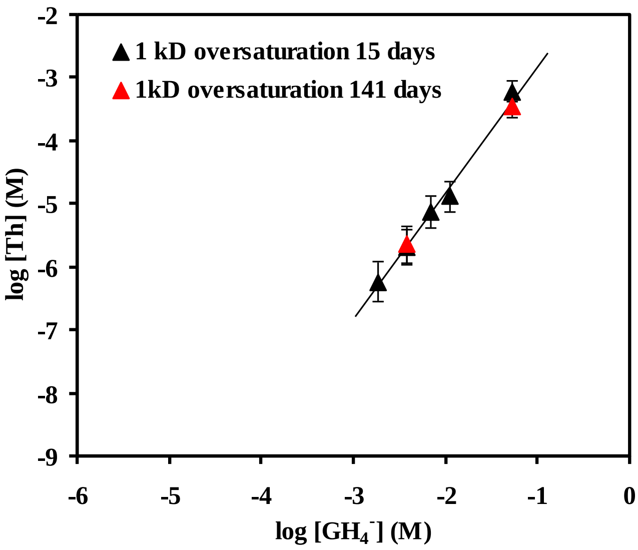

Figure 5-5. Comparison between results from oversaturation experiments in the thorium-gluconate system, after 1kD filtration. Black triangles: after 15 days. Red triangles: after 141 days.

It can be concluded that if the organic ligand concentration is low ($[GH_4^-]<3\cdot10^{-4}$M), adsorption of gluconate dominates and little thermodynamic information can be gained about aqueous speciation. If the gluconate concentration is high ($[GH_4^-]>1\cdot10^{-1}$ M), disagreements between the experiments form oversaturation and undersaturation are observed. Those phenomena constrain the range of gluconate concentrations that can be explored by the solubility method (from undersaturation direction) in the thorium-gluconate system.

- *Influence of pH*

Thorium hydroxide solubility measurements at pH range between 10 and 12.5 were performed (see Figure 5-6 and Paper I). Similar concentrations of thorium were measured for all pH values, suggesting that a similar thorium gluconate complex could be formed in all the studied pH range.

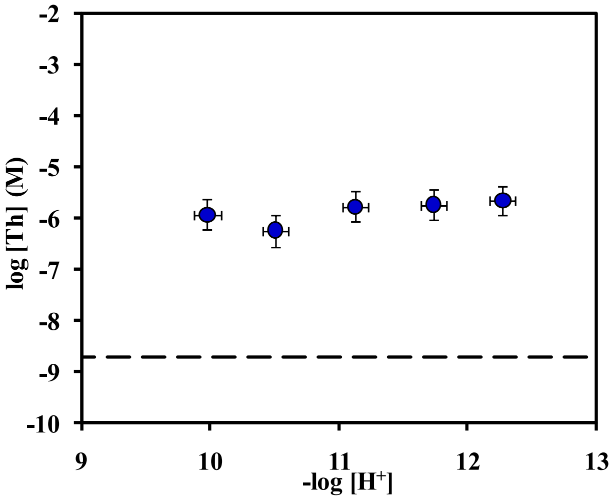

Figure 5-6. Solubility of thorium hydroxide as a function of pH$_c$ and initial gluconate concentration 4.5·10^{-3} M after 1 kD filtration (I = 0.5 M, $NaClO_4$). Dashed line is thorium hydroxide solubility in the absence of gluconate.

5.4 Determination of thorium-gluconate stability constants (Paper I)

From the experimental results presented in section 5.3 and Paper I, the following conclusions can be obtained:

- Thorium colloids are removed from solution by using 1kD polyethersulphone membrane filters.
- Similar concentrations of thorium were measured for all pH values in the pH range between 10 and 12.5.
- The range of gluconate concentrations that can be explored by the solubility method (from undersaturation direction) in the thorium-gluconate system is limited.

Taking into account those observations, values in agreement from both undersaturation and oversaturation directions after 1kD filtration at pH_c=12 were evaluated to provide thermodynamic stability constants for the formation of Th-GLU complexes. The measured values were evaluated by using FITEQL (Herbelin & Westall 1999) for parameter adjustment, using the thermodynamic database described in section 13.

The formation of a 1:1 Th:gluconate complex (r. 5-1 and solid line in Figure 5-1), provided an explanation for the measured thorium concentrations in solution (see Paper I).

$$Th(OH)_4 + GH_4^- = Th(OH)_n(GH_x)^- \quad \log K(I=0.5) = 5.6\pm0.6 \quad \text{r. 5-1}$$

A difficult aspect of establishing a reaction stoichiometry is to know the proton composition of the complex. Experimental measurements at pH_c between 10 and 12.5 indicate that the formation of the thorium-gluconate complex does not depend on pH under this particular range. However, the experimental information gathered does not allow differentiating if this is caused by the gluconate coordination through diol functions or by the presence of hydroxyls (OH^-) in the metal coordination sphere. As a consequence, the values of “n” and “x” in r. 5-1 cannot be determined independently only with those data. Further discussion on this issue is provided in section 5.5.1

The stability constant obtained at I = 0.5M was recalculated to I = 0 using the SIT model (section 13.4).

$$Th(OH)_4 + GH_4^- = Th(OH)_n(GH_x)^- \quad \log K^o= 5.6\pm0.6 \quad \text{r. 5-2}$$

The stability constant of the 1:1 Th:gluconate complex was determined using the experimental data where both oversaturation and oversaturation results were in agreement. However, the formation of a 1:2 Th:gluconate complex cannot be discarded if the results from the oversaturation experiments at high ligand concentrations are taken into account. Thus, an approximate stability constant for the formation of a 1:2 Th:gluconate complex was calculated using FITEQL. The result is shown in r. 5-3 and r. 5-4.

$$Th(OH)_4 + 2GH_4^- = Th(OH)_n(GH_x)_2^{2-} \qquad \log K(I=0.5) \approx 7.8 \qquad \text{r. 5-3}$$
$$Th(OH)_4 + 2GH_4^- = Th(OH)_n(GH_x)_2^{2-} \qquad \log K^o \approx 7.5 \qquad \text{r. 5-4}$$

Figure 5-7 shows the modelling of the results obtained if both the 1:1 and the 1:2 complexes are taken into account.

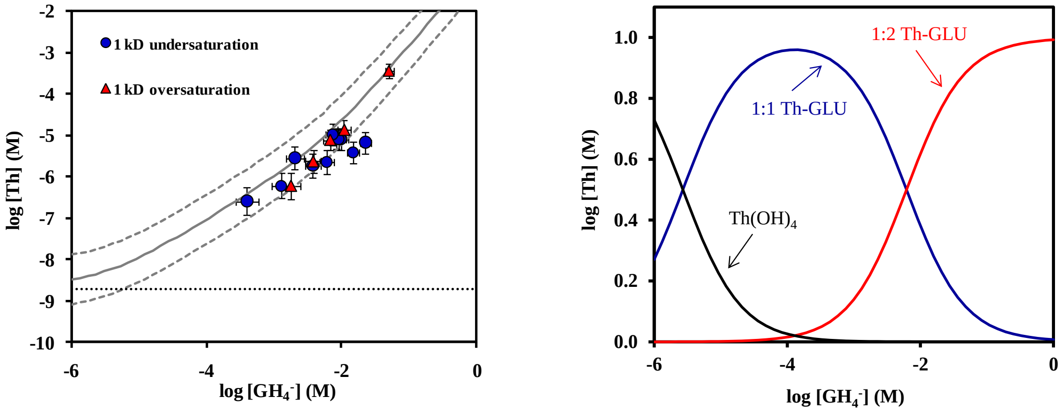

A B

Figure 5-7. A) Solubility of thorium hydroxide in I=0.5M $NaClO_4$ media at pH_c=12 as a function of measured gluconate concentration, after 1 kD filtration. Triangles: oversaturation direction. Circles: undersaturation direction. Solid grey line is calculated thorium hydroxide solubility taking into account 1:1 and 1:2 Th:gluconate formation (with uncertainty, dashed lines). Dotted line is calculated solubility in the absence of organic ligands. B) Th-gluconate speciation in agreement with the results obtained in present work.

5.4.1 Discussion on the obtained results

The acidity of a given element shows a dependency with the charge/radius ratios (z/r, z^2/r or z/r^2) of the element. Brown et al. (Brown et al. 1985) further developed this relationship in order to obtain the function shown in eq. 5-1:

$$g_1(z/r^2+g_2) \qquad \text{eq. 5-1}$$

where z is the charge of the ion, r is the ionic radii and g_1 and g_2 are functions of the charge (z) and the electronic structure of the metal ion[4].

This equation ($g_1(z/r^2+g_2)$) can be used to compare the stability constant for the 1:1 Th:gluconate complex obtained in present work with data for other metal-gluconate complexes, taking into account its corresponding acidity. The results of the comparison are shown in Figure 5-8. The thorium-gluconate stability constant obtained in present work is shown in red in the figure. Blue symbols represent the stability constants for metal-gluconate complexes reported by Sawyer (Sawyer 1964), who undertook the first extensive review on the metal complexes formed by gluconic acid.

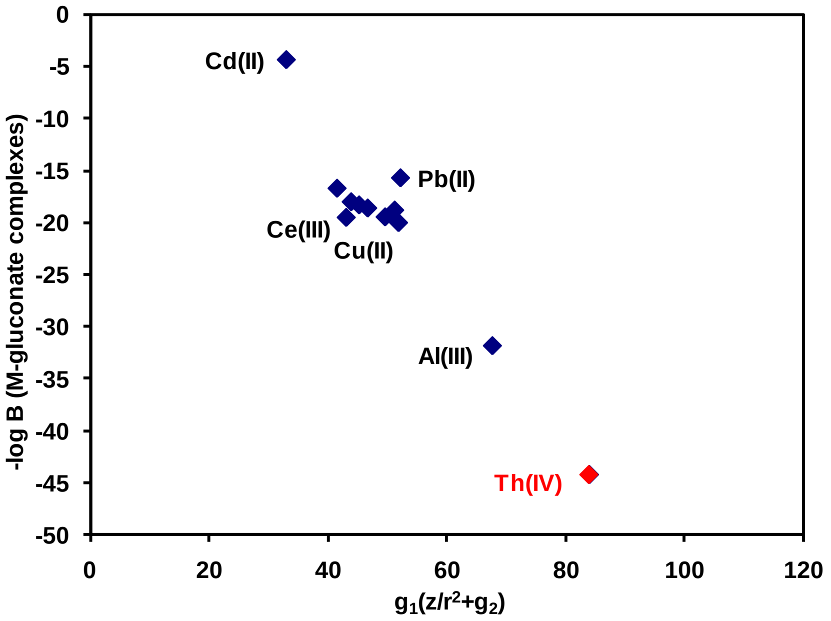

Figure 5-8. Stability constants of metal complexes with gluconate, versus $g_1(z/r^2+g_2)$ (Brown et al. 1985). Blue symbols are stability constants reported by (Sawyer 1964). Red symbol stands for thorium-gluconate stability constant obtained in present work.

Figure 5-8 shows that the stability constants for metal-gluconate complexes (including the thorium-gluconate complex) follow a linear relationship with the z/r^2 function, which increases the confidence on the results obtained in present work.

---

[4] g_1 and g_2 values for the different metal complexes are reported by (Brown et al. 1985).

g_1 and g_2 functions are not available for other tetravalent actinides such as Np(IV) or Pu(IV). The correlation between the stability constants and the Gibbs free energy of An(IV) (linear free-energy relationship) can also be used to assess the reliability of stability constants along the An(IV) series (Choppin et al. 2006, Gaona et al. 2008, Meyer et al. 2007, Rojo et al. 2013). The results of the correlation are shown in Figure 5-9; the thorium-gluconate stability constant obtained in present work is shown in red. As seen in the figure, the result shows a good agreement with other data available in the literature for An(IV)-gluconate complexes.

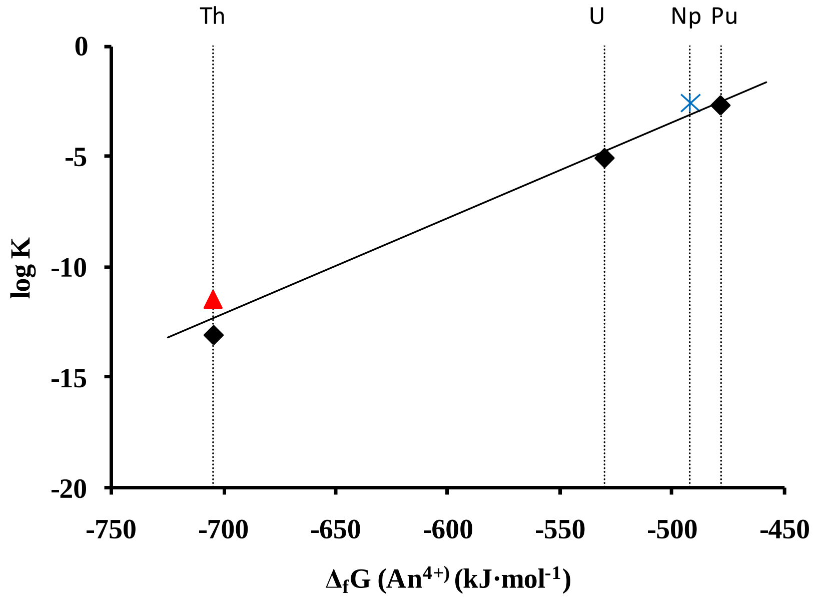

Figure 5-9. Relationship between the stability constants of An(IV)-gluconate complexes with $\Delta_f G(An^{4+})$, adapted from (Rojo et al. 2013). Red triangle stands for thorium-gluconate stability constant obtained in present work. Blue cross: from (Rojo et al. 2013). Black symbols: values recalculated from (Cross et al. 1989, Felmy 2004, Moreton 1993, Warwick et al. 2004).

5.5 Structure of the thorium-gluconate complex (Paper II)

The coordination sites of polyhydroxycarboxilic compounds (such as gluconate) may be the carboxylic groups, the hydroxyl groups or the ionized hydroxyl groups (ionized diol functions). In the later case, polyalcohols may lose one or more hydroxylic protons to give a metal-alcoholate complex under alkaline solutions in the presence of metals (Rendleman 1978).

EXAFS experiments were done in order to investigate the structure of the thorium-gluconate species formed at alkaline pH values, being the main objective to check if the coordination was taking place through a bidentate coordination to the carboxylic function or through ionized diol functions.

Two different samples were prepared: a Th-gluconate sample (total gluconate concentration of 0.46 M at pH=11.8), and a Th-carbonate sample (total carbonate concentration 0.1 M at pH=9.14). The preparation of both samples is described in Paper II. The Th-carbonate sample provides a clear example of a bidentate coordination of thorium to the carboxylic function, as shown in Figure 5-10, and was used for comparison purposes in order to evaluate if the bidentate coordination was occurring in the Th-gluconate sample.

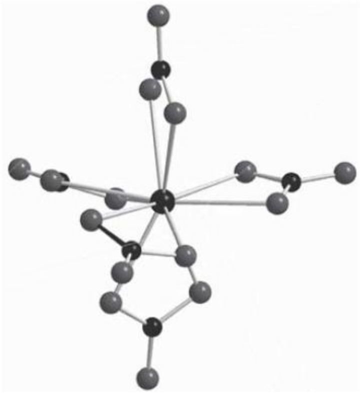

Figure 5-10. Structure of $Th(CO_3)_5^{6-}$ complex, from (Rand et al. 2009).

The Fourier transformation magnitude of the EXAFS spectra of Th-gluconate and Th-carbonate are shown in Figure 5-11. In both cases, EXAFS spectra are dominated by the oxygen atoms in the first thorium coordination shell. In addition, another significant feature is present at uncorrected distances of ≈3.5 and ≈3.7 Å respectively.

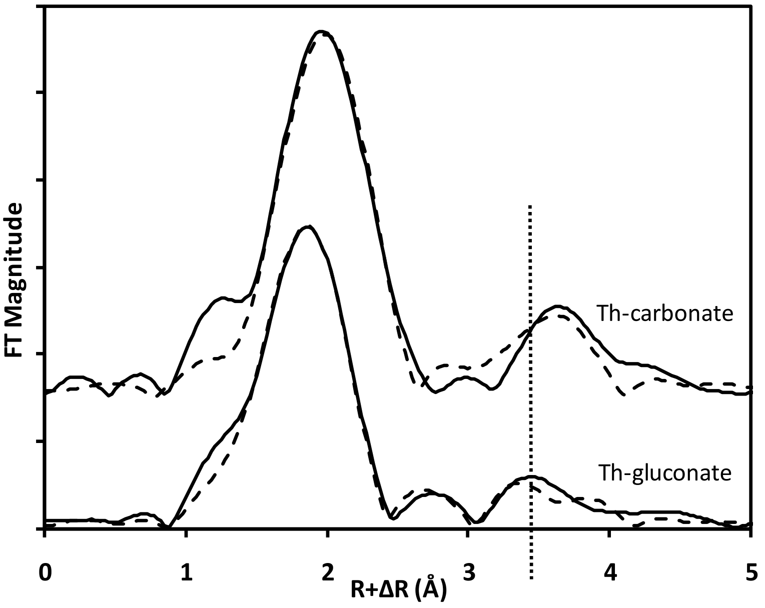

Figure 5-11. Experimental data of EXAFS fourier transforms of Th L_{III} edge for Th-gluconate and Th-carbonate solutions. The solid lines are the experimental data, and dashed lines correspond to preliminary theoretical fits.

In the case of the thorium carbonate sample, the feature at uncorrected distance of ≈3.7 Å corresponds to the Th-O_{dist} single scattering path and the corresponding Th-C-O_{dist} and Th-C-O_{dist}-C multiple scattering paths. Those multiple scattering paths are especially important when the scattering angle at the middle atom is near 180ºC. This is the case in thorium-carbonate coordination (see Figure 5-10), as carbonate adopts a symmetric bydentate geometry where the distal oxygen atom is collinear with the carbon atom (Allen et al. 1996, Altmaier et al. 2006).

If thorium was coordinated to the gluconate sample through the carboxylic function, the Th-C_{dist} path and the corresponding Th-C-C_{dist} and Th-C-C_{dist}-C multiple scattering paths would be expected to appear at a *longer* distances (in comparison with the feature in the thorium-carbonate spectra, see Figure 5-12). On the contrary, the feature on the thorium-gluconate spectra appears at a *shorter* distance (≈3.5 Å, see Figure 5-11).

This qualitative comparison may indicate that the feature at ≈3.5 Å in the thorium-gluconate spectra may not correspond to a Th-C_{dist} path. In this case, thorium coordination to gluconate carboxylic function in a bidentate way would not be occurring.

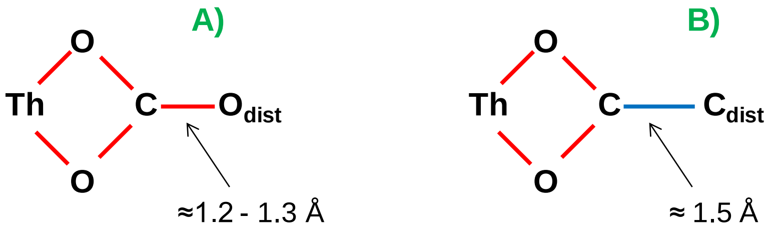

Figure 5-12. Comparison between thorium coordination to carbonate (A) and theoretical thorium coordination to gluconate through the carboxylic function (B). As seen in the figure, Th-O_{dist} distance would be expected to be shorter than the Th-C_{dist} distance.

In case that dimeric or higher polynuclear complexes are formed, the presence of a Th-Th backscatter could lead to the appearance of peaks at uncorrected distances near 4 Å (Xia et al. 2003). Nevertheless, the attempts to fit the spectra using a Th-Th backscatter resulted in unrealistic Th-Th distances of ≈3.7 Å in the studied samples. Those distances are too short for a real Th-Th interaction, which is usually ca. 3.99 Å (Rothe et al. 2002, Toraishi et al. 2002). An additional check was conducted by using a similar procedure to the one described by Allen and co-workers (Allen et al. 1996). The peak contribution was isolated by subtracting the fit of the first Th-O shell. The residual signal was then Fourier-filtered in the range 3-5 Å to remove noise. According to Allen et al., if the 3.7 Å peak were due to an interaction of Th with a high atomic number atom (such as another Th atom), an increase of the amplitude with k would be expected in this residual spectra, what is not observed in the results (Figure 5-13). According to those results, the presence of dimeric complexes in significant concentrations in the sample would not be observed.

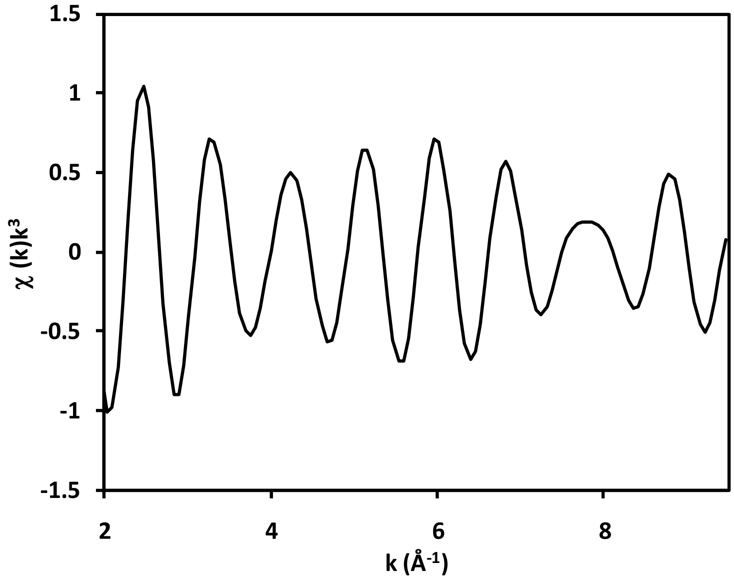

Figure 5-13. Fourier-filtered peak at an uncorrected distance of ca. 3.5 Å

5.5.1 Discussion on the obtained results

A general coordination-ionization scheme describing the changes in the structure of the metal-polyhydroxycarboxilates as a function of pH was described by Van Duin et al. (Van Duin et al. 1989) and is summarized in Figure 5-14.

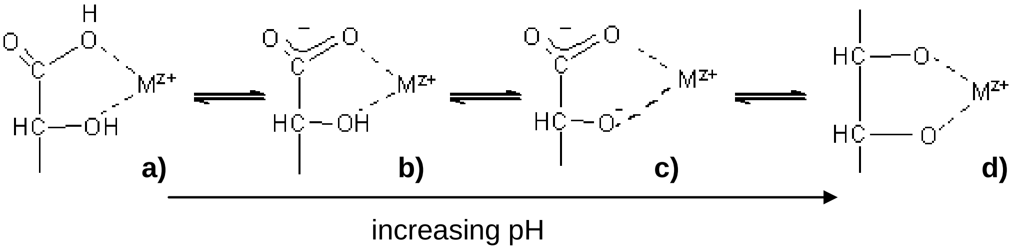

Figure 5-14. Coordination-ionization scheme of metal-polyhydroxycarboxylic complexes as a function of increasing pH, from (Van Duin et al. 1989).

The effect of pH in the coordination is correlated with the acidity of the hydrated metal cation (Van Duin et al. 1989). There is a relation between the acidity of the metal ion and the pH regions where the species shown in Figure 5-14 have their maximum concentrations. For example, alkali metal ions, which have a low acidity (low z/r^2

values), are suggested to coordinate with the structure “a” at low pH values (<4) and with structure “b” at pH values higher than 4. On the contrary, Al(III), which is more acidic (higher z/r^2 values), is suggested to coordinate mainly with the structure “c” at pH values between 3 and 10. As Th(IV) is a very acidic cation (high z/r^2 values), it would be expected to coordinate to polyhydroxycarboxylic acids as gluconate by an ionized-diol function at high pH values (structure “d” in Figure 5-14). The formation of $Th(OH)_n(GH_x)^-$ complex (r. 5-5) suggested in present work is in agreement with those arguments.

$$Th(OH)_4 + GH_4^- = Th(OH)_n(GH_x)^- \quad \text{r. 5-5}$$

The values of “n” and “x” in $Th(OH)_n(GH_x)^-$ will depend on the structure of the complex. Taking into account the results obtained in present work, the formation of a $Th(OH)_2(GH_2)^-$ species (“n”=2 and “x”=2) may be suggested:

-experimental values at pH_c between 10 and 12.5 indicate that the formation of the thorium-gluconate complex does not depend on pH under the studied conditions.

-EXAFS indicated that thorium coordination to gluconate could take place through a diol function, in agreement with the hypothesis in Van Duin et al. (Van Duin et al. 1989).

-the presence of a Th-Th backscatter was not observed.

It is however acknowledged that the exact values for “n” and “x” could only be confirmed if additional data were available.

5.6 Summary and conclusions

- Thorium hydroxide solubility at $pH_c=12$ increases approximately one order of magnitude with one order of magnitude increase in the gluconate concentration.
- Results of filtration test show that 1 kD filtration with Pall Microsept polyethersulfone filters and ultracentrifugation are useful for studying the thorium-gluconate system. Microsept 300 kD filters led to higher thorium concentrations, suggesting a formation of gluconate-bridged thorium colloids.

- The range of gluconate concentrations that can be explored by the solubility method (from undersaturation direction) in the thorium-gluconate system is limited.
- The formation of a 1 : 1 Th : gluconate (r. 5-1) and and a 1:2 Th:gluconate complex (r. 5-3) provided an explanation for the results obtained in the solubility experiments.

$Th(OH)_4 + GH_4^- = Th(OH)_n(GH_x)^-$ log K(I=0.5) = 5.6±0.6 r. 5-1

$Th(OH)_4 + 2GH_4^- = Th(OH)_n(GH_x)_2^{2-}$ log K(I=0.5) ≈ 7.8 r. 5-3

- Experiments performed at pH_c values between 10 and 12.5 indicate that a similar thorium gluconate complex could be formed in all this pH range.
- The information obtained through EXAFS experiments seem to indicate that thorium is not binding to the carboxylic function of gluconate in a bidentate way.
- According to the EXAFS results, dimeric or higher polynuclear complexes, with a direct Th-Th interaction, would not be present in solution after filtration.

6 Comparison between gluconate and isosaccharinate influence on thorium solubility (Paper II)

6.1 Introduction

The cellulose degradation process has been studied by several authors (Glaus & Van Loon 2008, Pavasars et al. 2003, Van Loon et al. 1999). Isosaccharinate is the main product of the degradation of cellulosic materials (pure cellulose, cotton, tissues, paper…) in an alkaline pH environment.

Due to the large amount of cellulose present among radioactive wastes, isosaccharinate is of major concern in many performance assessments of radioactive waste repositories. However, the amount of thermodynamic data available for the complexation of isosaccharinate with metals in the alkaline pH range are limited (Hummel et al. 2005).

Allard et al. (Allard & Ekberg 2006a, Allard & Ekberg 2006b) studied the thorium isosaccharinate system at pH=8 using liquid-liquid extraction experiments. The authors suggested the formation of 1:1, 1:2 and 1:3 Th:ISA complexes. However, they did not take into account the possible formation of diol coordinated complexes (see Figure 1-4) or the presence of hydroxyls (OH^-) in the metal coordination sphere. As a consequence, their conclusions cannot be extrapolated to higher pH values (Rai et al. 2009).

In the alkaline pH range and in the absence of calcium, only two studies are available. Vercammen et al. (Vercammen 2000, Vercammen et al. 1999, Vercammen et al. 2001) studied the complexation of Th(IV) by ISA in the pH range from 10.7 to 13.3 by batch sorption experiments using materials such as feldspar ($KAlSi_3O_8$), polyallomer centrifugue tubes or cation-exchange resin as sorbents. Based on best-fit analysis of the sorption data, the authors postulated that 1:1 Th:ISA complexes were formed. Rai and co-workers (Rai et al. 2009) studied the influence of ISA on $Th(OH)_4(am)$ solubility, suggesting the formation of $Th(OH)_4(ISA)_2^{2-}$ complexes in the alkaline pH range. The results from the solubility experiments by Rai and co-workers are not in agreement with the sorption studies by Vercammen et al.

On the other hand, isosaccharinate and gluconate structures are very similar, as shown in Figure 6-1. As a consequence gluconate has been used as an analogue for isosaccharinate in some experimental works (Birjkumar et al. 2012b).

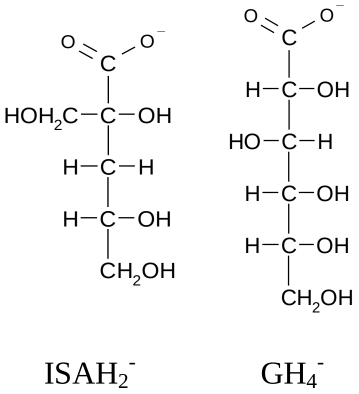

Figure 6-1. Comparison between isosaccharinate (ISAH$_2^-$, left) and gluconate (GH$_4^-$, right) chemical structure.

6.2 Objectives

The objective of this part of the work was to obtain thermodynamic data (stability constants) for the thorium-isosaccharinate system in the alkaline pH range and to investigate the gluconate-isosaccharinate analogy. The procedure followed was:

1-Study the thorium hydroxide solubility in the presence of isosaccharinate and determination of the stability constants for aqueous thorium-isosaccharinate complexes (section 6.3 and Paper II).

2-Study of the structure of the Th-isosaccharinate complexes by EXAFS (section 6.4).

3-Comparison between the results obtained in the Th-gluconate and the Th-isosaccharinate systems (section 6.5).

4-An extensive comparison between the results obtained in present work and previous literature values was also done (section 6.6).

5-Conclusions are provided in section 6.7.

6.3 Thorium hydroxide solubility in the presence of isosaccharinate (Paper II)

Thorium hydroxide solubility studies in the alkaline pH range were carried out using the experimental set-up described in section 3.3, from both undersaturation and oversaturation direction. Results are provided below.

6.3.1 Determination of the thorium-isosaccharinate stability constants (Paper II)

Results of thorium hydroxide solubility studies are provided in Figure 6-2. As in the case of the thorium-gluconate system, thorium hydroxide solubility at $pH_c=12$ increases significantly in the presence of isosaccharinate (symbols in Figure 6-2) in comparison with the solubility under the same conditions in the absence of organic ligands (dotted black line in the figure).

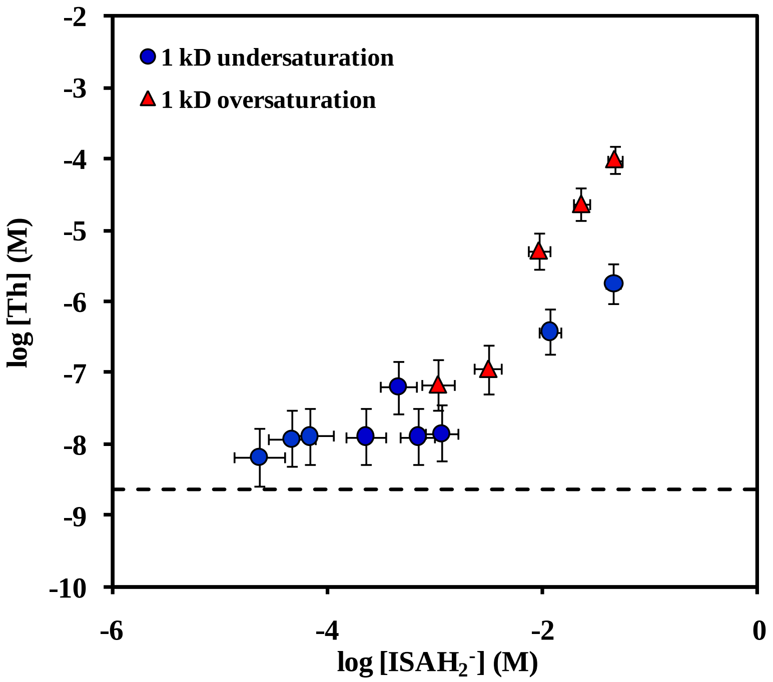

Figure 6-2. Solubility of thorium hydroxide in I=0.5M $NaClO_4$ media, pH_c=12, as a function of measured isosaccharinate concentrations in solution, after 1 kD filtration. Blue circles: from undersaturation direction. Red triangles: from oversaturation direction.

At $[ISA]_T>10^{-2}$ M, undersaturation and oversaturation results are not in agreement. Similar results were obtained in the thorium-gluconate system (see section 5.3). The range of isosaccharinate concentrations that can be explored from undersaturation direction in the thorium-isosaccharinate system is then limited.

Taking into account the discussion presented in section 5.3 (thorium-gluconate system), modelling of the results obtained has not taken into account the results obtained from undersaturation direction at higher and lower ligand concentrations (open symbols in Figure 6-3).

Results on thorium isosaccharinate system can be explained with the formation of a 1:1 and 1:2 thorium-isosaccharinate species (r. 6-1 and r. 6-2 respectively). Figure 6-3 shows the results of the modelling of when both species are taken into account.

$Th(OH)_4 + ISAH_2^- = Th(OH)_n(ISAH_x)^-$ log K(I=0.5) ≈ 4.2 r. 6-1
$Th(OH)_4 + 2ISAH_2^- = Th(OH)_n(ISAH_x)_2^{2-}$ log K(I=0.5) = 7.3 ± 1.0 r. 6-2

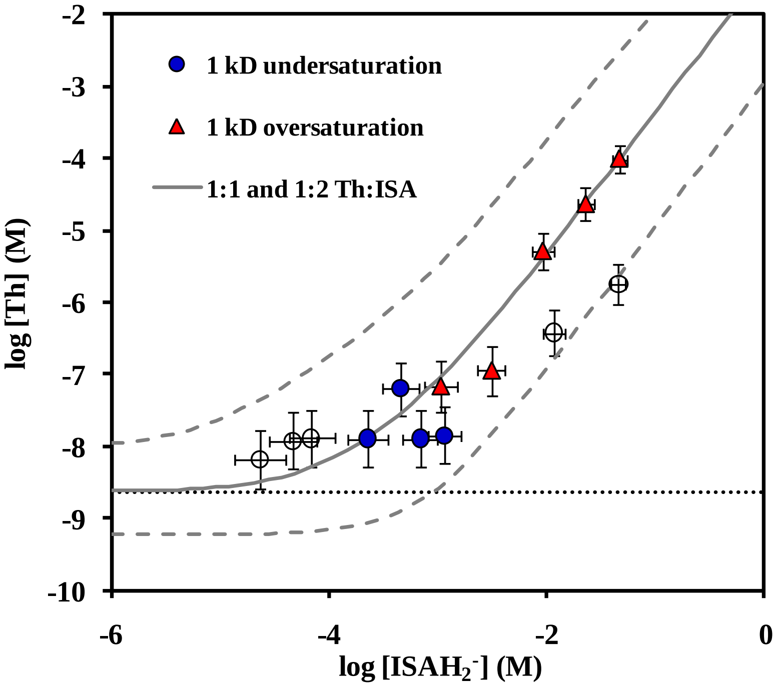

Figure 6-3. Solubility of thorium hydroxide in I=0.5M $NaClO_4$ media as a function of measured isosaccharinate concentrations in solution, after 1 kD filtration. Circles: from undersaturation direction. Triangles: from oversaturation direction. Only solid symbols were used in the calculations (see text). Grey solid line: calculated solubility taking into account the formation of both 1:1 and 1:2 Th:ISA complexes (with uncertainty, dashed lines). Dotted black lines indicate thorium hydroxide solubility in the absence of organic ligands.

The corresponding thorium aqueous speciation is shown in Figure 6-4. As shown in the figure, in the zone where the 1:1 complex is formed ($[ISA]_T \approx 2 \cdot 10^{-4}$ M), measured thorium concentrations show a significant scatter. Thus, the constant suggested for the 1:1 Th-isosaccharinate complex is only approximate (r. 6-1).

The uncertainty for the 1:2 Th-isosaccharinate complex (r. 6-2) has been calculated in order to cover all the experimental data obtained, including the results from both undersaturation and oversaturation directions. Because of that, a high uncertainty (±1) has been determined.

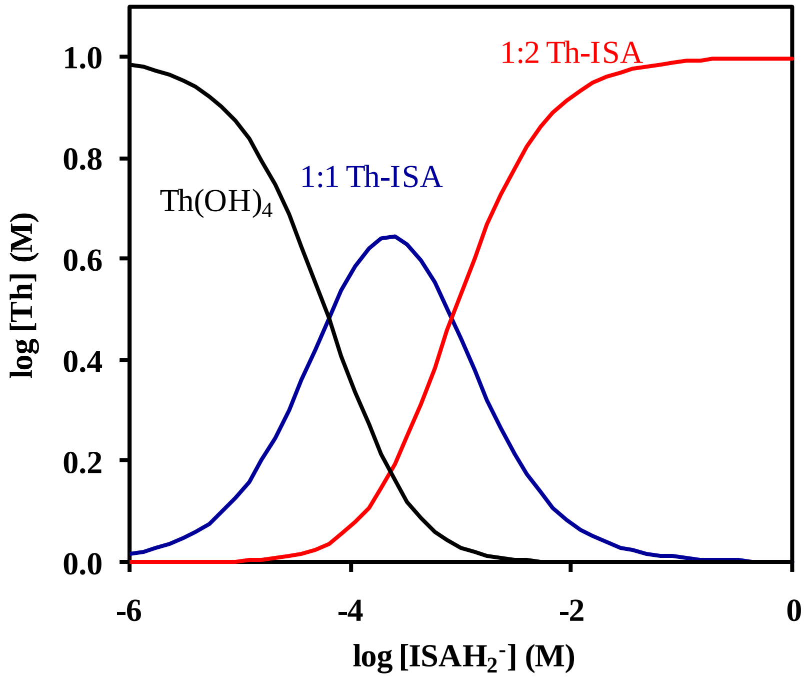

Figure 6-4. Calculated thorium aqueous speciation in Figure 6-3 (thorium hydroxide solubility in the presence of isosaccharinate), in agreement with the stability constants determined in present work.

The values obtained were corrected to I=0 using SIT (r. 6-3 and r. 6-4), as described in appendix B (section 13.4).

$Th(OH)_4 + ISAH_2^- = Th(OH)_n(ISAH_x)^-$ log K° ≈ 4.2 r. 6-3
$Th(OH)_4 + 2ISAH_2^- = Th(OH)_n(ISAH_x)_2^{2-}$ log K° = 7.0 ± 1.0 r. 6-4

6.4 Structure of the thorium-isosaccharinate complex

The information obtained with EXAFS experiments indicated that thorium was not binding to the carboxylic function of gluconate in a bidentate way (section 5.5). Given the similarities between gluconate and isosaccharinate, a similar conclusion would be expected in the case of thorium-isosaccharinate complexes. EXAFS experiments were done in order to confirm this hypothesis.

6.4.1 EXAFS experiments

For EXAFS experiments, an aqueous Th-isosaccharinate sample was prepared from a solution of isosaccharinate concentration of 0.1 M at pH_c=12.2 by adding a total thorium concentration of $[Th]_0=1\cdot10^{-3}$. The thorium-isosaccharinate sample was compared with a Th-carbonate solution (with a total thorium concentration of $[Th]_0=1\cdot10^{-3}$ and a carbonate concentration of 0.1 M at pH_c=9.1) and a thorium gluconate solution (a total thorium concentration of $[Th]_0=1\cdot10^{-3}$ and a gluconate concentration of 0.1 M at pH_c=11.7).

The Fourier transformation magnitudes of the EXAFS spectra are shown in Figure 6-5. Thorium-isosaccharinate and thorium-gluconate samples are similar; a similar structure may be expected for both complexes. Furthermore, as in the case of EXAFS experiments with gluconate, the comparison between the thorium-isosaccharinate and thorium-carbonate indicates that thorium is not coordinating to isosaccharinate carboxylic function in a bidentate way (see the complete discussion in section 5.5).

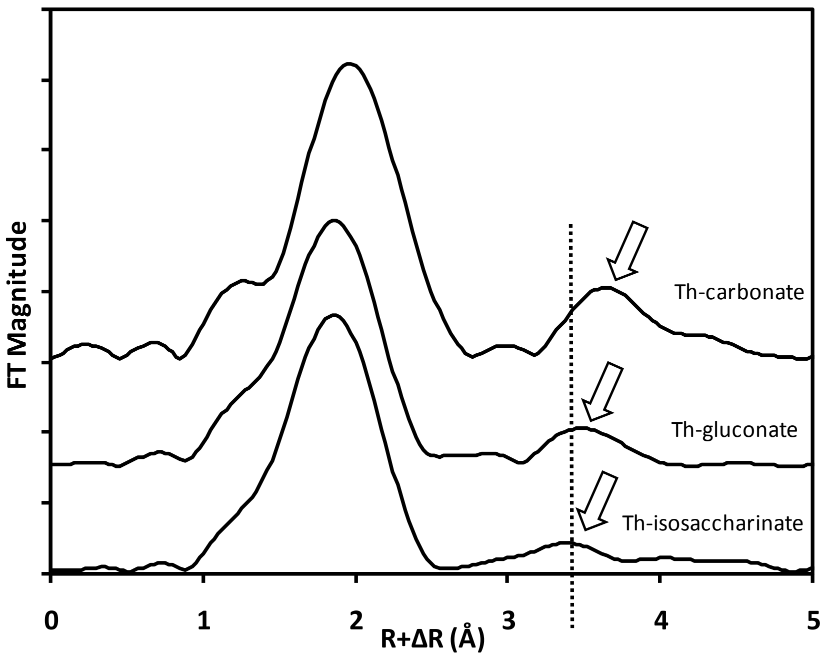

Figure 6-5. Experimental data of EXAFS fourier transforms of Th L_{III}-edge for Th-isosaccharinate, Th-gluconate and Th-carbonate solutions. The exact composition of each sample are described in the text.

6.5 Comparison between gluconate and isosaccharinate

The comparison of the measured thorium concentrations in solubility experiments for both Th-gluconate and Th-isosaccharinate solutions is provided in Figure 6-6.

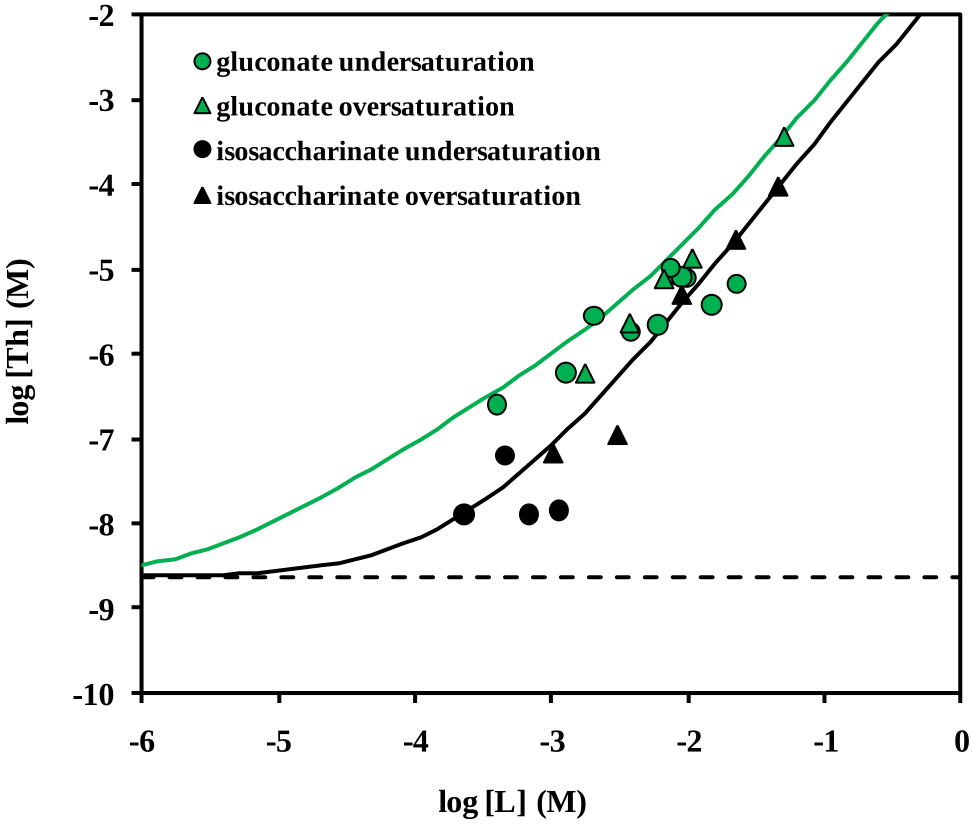

Figure 6-6. Solubility of thorium oxyhydroxide from undersaturation (circles) and oversaturation (triangles) direction as a function of the concentration of organic ligand, at fixed pH_c=12 (I=0.5M, $NaClO_4$). Black symbols: in the presence of isosaccharinate. Green symbols: In the presence of gluconate. Black solid line: calculated solubility taking into account the formation of a 1:1 and 1:2 Th-ISA complex. Green line: calculated solubility taking into account the formation of a 1:1 and 1:2 Th-gluconate complex. Dashed line: calculated solubility in the absence of organic ligands.

The solubility of thorium in the presence of isosaccharinate is slightly smaller than the one in the presence of gluconate. This agrees with the slightly smaller stability constants determined for the thorium-isosaccharinate complexes than for the gluconate-thorium complexes.

A weaker sorption of isosaccharinate on cement, compared to that of gluconate, was reported by Glaus et al. (Glaus et al. 2006). This behaviour suggests that the differences between the structure of gluconate and isosaccharinate, although small, do play a role in the behaviour of those organic ligands. A similar conclusion was recently reported by Birjkumar and co-workers (Birjkumar et al. 2012b) for uranyl-gluconate and isosaccharinate complexes. Density functional theory studies conducted by those authors revealed similarities in structure, bonding and coordination geometry; but also differences in ΔG values for ligand replacement reactions, suggesting that some differences exist between thermodynamic properties of gluconate and isosaccharinate uranyl complexes.

Summarizing, gluconate and isosaccharinate show a similar behaviour towards thorium complexation. However, a slightly smaller stability for the thorium-isosaccharinate than for the gluconate-thorium complexes may be expected. Thus, using gluconate as a direct analogue for isosaccharinate could be considered a conservative approach (the effect of isosaccharinate on thorium mobility would be overestimated).

6.6 Comparison with literature values

The thermodynamics of ISA complexation with thorium had already been described in the literature. Different techniques such as solubility experiments (Rai et al. 2009), sorption experiments (Vercammen 2000, Vercammen et al. 1999, Vercammen et al. 2001) and liquid-liquid extraction experiments (Allard & Ekberg 2006a, Allard & Ekberg 2006b) were used. The values obtained in those publications show several disagreements, justifying the necessity of the studies presented in this work.

The results of the literature studies, as well as the ones obtained in present work, are summarized in Table 6-1.

Table 6-1. Summary of stability constants for the formation of Th-ISA complexes (in the near-neutral to alkaline pH range).

Reaction	log K	Source
$Th^{4+} + ISAH_2^- = Th(OH)_n(ISAH_x)^- + 4H^+$	$\approx -15.3^a$	(This work)
$Th^{4+} + 2ISAH_2^- = Th(OH)_n(ISAH_x)_2^{2-} + 4H^+$	-12.2 ± 1.0^a	
$Th^{4+} + 2ISAH_2^- + 4H2O = Th(OH)_4(ISAH_2)_2^{2-} + 4H^+$	-12.5 ± 0.5^b	(Rai et al. 2009)
$Th^{4+} + ISA^- = Th(ISA)^-_{-4H+} + 4H^+$	-10.1 ± 0.2^c	(Vercammen 2000) (Vercammen et al. 1999) (Vercammen et al. 2001)
$Th^{4+} + ISA^- = Th(ISA)^{3+}$	12.56 ± 5.01^d	(Allard & Ekberg 2006a, Allard & Ekberg 2006b)
$Th^{4+} + 2ISA^- = Th(ISA)_2^{2+}$	19.38 ± 0.95^d	
$Th^{4+} + 3ISA^- = Th(ISA)_3^+$	21.30 ± 5.01^d	

a: data at I=0.5M $NaClO_4$

b: data at I=0

c: data at I=0.3M $NaClO_4$, dependent of the thorium hydrolysis reactions reported in the original work

d: data at I=1M $NaClO_4$

1) Solubility experiments

Rai et al. (Rai et al. 2009) performed thorium hydroxide solubility experiments from undersaturation direction at different pH values and different isosaccharinate concentrations. The authors suggested the formation of 1:2 Th:isosaccharinate complexes (see Table 6-1).

Figure 6-7 shows thorium concentrations measured by those authors at pH=12 (symbols) and the calculated data using the Th-isosaccharinate stability constants obtained in present work. A reasonable agreement between measured and calculated values is obtained; however, the calculated model slightly overestimates some of the measured values.

It must be noticed that Rai et al. did not measure isosaccharinate concentrations in solution; as a consequence, the “x” axis in Figure 6-7 represents total isosaccharinate concentrations and not the measured ones. It could then be suspected that, if measured isosaccharinate concentrations were available in Rai and co-workers experiments, the agreement would be better.

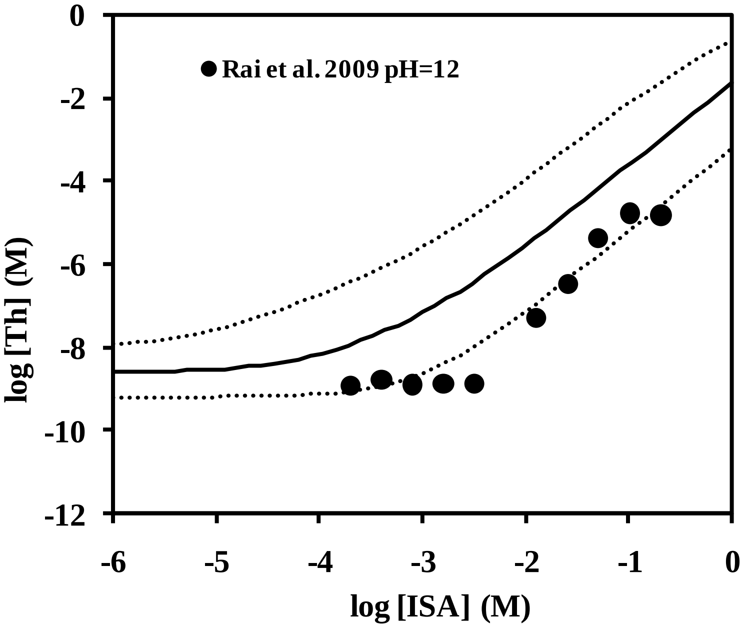

Figure 6-7. Symbols: Solubility of thorium hydroxide as a function of total isosaccharinate concentrations in solution at pH=12, from (Rai et al. 2009). Black solid line: calculated solubility taking into account the formation of both 1:1 and 1:2 Th:ISA complexes calculated in present work (with uncertainty, dotted lines).

2) Sorption experiments

Vercammen et al. (Vercammen 2000, Vercammen et al. 1999, Vercammen et al. 2001) studied the complexation of thorium with isosaccharinate in the pH range from 10.7 to 13.3 by batch sorption experiments. The authors used different sorption materials depending on pH: feldspar at pH=10.7, polyallomer tubes (ethylene-propilene copolymer) at pH=12 and ionic exchange resin at pH=13.3. Based on best-fit analysis of the sorption data, the authors postulated that 1:1 Th:ISA complexes were formed in the absence of Ca, with log K = −10.1 at I = 0.3M (see Table 6-1).

The authors did not take into account the same thorium hydrolysis constants as the ones used in present work. In order to allow a consistent comparison, the log K value was recalculated using the NEA thermodynamic database for thorium (section 12). Recalculated values are shown in r. 6-5.

$Th^{4+} + ISA^{-} = Th(ISA)^{-}_{-4H+} + 4H^{+}$	log K° = -11.8±0.2	r. 6-5	(Vercammen 2000), (Vercammen et al. 1999), (Vercammen et al. 2001) recalculated in present work

Symbols in Figure 6-8 represent measured K_d values for thorium sorption experiments on polyallomer tubes at pH=12 (Vercammen 2000). Calculated K_d values (solid line in Figure 6-8) were obtained using the stability constants obtained in present work. The calculated values overestimate thorium sorption, that is, the formation of thorium-isosaccharinate complexes is underestimated. A definitive explanation for this discrepancy was not found.

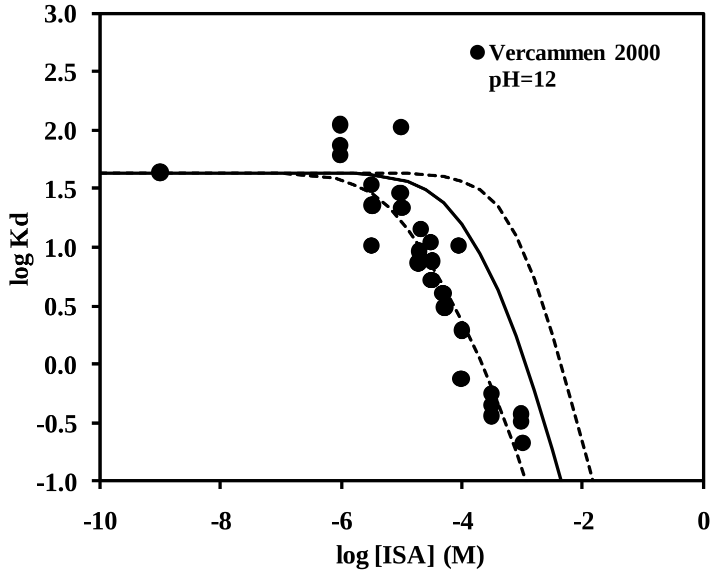

Figure 6-8. Symbols: Influence of ISA on the sorption of thorium on a polyallomer tube wall at pH=12, from (Vercammen 2000). Black solid line: calculated K_d values taking into account the formation of both 1:1 and 1:2 Th:ISA complexes obtained in present work (with uncertainty, dotted lines).

3) Liquid-liquid extraction experiments

Allard et al. (Allard & Ekberg 2006a, Allard & Ekberg 2006b) studied the formation of thorium-isosaccharinate complexes using liquid-liquid extractions with acetylacetone at $pH_c \approx 8$. According to their publications, their experimental results suggest the formation of a 1:2 Th:ISA complex, with minor contributions of additional 1:1 and 1:3 complexes.

Allard et al. did not take into account the role of isosaccharinate hydroxyl groups in their calculations (notice that the experiments were conducted only at a single pH values, which justifies this decision). As a consequence, the authors interpreted their results in terms of formation of complexes such as $Th(ISAH_2)_2^{2+}$, instead of $Th(OH)_4(ISAH_2)_2^{2-}$ or $Th(ISA)_2^{2-}$. However, it is possible to explain their experimental data using the stability constants obtained in solubility experiments in present work, as shown below.

Thorium concentration in liquid-liquid extraction experiments can be calculated using eq. 6-1:

$$D_{Th} = \frac{\lambda_4 \beta_{140} (Aa^-)^4}{1 + \beta_{140}(Aa^-)^4 + \frac{K_1 [ISA]^1}{[H^+]^4} + \frac{K_2 [ISA]^2}{[H^+]^4}} \qquad \text{eq. 6-1}$$

Where:

-D_{Th} is the distribution coefficient for thorium between the organic phase (acetylacetone, Aa) and the aqueous phase.

-λ_4 is the distribution of the Th-acetylacetone complex between the organic phase and the aqueous phase. λ_4=420 at 25ºC (Allard & Ekberg 2006b).

-β_{140} is the stability constant for the formation of Th-acetylacetone complex ($Th(Aa)_4$). log β_{140} =27.4±0.2 at I=1M $NaClO_4$ (Ekberg et al. 2000).

-(Aa) is total acetylacetone concentration in the liquid-liquid experiments ($8.72 \cdot 10^{-4}$ M or $1.12 \cdot 10^{-3}$ M depending on the experiment)

-$[H^+]$ is proton concentration in each experimental point.

-K_1 is the stability constant for the formation of the 1:1 Th-ISA complex, and K_2 is the stability constant for the formation of the 1:2 Th-ISA complex, obtained in present work, after correction to I=1M (r. 6-6 and r. 6-7).

$Th^{4+} + ISAH_2^- = Th(OH)_n(ISAH_x)^- + 4H^+$ log K(I=1M) ≈ -15.6 r. 6-6
$Th^{4+} + 2ISAH_2^- = Th(OH)_n(ISAH_x)_2^{2-} + 4H^+$ log K(I=1M) = -12.5 r. 6-7

As seen in Figure 6-9, the distribution coefficients calculated using eq. 6-1 with the constants obtained in present work (solid line in the figure) are in good agreement with the experimental values obtained by Allard and co-workers.

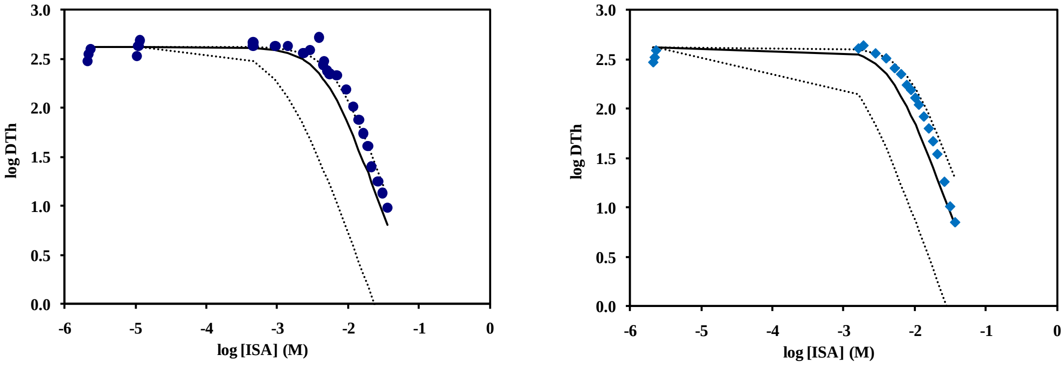

Figure 6-9. Symbols: Measured distribution coefficients for liquid-liquid extraction data at 25ºC and pH≈8, at total acetylacetone concentrations of $8.72 \cdot 10^{-4}$M (left) or $1.12 \cdot 10^{-3}$M (right), from (Allard & Ekberg 2006a, Allard & Ekberg 2006b). Solid lines: Calculated distribution coefficients using Th-ISA complexes obtained in present work. For the meaning of dotted lines, see text.

The main source of uncertainty in this calculation is the exact pH_c value in the experiments, as the exact proton concentration used in eq. 6-1 has a great influence in the calculated D value. Because of this, the solid lines in Figure 6-9 were calculated using the average $[H^+]$ values in the experiments reported by (Allard & Ekberg 2006a, Allard & Ekberg 2006b). Dotted lines in the figure were obtained by using the maximum and minimum $[H^+]$ reported by the authors.

4) Summary

A comparison of previous literature values with the stability constants determined in present work has been done.

Certain agreement between previous solubility experiments (Rai et al. 2009) and the results obtained in present work is observed. The lack of measured isosaccharinate concentrations in solution in Rai et al. experiments limits the comparison between both data sets.

Modelling of sorption experiments (Vercammen 2000, Vercammen et al. 1999, Vercammen et al. 2001) results in Th-isosaccharinate stability constants that are higher than the ones obtained in present work.

Liquid-liquid extraction experiments (Allard & Ekberg 2006a, Allard & Ekberg 2006b) can be explained with the stability constants obtained in present work.

Summarizing, the stability constants for thorium-isosaccharinate complexes obtained in present work agree with previous solubility experiments but also with liquid-liquid extraction measurements, which provides additional confidence on the results obtained.

6.7 Summary and conclusions

- Both isosaccharinate and gluconate ligands are able to significantly increase the thorium solubility at alkaline pH values.
- The results suggest the coordination of one Th(IV) by one or two polyhydroxycarboxylic ligands, depending on the ligand concentration in solution.
- Stability constants for the formation of those complexes were determined (r. 6-1 and r. 6-2).

$Th(OH)_4 + ISAH_2^- = Th(OH)_n(ISAH_x)^-$ log K(I=0.5) ≈ 4.2 r. 6-1
$Th(OH)_4 + 2ISAH_2^- = Th(OH)_n(ISAH_x)_2^{2-}$ log K(I=0.5) = 7.3±1.0 r. 6-2

- The information obtained through EXAFS experiments may indicate that thorium is binding isosaccharinate through the diol functions rather than through the carboxylic function in a bidentate way.
- The Fourier transformation magnitude of the EXAFS spectra for both thorium-isosaccharinate and thorium-gluconate samples are similar, which could indicate similar structure of the complexes.

- A slightly smaller stability for the thorium-isosaccharinate than for the gluconate-thorium aqueous species was determined.
- The stability constants for thorium-isosaccharinate complexes obtained in present work agree with previous solubility experiments (Rai et al. 2009) and with liquid-liquid extraction measurements (Allard & Ekberg 2006a, Allard & Ekberg 2006b) from the literature.

7 Thorium behaviour in the presence of EDTA (Paper III)

7.1 Introduction

In alkaline conditions few studies on EDTA complexation capacity towards thorium are available. Xia and co-workers (Xia et al. 2003) studied thorium hydroxide solubility in the presence of EDTA at alkaline pH values (pH range 9-11). Those authors reported the formation of $Th(OH)_2(EDTA)^{2-}$ and determined the stability constant for this aqueous species. In the experiments at low EDTA concentrations, the authors observed the disappearance of the EDTA from the solutions. Xia et al. described that in those solutions with low organic ligand concentrations the EDTA was completely adsorbed on the thorium hydroxide solid.

The adsorption was dependant on the amount of thorium hydroxide on the experiment.

7.2 Objectives

The main objective has been the study of the effect of EDTA on thorium hydroxide solubility at pH 12, above the pH range previously studied by Xia and co-workers (Xia et al. 2003).

7.3 Solubility experiments

Taking into account the results obtained by Xia and co-workers, were the adsorption of EDTA was dependant on the amount of thorium hydroxide on the experiment, in present work thorium hydroxide solubility experiments in the presence of EDTA were performed at two different solid-to-liquid ratios (0.4 and 2.5 g/l). As shown in Figure 7-1, measured thorium concentrations in solutions are independent from the solid/liquid ratio, which indicates that sorption of EDTA on the solid is negligible under the conditions studied.

Furthermore, thorium measurements from both 1kD and 300kD filtration were in agreement, probably because measured thorium concentrations are low, below the concentration needed to form of ligand-bridged colloids.

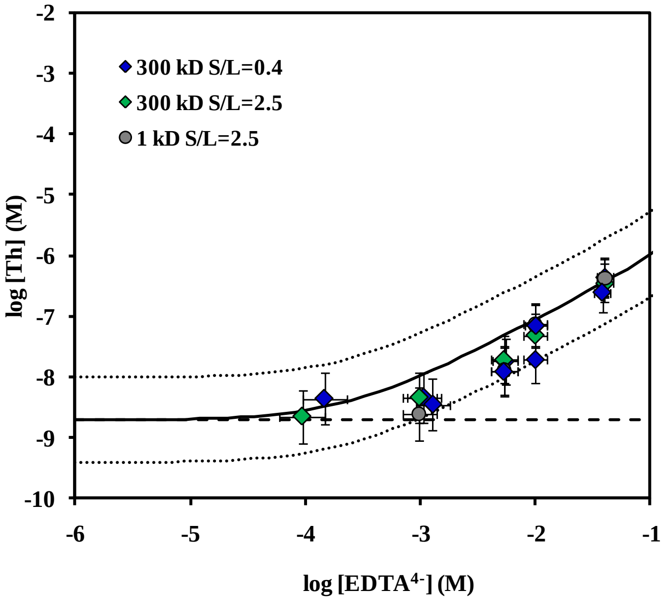

Figure 7-1. Solubility of $ThO_2 \cdot xH_2O$ as a function of EDTA concentration, at fixed pH_c=12 (I=0.5M, $NaClO_4$). Blue diamonds: experiments at solid-to-liquid ratios =0.4 g/l, 300kD filtration. Green diamonds: experiments at solid-to-liquid ratios =2.5 g/l, 300kD filtration. Grey circles: experiments at solid-to-liquid ratios =2.5 g/l, 1kD filtration. Solid line is calculated solubility by considering the formation of $Th(OH)_2(EDTA)^{2-}$ complex (with uncertainty, dotted line). Dashed line is thorium hydroxide solubility in the absence of organic ligands.

The solubility of thorium increases approximately one order of magnitude when increasing one order of magnitude the concentration of EDTA (Figure 7-1), indicating the formation of a 1:1 Th-EDTA species in the EDTA concentration range from 10^{-3} to 10^{-1} M.

The aqueous EDTA speciation is significantly affected by the presence of sodium in the system (r. 7-1); the corresponding aqueous speciation scheme was considered in the calculations.

$Na^+ + EDTA^{4-} = NaEDTA^{3-}$ logK = 2.8±0.2 r. 7-1

The calculated stability constant is shown in r. 7-2.

$ThO_2 \cdot xH_2O + EDTA^{4-} + 2H^+ = Th(OH)_2(EDTA)^{2-} + xH_2O$ $\log K_s(I=0.5) = 20.2 \pm 0.7$ r. 7-2

After correction to I=0 using SIT (see section 13.4) the data shown in r. 7-3 were obtained.

$Th^{4+} + EDTA^{4-} + 2H_2O = Th(OH)_2(EDTA)^{2-} + 2H^+$ $\log K^o = 13.4 \pm 0.7$ r. 7-3

Data obtained were in agreement with the formation of $Th(OH)_2EDTA^{2-}$ species reported by Xia and co-workers, r. 7-4 (Xia et al. 2003).

$Th^{4+} + EDTA^{4-} + 2H_2O = Th(OH)_2(EDTA)^{2-} + 2H^+$ $\log K^o = 13.2$ (Xia et al. 2003) r. 7-4

7.4 Summary and conclusions

- The solubility of thorium slightly increases in the presence of EDTA at alkaline pH values.
- The results obtained suggest the formation of $Th(OH)_2EDTA^{2-}$ species at pH_c=12, in agreement with previous literature works (Xia et al. 2003).

8 The effect of gluconate and EDTA on thorium solubility under simulated cement porewater conditions (Paper III)

8.1 Introduction

Cementitious systems are characterized by the alkaline pH and by the presence of calcium concentrations in solution. Those systems evolve with time, and different chemical conditions (different pH and calcium concentrations) are encountered as the reactive cement phases dissolve (see section 1.1). For example, in degradation state II, the chemical composition of the porewater is dominated by equilibrium with portlandite, $Ca(OH)_2$ giving a pH of 12.2. Calcium concentrations at this degradation state are in the order of 10^{-2} M (Ochs et al. 1998, Ochs et al. 2002).

Calcium forms complexes with organic ligands such as gluconate and EDTA (Hummel et al. 2005, Schubert & Lindenbaum 1952, Tits et al. 2005). The speciation of those ligands at pH=12 (and I=0.5 M $NaClO_4$) as a function of calcium concentration in the system has been calculated in present work using the data available in the literature (see appendix B, section 13) and is shown in Figure 8-1. As seen in the figure, gluconate is affected by the presence of calcium, and the aqueous EDTA speciation is significantly affected by the presence of both sodium (as already mentioned in section 7.3) and calcium.

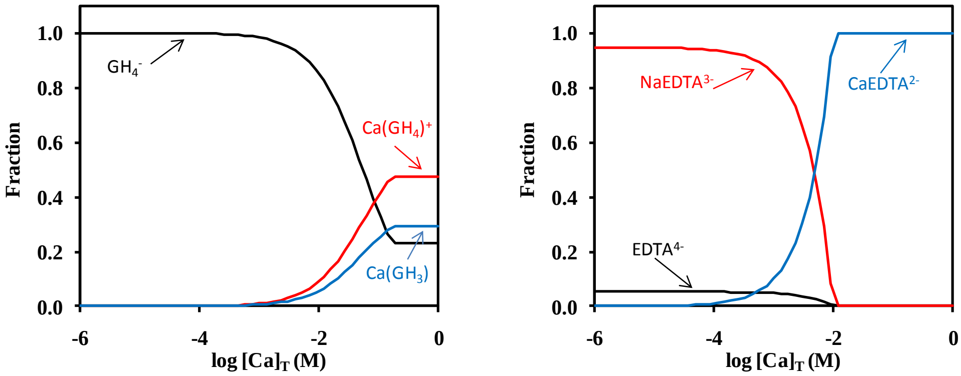

Figure 8-1. Gluconate (left) and EDTA (right) speciation in I=0.5M $NaClO_4$ media as a function of total calcium concentration in the system. $[L]_T=1\cdot10^{-2}$M, pH=12.

The stabilization of anionic hydroxide complexes in the alkaline pH range by strong interaction with calcium, as a result of either ion association or ion pair formation, has been previously reported (Altmaier et al. 2008, Brendebach et al. 2007). In those works, high solubility of Th(IV) hydrous oxides at pH_c = 11 to 12 in concentrated $CaCl_2$ solutions were observed. The solubility increase was attributed to the formation of $Ca_4[Th(OH)_8]^{4+}$. As Altmaier et al. discuss in their publication, the formation of $Ca_4[Th(OH)_8]^{4+}$ is “of particular interest for the storage of nuclear waste in underground salt mines, where concentrated alkaline $CaCl_2$ porewaters may be present”. However, speciation calculations performed in present work (see Figure 8-2) indicate that at pH=12, precipitation of $Ca(OH)_2$(s) limits the formation of this complex.

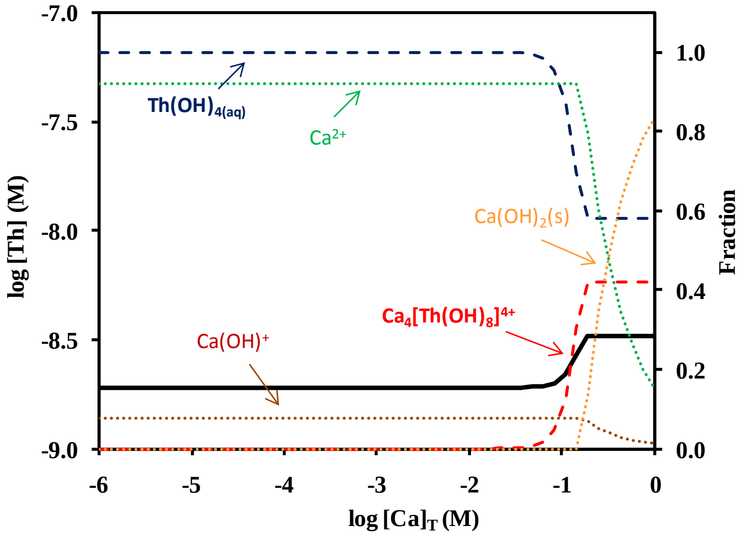

Figure 8-2. Amorphous thorium hydroxide solubility (black solid line) and underlying thorium aqueous speciation (dashed lines) and calcium aqueous speciation (dotted lines) as a function of calcium concentration in the system. pH=12, I=0.5 M $NaClO_4$.

The formation of ternary M-gluconate-Ca complexes (with M=Fe(III) or Th(IV)) has been suggested in several publications (Bechtold et al. 2002, Tits et al. 2005, Venema 1992, Vercammen et al. 1999). On the contrary, similar complexes have not been reported for nickel, europium or uranium, even under similar experimental conditions (Baraniak et al. 2002, Greenfield et al. 1997, Tits et al. 2005).

Venema (Venema 1992) studied the structure of the Al(III) complexes with hydroxycarboxylic acids in the presence of Ca by NMR. The author determined the structure of some Ca-M-L complexes, as the Ca-Al(III)-glucarate complex shown in Figure 8-3, formed at pH=11.5. As Th(IV), Al(III) is a hard metal ion with high affinity for hard bases, i.e. negatively charged oxygen donors such as deprotonated hydroxy and carboxylate groups. In addition, glucarate is a polyhydroxycarboxilic acid very similar to gluconate, although it has two carboxylic functions instead of one. Taking into account those similarities, the formation of Ca-Th-gluconate complexes seems likely. However, Venema used concentrated solutions[5], with equimolar Al(III) and glucarate concentrations and 0.5 equivalents of Ca for each mol of aluminium. Furthermore, data provided by the author do not allow calculating any stability constant for the formation of the complexes, as the studies of Venema are focused only on the elucidation of their structures.

---

[5] The exact concentrations of the solutions are not reported in (Venema 1992).

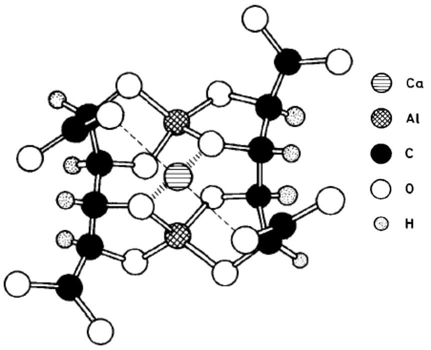

Figure 8-3. Representation of a 2:2:1 Ca-Al(III)-glucarate complex, from (Venema 1992).

The formation of Ca-Th-GLU complexes was not observed in Th sorption experiments with natural clays, sandstone or volcanic rocks reported by Baston and co-workers (Baston et al. 1992). Baston et al. reported significant sorption of both gluconate and the complex Th-GLU onto the natural materials. The system studied by Baston et al. was also influenced by the dissolution of the natural materials used in the experiments, and the introduction of further ionic species and complexing agents (for example carbonate) in the system.

Tits et al. (Tits et al. 2005, Tits et al. 2002) suggested the formation of a $CaTh(OH)_4(GH_4)_2(aq)$ species to explain their results on thorium sorption experiments in calcite in the presence of gluconate. The authors used the results obtained by Vercammen (Vercammen 2000, Vercammen et al. 2001) to support their hypothesis. However, they did not take into account the possible formation of Th-GLU complexes (without calcium) in their data treatment.

Vercammen et al. studied the influence of ISA on the sorption of Th on a polyallomer tube wall at pH 12.0 in the absence and presence of calcium. In the presence of calcium, the authors suggested the formation of a Th(IV)–ISA–Ca complex. Experimental data from Vercammen et al. are shown in Figure 8-4. As seen in the figure, the results obtained in the sorption experiments do not shown clear differences between the experiments in the absence and in the presence of $[Ca]_T$=0.7 mM. In the case of the experiments at $[Ca]_T$=10 mM, a high dispersion of the data is noticed. Thus, the formation of the Th(IV)–ISA–Ca complex may be uncertain.

In the case of EDTA, Rai et al. (Rai et al. 2008) studied Pu(IV) solubility in the system Pu(IV)-EDTA-Ca and Fe(III)-EDTA-Ca. Those authors did not observe the formation of ternary Ca-Pu(IV)-EDTA complexes.

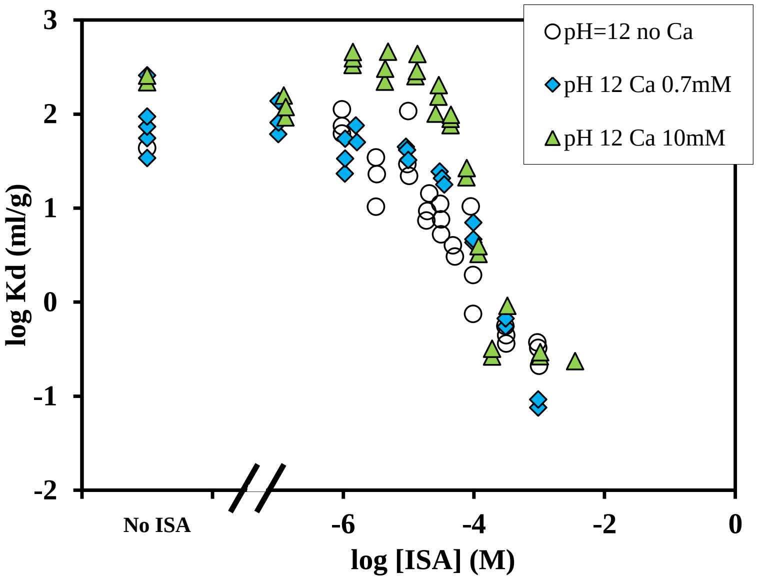

Figure 8-4. Influence of ISA on the sorption of Th on a polyallomer tube wall at pH 12.0 in the absence of calcium (empty circles) in the presence of 0.7mM Ca (blue diamonds) and in the presence of 10mM Ca (green triangles). Experimental data from (Vercammen 2000, Vercammen et al. 2001).

8.2 Objectives

The main objective of this chapter is to study the influence of calcium on thorium oxyhydroxide solubility in the presence of gluconate or EDTA at pH=12.

The procedure reported below has been followed:

1-Study of the thorium hydroxide solubility in the presence of gluconate and calcium (section 8.3.1 and Paper III), including a detailed analysis of calcium behaviour (section 8.3.2 and Paper III).

2-Study of the structure of the potential Ca-Th-gluconate system in comparison with the Th-gluconate system, by EXAFS (section 8.3.3 and Paper III).

3-Study the thorium hydroxide solubility in the presence of EDTA and calcium (section 8.4 and Paper III).

The maximum calcium concentrations studied are in the order of 10^{-2} M, characteristic of cement porewaters corresponding to cement compositions at the second degradation stage but below the concentrations that could lead to the precipitation of portlandite in the experiments.

8.3 Thorium behaviour in the presence of gluconate and calcium

8.3.1 Solubility experiments

Thorium hydroxide solubility experiments in the alkaline pH range, in the presence of both gluconate and calcium, were carried out using the set-up described in section 3. Figure 8-5 shows the experimental results in the presence of both calcium and gluconate (solid symbols), compared to the measured solubilities in the absence of Ca at pH=12. Only at higher calcium concentrations, $[Ca]=2.2\cdot10^{-2}$ M (green triangles in the figure), a small increase in solubility (in comparison with the data in absence of calcium) is observed.

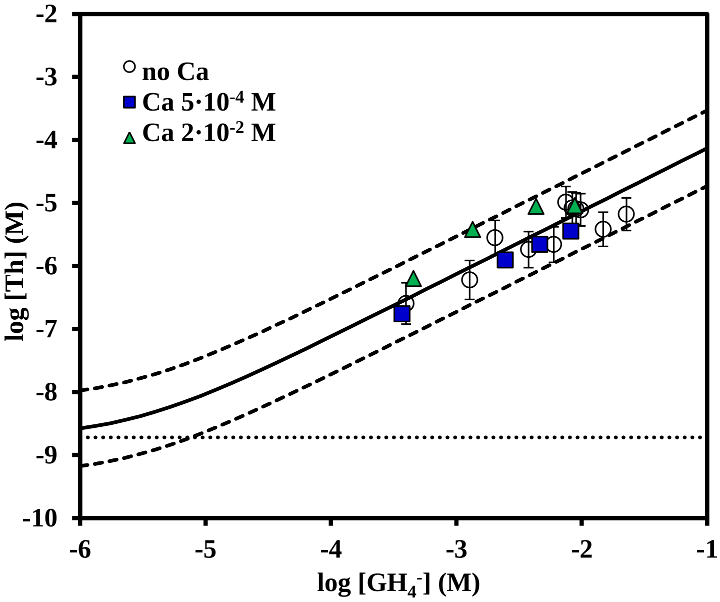

Figure 8-5. Solubility of thorium oxyhydroxide from undersaturation direction as a function of measured gluconate concentration at fixed $pH_c=12$ (I=0.5M, $NaClO_4$), time>39 days. Open circles: in the absence of calcium. Blue squares: $[Ca]=5\cdot10^{-4}$ M. Green triangles: $[Ca]=2\cdot10^{-2}$ M. Solid line is calculated thorium hydroxide solubility taking into account $Th(OH)_2(GH_2)^-$ formation (with uncertainty, dashed line) as reported in section 5.4. Dotted line is calculated solubility in the absence of organic ligands.

Taking into account the large uncertainty for the observed thorium oxyhydroxide solubility in the presence of gluconate (see dotted lines in Figure 8-5), the formation of the $Ca:Th:GH_4$ complex cannot be confirmed under the studied conditions. The small apparent solubility increase only allow the calculation of an upper limit value for the formation of a Ca:Th:L complex (r. 8-1).

$$ThO_2\cdot xH_2O + GH_4^- + Ca^{2+} = Ca:Th:GH_4 \qquad \log K(I=0.5) \leq -0.9 \quad \text{r. 8-1}$$

8.3.2 Calcium analysis

A decrease of the aqueous calcium concentrations was observed at $5 \cdot 10^{-4}$ and $2 \cdot 10^{-2}$ M initial calcium concentrations (see Figure 8-6). This may indicate that a significant part of the available calcium in solution is being sorbed (or precipitated) on the solid surface[6]. However, with the available data it is not possible to evaluate whether the decrease in measured calcium concentrations is due to the sorption of free Ca^{2+} or to the sorption of a Ca:gluconate complex on the solid surface of thorium oxyhydroxide.

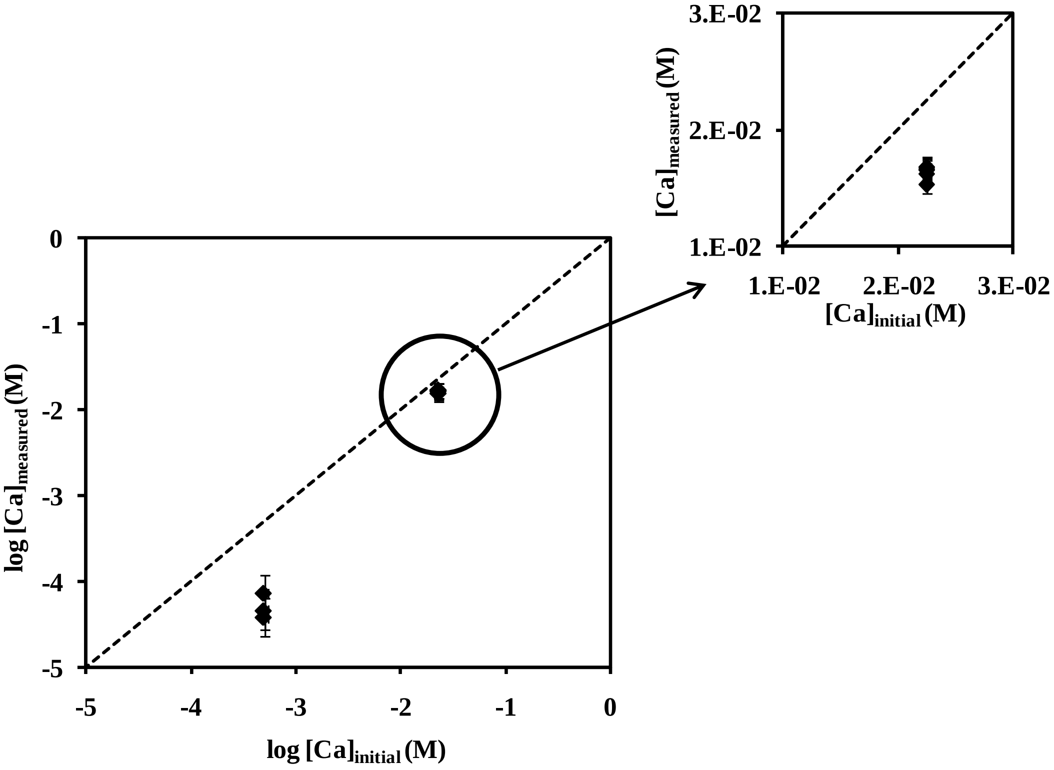

Figure 8-6. Measured vs. initial calcium concentrations in thorium hydroxide solubility experiments at pH_c=12 in the presence of both calcium and gluconate. Black dotted line indicates $Ca]_{measured}$=$[Ca]_{initial}$.

---

[6] Calcium sorption on tetravalent hydroxides surfaces had already been reported in the literature (Stankovic et al. 1990). The sorption of organic ligands onto the solid thorium hydroxide surface was also described in previous sections.

An additional attempt to investigate the influence of calcium on the system was done by means of SEM (Scanning Electron Microscopy) and SEM-EDX (Scanning Electron Microscopy coupled with Energy Dispersive X-ray Spectroscopy) analysis.

SEM measurements of thorium hydroxide solid showed very similar morphology of the solid in the absence or the presence of calcium, as reported in Paper III. Altmaier and co-workers (Altmaier et al. 2008) reported changes (detected by SEM and XRD analysis) in a solid thorium hydroxide sample that had been in contact with a calcium solution at pH>11.5. According to (Altmaier et al. 2008), SEM showed needle-like crystals lying on the bulk heap of amorphous thorium hydroxide particles. Those needles were not observed in the present samples (see Figure 8-7); the much higher calcium concentrations ([Ca]>1M) and longer reaction times used by Altmaier and co-workers explain the apparent discrepancy between the results.

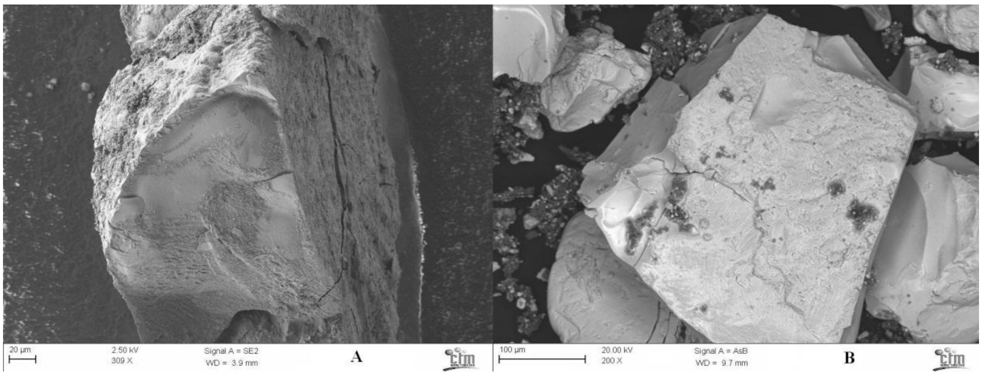

Figure 8-7. SEM images for amorphous thorium oxyhydroxide after contact with 0.5 M $NaClO_4$ solution at pH_c=12 for >70 days. A) $[GH_4^-]=1.0\cdot10^{-2}$ M, no calcium B) $[GH_4^-]=1.7\cdot10^{-3}$ M, $[Ca]=2.2\cdot10^{-2}$ M.

SEM-EDX analysis (Scanning Electron Microscopy coupled with Energy Dispersive X-ray Spectroscopy) was used for the elemental analysis of the surface of the sample. The solid analysed remained for >190 days in contact with a 0.5M $NaClO_4$ solution at pH=12, with $[GH_4^-]_T=1.7\cdot10^{-3}$ M and $[Ca]_T=2.2\cdot10^{-2}$ M. The solid was filtered, washed with MilliQ water and dried in a vacuum desiccator before the analysis.

As seen in Figure 8-8, the presence of calcium was shown in the spectrum. However, significant amounts of Cl were also detected. The presence of Cl may indicate that, during the preparation of the sample for the SEM-EDX analysis, some $NaClO_4$ was not washed off and was still present in the surface when the solid was dried and analysed. Thus Ca detected in the EDX analysis could be adsorbed on the thorium hydroxide surface or may be present in the sample due to an insufficient washing before the analysis. It was then not possible to confirm the sorption or the precipitation of calcium on the surface using SEM-EDX results.

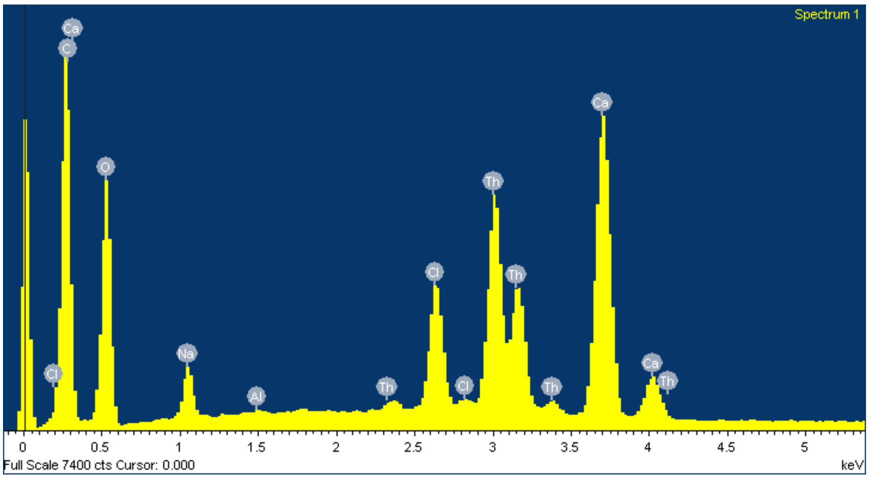

Figure 8-8. EDX results for amorphous thorium oxyhydroxide after contact with $[GH_4^-]=1.7\cdot10^{-3}$ M, $[Ca]=2.2\cdot10^{-2}$ M, 0.5M $NaClO_4$ solution at pH=12 for >190 days.

8.3.3 EXAFS experiments

EXAFS analyses were also done in the Ca-Th-GH_4^- system in the alkaline pH range. Two samples from oversaturation direction were prepared from a solution of $[Th]_0=1\cdot10^{-3}$ M and $[GH_4^-]=0.1$ M at pH≈11.8 for EXAFS analysis. One of the samples did also contain calcium, with a total concentration of $1\cdot10^{-2}$ M. The Fourier transformation magnitudes of the EXAFS spectra are shown in Figure 8-9. It can be seen that both spectra are very similar, which may indicate a similar coordination environment for thorium in both cases. Then, if a Ca:Th:GH_4 complex is formed, calcium coordination in the sample does not seem to influence significantly the results obtained with EXAFS.

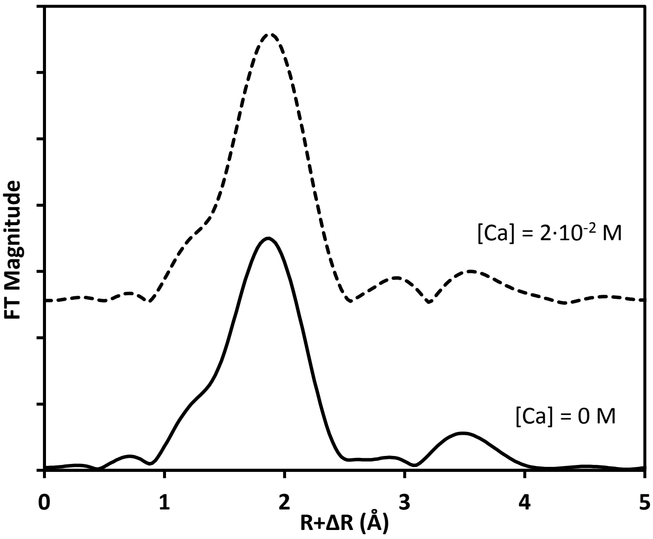

Figure 8-9. Experimental data of EXAFS Fourier transforms of Th L_{III}-edge for Th-gluconate solutions, $[Th]_0=1\cdot10^{-3}$ M and $[GH_4^-]=0.1$ M at pH≈11.8. Solid line: in the absence of calcium. Dashed line: $[Ca]_0=1\cdot10^{-2}$ M.

8.4 Thorium behaviour in the presence of EDTA and calcium

As well as the Ca-Th-gluconate system, the Ca-Th-EDTA system was also investigated (see Paper III).

In the presence of both calcium and EDTA (colour symbols in Figure 8-10), measured thorium aqueous concentrations show that Ca concentrations of $2.0\cdot10^{-3}$ M do not affect thorium oxyhydroxide solubility. Hence, the results obtained in both, the presence (colour symbols in Figure 8-10) and the absence of Ca (open circles in Figure 8-10) can be explained by assuming only the formation of $Th(OH)_2(EDTA)^{2-}$ complex already described in section 7. This is probably due to the structure of the EDTA ligand itself, that chelates thorium without leaving free coordination sites (Bogucki & Martell 1958).

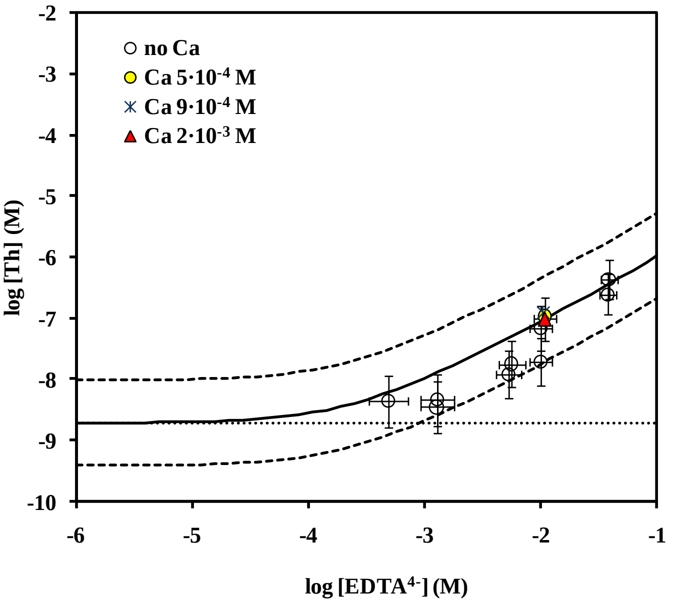

Figure 8-10. Solubility of thorium oxyhydroxide from undersaturation direction as a function of measured EDTA concentration at fixed pH_c=12 (I=0.5M, $NaClO_4$), time>19 days. Open circles: in the absence of calcium. Yellow circle: $[Ca]=5\cdot10^{-4}$ M. Blue cross: $[Ca]=9\cdot10^{-4}$ M. Red triangle: $[Ca]=2\cdot10^{-3}$ M. Solid line is thorium hydroxide solubility taking into account $Th(OH)_2(EDTA)^{2-}$ formation (with uncertainty, dashed line). Dotted line is calculated solubility in the absence of organic ligands.

8.5 Summary and conclusions

- According to the previous literature data, the formation of $Ca:Th:GH_4$ complexes seems to be uncertain.
- The influence of gluconate or EDTA on thorium solubility in the presence of calcium at pH=12 was studied in present work.
- Solubility experiments do not allow to confirm neither disregard the formation of any $Ca:Th:GH_4$ or Ca:Th:EDTA complex.
- A decrease in measured calcium concentrations in solution (in relation with initial calcium concentrations) was observed. This decrease could be explained by the

sorption of Ca^{2+} itself or even to the sorption of the Ca:gluconate complex on the solid surface of thorium oxyhydroxide.

- The Fourier transformation magnitudes of the EXAFS spectra for thorium-gluconate complexes are similar in both the presence and the absence of calcium.

9 Complexation of U(VI) by gluconate (Paper IV)

9.1 Introduction

The complexation of U(VI) with gluconate was studied by Sawyer and co-workers (Sawyer & Kula 1962). The authors studied the complexation of U(VI) with gluconate under alkaline conditions characteristic of cement environments. On the basis of the results obtained from spectrophotometry, polarography, polarimetry, and pH measurements, they reported the formation of an $(UO_2)(GH_4)(OH)_2^-$ complex. The authors considered the reaction r. 9-1 as the representative one for the formation of the complex and used it to calculate the corresponding stability constant (log K=6.3).

According to uranium thermodynamic data (Guillaumont et al. 2003), the speciation of U(VI) in solution under alkaline pH values (pH≈11 and higher) in the absence of organic ligands is dominated by $UO_2(OH)_3^-$ and $UO_2(OH)_4^{2-}$, and not by $UO_2(OH)^+$. This implies that the stability constant suggested by Sawyer and Kula is not in agreement with the expected U(VI) chemical speciation in the absence of organic ligands. Thus, the value suggested by (Sawyer & Kula 1962) should be revised. However, the original publication (Sawyer & Kula 1962) does not provide all the necessary details in order to perform a reevaluation.

$$UO_2(OH)^+ + OH^- + GH_4^- = (UO_2)(GH_4)(OH)_2^- \quad \text{(Sawyer \& Kula 1962)} \qquad \text{r. 9-1}$$

Baraniak and co-workers (Baraniak et al. 2002) studied the influence of several organic ligands (including gluconate) into U(VI) sorption onto natural materials that included uncertain quantities of calcium and carbonate. The complexity of the system and the poor sorption of uranium in the studied solids did not allowed to obtain any stability constant for the formation of uranium-gluconate complexes.

Evans (Evans 2003) suggested the formation of $UO_2GH_4^+$ in the U(VI)-GLU system. The author suggested different stability constants for the same complex at different pH values; this may indicate the formation of different complexes depending on pH, a possibility that was not taken into account in the original publication. In addition, the formation of a positively charged species in alkaline media seems unlikely.

Taking into account the analogy between gluconate and isosaccharinate (see section 6 of present work) the available data for U(VI)-ISA system was also investigated. In the NEA thermodynamic series (Hummel et al. 2005), the authors raised the hypothesis of the existence of $UO_2(OH)_n(ISAH_{-x})^{(1-n-x)}$-like complexes in alkaline solutions. However, no thermodynamic data for the uranium-isosaccharinate system were selected in the review.

Warwick and co-workers (Warwick et al. 2006) studied the U(VI)-isosaccharinate system using as a basis the solubility of sodium uranate at different pH values in the presence of the organic ligand. At pH=13.3 the authors reported a value of $\log_{10}\beta = 18.8\pm1.6$ for the formation of a $UO_2ISA(OH)_4$ complex (the charge of the species formed was omitted by the authors).

$$UO_2^{2+} + ISA + 4OH^- = UO_2ISA(OH)_4 \quad \text{(Warwick et al. 2006)} \quad \text{r. 9-2}$$

It must be taken into account that the uranium hydrolysis constants used in the calculations by Warwick and co-workers were those in the NIST database ($\log_{10}\beta(UO_2(OH)_4^{2-})$=22.2 and $\log_{10}\beta(UO_2(OH)_3^-)$=22.2), which are slightly different from the ones used in present work.

From the results of those literature publications it can be concluded that the formation of U(VI)-gluconate complexes at alkaline pH values is likely. However, the stability of the complexes is not clear.

9.2 Objectives

The main objective of this chapter is the study and determination of the formation of U(VI)-gluconate complexes by following the procedure reported below:

1-Study of uranates solubility in the presence of gluconate (section 9.3 and Paper IV).

2-Study of U(VI) complexes in the presence of gluconate, by using UV-VIS experiments, and determination of the stability constant for the formation of U(VI)-gluconate complex (section 9.4 and Paper IV).

3-Evaluation of the stability constants calculated in UV-VIS studies in comparison with the results obtained in the solubility studies (section 9.5 and Paper IV).

9.3 Solubility experiments

The presence of gluconate was shown to increase significantly the solubility of uranates at pH=12, thus suggesting the formation of a U(VI)-gluconate complex.

- *Solubility studies from oversaturation direction*

Solubility tests from oversaturation direction were performed in 1 M $NaClO_4$ media, by spiking gluconate solutions under alkaline conditions with an acidic uranyl nitrate solution. The final U(VI) concentration was 10^{-4} M and the final pH value of the medium was 12. Results are shown in Figure 9-1. Under such conditions, and according to the experiments presented in section 4.3, sodium uranate solid should precipitate and total U(VI) concentrations in the aqueous phase should be near 10^{-6} M (grey zone in Figure 9-1). On the contrary, measurements indicate that all uranium added is maintained in solution (symbols in Figure 9-1), suggesting the formation of an U(VI)-gluconate complex.

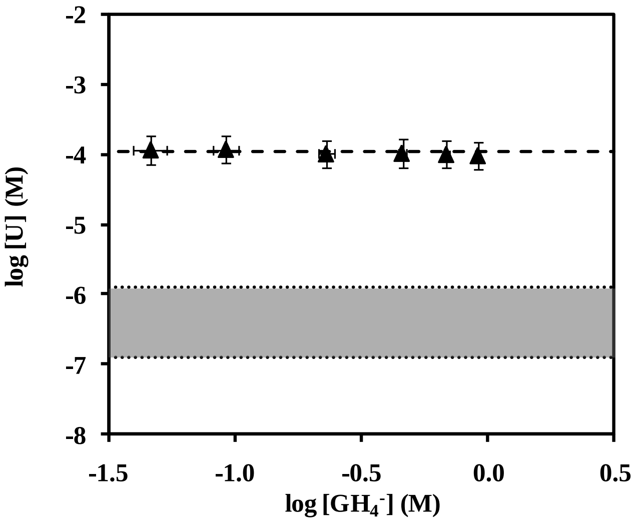

Figure 9-1. Results from solubility (oversaturation) experiments. Triangles: Measured uranium concentrations in solution as a function of gluconate concentration at fixed pH_c=12 (I=1 M $NaClO_4$), after filtration. Dashed line: total uranium concentration added ($1·10^{-4}$ M). Grey zone: expected $Na_2U_2O_7$ solubility under those conditions in the absence of organic ligands.

- *Solubility studies from undersaturation direction*

Undersaturation solubility tests were performed by contacting sodium uranate with 0.5M KCl solutions and different gluconate concentrations; results are shown in Figure 9-2. Under those conditions and in the absence of organic ligands, total U(VI) concentrations in the aqueous phase should be near 10^{-6} M (grey zone in Figure 9-2). On the contrary, at [GLU]>$5·10^{-3}$M, measured uranium concentrations in solution are significantly higher (symbols in Figure 9-2). As in the case of oversaturation experiments, those results suggest the formation of an U(VI)-gluconate complex.

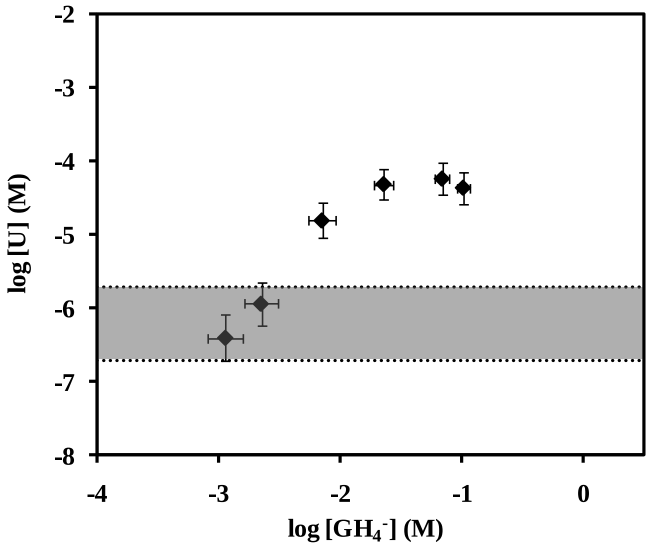

Figure 9-2. Results from solubility (undersaturation) experiments. Diamonds: Measured uranium concentrations in solution as a function of gluconate concentration at fixed pH$_c$=12 (I=0.5 M KCl), after filtration. Grey zone: expected $K_2U_2O_7$ solubility under those conditions in the absence of organic ligands.

9.4 UV-VIS experiments

UV-Vis experiments were performed to study U(VI)-L complexation in the alkaline range.

UV-VIS spectra shown in Figure 9-3 were recorded in alkaline solutions with a constant uranium concentration ($5 \cdot 10^{-3}$ M) and a variable gluconate concentration (ranging from $2 \cdot 10^{-4}$ to $4 \cdot 10^{-3}$ M). Samples were measured immediately after preparation, without filtration. The measured absorbance increases with the gluconate concentration in the system, compared with the absorbance in the absence of organic ligand (red dashed line in Figure 9-3). Furthermore, a displacement on the wavelength that shows the maximum absorbance signal is also noticed. This suggests the formation of U(VI)-gluconate complexes.

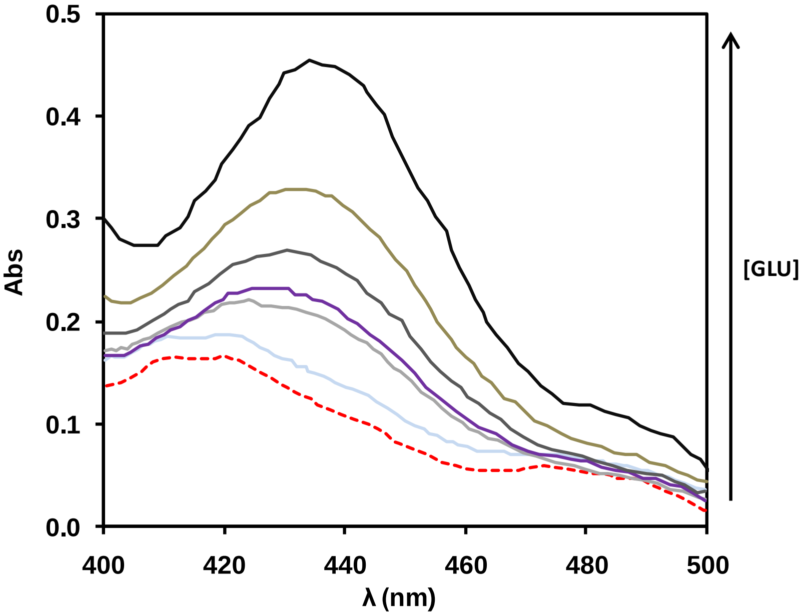

Figure 9-3. Spectra for solutions with a constant uranium concentration ($5\cdot10^{-3}$ M) and increasing gluconate concentrations (from $2\cdot10^{-4}$ to $4\cdot10^{-3}$ M) at pH=12. Dashed red line indicates the absorbance in the absence of organic ligand.

Using UV-VIS spectroscopy, two additional experiments (using the continuous variation method and the molar variation method) were conducted.

- *The continuous variation method*

In this method the sum of metal and ligand concentrations ([M]+[L]) in solution is constant in all the samples (Bruneau et al. 1992, Rossotti & Rossotti 1961, Sawyer & Kula 1962). Measurements were performed at λ=435nm, which is expected to be the absorbance maximum of the uranium-gluconate complex (Sawyer & Kula 1962). The sum of metal and ligand concentrations was kept constant at $[U]+[L]=1\cdot10^{-2}$ M. The results obtained (Figure 9-4) showed an inflection point at a mole fraction of 0.5, suggesting the formation of a 1:1 U(VI):gluconate complex.

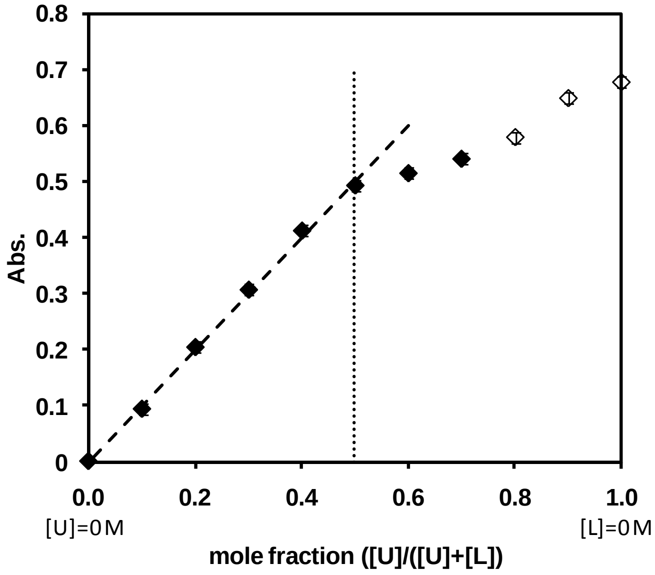

Figure 9-4. UV-VIS results in the continuous variation method for uranium-gluconate samples at pH≈12; $[U]+[L]=1\cdot10^{-2}$ M. The plot shows absorbance at λ=435nm vs. the mole fraction for uranium. Open symbols indicate the samples where a yellow precipitate was observed.

After 1 week of sample preparation, a yellow precipitate appeared in tubes with uranium molar fractions higher than 0.75 (open symbols in Figure 9-4). TMAOH (with a final concentration of 0.1 M) was used to adjust the pH to 12 in UV-VIS samples. The tetramethylammonium counterion was expected to suppress formation of uranate salts, as reported by Clark et al. (Clark et al. 1999). However, other solids may limit U(VI) solubility under alkaline conditions. In the absence of any complexing agent, schoepite ($UO_2(OH)_2(s)$) may precipitate. Thus, the formation of schoepite in the samples with low gluconate concentrations (open symbols in Figure 9-4) seems likely.

- *The molar variation method*

In the molar variation method the metal concentration is constant and the concentration of the ligand is increased in each sample (Rossotti & Rossotti 1961, Sawyer & Kula 1962).

The ligand concentration in sample solutions was varied from 0 to $7\cdot10^{-3}$ M. Uranium concentration in each sample was kept constant at $[U(VI)]_{total}=1\cdot10^{-3}$ M. The results obtained by applying this method are shown in Figure 9-5.

8 days after its preparation, a yellow precipitate was present in those samples with no gluconate present or with low gluconate concentrations (open symbols in Figure 9-5). As in the continuous variation method experiments, this may be due to the formation of schoepite in the solutions. Preliminary tests with lower uranium concentration (which would have avoided the formation of schoepite in the samples) did not provide useful results, as measured absorbance was very small. Thus, it was decided to filter the samples before absorbance measurements were done.

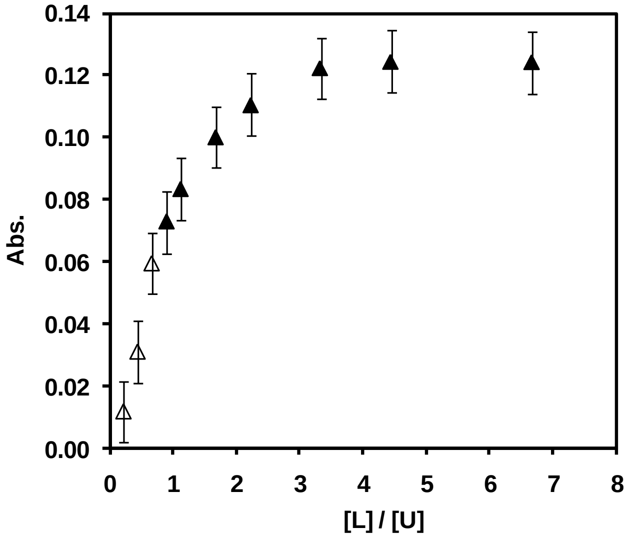

Figure 9-5. UV-VIS results in the molar variation method for uranium-gluconate samples at pH≈12; $[U]_{total}=1\cdot10^{-3}$ M. The graph shows absorbance at λ=435nm vs. the ratio [L]/[U], after sample filtration. Open symbols: samples were precipitation was observed before filtration.

The results from the molar variation method allowed the calculation of a stability constant for the formation of the 1:1 U(VI):gluconate complex:

1) The molar absorptivity ε_{ML} for the 1:1 U(VI):gluconate complex was calculated from the measured absorbance A at higher ligand concentrations by using the Beer's law (eq.

9-1). Under those conditions, uranium-gluconate complex is expected to be the main species in solution, and the contribution of the non-complexed uranium species ($UO_2(OH)_3^-$ and $UO_2(OH)_4^{2-}$) to the total signal should be less than 10%.

$$A = \varepsilon_{ML} l [ML] \quad \text{eq. 9-1}$$

2) The amount of free gluconate ligand $[L]_{free}$ was calculated in the samples around the inflection point by considering that all measured absorbance was due to the formation of the U(VI):gluconate complex (eq. 9-2).

$$[L]_{free} = [L]_T - \frac{A}{\varepsilon_{ML} l} \quad \text{eq. 9-2}$$

3) Those data (total uranium and gluconate concentration and calculated free gluconate ligand) were used as an input data in FITEQL in order to calculate the formation constant for the 1:1 U(VI):gluconate complex.

Prior to this calculation, it was mandatory to know the number of protons involved in the reaction. However, the structure of the complex remains unclear, as data were only acquired at one single pH value and no EXAFS or NMR data were available. Recently, Birjkumar et al. (Birjkumar et al. 2012a) studied the geometries of U(VI)-gluconate complexes using density functional theory (DFT). The authors studied different chelating modes, including $UO_2(OH)_2(GH_3)^{2-}$, and suggested that the formation of this complex was likely at high pH values. The formation of this complex was then suggested in order to explain the results obtained in present work.

The formation constant for the 1:1 U(VI):gluconate complex was then calculated as shown in r. 9-3.

$$UO_2(OH)_3^- + GH_4^- = UO_2(OH)_2(GH_3)^{2-} + H_2O \qquad \log K^o \approx 3.9 \pm 1 \qquad \text{r. 9-3}$$

9.5 Discussion of the obtained results

The formation constant for the 1:1 U(VI):gluconate complex shown in r. 9-3 was used to calculate the expected uranates solubility; then the calculations were compared with the results from oversaturation and undersaturation experiments described in section 9.3.

As shown in Figure 9-6, the observed results in experiments from oversaturation direction can be partially explained by the formation of the U-gluconate complex reported in r. 9-3. According to the calculations, even higher uranium concentrations could be maintained in solution with [GLU]>10^{-2} M, if these data were available.

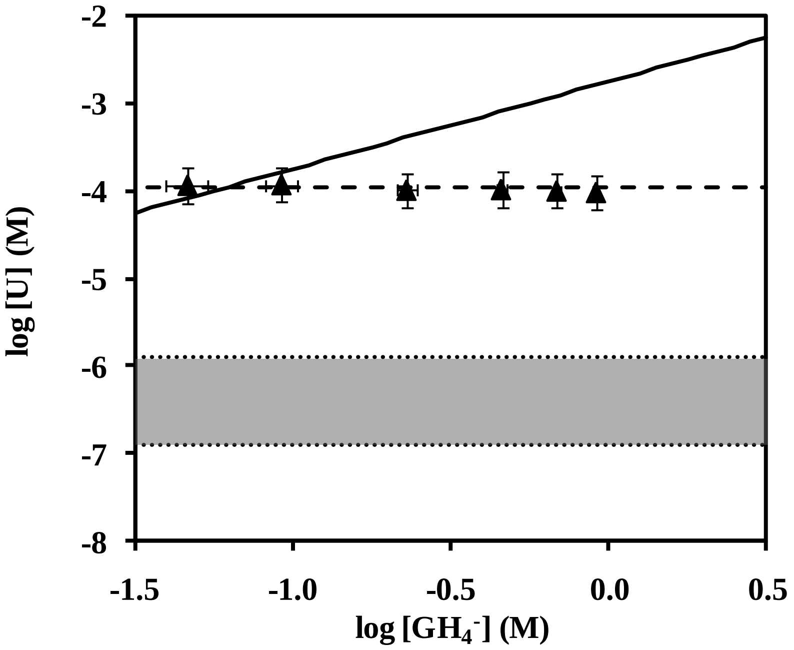

Figure 9-6. Results from solubility (oversaturation) experiments. Triangles: Measured uranium concentrations in solution as a function of gluconate concentration at fixed pH_c=12 (I=1 M $NaClO_4$), after filtration. Dashed line: total uranium concentration added ($1\cdot10^{-4}$ M). Grey zone: expected $Na_2U_2O_7$ solubility under those conditions in the absence of organic ligands. Black solid line: calculated solubility taking into account the formation of the 1:1 U(VI):gluconate complex.

The undersaturation results can be partially explained taking into account the formation of the U-gluconate with the stability constant shown in r. 9-3. However, the high uncertainty observed for both the uranate solubility and the U-gluconate complex complicates the interpretation of the data. At high gluconate concentrations (≈10^{-1} M) the dissolution of the solid seems to be limited; this behaviour is similar to the one observed in the experiments with thorium hydroxide.

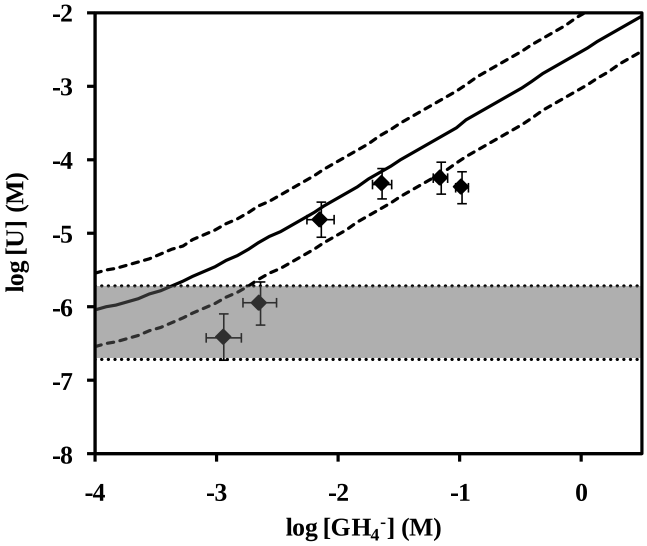

Figure 9-7. Results from solubility (undersaturation) experiments. Diamonds: Measured uranium concentrations in solution as a function of gluconate concentration at fixed pH_c=12 (I=0.5 M KCl), after filtration. Grey zone: expected $K_2U_2O_7$ solubility under those conditions in the absence of organic ligands. Black solid line: calculated solubility taking into account the formation of a 1:1 U(VI):gluconate complex, with uncertainty (dotted lines).

As already mentioned, the structure of the complex (i.e. the number of protons involved in the reaction) remains unclear. The solubility and UV-VIS data obtained have been evaluated by considering r. 9-4. This hypothesis is in agreement:

-With the observations from Birjkumar et al. (Birjkumar et al. 2012a)

-With the fact that $UO_2(OH)_3^-$ is one of the main U(VI) species in solution under the conditions studied in the absence of organic ligands.

$$UO_2(OH)_3^- + GH_4^- = UO_2(OH)_2(GH_3)^{2-} + H_2O \qquad \log K^o \approx 3.9 \pm 1 \qquad \text{r. 9-4}$$

As a result of this hypothesis, speciation calculations indicate that $UO_2(OH)_2(GH_3)^{2-}$ could be formed even at near-neutral pH values (see Figure 9-8). Taking into account that the experiments were done only at pH=12, it is not possible to ensure that those speciation calculations are realistic.

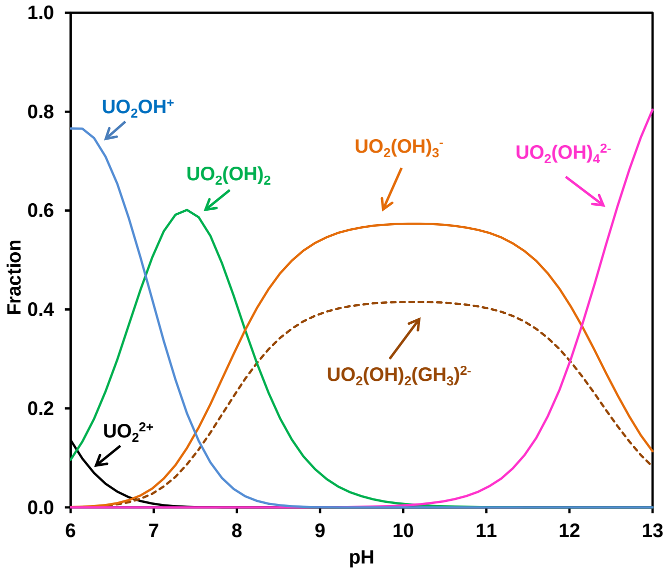

Figure 9-8. U(VI) speciation in the presence of gluconate, taking into account the results obtained in present work (reaction 9-4). $[U(VI)]_T=1\cdot10^{-9}$M, $[GH_4^-]_T=1\cdot10^{-4}$M. The possible precipitation of solids has not been taken into account in the calculations.

It should be taken into account that the speciation of U(VI) in solution under alkaline pH values (pH≈11 and higher) in the absence of organic ligands is dominated by both $UO_2(OH)_3^-$ and $UO_2(OH)_4^{2-}$. Thus, it may be possible that the reaction occurring in the system is the one shown in r. 9-5 instead of the one reported in r. 9-4 (the undersaturation results can also be partially explained taking into account r. 9-5, see Figure 9-9).

$$UO_2(OH)_4^{2-} + GH_4^- = UO_2(OH)_3(GH_3)^{3-} + H_2O \qquad \log K^o \approx 4.1 \qquad \text{r. 9-5}$$

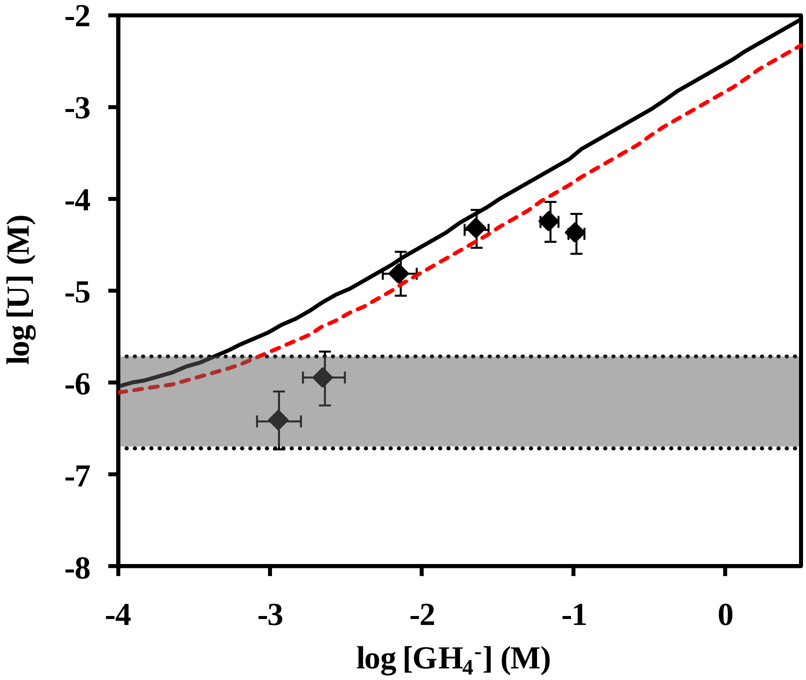

Figure 9-9. Reevaluation of the results from solubility (undersaturation) experiments. Diamonds: Measured uranium concentrations in solution as a function of gluconate concentration at fixed pH_c=12 (I=0.5 M KCl), after filtration. Grey zone: expected $K_2U_2O_7$ solubility under those conditions in the absence of organic ligands. Black solid line: calculated solubility taking into account reaction 9-4. Red dotted line: calculated solubility taking into account reaction 9-5.

If r. 9-5 is the most significant one occurring in the system, the speciation of U(VI) in the presence of organic ligands as a function of pH will change significantly (see Figure 9-10).

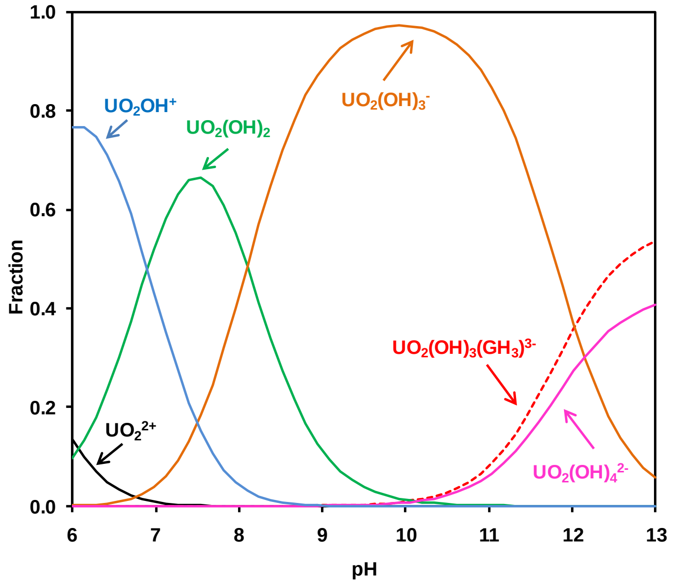

Figure 9-10. U(VI) speciation in the presence of gluconate, taking into account the results in reaction 9-5. $[U(VI)]_T=1\cdot10^{-9}$M, $[GH_4^-]_T=1\cdot10^{-4}$M. The possible precipitation of solids has not been taken into account in the calculations.

It is then necessary to obtain further data on the structure of the complex before the conclusions obtained in present work could be extrapolated to pH values different than 12.

9.6 Summary and conclusions

In neutral and alkaline solutions, and in the presence of major cations such as Na^+, K^+, $Ca^{2+}$and Mg^{2+} in the media, U(VI) may precipitate in the form of uranates. Formation of these solids have been reported even at I = 0.1 M $NaClO_4$ (Meinrath 1998a). The study of the U(VI)-gluconate system in the alkaline pH range is then complicated due to the formation of those sparingly soluble solids even at low ionic strengths.

As a consequence, different approaches were used in present work in order to investigate the formation of U(VI)-gluconate complexes (see a summary in Figure 9-11).

- Solubility studies from both oversaturation and undersaturation direction, that demonstrated the formation of U(VI)-gluconate complexes,
- Results from UV-VIS studies allowed the calculation of an approximated stability constant for 1:1 U(VI):gluconate,
- And finally, the stability constants calculated in UV-VIS experiments were used to justify the results obtained in the solubility studies.

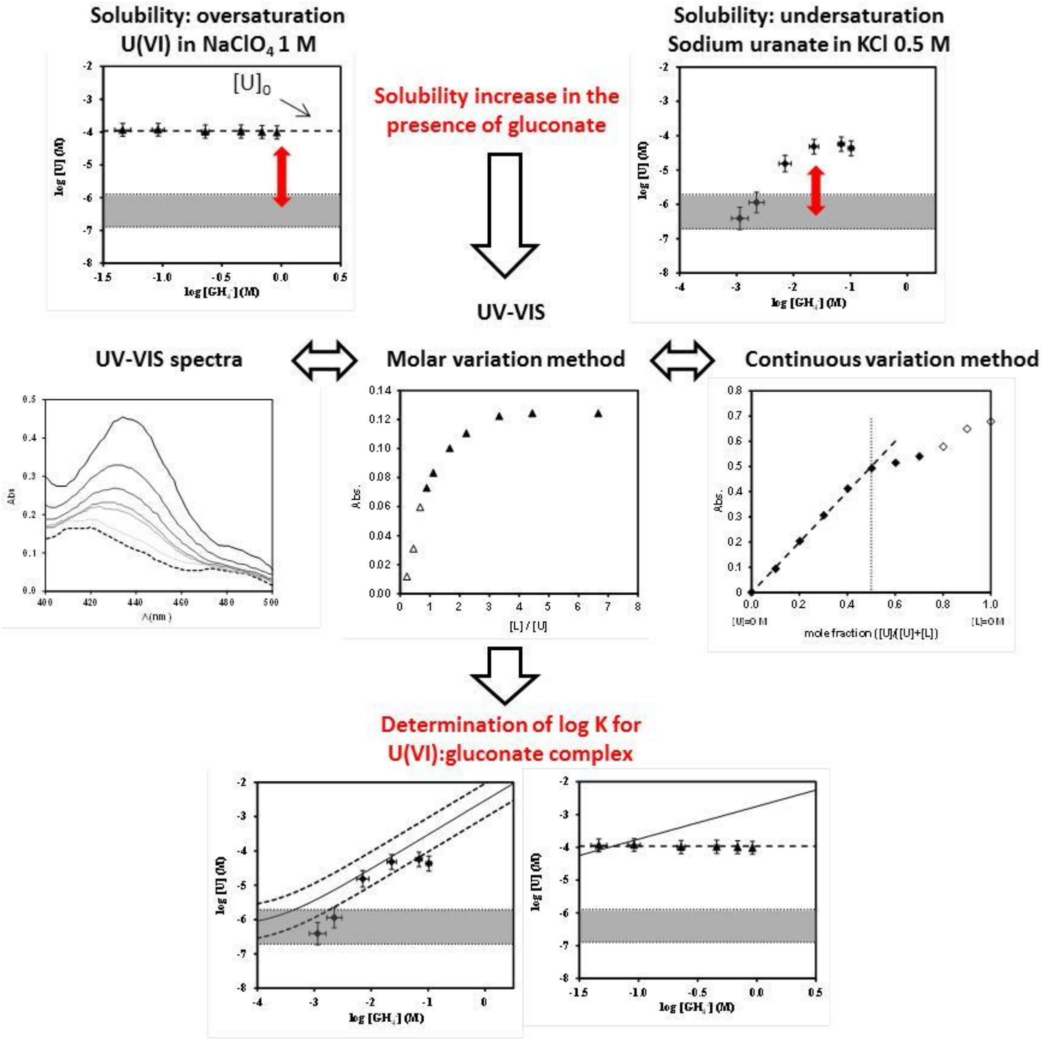

Figure 9-11. Summary of the experiments for the study of U(VI) complexation with gluconate.

Main conclusions obtained are summarized below:

- Both solubility and UV-VIS experiments showed the formation of U(VI)-gluconate complexes at pH=12.
- Results of UV-VIS experiments allowed to calculate an stability constant for the formation of a 1:1 U(VI)-gluconate complex.
- The stability constant obtained allows explaining reasonably well the results from solubility experiments.
- The structure of the complex remains unclear. This is one of the main limitations of the work performed.

10 Complexation of U(VI) by EDTA (unpublished results)

10.1 Introduction

U(VI) is predominantly penta coordinated, with all exchangeable ligands perpendicular to the O=U=O axis. The geometry of UO_2^{2+} and that of EDTA only permits coordination of at most one iminodiacetate moiety. Consequently, the relative stability of U(VI)-EDTA complex is lower than the stability of the complexes of EDTA with other cations (Glaus et al. 2000).

A wide variety of U(VI)-EDTA species have been suggested in different studies (Hummel et al. 2005), as shown in Table 10-1. However, there is a lack of stability data for U(VI)-EDTA complexation in alkaline environments. In fact, the data available in the alkaline pH range, highlighted in grey in Table 10-1, are not based on experimental measurements, but on the use of estimation methodologies to determine stability constants; only upper limit values are suggested in some cases (Hummel 1993).

Table 10-1. Stability constants available in the literature for U(VI)-EDTA complexation.

Species	Log K	Reference	Comments
$UO_2(EDTA)^{2-}$	13.70	(Hummel et al. 2005)	
$(UO_2)_2(EDTA)(aq)$	20.60	(Hummel et al. 2005)	
$UO_2(HEDTA)$-	19.61	(Hummel et al. 2005)	
$UO_2(OH)(EDTA)^{3-}$	5.9	(Hummel 1993)	(1)
$UO_2(OH)_2(EDTA)^{4-}$	< -3.1	(Hummel 1993)	(1)
$UO_2(OH)_3(EDTA)^{5-}$	< -16.1	(Hummel 1993)	(1)
$(UO_2)_2(EDTA)_2^{4-}$	26.77	(Rihs et al. 2004)	(2)
$(UO_2)_2(OH)(EDTA)^{-}$	13.06	(Rihs et al. 2004)	(2)
$(UO_2)_4(OH)_4(EDTA)_2^{4-}$	15.34	(Rihs et al. 2004)	(2)
$(UO_2)_6(OH)_4(EDTA)_3^{4-}$	34.3	(Rihs et al. 2004)	(2)

(1) Estimated value.
(2) Original source (Silva & Simoes 1968), not corrected to I=0.

From the data shown in Table 10-1, the results in Figure 10-1 can be obtained. According to that figure, the ternary species $UO_2(OH)_2(EDTA)^{4-}$, if existing, could play an important role in the U(VI)-EDTA systems under alkaline environments. However, no experimental evidences of the formation of these species are available.

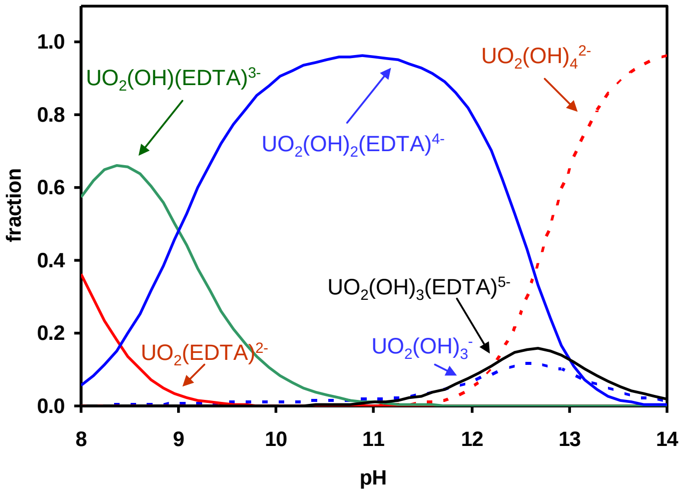

Figure 10-1. Suggested speciation scheme for the U(VI)-EDTA system, according to the stability constants in Table 10-1. $[U]=1\cdot10^{-7}$ M, $[EDTA]=1\cdot10^{-4}$ M.

10.2 Objectives

The main objective of this work was the study of the role of EDTA on U(VI) solubility.

10.3 Solubility experiments

The determined solubility of sodium uranate at the different EDTA concentrations is shown in Figure 10-2 (blue diamonds). There is no influence of EDTA on the solubility of the solid for EDTA concentrations $-4 < \log [EDTA] < -2.5$. Nevertheless, if the speciation scheme shown in Table 10-1 is taken into account, a solubility increase would be expected (red line in the figure).

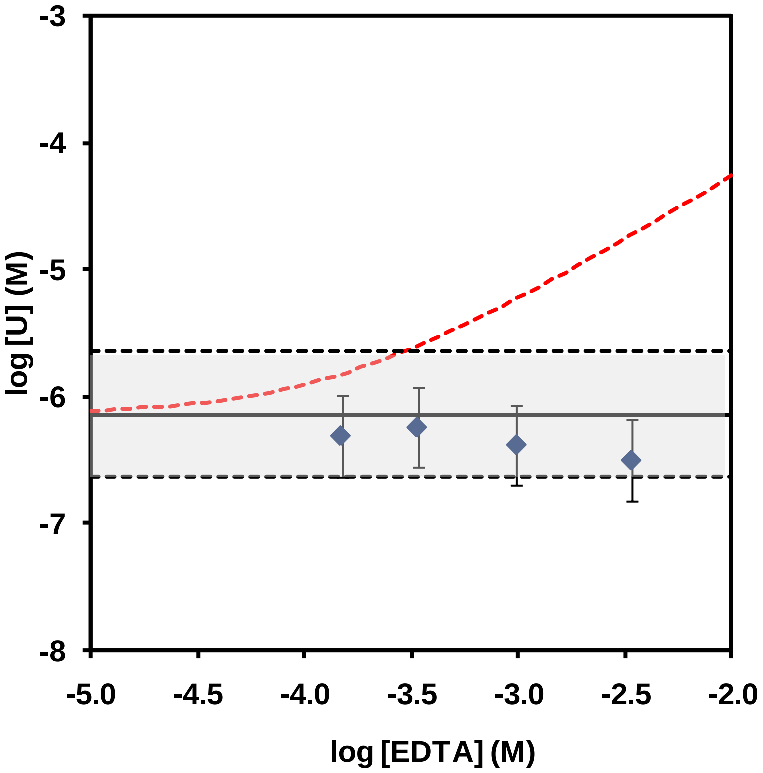

Figure 10-2. Blue diamonds: Sodium uranate solubility (undersaturation direction) in I=0.5M $NaClO_4$ media at pH=11.8 and different EDTA concentrations (>26 days). Grey zone: Sodium uranate solubility in the absence of organic ligands. Solid red line: calculated sodium uranate solubility using U(VI)-EDTA stability constants highlighted in grey in Table 10-1.

Thus, EDTA concentrations in the range -4 < log [EDTA] < -2.5 do not increase the solubility of uranium at pH=11.8. If $UO_2(OH)_x(EDTA)^{(x+2)-}$ species exist, their stability constants are lower than the ones suggested in Table 10-1.

10.4 Summary and conclusions

- EDTA concentrations in the range -4 < log [EDTA] < -2.5 do not increase the solubility of sodium uranate at pH=11.8.
- The experimental data do not allow to deny neither confirm the existence of $UO_2(OH)_n(EDTA)^{(n+2)-}$ species.

- If existing, stability constants for $UO_2(OH)_n(EDTA)^{(n+2)-}$ species would be lower than the ones estimated in the literature.

11 Summary and further work

11.1 Summary

In this work the effect of organic ligands (gluconate, isosaccharinate and EDTA) in the solubility of radionuclides (Th(IV), U(VI)) under alkaline conditions were investigated.

Results show that all the studied ligands are able to significantly enhance the solubility of thorium under the studied conditions. Nevertheless, in the alkaline pH range the complexation strength of the polyhydroxycarboxylic acids (gluconate and isosaccharinate) towards thorium is higher than that of the studied polyaminocarboxylic acid (EDTA). A high complexation capacity in the alkaline pH range is characteristic of polyalcohols (and polyhydrocarboxylic acids), due to the deprotonation of alcoholic hydroxy groups (Gyurcsik & Nagy 2000).

Although gluconate is usually used as a chemical analogue for isosaccharinate, the small differences obtained in solubility experiments in the presence of both ligands suggest that this analogy should be used with caution, being gluconate effect on thorium hydroxide solubility higher than that of isosaccharinate.

EXAFS studies do not provide a definitive model of the structure of Th-polyhydroxylic acid complexes. However, the results seem to be consistent with the coordination between the metal and the ligand through an ionized-diol function, instead of a bidentate coordination through the carboxylic group, in agreement with the deprotonation of alcoholic hydroxy groups mentioned before. No evidences of the formation of polynuclear complexes have been found under the studied conditions.

The EDTA structure is significantly different from that of gluconate or isosaccharinate, as it does not contain alcoholic hydroxy groups. With increasing pH, the hydrolysis of the metal ion may prevent the coordination of the EDTA ligand to thorium. For the same reason, thorium complexation with EDTA is significantly affected by the competitive formation of $NaEDTA^{3-}$ and $Ca(EDTA)^{2-}$ complexes, as Na or Ca are less acidic than Th.

The presence of competing ions should then be taken into account when calculating the influence of the organic ligands on radionuclide mobility. The case of calcium is particularly significant, taking into account that this element is one of the main components of cement (a material ubiquitous in the radioactive waste repositories).

Calcium was shown to be a significant competitor for thorium, due to the formation of Ca-EDTA complexes. Thus, the presence of calcium reduces thorium mobility in the presence of EDTA.

The formation of ternary Ca-Th-L species (where L is a polyhydroxycarboxylic acid), although reported in some publications, was not confirmed in present work. It was concluded that, in alkaline systems (pH=12) where gluconate is present, calcium concentrations below 10^{-2}M may not enhance significantly thorium hydroxide solubility. In the same sense, EXAFS studies did not allow to observe any changes in the structure of the thorium-gluconate complex when calcium was present in the media.

U(VI)–gluconate and U(VI)-EDTA complexes in the alkaline pH range were also investigated. The formation of $UO_2(OH)_n(GH_3)^{n-}$ increases significantly sodium and potassium uranates solubility at pH=12 and gluconate concentrations higher than 10^{-2} M, thus affecting the mobility of U(VI). However, the stoichiometry of this complex remains unclear; further studies are necessary before those conclusions can be extrapolated to other pH values.

U(VI) is predominantly penta coordinated, with all exchangeable ligands perpendicular to the O=U=O axis (Glaus et al. 2000). On the contrary Th(IV) is expected to have a coordination number of 9 or 10 (Szabo et al. 2006) and has a higher tendency to hydrolysis. As a consequence, the complexation of U(VI) with a polyhydroxycarboxylic acid such as gluconate is expected to be weaker than the complexation of Th(IV) with the same ligand.

EDTA concentrations in the range -4 < log [EDTA] < -2.5 do not increase the solubility of sodium uranate at pH=11.8; the experimental data obtained do not allow to deny neither confirm the existence of U(VI)-OH-EDTA species. The geometry of UO_2^{2+} and that of EDTA only permits coordination of at most one iminodiacetate moiety. Consequently, the relative stability of U(VI)-EDTA complexes is expected to be lower than the stability of the complexes of EDTA with other cations (Glaus et al. 2000), as for example Th(IV).

11.2 Further work

In present work, some questions that deserve further investigation have been raised.

First of all, some differences have been observed in solubility experiments from undersaturation and oversaturation directions under high gluconate or isosaccharinate concentrations. Artifacts due to kinetic factors or insufficient solid separation were discarded in several tests done in present work. Further studies are necessary to investigate the reasons behind these observations.

The particular structure of the complexes formed also deserves further investigation. EXAFS techniques have been successfully used to increase the knowledge on this particular subject. Nevertheless, the use of additional techniques as nuclear magnetic resonance (NMR) spectroscopy could also provide valuable information.

Paper I

(Published)

E. Colàs, M. Grivé, I. Rojo and L. Duro
Solubility of $ThO_2 \cdot xH_2O$(am) in the presence of gluconate
Radiochimica Acta 99, 269–273 (2011) / DOI 10.1524/ract.2011.1837

Radiochim. Acta **99**, 269–273 (2011) / **DOI** 10.1524/ract.2011.1837
© by Oldenbourg Wissenschaftsverlag, München

Solubility of $ThO_2 \cdot xH_2O(am)$ in the presence of gluconate

By E. Colàs[1,*], M. Grivé[1], I. Rojo[2] and L. Duro[1]

[1] Amphos 21, Pg. Garcia i Fària, 49-51, 08019 Barcelona, Spain
[2] CTM Centre Tecnològic, Av. Bases de Manresa, 1, 08242 Manresa, Spain

(Received February 18, 2010; accepted in revised form February 15, 2011)

Thorium(IV) / Solubility / Gluconate / Complexation

Summary. Thorium complexation with gluconate has been studied from solubility experiments at gluconate concentrations between 10^{-6} and 10^{-1} mol/l, with pH_c between 9 and 13 and $I = 0.5$ M ($NaClO_4$).
Solubility experiments indicate the formation of a 1 : 1 thorium : gluconate complex. The stability constant for this species, extrapolated to I = 0 by using the SIT (specific interaction theory), has been determined to be $\log 10\ K^\circ = -11.5 \pm 0.6$ for the reaction:

$$Th^{4+} + GH_4^- + 2H_2O = Th(OH)_2(GH_2)^- + 4H^+$$

In the presence of $ThO_2 \cdot xH_2O$, sorption of the organic ligand onto solid surface seems to limit thorium dissolution.

1. Introduction

Concrete and cement materials used in radioactive waste disposal must fulfill several requirements to ensure mechanical stability and durability of the structures. Their water to total cement material ratio is usually minimized, and a highly compact concrete, with a low porosity, is used, in order to reduce radionuclide mobility [1]. In these materials, organic admixtures are necessary to compensate the low water content and to achieve the fluidity necessary for cement pouring. Gluconic acid (HGH_4, Fig. 1) is a polyhydroxy carboxylic acid commonly used as an additive in concrete formulations [2]. As a consequence, it may be found in radioactive waste repositories, where cement materials are used. It can also be used as a simple molecule representative of the effect that complex superplastizers (such as carboxylic ether polymers) may have under cementitious conditions. Its structure is similar to that the one of isosaccharinate, the most important product of alkaline degradation of cellulose which is of major concern in many performance assessments of radioactive waste repositories [3].

A number of investigations indicate that actinides may form stable complexes with polyhydroxy carboxylic acids such as gluconate [4–10] or isosaccharinate [7, 8, 11–14], which may lead to an enhancement of their mobility. However, as far as the authors know the number of studies involving thorium and gluconate is limited [5, 8], and data in absence of calcium is unpublished [6].

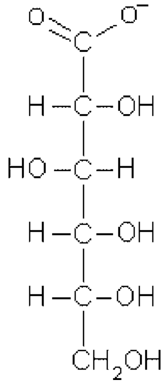
Fig. 1. GH_4^- chemical structure. H_4 refers to the hydrogens of the secondary alcohols in the molecule [15].

The present work aims at quantifying the influence of gluconate on thorium solubility, especially in the alkaline pH range characteristic of cementitious environments. The data, obtained in the absence of calcium, will be complemented with further information related with the influence of calcium in the system in subsequent publications.

2. Experimental

2.1 Reagents and solutions

$NaClO_4 \cdot H_2O(s)$ (p.a.) and sodium gluconate ($NaC_6H_{11}O_7$, p.a.) were purchased from Sigma Aldrich, and NaOH(s) from Panreac. Thorium nitrate solution was obtained from J.T. Baker. All solutions were prepared with ultra pure water purified with a MilliQ-academic (Millipore) apparatus. Reagents and solutions were CO_2-free and were prepared and stored inside a nitrogen glove box.

pH_c was determined using an alkaline resistant combined glass electrode (Crison) where the reference electrolyte had been replaced by the background electrolyte used in the experiments (0.5 M $NaClO_4$) [16]. The electrode was calibrated using a Gran titration procedure [17] where 50 ml of 0.5 M $NaClO_4$ were titrated with a 0.06 M $HClO_4$ solution.

.2 Solubility experiments

Thorium hydroxide was prepared by slow titration under constant stirring of a thorium nitrate solution with carbonate-free NaOH up to pH 10 under nitrogen atmosphere [18].

---

[*] Author for correspondence (E-mail: eli.colas@amphos21.com).

The precipitate was afterwards filtered through 0.22 μm nylon filters under nitrogen atmosphere, washed several times with carbonate-free water, and dried in a vacuum desiccator for one week. X-ray diffraction analysis of the solid showed broad bands, indicating a low cristallinity degree of the material.

Solubility experiments from both oversaturation and undersaturation direction were done using polypropylene tubes (20–50 ml) at 25 ± 2 °C. Undersaturation experiments were performed by contacting 0.06g of solid thorium hydroxide with 20 ml of solution containing different concentrations of gluconate. In the case of experiments from oversaturation direction, the solution was spiked with an acidic concentrated thorium nitrate solution (4×10^{-2} M), so that the final thorium concentration in the tubes was 1×10^{-3} M. In both cases CO_2-free NaOH was used to adjust the solutions to the desired pH values. Ionic strength was kept at $I = 0.5$ M ($NaClO_4$-NaOH-Na(GH_4)). The tubes were kept under constant stirring for different time intervals. Preliminary experiments did not show significant sorption on tube walls within thorium detection limits (1×10^{-9} M).

1 ml aliquots of the samples were filtered through polyether sulfone membrane filters (Microsept™ 1 kDa, pore size ≈ 1.2 nm or 300 kDa, pore size ≈ 20 nm [19]) prior to thorium analysis. These filters have been reported to allow successful separation of thorium colloids [19].

Thorium concentrations were determined by ICP-MS (Agilent 7500cx). Detection limit for Th in the original solutions (after dilution with HNO_3 2%) was 1×10^{-9} mol/l. SEM analyses were carried out with a field emission Ultra Plus ZEISS equipment. Gluconate has been measured as total organic carbon concentration using TOC equipment (Shimadzu TOC-5050A) after dilution and acidification of the samples.

3. Results

Prior to the experiments in the presence of gluconate, the solubility of amorphous thorium hydroxide in the absence of organic ligands was determined. Results are shown in Fig. 2, in comparison with previous literature data. Evaluation of measured thorium concentrations (solid symbols in the figure) by using FITEQL [20], with thermodynamic data and SIT coefficients based on [21] (see Tables 1 and 2), results in the solubility constant (with 2σ uncertainty) reported in Eq. (1).

$$ThO_2 \cdot xH_2O + 4H^+ = Th^{4+} + (2+x)H_2O$$
$$\log_{10} K^\circ = 8.8 \pm 0.6 \qquad (1)$$

$\log_{10} K^\circ = 8.8 \pm 0.6$ is in agreement within the uncertainty limits with $\log_{10} K^\circ = 8.5 \pm 0.9$ for ThO_2(am, hyd, aged) solid reported in the 2009 NEA-OECD thermodynamic data review of thorium [21].

In the presence of GH_4^-, SEM images (Fig. 3) provide evidences of the reaction of solid thorium hydroxide with a gluconate solution at alkaline pH values ($pH_c = 12$). The solid particles in Fig. 3a, which were not in contact with gluconate, present sharp edges even after 500 d in contact with a $pH_c = 12$ solution. On the contrary, thorium hydrox-

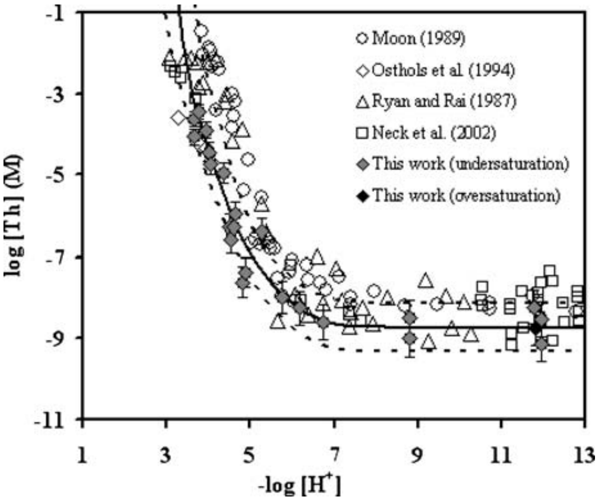

Fig. 2. Solubility of $ThO_2 \cdot xH_2O$ ($I = 0.5$ M, $NaClO_4$) from undersaturation (grey solid symbols) and oversaturation (black solid symbols) after > 40 d and 1 kDa or 300 kDa filtration, and comparison with previous literature data [18, 22–24]. Solid line stands for the calculated thorium hydroxide solubility in the absence of organic ligands, using the data in Tables 1 and 2 (with 2σ corresponding uncertainty, dashed line).

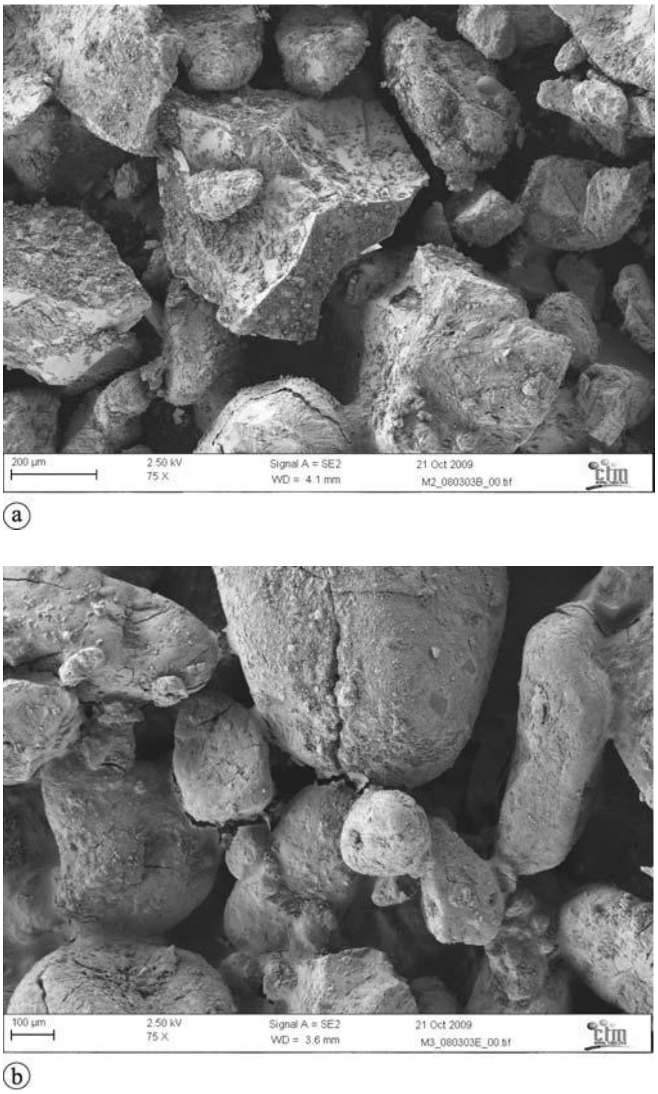

Fig. 3. SEM images of thorium hydroxide after contact with 0.5 M $NaClO_4$ solution for > 500 d. (**a**) No organic ligand, $pH_c = 12$, (**b**) $[GH_4^-] = 0.01$ M, $pH_c = 12$.

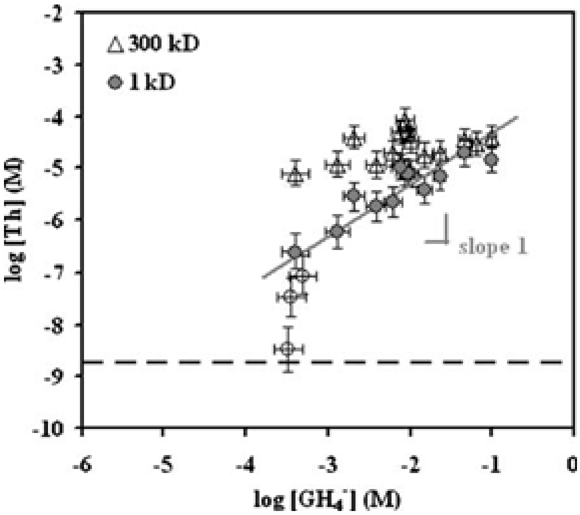

Fig. 4. Solubility of $\mathrm{ThO_2 \cdot xH_2O}$ after > 39 d as a function of measured gluconate concentration at fixed $\mathrm{pH_c} = 12$ ($I = 0.5$ M, $\mathrm{NaClO_4}$). Open triangles: after 300 kDa filtration. Circles: after 1 kDa filtration. Open circles indicate the samples where gluconate may be sorbed on the solid (see text). Dashed line is thorium hydroxide solubility in the absence of gluconate.

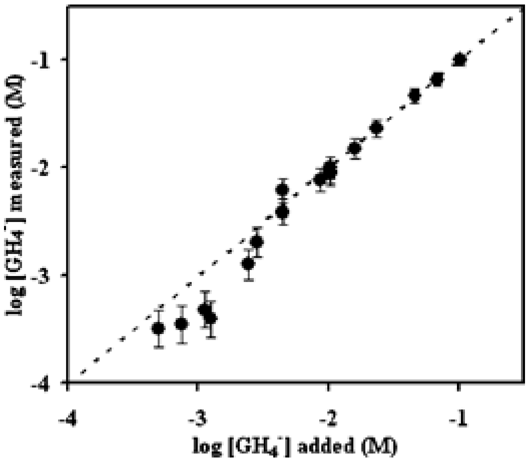

Fig. 5. Added *vs.* measured gluconate concentrations in solution. Detection limit of measured gluconate is 1×10^{-4} M.

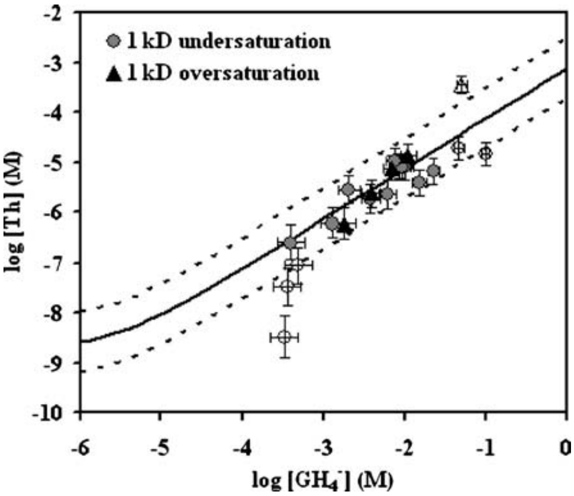

Fig. 6. Solubility of $\mathrm{ThO_2 \cdot xH_2O}$ as a function of gluconate concentration at fixed $\mathrm{pH_c} = 12$ ($I = 0.5$ M, $\mathrm{NaClO_4}$) after 1 kDa filtration. Solid black triangles: oversaturation direction, (15 or 149 d). Circles: undersaturation direction, $t > 39$ d. Solid line is thorium hydroxide solubility taking into account $\mathrm{Th(OH)_2(GH_2)^-}$ formation (with uncertainty as 2σ, dotted line).

ide sample that has been in contact with gluconate presents blunt edges (Fig. 3b).

The solubility of $\mathrm{ThO_2 \cdot xH_2O}$ (from undersaturation direction) as a function of measured gluconate concentration at fixed $\mathrm{pH_c} = 12$ has been studied. Microsept 1 kDa filters (grey circles in the figure) led to lower thorium concentrations after filtration than 300 kDa filters (triangles in the figure), specially at thorium concentrations higher than 5×10^{-7} M (see Fig. 4). This may be due to the formation of different gluconate-containing species, some of them larger than 1.2 nm, which would not pass the 1 kDa filter. A similar situation had been described for thorium hydroxide solubility in the presence of carbonates [19]; in this case, higher thorium solubilities were measured after 220 nm filtration than after 1.2 nm filtration. These differences were suggested to be caused by the formation of carbonate bridged thorium colloids [19].

Thorium hydroxide solubility increases approximately one order of magnitude with one order of magnitude increase in the gluconate concentration (Fig. 4). Steady state concentrations, (where thorium aqueous concentrations do not vary within 5%) are reached in approximately 30 d. Fig. 4 includes data measured between 39 and 113 d in different experimental sets. The possibility of all thorium hydroxide solid being dissolved (as mentioned for example in [25] in the case of thorium solubility experiments in the presence of EDTA) has been discarded, as solid is still visible at the bottom of the tubes after the end of the experiment.

Additions of small amounts of gluconate result in a decrease in measured gluconate concentration in solution (see Fig. 5). This observation would indicate that gluconate is sorbing onto the solid thorium hydroxide surface, preventing the formation of aqueous thorium-gluconate complexes, specially at low gluconate concentrations (open circles in Fig. 4). Previous literature data on EDTA [25] and citrate [26] are in agreement with those suggestions.

The observed decrease of measured gluconate with respect the initial gluconate concentrations in the experiments with solid thorium hydroxide initially present, led to the performance of several additional solubility experiments from oversaturation direction. The comparison between the results from both oversaturation and undersaturation (see Fig. 6), indicate that measured thorium concentrations from both directions are not in agreement at high gluconate concentrations ($> 2 \times 10^{-2}$ M). Given that in both cases samples have reached equilibrium (thorium aqueous concentrations measured in oversaturation experiments are identical after 15 or 141 d) the disagreement seems not to be related to kinetic factors.

Taking into account the high amount of gluconate present in the system, sorption (or even coprecipitation) of gluconate onto the solid surface could limit thorium dissolution in the experiments from undersaturation direction with higher gluconate concentrations.

As a consequence, only data in agreement from both undersaturation and oversaturation directions have been evaluated to provide thermodynamic stability constants for the formation of Th-GLU complexes.

Table 1. Thermodynamic data used in the calculations.

Reaction	$Log_{10}K^0$	Reference
$Th^{4+} + H_2O = Th(OH)^{3+} + H^+$	-2.5±0.5	[21]
$Th^{4+} + 2H_2O = Th(OH)_2^{2+} + 2H^+$	-6.2±0.5	[21]
$Th^{4+} + 3H_2O = Th(OH)_3^{+} + 3H^+$	-11.0±1.0	[29][1]
$Th^{4+} + 4H_2O = Th(OH)_4(aq) + 4H^+$	-17.4±0.7	[21]]
$6Th^{4+} + 14H_2O = Th_6(OH)_{14}^{10+} + 14H^+$	-36.8±1.2	[21]
$6Th^{4+} + 15H_2O = Th_6(OH)_{15}^{9+} + 15H^+$	-36.8±1.5	[21]
$4Th^{4+} + 12H_2O = Th_4(OH)_{12}^{4+} + 15H^+$	-26.6±0.2	[21]
$Th^{4+} + GH_4^- + 2H_2O = Th(OH)_2(GH_2)^- + 4H^+$	-11.5±0.6	This work
$ThO_2{\cdot}xH_2O + 4H^+ = Th^{4+} + (2+x)H_2O$	8.8±0.6	This work

[1] Upper limit value (see [21])

Table 2. SIT ion interaction parameters used in the calculations.

j	*k*	$\varepsilon_{(j,k)}$	Reference
H^+	ClO_4^-	0.14	[21]
Th^{4+}	ClO_4^-	0.70	[21]
$Th(OH)^{3+}$	ClO_4^-	0.48	[21]
$Th(OH)_2^{2+}$	ClO_4^-	0.33	[21]
$Th(OH)_3^{+}$	ClO_4^-	0.15	[21]
$Th_6(OH)_{14}^{10+}$	ClO_4^-	2.2	[21]
$Th_6(OH)_{15}^{9+}$	ClO_4^-	1.85	[21]
$Th_4(OH)_{12}^{4+}$	ClO_4^-	0.56	[21]
Na^+	GH_4^-, $Th(OH)_2(GH_2)^-$	-0.07	This work[1]

[1] In analogy with $\varepsilon(Na^+, Hox^-)$ reported in [21].

Data from both oversaturation and undersaturation directions after 1 kDa filtration with gluconate concentrations between 2×10^{-2} and 4×10^{-4} M (filled symbols in Fig. 6) have been evaluated by using FITEQL [20] for parameter adjustment. The formation of a 1 : 1 Th : gluconate complex (Eq. (2)), with $\log_{10} K = -13.9 \pm 0.6$ at $I = 0.5$ (solid line in Fig. 6), provides an explanation for the measured concentrations in solution in oversaturation experiments. The value of WSOS/DF obtained (1.2) indicates a satisfactory optimization procedure, as values $0.1 < \text{WSOS/DF} < 20$ are common for a reasonable good fit [20].

$$Th^{4+} + GH_4{}^- + 2H_2O = Th(OH)_2(GH_2)^- + 4H^+ \qquad (2)$$

Measured thorium hydroxide solubility does not allow to differentiate between the formation of $Th(OH)_2(GH_2)^-$ (Eq. (2)) or other species such as $Th(OH)_4(GH_4)^-$ or $Th(G)^-$. Polyhydroxylic compounds (such as gluconate) may lose one or more hydroxylic protons to give a metal-alcoholate complex under alkaline solutions and in the presence of metals [10, 27]. In the case of thorium, coordination has been suggested to occur by an ionized-diol function in the alkaline pH range (pH > 9) [28]. This hypothesis agrees with the formation of $Th(OH)_2(GH_2)^-$ (Eq. (2)). EXAFS studies are on-going to characterize the actual structure of the complex formed in solution.

The stability constant obtained at $I = 0.5$ M has been recalculated to $I = 0$ using the SIT model. As $\varepsilon(Na^+, GH_4{}^-)$ and $\varepsilon(Na^+, Th(OH)_2(GH_2)^-)$ are not available, they have been estimated to be -0.07 (in analogy with $\varepsilon(Na^+, Hox^-)$ reported in [21]). A similar approach has been used previously in the case of isosaccharinate complexes with thorium [14].

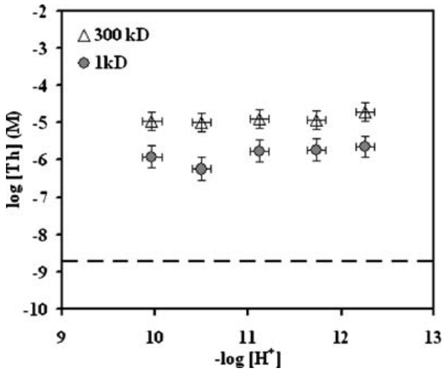

Fig. 7. Solubility of $ThO_2 \cdot xH_2O$ as a function of pH_c and initial gluconate concentration 4.5×10^{-3} M after 112 d ($I = 0.5$ M, $NaClO_4$). Open triangles: after 300 kDa filtration. Solid circles: after 1 kDa filtration. Dashed line is thorium hydroxide solubility in the absence of gluconate.

Equilibrium constants and ion interaction coefficients used in the calculations are reported in Tables 1 and 2.

As far as the authors are aware, the only work dealing with the solubility of Th in the presence of gluconate (and in the absence of calcium) is an unpublished work from Felmy [6]. Felmy [6] studied the influence of gluconate 1×10^{-2} M on the solubility of thorium hydroxide at different pH values at $I = 0.5$ M. The experimental data in the pH range 9–12 showed an increase of the solubility with a slope of approx. +1, which may indicate the loss of a proton in agreement with the reaction: $ThO_2(am) + GH_4{}^- + 2H_2O = Th(OH)_4(GH_3)^{2-} + H^+$ [2]. This trend is not observed in the data at different pH values obtained in the present work (see Fig. 7). Lack of detailed experimental information in [6] makes difficult a detailed investigation on this disagreement.

4. Conclusions

Results show that gluconate is able to significantly enhance thorium hydroxide solubility at alkaline pH values. The coordination between the metal and the ligand may take place through an ionized-diol function. Differences observed after filtration with 300 kDa (≈ 20 nm) or 1 kDa (≈ 1.2 nm) pore-size filters suggest that additional gluconate-containing polynuclear species may also be formed in solution.

The results suggest the coordination of one Th(IV) by one gluconate ligand. A stability constant for the formation of this complex has been calculated.

Differences have been observed in solubility experiments from undersaturation and oversaturation directions under high gluconate concentrations. These differences may be attributed to the sorption (or coprecipitation) of gluconate onto solid thorium hydroxide surface, resulting in a limitation of the thorium dissolved in the aqueous phase.

Further spectroscopic studies are on-going to provide a) evidences on the coordination suggested for the Th-gluconate complex and b) a definitive explanation for the differences observed on measured thorium concentrations between solubility experiments from oversaturation and undersaturation direction.

Acknowledgment. This work has been financially supported by ANDRA. Eric Giffaut is acknowledged for fruitful scientific discussions. Thanks are due to the reviewers for their comments, which improved the quality of the original manuscript. I.R. acknowledges the Generalitat de Catalunya for her research contract ("Beatriu de Pinós" program).

References

1. ANDRA. Dossier 2005 Argile -architecture and management of a geological disposal system. ANDRA Report Series (2005).
2. Gaona, X., Montoya, V., Colàs, E., Grivé, M., Duro, L.: Review of the complexation of tetravalent actinides by ISA and gluconate under alkaline to hyperalkaline conditions. J. Contam. Hydrol. **102**, 217 (2008).
3. Hummel, W., Anderegg, G., Rao, L., Puigdomènech, I., Tochiyama, O.: Chemical thermodynamics of compounds and complexes of U, Np, Pu, Am, Tc, Se, Ni and Zr with selected organic ligands. In: *Chemical Thermodynamics*. Vol. 9 (Mompean, F. J., Illemassène, M., Perrone, J., eds.) Elsevier, North-Holland, Amsterdam (2005).
4. Sawyer, D. T., Kula, R. J.: Uranium(VI) gluconate complexes. Inorg. Chem. **1**, 303 (1962).
5. Baston, G. M. N., Berry, J. A., Bond, K. A., Brownsword, M., Linklater, C. M.: Effects of organic degradation products on the sorption of actinides. Radiochim. Acta **52/53**, 249 (1992).
6. Felmy, A. R.: Chemical speciation of Americium, Curium and selected tetravalent actinides in high level waste. Technical report, PNNL. EMSP Project 73749 (2004).
7. Warwick, P., Evans, N., Hall, T., Vines, S.: Stability constants of uranium(IV)-α-isosaccharinic acid and gluconic acid complexes. Radiochim. Acta **92**, 897 (2004).
8. Tits, J., Wieland, E., Bradbury, M. H.: The effect of isosaccharinic acid and gluconic acid on the retention of Eu(III), Am(III) and Th(IV) by calcite. Appl. Geochem. **20**, 2082 (2005).
9. Zhang, Z., Clark, S. B., Tian, G., Zanonato, P. L., Rao, L.: Protonation of D-gluconate and its complexation with Np(V) in acidic to nearly neutral solutions. Radiochim. Acta **94**, 531 (2006).
10. Zhang, Z., Helms, G., Clark, S. B., Tian, G., Zanonato, P. L., Rao, L.: Complexation of uranium(VI) by gluconate in acidic solutions: a thermodynamic study with structural analysis. Inorg. Chem. **48**, 3814 (2009).
11. Rai, D., Rao, L., Moore, A.: The influence of isosaccharinic acid on the solubility of Np(IV) hydrous oxide. Radiochim. Acta **83,** 9 (1998).
12. Vercammen, K., Glaus, M. A., Van Loon, L. R.: Complexation of Th(IV) and Eu(III) by α-isosaccharinic acid under alkaline conditions. Radiochim. Acta **89**, 393 (2001).
13. Allard, S., Ekberg, C.: Complexing properties of alpha-isosaccharinate: Stability constants, enthalpies and entropies of Th-complexation with uncertainty analysis. J. Solut. Chem. **35**, 1173 (2006).
14. Rai, D., Yui, M., Moore, D. A., Rao, L.: Thermodynamic model for ThO_2(am) solubility in isosaccharinate solutions. J. Solut. Chem. **38**, 1573 (2009).
15. Sawyer, D. T.: Metal-gluconate complexes. Chem. Rev. **64**, 633 (1964).
16. Kitamura, A., Kohara, Y.: Carbonate complexation of neptunium(IV) in highly basic solutions. Radiochim. Acta **92**, 583 (2004).
17. Gran, G.: Determination of the equivalence point in potentiometric titrations. Part II. Analyst **77**, 661 (1952).
18. Neck, V., Müller, R., Bouby, M., Altmaier, M., Rothe, J., Denecke, M. A., Kim, J. I.: Solubility of amorphous Th(IV) hydroxide – application of LIBD to determine the solubility product and EXAFS for aqueous speciation. Radiochim. Acta **90**, 485 (2002).
19. Altmaier, M., Neck, V., Müller, R., Fanghänel, T.: Solubility of $ThO_2 \cdot H_2O$(am) in carbonate solution and the formation of ternary Th(IV) hydroxide-carbonate complexes. Radiochim. Acta **93**, 83 (2005).
20. Herbelin, A. L., Westall, J. C.: FITEQL 4.0: a computer program for determination of chemical equilibrium constants from experimental data. Technical Report 99-01. Department of Chemistry, Oregon State University, Corvallis (1999).
21. Rand, M., Fuger, J., Grenthe, I., Neck, V., Rai, D.: Chemical thermodynamics of thorium. In: *Chemical Thermodynamics*. Vol. 11 (Mompean, F. J., Perrone, J., Illemassène, M., eds.) Elsevier, North-Holland, Amsterdam (2009).
22. Moon, H. C.: Equilibrium ultrafiltration of hydrolized Thorium(IV) solutions. Bull. Korean Chem. Soc. **10,** 270 (1989).
23. Ryan, J. L., Rai, D.: Thorium(IV) hydrous oxide solubility. Inorg. Chem. **26**, 4140 (1987).
24. Osthols, E., Bruno, J., Grenthe, I.: On the influence of carbonate on mineral dissolution III. The solubility of microcrystalline ThO_2 in CO_2-H_2O media. Geochim. Cosmochim. Acta **58**, 613 (1994).
25. Xia, Y., Felmy, A. R., Rao, L., Wang, Z., Hess, N. J.: Thermodynamic model for the solubility of ThO_2(am) in the aqueous Na^+-H^+-OH^--NO_3^--H_2O-EDTA system. Radiochim. Acta **91**, 751 (2003)
26. Felmy, A. R., Cho, H., Dixon, D. A., Xia, Y., Hess, N. J., Wang, Z.: The aqueous complexation of thorium with citrate under neutral to basic conditions. Radiochim. Acta **94**, 205 (2006).
27. Rendleman, J. A.: Metal-polysaccharide complexes: part I. Food Chem. **3**, 47 (1978).
28. Van Duin, M., Peters, J. A., Kieboom, A. P. G., Van Bekkum, H.: A general coordination-ionization scheme for polyhydroxy carboxylic acid in water. Recl. Trav. Chim. Pays-Bas **108**, 57 (1989).
29. Neck, V., Kim, J. I.: Solubility and hydrolysis of tetravalent actinides. Radiochim. Acta **89**, 1 (2001).

Paper II

(In preparation)

E. Colàs, M. Grivé, I. Rojo and L. Duro
Comparison between gluconate and isosaccharinate influence on thorium solubility
In preparation

Comparison between gluconate and isosaccharinate influence on thorium solubility

Elisenda Colàs[1,*], Mireia Grivé[1], Isabel Rojo[2] and Lara Duro[1]

1 Amphos 21, Pg. Garcia i Faria, 49-51, 08019 Barcelona, Spain.
2 Fundació CTM Centre Tecnològic, Av. Bases de Manresa, 1, 08242 Manresa, Spain

Thorium / Solubility / Gluconate / Isosaccharinate / EXAFS

Abstract.

Gluconate ($C_6H_{11}O_7$) and isosaccharinate ($C_6H_{11}O_6$) are organic substances representative of generic polyhydroxycarboxylic acids that can be present in low- and intermediate- level radioactive wastes. In order to guarantee the safety of the repository, it is necessary to quantitatively predict the reactions that are likely to occur between radionuclides and those complexing agents. The objective of this work is to study the stability behaviour of Th(IV) towards gluconate and isosaccharinate under alkaline conditions.

The study was conducted by means of both solubility and EXAFS experiments; special attention was paid to sample filtration, to allow a successful separation of thorium colloids. Solubility experiments have shown that both gluconate and isosaccharinate are able to significantly increase thorium hydroxide solubility at alkaline pH values. The influence of isosaccharinate on thorium solubility is smaller than the one of gluconate, what is likely due to the differences in the chemical structure of both organic ligands. EXAFS results are consistent with a coordination of the ligand trough ionized diol functions.

Introduction

Low- and intermediate- level radioactive wastes usually have a very diverse origin and composition. A wide variety of materials, some of them made of organic polymers (such as packaging plastics, clothes, paper, gloves, or ion-exchange resins), are generally present in those types of wastes [1,2]. Among these materials, different organic substances in the waste or in degradation products emanating from it, and chemicals added during the building of cementitious barriers in the repository, may exhibit complexing properties towards radionuclides [3].

Gluconate ($C_6H_{11}O_7$) and isosaccharinate ($C_6H_{11}O_6$) are polyhydroxycarboxylic acids that can be present in nuclear waste repositories. Sodium gluconate was suggested as a representative model-compound for a wide variety of additives used by cement manufacturers [4]. In spite of being a “simple” molecule compared to the complex chemical structures of commercial cement additives, gluconate complexation capacity towards radionuclides is very high. Isosaccharinate is the main degradation product from cellulose in alkaline conditions.

The study of potential migration of radionuclides from radioactive waste disposal installations is considered in any safety assessment. To this aim, the complexing capacity of the different compounds present in the wastes and radionuclides must be quantitatively assessed [5]. The complexation of radionuclides by short-chain organic ligands present in the wastes is not completely understood. Although a reasonable amount of information on the gluconate complexation with transition metals exists in the literature [6], the level of knowledge on the system gluconate-radionuclide is far from complete [7], and the number of experimental studies dealing with isosaccharinate-radionuclide complexes is really scarce [5].

The objective of this work is the study of the complexation of actinides with gluconate and isosaccharinate under alkaline conditions. Tetravalent actinides are expected to dominate under the reducing conditions of the repository [3], so the experimental work was conducted with Th(IV). The advantages of using Th(IV) instead of other actinides are a) its low radioactivity when natural thorium is used in the experiments, making its manipulation easier and b) the fact that thorium is not redox sensitive, so that no special procedures to exclude oxygen from the experiments are needed, as it would have been the case if U(IV) was used instead.

Experimental

Reagents and solutions

$NaClO_4 \cdot H_2O(s)$ (p.a.) and sodium gluconate ($NaC_6H_{11}O_7$, p.a.) were purchased from Sigma Aldrich, $Na_2CO_3(s)$ and $NaHCO_3(s)$ from Scharlau and NaOH(s), from Panreac. Thorium nitrate solution (1% w/v) was obtained from J.T. Baker. Ultrapure water from a Milli-Q Academic water purification system was degassed by boiling and cooling in a $N_2(g)$ atmosphere and used in all experiments. Reagents and solutions were CO_2-free and were prepared and stored inside a nitrogen glove box.

pH_c was determined using an alkaline resistant combined glass electrode (Crison 52.22) where the reference electrolyte had been replaced by the background electrolyte used in the experiments (0.5 M $NaClO_4$) [8]. The electrode was calibrated using a Gran titration procedure [9], where 50 ml of $NaClO_4$ 0.5M were titrated with a 0.06M $HClO_4$ solution.

Sodium isosaccharinate was synthetized following the procedure reported by Whistler and co-workers [10] with some modifications [11,12]. Calcium isosaccharinate was obtained through the alkaline degradation of α-lactose hydrate (Sigma Aldrich) in saturated aqueous $Ca(OH)_2(s)$ (Panreac) solutions. The X-ray diffraction pattern (Bruker D-5005) of the calcium solid obtained was in agreement with the one reported in Rai and co-workers [13] for crystalline calcium isosaccharinate. Isosaccharinate sodium salt was obtained exchanging calcium against sodium with a cation exchange resin (Chelex 100, Bio-Rad) in the sodium form [14-16]. Isosaccharinate sodium salt was characterized by nuclear magnetic resonance spectroscopy (Bruker ARX 300); $^{13}C\{^1H\}$ NMR (75.47 MHz) spectra obtained confirmed the purity of the organic ligand, by comparison with the spectra reported by Cho et al. [17].

Thorium hydroxide for undersaturation experiments was prepared from a thorium nitrate solution by slow titration with carbonate-free NaOH up to pH 10 with constant stirring under a nitrogen atmosphere [18]. A complete description of the preparation and characterization of the solid is available in a previous work [19]. Solubility measurements of this solid in the absence of organic ligands are in agreement with data reported in previous publications [20].

Solubility experiments

The solubility experiments were done in polypropylene tubes (20-50 ml) at 25±2 ºC. CO_2-free NaOH was used to adjust the solutions to the desired pH value (pH=12). Ionic strength was kept constant at I=0.5M ($NaClO_4$-NaOH-NaL, where L is isosaccharinate or gluconate organic ligand), being $NaClO_4$ the main electrolyte in solution. Tubes were kept under constant stirring for different time intervals. The possible sorption of thorium onto the tube walls was tested by leaching them with 2% HNO_3 after their use; the analysis of the solutions with ICP-MS did not show significant thorium sorption on tube walls within detection limits.

The complexation behaviour was investigated through solubility experiments from both undersaturation and oversaturation directions. Undersaturation experiments were done by contacting 0.06g of solid thorium hydroxide with 20 ml of a solution containing a given organic ligand concentration (10^{-5} to 0.5 M) at pH≈12. Oversaturation experiments were done by preparing 20 ml of a solution containing a given organic ligand concentration (10^{-5} to 0.5 M) at pH≈12 and adding a spike of acidic concentrated thorium solution, being the total thorium concentration in the tubes of 10^{-3} M.

Samples where measured at equilibration times between 29 and 113 days (from undersaturation direction) or between 12 and 141 days (from oversaturation direction). Equilibrium in solubility experiments was assumed to have been reached when thorium concentrations did not vary more than 5% within 48 hours or more. Preliminary test indicated that 10 days were enough to reach equilibrium, which is in agreement with previous observations reported in the literature [21,22].

Aliquots of 1 ml solution were taken and filtered through polyether sulfone membrane filters (Microsept TM 1 kD, pore size ≈1.2 nm [23]) prior to thorium analysis. Those filters were reported to allow successful separation of thorium colloids [23].

Thorium concentrations were determined by ICP-MS (Agilent 7500cx). Detection limit for Th in the original solutions (after dilution with HNO_3 2%) was $1 \cdot 10^{-9}$mol/l. Isosaccharinate and gluconate were measured as total organic carbon concentration using TOC equipment (Shimadzu TOC-5050A) after dilution and acidification of the samples.

EXAFS experiments

EXAFS experiments were conducted in an attempt to increase the knowledge on the structure of the aqueous complexes formed between thorium and polyhydroxycarboxylic acids. The majority of the samples in the solubility experiments presented too low aqueous thorium concentrations to provide useful information, so two concentrated samples were prepared in order to obtain EXAFS data:

-An aqueous Th-gluconate sample was prepared from a solution of gluconate concentration of 0.46 M at pH=11.8 by adding a total thorium concentration of $[Th]_0=1\cdot10^{-3}$, and

-For comparison purposes, a Th-carbonate sample was prepared from a solution of carbonate concentration 0.1 M at pH=9.14, by adding a total thorium concentration of $[Th]_0=1\cdot10^{-3}$ [24]. Under such conditions, both $Th(CO_3)_5^{6-}$ and $Th(OH)(CO_3)_4^{5-}$ are expected to be present in solution.

Samples were filtered using polyether sulfone membrane filters and stored and measured in polyethylene holders.

Thorium L_{III}-edge EXAFS spectra were collected at the ROssendorf Beam Line (ROBL) at the European Synchrotron Radiation Facility (ESRF) located in Grenoble (France). Spectra were collected in fluorescence mode at room temperature. Nine scans for the Th-carbonate sample and ten scans for Th-gluconate sample were collected, pre-treated and averaged using Sixpack [25]. Data analysis was performed using the WinXAS [26] software. Theoretical scattering amplitudes for each absorber and backscattered pair were calculated with the FEFF 8.20 code [27]. The amplitude reduction factor, S_0^2, was defined as 1.0 and a single value of the shift in threshold energy, ΔE_0, was allowed to vary for all coordination shells of a given sample.

The EXAFS spectra were fitted using as a reference the crystal structures of calcium gluconate [28], manganese citrate [29,30] or guanidinium pentacarbonato thorate [31,32]. Those structures allow the identification of the characteristic paths for diol coordination (in calcium gluconate or manganese citrate) or bidentate carbonate coordination (in pentacarbonato thorate). The atomic positions for the calcium gluconate and manganese citrate crystal structures were modified prior to FEFF calculation of the scattering paths to compensate for the difference in atomic radii between Ca(II), Mn(III) and Th(IV).

Results and discussion

Solubility experiments

Previous results [19] showed that gluconate is able to significantly enhance thorium hydroxide solubility at alkaline pH values. Total gluconate concentrations of $4.5\cdot10^{-3}$ M increase the solubility of solid thorium hydroxide ($ThO_2\cdot xH_2O(am)$) by more than two orders of magnitude at pH=12. The experiments suggested the formation of a 1 : 1 thorium : gluconate complex with a stability constant reported in eq. 1.

$$Th^{4+} + GH_4^- + 2H_2O = Th(OH)_2(GH_2)^- + 4H^+$$

$$\log_{10}K(I = 0.5) = -13.9\pm0.6 \qquad (1)\ [19]$$

Similar solubility experiments were conducted to study the complexation capacity of isosaccharinate with Th(IV). Results obtained from undersaturation direction (black circles in Fig.1) show that, in the presence of isosaccharinate, thorium solubility enhancement is slightly lower than the one observed for gluconate.

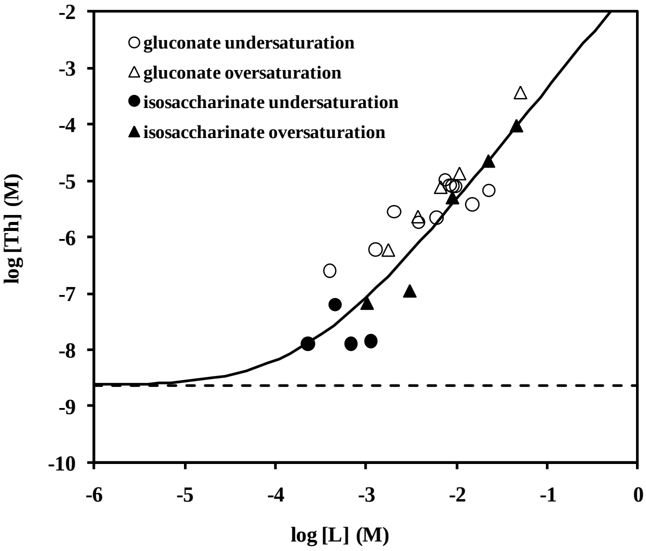

Fig. 1. Solubility of thorium oxyhydroxide from undersaturation (circles) and oversaturation (triangles) direction as a function of the concentration of organic ligand, at fixed pH_c=12 (I=0.5M, $NaClO_4$). Open symbols: In the presence of gluconate [19]. Solid black symbols: in the presence of isosaccharinate (present work). Black solid line: calculated solubility taking into account the formation of a $Th(OH)_2(ISA)^-$ and a $Th(ISA)_2^{2-}$ complex. Dashed line: calculated solubility in the absence of organic ligands.

Results in the presence of gluconate [19] were explained with the formation of a $Th(OH)_2(GH_2)^-$ species in the pH range 10-12.5. A similar species ($Th(OH)_2(ISA)^-$) could be expected to form in the case of thorium-isosaccharinate system. Additional measurements at different pH values are needed to confirm this suggestion and to definitely identify the number of protons involved in the reaction.

At relatively high isosaccharinate concentrations, (log ISA> -2.5) results obtained seem to indicate the formation of a 1 : 2 thorium-isosaccharinate species (Fig. 1). The formation of a 1 : 2 thorium-isosaccharinate complex had already been suggested in previous thorium hydroxide solubility investigations in the presence of isosaccharinate [21].

$$Th^{4+} + ISAH_2^- + 2H_2O = Th(OH)_2(ISA)^- + 4H^+$$
$$\log_{10}K(I = 0.5) \approx -15.3 \qquad (2)\ \text{p.w.}$$

$$Th^{4+} + 2ISAH_2^- = Th(ISA)_2^{2-} + 4H^+$$
$$\log_{10}K(I = 0.5) = -12.2 \pm 1.0 \qquad (3)\ \text{p.w.}$$

The log K value for the formation of these complexes were optimized by using the FITEQL program [33], and the result is shown in eq. 2. The value of WSOS/DF obtained (0.24) indicates a reasonable optimization procedure, as values 0.1 < WSOS/DF < 20 are common for an acceptable fit [33]. An increase in the number of experimental data points would be necessary to reduce this uncertainty. In addition, the points in the region were the 1 : 1 complex is formed show a significant scatter; because of that, the constant obtained has been considered only as approximate.

Both gluconate and isosaccharinate are polyhydroxycarboxylic acids with a similar chemical structure. Similar behaviour for both ligands in front of thorium complexation is observed, with slightly smaller stability for the isosaccharinate than for the gluconate-thorium complex (Fig. 1). A similar conclusion was recently reported by Birjkumar and co-workers [34] for uranyl-gluconate and isosaccharinate complexes. Density functional theory studies conducted by those authors revealed similarities in structure, bonding and coordination geometry but also differences in ΔG values for ligand replacement reactions, suggesting that some differences exist between thermodynamic properties of gluconate and isosaccharinate uranyl complexes. A weaker sorption of isosaccharinate on cement, compared to that of gluconate, was reported by Glaus et al. [35], suggesting a similar trend in both complexation and sorption behaviour of those organic ligands. The acidity of the α-hydroxyl group [17,36,37] may play a key role in the metal-ligand complexation, specially if the coordination between the metal and the ligand takes place through an ionized-diol function [37-39].

EXAFS experiments

The Fourier transformation magnitude of the EXAFS spectra of Th-gluconate (total gluconate concentration of 0.46 M at pH=11.8) and Th-carbonate (total carbonate concentration 0.1 M at pH=9.14) samples are shown in Fig. 2. EXAFS spectra are dominated by ≈10 O atoms in the first thorium coordination shell. In addition, another significant feature is present at uncorrected distances of ≈3.5 and ≈3.7 Å respectively.

The relatively low Th concentration and the high disorder characteristic of aqueous samples result in a limited data quality. Nevertheless, data allow obtaining relevant information.

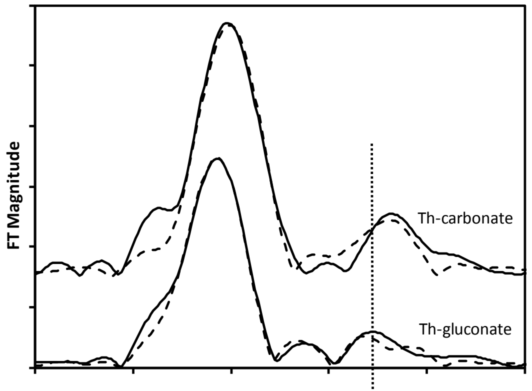

Fig. 2. Experimental data of EXAFS fourier transforms of Th L_{III} edge for Th-gluconate and Th-carbonate solutions (see text). The solid lines are the experimental data, and dashed lines correspond to preliminary theoretical fits. For the meaning of dotted vertical line, see text.

Besides the first oxygen shell, the fits of the Th-gluconate sample indicate the presence of ≈2 carbon atoms at *ca.* 3.4 Å, which can be related to the formation of a complex between Th and the gluconate ligand. The high uncertainty in the coordination number does not allow confirming the number of gluconate ligands involved in the formation of the complex.

The fits of the feature appearing at an uncorrected distance of ≈3.5 Å are only reasonable by assuming the presence of O atoms of an hydroxyl group. Simulations including multiple scattering paths (Th-C-O_{dist}) have not improved significantly the quality of the fit.

Peaks at similar uncorrected distances could also be due to the presence of a Th-Th backscatter that could indicate the formation of dimeric or higher polynuclear complexes [22]. However, the fits using this paths result in unrealistic Th-Th distances of ≈3.7 Å in the studied samples. Those distances are too short for a real Th-Th interaction, which is usually *ca.* 3.99 Å [40,41]. An additional check was conducted by using a similar procedure to the one described by Allen and co-workers [42]. The peak contribution was isolated by subtracting the fit of the first Th-O shell. The residual signal was then Fourier-filtered in the range 3-5 Å to remove noise. According to Allen et al. [42], if the 3.7 Å peak were due to an interaction of Th with a high atomic number atom (such as another Th atom), an increase of the amplitude with k would be expected in this residual spectra, what is not observed in the results (Fig. 3). As a conclusion, the presence of dimeric complexes in significant concentrations in the sample has been discarded.

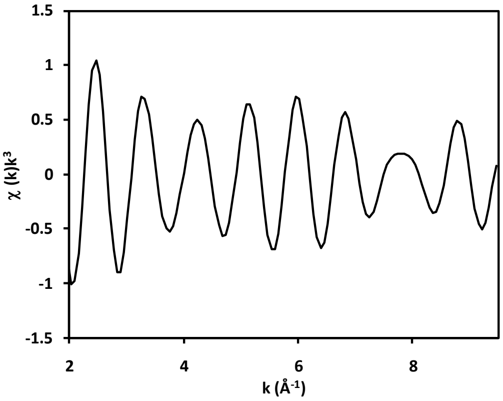

Fig. 3. Fourier-filtered peak at an uncorrected distance of *ca.* 3.5 Å (see text).

In the Th-carbonate spectrum, a similar feature appears at longer uncorrected distances (≈3.7 Å, see dotted vertical line in Fig. 2). In this sample, multiple scattering paths (Th-C-O_{dist} and Th-C-O_{dist}-C) are expected to enhance the observed amplitude, due to the fact that carbonate adopts a symmetric bydentate geometry where the distal oxygen atom is collinear with the carbon atom [24,42]. Those multiple scattering paths have not been identified in the Th-gluconate sample, which may indicate that gluconate is not binding through a bidentate carboxylate function.

Conclusions

This work provides experimental data on the complexation strength of both gluconate and isosacharinate towards thorium and on the potential aqueous species formed. Both ligands are able to significantly increase the thorium solubility at alkaline pH values. The results suggest the coordination of one Th(IV) by one or two polyhydroxycarboxylic ligands, depending on the ligand concentration in solution. Stability constants for the formation of those complexes were determined. Differences between results obtained from oversaturation and undersaturation direction at high ligand concentrations were observed, although a definitive explanation for this phenomenon is still under debate.

EXAFS studies do not provide a definitive model for the coordination in the Th-polyhydroxylic acid complexes. However, the results seem to be consistent with the coordination between the metal and the ligand through an ionized-diol function (options b or c in Fig. 4), instead of a bidentate coordination through the carboxylic group (option a in Fig. 4). No evidences of the formation of polynuclear complexes have been found under the studied conditions.

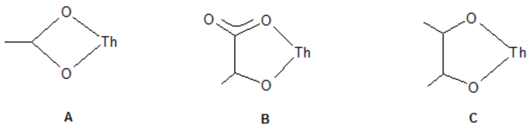

Fig. 4. Scheme for the possible coordination of polyhydroxylic acid complexes with thorium a) bidentate coordination through the carboxylic group b,c) different coordination modes through an ionized-diol function.

Finally, although gluconate is usually used as a chemical analogue for isosaccharinate, the small differences obtained in solubility experiments in the presence of these ligands suggest that this analogy should be used with caution, being gluconate effect on thorium hydroxide solubility higher than isosaccharinate effect in the alkaline pH range.

Acknowledgements. The authors would like to thank the French National Agency for Radioactive Waste Management (ANDRA) for funding this work through the ThermoChimie project. E. Giffaut is acknowledged for fruitful scientific discussions. We acknowledge the ESRF for provision of synchrotron radiation facilities and we would like to thank A. Scheinost and C. Henning for help in using ROBL beamline and with EXAFS data elucidation. We would also thank C. Viñas for NMR analysis of solid isosaccharinate samples.

References

1. ANDRA. Dossier 2005 argile - safety evaluation of a geological repository, ANDRA (2005).
2. ANDRA. Inventaire national des matières et déchets radioactifs 2009, ANDRA (2009).
3. ANDRA. Dossier 2005 Argile. Référentiel de comportement des radionucléides et des toxiques chimiques d'un stockage dans le Callovo-Oxfordien jusqu'à l'homme. Site de Meuse/Haute-Marne, ANDRA (2005).
4. Bradbury, M.H; Van Loon, L.R. Cementitious near-field sorption databases for performance assessment of a L/ILW repository in a Palfris Marl host rock. CEM-94: Update I, June 1997. Technical Report 98-01, PSI (1998).
5. Hummel, W; Anderegg, G; Rao, L; Puigdomènech, I; Tochiyam, O. Chemical Thermodynamics 9: Chemical Thermodynamics of Compounds and Complexes of U, Np, Pu, Am, Tc, Se, Ni Zr with Selected Organic Ligands, OECD Publishing, (2005).
6. Sawyer, D.T. Metal-gluconate complexes, Chem. Rev., **64** (6), 633 (1964).
7. Keith-Roach, M.J; The speciation, stability, solubility biodegradation of organic co-contaminat radionuclide complexes: a review, Sci. Total Environ., **396**, 1 (2008).
8. Kitamura, A; Kohara, Y; Carbonate complexation of Neptunium(IV) in highly basic solutions, Radiochim. Acta , **92**, 583 (2004).
9. Gran, G. Determination of the equivalence point in potentiometric titrations. Part II, The Analyst, **77**, 661 (1952).
10. Whistler, R.L; BeMiller, J.N. Methods in Carbohydrate Chemistry, vol. 2, Reactions of Carbohydrates, chapter α-D-Isossacharino-1,4-lactone. Action of lime water on lactose, pages 477–479. Academic Press, New York (1961).
11. Evans, N.D.M. Studies on metal alpha-isosaccharinic acid complexes. PhD thesis, Loughborough University, (2003).
12. Vercammen, K. Complexation of Calcium, Thorium Europium by alpha-Isosaccharinic Acid under Alkaline Conditions, PhD thesis, Swiss Federal Institute of Technology Zurich, (2000).
13. Rai, D; Rao, L; Moore, A. The influence of isosaccharinic acid on the solubility of Np(IV) hydrous oxide, Radiochim. Acta **83**, 9 (1998).
14. Glaus, M.A; Van Loon, L.R; Achatz, S; Chodura, A; Fischer, K. Degradation of cellulosic materials under the alkaline conditions of a cementitious repository for low intermediate level radioactive waste - Part I: Identification of degradation products, Anal. Chim. Acta, **398**, 111 (1999).
15. Pointeau, I; Hainos, D; Coreau, N; Reiller, P. Effect of organics on selenite uptake by cementitious materials, Waste Management, **26**, 733 (2006).
16. Rai, D; Rao, L; Moore, R.C; Bontchev, R; Holt, K. Development of biodegradable isosaccharinate-containing foams for decontamination of actinides: Thermodynamic kinetic reactions between isosaccharinate actinides on metal concrete surfaces, USDOE Technical Report, EMSP-82715-2004 (2004).
17. Cho, H; Rai, D; Hess, N.J; Xia, Y; Rao, L. Acidity structure of isosaccharinate in aqueous solution: A nuclear magnetic resonance study, J. Solution Chem., **32**, 691 (2003).
18. Neck, V; Müller, R; Bouby, M; Altmaier, M; Rothe, J; Denecke, M.A; Kim, J.I. Solubility of amorphous Th(IV) hydroxide – application of LIBD to determine the solubility product EXAFS for aqueous speciation, Radiochim. Acta, **90** 485 (2002).

19. Colàs, E; Grivé, M; Rojo, I; Duro, L. Solubility of ThO_2•xH_2O(am) in the presence of gluconate, Radiochim. Acta, **99**, 269 (2011).

20. Rand, M; Fuger, J; Grenthe, I; Neck, V; Rai, D. Chemical Thermodynamics 11: Chemical Thermodynamics of Thorium, volume 11 of Chemical Thermodynamics. OECD Publishing, (2009).

21. Rai, D; Yui, M; Moore, D.A. Thermodynamic model for ThO_2(am) solubility in isosaccharinate solutions. J. Solution Chem., **38**, 1573 (2009).

22. Xia, Y; Felmy, A.R; Rao, L; Wang, Z; Hess, N.J. Thermodynamic model for the solubility of ThO_2(am) in the aqueous Na^+-H^+-OH^--NO_3^--H_2O-EDTA system. Radiochim. Acta, **91**, 751 (2003).

23. Altmaier, M; Neck, V; Muller, R; Fanghanel, T. Solubility of ThO_2•H_2O(am) in carbonate solution the formation of ternary Th(IV) hydroxide-carbonate complexes, Radiochim. Acta, **93**, 83 (2005).

24. Altmaier, M; Neck, V; Denecke, M.A; Yin, R; Fanghänel, T; Solubility of ThO_2•xH_2O(am) the formation of ternary Th(IV) hydroxide-carbonate complexes in $NaHCO_3$-Na_2CO_3 solutions containing 0 to 4 M NaCl, Radiochim. Acta, **94**, 495 (2006).

25. Webb, S.M. SIXPack: a graphical user interface for XAS analysis using IFEFFIT. Physica Scripta, **T115**, 1011 (2005).

26. Ressler, T. WinXAS: a program for X-ray absorption spectroscopy data analysis under MS-Windows. Journal of Synchrotron Radiation, **5**, 118 (1998).

27. Rehr, J.J; Albers, R.C. Theoretical approaches to X-ray absorption fine structure. Reviews of Modern Physics, **72**, 621 (2000).

28. Wieczorek, M.W; Blaszczyk, J; Krol, B.W. Effects of cation interactions on sugar anion conformation in complexes of lactobionate and gluconate with calcium, sodium or potassium. Acta Crystallogr., Sect. C: Cryst. Struct. Commun., **52**, 1193 (1996).

29. Felmy, A.R; Cho, H; Dixon, D.A; Xia, Y; Hess, N.J; Wang, Z. The aqueous complexation of thorium with citrate under neutral to basic conditions, Radiochim. Acta, **94**, 205 (2006).

30. Matzapetakis, M; Karligiano, N; Bino, A; Dakanali, M; Raptopoulou, C.P; Tangoulis, V; Terzis, A; Giapintzakis, J; Salifoglou, A. Manganese citrate chemistry: Syntheses, spectroscopic studies, structural characterizations of novel mononuclear, water-soluble manganese citrate complexes. Inorg. Chem., **39**, 4044 (2000).

31. Felmy, A.R; Rai, D; Sterner, S.M; Mason, M.J; Hess, N.J; Conradson, S.D. Thermodynamic models for highly charged aqueous species: Solubility of Th(IV) hydrous oxide in concentrated $NaHCO_3$-Na_2CO_3 solutions, J. Solution Chem., **26**, 233 (1997).

32. Voliotis, S; Rimsky, A. Etude structurale des carbonates complexes de cerium et de thorium. II. Structure cristalline et moleculaire du pentacarbonatothorate de guanidine tetrahydrate. Acta Crystallogr., Sect. B: Struct. Sci., **31**, 2612 (1975).

33. Herbelin, A.L; Westall, J.C. FITEQL 4.0: a computer program for determination of chemical equilibrium constants from experimental data, Technical report 99-01. Department of Chemistry, Oregon State University, Corvallis, (1999).

34. Birjkumar, K.H; Bryan, N.D; Kaltsoyannis, N. Is gluconate a good model for isosaccharinate in uranyl(VI) chemistry? A DFT study, Dalton Trans., **41**, 5542 (2012).

35. Glaus, M.A; Laube, A; Van Loon, L.R. Solid–liquid distribution of selected concrete admixtures in hardened cement pastes, Waste Management, **26**, 741 (2006).

36. Gaona, X; Montoya, V; Colàs, E; Grivé, M; Duro, L. Review of the complexation of tetravalent actinides by ISA gluconate under alkaline to hyperalkaline conditions, J. Contam. Hydrol., **102**, 217 (2008).

37. Zhang, Z; Clark, S.B; Tian, G; Zanonato, P.L; Rao, L. Protonation of D-gluconate and its complexation with Np(V) in acidic to nearly neutral solutions, Radiochim. Acta, **94**, 531 (2006).

38. Rendleman, J.A. Metal-polysaccharide complexes: Part I. Food Chemistry, **3**, 47 (1978).

39. Van Duin, M; Peters, J.A; Kieboom, A.P.G;Van Bekkum, H. A general coordination-ionization scheme for polyhydroxy carboxylic acid in water, Recueil des Travaux Chimiques des Pays-Bas, **108**, 57 (1989).

40. Rothe, J; Denecke, M.A; Neck, V; Muller, R; Kim, J.I. XAFS investigation of the structure of aqueous thorium (IV) species, colloids, and solid thorium (IV) oxide/hydroxide, Inorg. Chem., **41**, 249 (2002).

41. Toraishi, T; Farkas, I; Szabo, Z; Grenthe, I. Complexation of Th(IV) and various lanthanides(III) by glycolic acid; potentiometric, ^{13}C-NMR and EXAFS studies, J. Chem. Soc., Dalton Trans., **20**, 3805 (2002).

42. Allen, P; Shuh, D.K; Bucher, J; Edelstein, N; Reich, T; Denecke, M.A; Nitsche, H. EXAFS determinations of uranium structures: The uranyl ion complexed with tartaric, citric, and malic acids, Inorg. Chem., **35**, 784 (1996).

Paper III

(Published)

E. Colàs, M. Grivé, I. Rojo and L. Duro

The effect of gluconate and EDTA on thorium solubility under simulated cement porewater conditions

Journal of Solution Chemistry (2013) / DOI 10.1007/s10953-013-0054-2

The effect of gluconate and EDTA on thorium solubility under simulated cement porewater conditions

Elisenda Colàs
Amphos 21. Pg. Garcia i Fària, 49-51, 08019 Barcelona, Spain.
T: +34 93 583 05 00
F: +34 93 307 59 28
eli.colas@amphos21.com

Mireia Grivé
Amphos 21. Pg. Garcia i Fària, 49-51, 08019 Barcelona, Spain.
T: +34 93 583 05 00
F: +34 93 307 59 28
mireia.grive@amphos21.com

Isabel Rojo
Fundació CTM Centre Tecnològic. Av. Bases de Manresa, 1, 08242 Manresa, Spain
T: +34 93 877 73 73
F: +34 93 877 73 74
isabel.rojo@ctm.com.es

Lara Duro
Amphos 21. Pg. Garcia i Fària, 49-51, 08019 Barcelona, Spain.
T: +34 93 583 05 00
F: +34 93 307 59 28
lara.duro@amphos21.com

Abstract

α-hydroxy carboxylate ligands like gluconate or polyaminocarboxylate ligands such as ethylenediaminetetraacetate (EDTA) are frequently used in decontamination procedures at nuclear power plants. The presence of these organic substances among nuclear wastes could enhance the solubility of actinides by forming soluble complexes. Thermodynamic data on the stability of gluconate and EDTA with actinides are essential to predict their increase in mobility, especially in high pH systems characteristic of cement environments of a nuclear waste repository.

In this work, the solubility of thorium oxyhydroxide in the presence of gluconate and EDTA has been studied. The results highlight the key role of these organics in increasing the solubility of thorium at pH_c=12. The presence of calcium at concentrations below 10^{-2} mol·dm^{-3} (characteristic of cement porewaters corresponding to cement compositions at the second degradation stage) does not seem to affect significantly thorium solubility under the studied conditions.

Thorium / Solubility / Gluconate / EDTA / Calcium

1 Introduction

Polyhydroxycarboxylic and polyaminocarboxylic acids are frequently used as cleaning agents in decontamination procedures in nuclear processes [1]. These types of organic ligands, like gluconate (GH_4^-) or ethylenediaminetetraacetate (EDTA), are present in radioactive wastes. A number of investigations indicate that actinides may form stable complexes with gluconate [2-8] or EDTA [1, 9-13] in a wide pH range. Nevertheless, the scarcity of data regarding the type of species formed and their stability results in a generally poor understanding of the potential migration of radionuclides, especially in the alkaline range of pH and in the presence of other cations such as calcium, which are the main conditions imposed by cementitious materials widely used in nuclear waste repositories.

One example of this poor understanding is the remaining open question on the formation of ternary M-L-Ca species (where L is a polyhydroxycarboxylic acid), and their role on the solubility of a given radionuclide [14]. The formation of ternary Th-gluconate-Ca complexes under cement porewater conditions (where the maximum calcium concentration can be limited due to the precipitation of portlandite), has been suggested in some publications [5, 15]. Tits et al. performed thorium sorption experiments on calcite in the presence of gluconate under alkaline conditions. The authors did not observe calcite dissolution in significant amounts, confirming that total aqueous calcium concentrations in the system were controlled. To explain their results, the authors suggested the formation of a $CaTh(OH)_4(GH_4)_2(aq)$ species, but did not take into account the possible formation of Th-gluconate complexes (without calcium) in their data treatment. Baston and co-workers [2] made thorium sorption experiments with natural clays, sandstone or volcanic rocks. Their results show that the presence of the organic species can cause a reduction in the sorption of the radionuclide on those materials. However, the study does not provide evidences of the formation of ternary Ca-Th-gluconate complexes. Those results highlight that the previous information on the formation of ternary Th-gluconate-Ca is scarce.

The present work aims at studying the influence of gluconate and EDTA on thorium solubility in the presence of calcium at $pH_c=12$. Maximum calcium concentrations studied are in the order of 10^{-2} $mol{\cdot}dm^{-3}$, characteristic of cement porewaters corresponding to cement compositions at the second degradation stage [16, 17] but below the concentrations that could lead to the precipitation of portlandite.

2 Experimental

2.1 Reagents and solutions

$NaClO_4 \cdot H_2O(s)$ (p.a.), sodium gluconate ($NaC_6H_{11}O_7$, p.a.) and disodium ethylenediaminetetraacetate ($Na_2C_{10}H_{14}N_2O_8 \cdot 2H_2O$, dihydrated disodium salt of EDTA, p.a.) were purchased from Sigma Aldrich, and NaOH(s) and $CaCl_2(s)$ from Panreac. Thorium nitrate solution (1% w/v) was obtained from J.T. Baker. Ultrapure water from a Milli-Q Academic water purification system was degassed by boiling and cooling in a $N_2(g)$ atmosphere and used in all experiments. Reagents and solutions were CO_2-free and were prepared and stored inside a nitrogen glove box.

pH_c was determined using an alkaline resistant combined glass electrode (Crison 52.22) where the reference electrolyte had been replaced by the background electrolyte used in the experiments (0.5 $mol \cdot dm^{-3}$ $NaClO_4$) [18]. The electrode was calibrated using a Gran titration procedure [19], where 50 ml of 0.5 $mol \cdot dm^{-3}$ $NaClO_4$ were titrated with a 0.06 $mol \cdot dm^{-3}$ $HClO_4$ solution.

2.2 Solubility experiments

Thorium hydroxide was prepared from a thorium nitrate solution by slow titration with carbonate-free NaOH up to pH_c 10 with constant stirring under a nitrogen atmosphere [20]. The precipitate was afterwards filtered through 0.22µm nylon filters under nitrogen atmosphere, washed several times with carbonate-free water, and dried in a vacuum desiccator for one week. X-ray diffraction (XRD) analysis of the solid showed broad bands, indicating the low crystallinity of the material and allowed the identification of the solid as $ThO_2 \cdot xH_2O$. Solubility measurements of this solid in the absence of organic ligands are in agreement with data reported in previous publications [14]. A complete description of those measurements was provided in a previous work [21]; its determined solubility constant in the absence of organic ligands is available in Table 1 and Table 2.

The solubility experiments undertaken in this work were done in polypropylene tubes (20-50 ml) at 25±2 ºC, by contacting 0.06g of solid thorium hydroxide with 20 ml of a solution containing a given calcium and organic ligand concentration. The possible sorption of thorium onto the tube walls was tested by leaching them with 2% HNO_3 after their use. The analysis of the solutions with Inductively Coupled Plasma Mass Spectrometry (ICP-MS) did not show thorium sorption on tube walls within detection limits.

Previous experiments in the thorium-gluconate system in the absence of calcium [21] showed that sorption of the organic ligand on the thorium solid surface constrains the range of gluconate concentrations that can be explored by the solubility method from undersaturation direction. Taking into account those observations, the range of concentration studied for the organic ligand was varied from 10^{-4} to 10^{-1} $mol \cdot dm^{-3}$.

Maximum calcium concentrations were 2×10^{-2} $mol \cdot dm^{-3}$; preliminary PhreeqC [22] calculations indicate that $Ca(OH)_2(s)$ should not precipitate under those conditions.

CO_2-free NaOH was used to adjust the solutions to the desired pH value (pH_c=12). Ionic strength was kept constant at I=0.5 $mol \cdot dm^{-3}$ ($NaClO_4$-NaOH-$Na(GH_4)$-$CaCl_2$ or $NaClO_4$-NaOH-Na_2EDTA-$CaCl_2$, with $NaClO_4$ the main electrolyte in solution). Tubes were kept under constant stirring for different time intervals up to 70 days. Equilibrium in solubility experiments was assumed to have been reached when thorium concentrations did not vary more than 5% within 48 hours or more. Preliminary test indicated that 10 days were enough to reach equilibrium, which is in agreement with previous observations reported in the literature [13, 23].

1 ml aliquots of solution were taken and filtered through polyether sulfone membrane filters (Microsept TM 1 kD, pore size ≈1.2 nm or 300 kD, pore size ≈20 nm [24]) prior to thorium analysis. These filters have been reported to allow successful separation of thorium colloids [24].

Thorium concentrations were determined by ICP-MS (Agilent 7500cx). Detection limit for Th in the original solutions (after dilution with HNO_3 2%) was 1×10^{-9} $mol \cdot dm^{-3}$. Calcium was measured using Inductively Coupled Plasma Optical Emission Spectrometry (ICP-OES) (Thermo ICAP 6300MCF DUO). Quantification limit for calcium in the original solutions was 2.5×10^{-5} $mol \cdot dm^{-3}$. Gluconate and EDTA were measured as Total Organic Carbon (TOC) concentration using TOC equipment

(Shimadzu TOC-5050A) after dilution and acidification of the samples. Scanning Electron Microscope (SEM) analyses of the solid morphology in the absence and in the presence of calcium were carried out with a field emission Ultra Plus ZEISS equipment.

2.3 EXAFS experiments

In addition to the solubility experiments described in the previous section, two additional samples were prepared from the oversaturation direction and measured with the Extended X-ray Absorption Fine Structure Spectroscopy (EXAFS) technique. Both samples were prepared from a solution of $[Th]_0$=1 x 10^{-3} mol·dm^{-3} and $[GH_4^-]$=0.1 mol·dm^{-3} at pH_c≈11.8. Sample 1 did not contain calcium; sample 2 contained $[Ca]_0$=1 x 10^{-2} mol·dm^{-3} to evaluate its effect in the system. EXAFS measurements were done after sample filtration through polyether sulfone membrane filters.

Thorium L_{III}-edge EXAFS spectra were collected at the ROssendorf Beam Line (ROBL) at the European Synchrotron Radiation Facility (ESRF) located in Grenoble (France). A minimum of 7 scans per sample were collected in fluorescence mode at room temperature. Scans were pre-treated and averaged using Sixpack [25]. Data analysis was performed using the WinXAS [26] software.

3 Results and discussion

3.1 Results in the absence of calcium

In the presence of gluconate and in the absence of calcium a 1:1 Th-gluconate complex is expected to form, as we reported in a previous work [21]. $\log_{10}K_s$(I=0.5) was calculated to be = -3.1±0.6 [21].

Likewise, the solubility of thorium increases approximately one order of magnitude when increasing one order of magnitude the concentration of EDTA, indicating the formation of a 1:1 Th-EDTA species in the EDTA concentration range from 10^{-3} to 10^{-1} mol·dm^{-3} (see open circles in Fig. 4). The stability constant for the formation of the Th-EDTA complex under the conditions studied was calculated to be $\log_{10}K_s$(I=0.5) =20.2±0.7 in present work by using the FITEQL program [27]. These results are in agreement with previous results from Xia and co-workers [13], who reported the formation of a $Th(OH)_2EDTA^{2-}$ species under similar conditions but in a lower pH range (pH 9-11).

3.2 Results in the presence of gluconate and calcium

3.2.1 Calcium effect on solid

SEM measurements of thorium hydroxide solid showed very similar morphology of the solid in the absence and in the presence of calcium (Fig. 1), and no changes were detected. Altmaier and co-workers [28] reported changes (detected by SEM and XRD analysis) in a solid thorium hydroxide sample that had been in contact with a calcium solution at $pH_c>11.5$. According to [28], SEM showed needle-like crystals lying on the bulk heap of amorphous thorium hydroxide particles. Those needles were not observed in the present samples; the much higher calcium concentrations ([Ca]>1 mol·dm^{-3}) and longer reaction times used by [28] may explain the apparent discrepancy between the results.

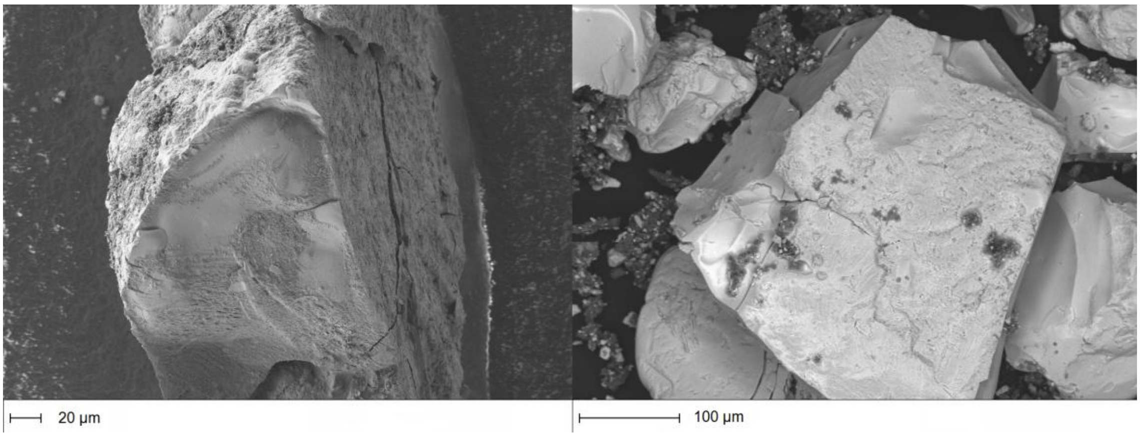

Fig. 1 SEM images for amorphous thorium oxyhydroxide after contact with 0.5 mol·dm^{-3} $NaClO_4$ solution at pH_c=12 for >70 days. A) [GH_4^-]=1.0 x 10^{-2} mol·dm^{-3}, no calcium B) [GH_4^-]=1.7 x 10^{-3} M, [Ca]=2.2 x 10^{-2} mol·dm^{-3}

The stabilization of anionic hydroxide complexes in the alkaline pH range by strong interaction with calcium, as a result of either ion association or ion pair formation, was also reported by [28, 29]. In those works, high solubilities of Th(IV) hydrous oxides at pH_c = 11 to 12 in concentrated $CaCl_2$ solutions (of particular interest for the storage of nuclear waste in underground salt mines) were observed. The solubility increase was attributed to the formation of $Ca_4[Th(OH)_8]^{4+}$. Speciation calculations indicate that at pH$_c$ values and calcium concentrations used in present work, $Ca_4[Th(OH)_8]^{4+}$ complexes are not formed.

3.2.2 Solubility experiments

Fig. 2 shows the experimental results for thorium solubility in the presence of both calcium and gluconate (solid symbols), compared to the measured solubilities in the absence of Ca (open circles) at pH$_c$=12.

At low calcium concentrations (grey squares, [Ca]=5 x 10^{-4} mol·dm^{-3}), results obtained are similar to those obtained in the absence of calcium (open circles), and can be explained by assuming that $Th(OH)_2(GH_2)^-$ is the only species responsible for the observed solubility increase (solid line in the figure). At higher calcium concentrations, [Ca]=2 x 10^{-2} mol·dm^{-3}, the small solubility increase observed may indicate the formation of a Ca:Th:GH$_4$ complex. However, the apparent solubility increase is not very significant, taking into account the large uncertainty for the observed thorium oxyhydroxide solubility in the presence of gluconate (see dotted lines in Fig. 2).

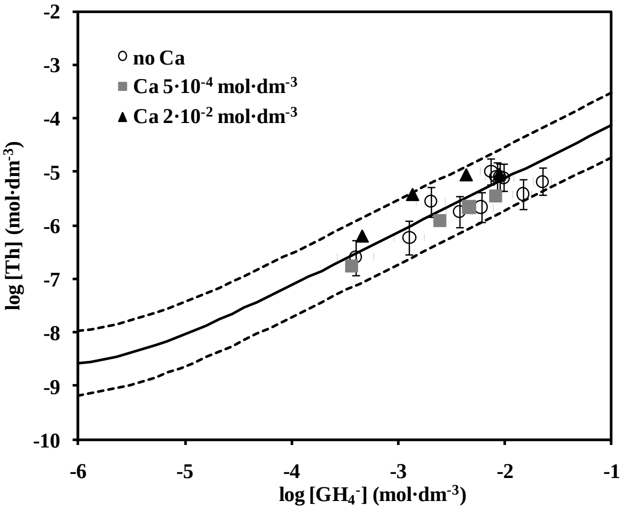

Fig. 2 Solubility of thorium oxyhydroxide from undersaturation direction as a function of measured gluconate concentration at fixed pH$_c$=12 (I=0.5 mol·dm^{-3}, NaClO$_4$), time>39 days. Open circles: in the absence of calcium. Grey squares: [Ca]=5 x 10^{-4} mol·dm^{-3}. Black triangles: [Ca]=2 x 10^{-2} mol·dm^{-3}. Solid line is calculated thorium hydroxide solubility taking into account $Th(OH)_2(GH_2)^-$ formation (with uncertainty as 2σ, dotted line)

The results obtained indicate that Th(IV)-gluconate-Ca species, if formed, should not have a significant influence on thorium hydroxide solubility under the studied conditions.

On the other hand, calcium could form complexes with the gluconate ligand itself (see Table 1), thus directly competing with thorium for the organic ligand. This competition is significant due to the higher calcium concentration when compared to thorium concentration in the system and was taken into account in the calculations.

Table 1 Stability constants in the Th-gluconate-Ca system

Reaction	*Log K*	*Original source*
$Ca^{2+} + GH_4^- \leftrightarrows Ca(GH_4)^+$	$\log_{10}K(I=0.5) = 1.1$	[30]
$Ca^{2+} + GH_4^- \leftrightarrows Ca(GH_3)(aq) + H^+$	$\log_{10}K(I=0.5) = -11.1$	[5]
$ThO_2 \cdot xH_2O \leftrightarrows Th(OH)_{4(aq)} + (x-2)H_2O$	$\log_{10}K_s(I=0.5) = -8.72 \pm 0.6$	[21]
$ThO_2 \cdot xH_2O + GH_4^- \leftrightarrows Th(OH)_2(GH_2)^- + xH_2O$	$\log_{10}K_s(I=0.5) = -3.1 \pm 0.6$	[21]

After the experiments, measurements of calcium concentrations in solution were performed. A decrease of the aqueous calcium concentrations was observed at both 5×10^{-4} $mol \cdot dm^{-3}$ and 2×10^{-2} $mol \cdot dm^{-3}$ initial calcium concentrations, being more significant at $[Ca]_0 = 5 \times 10^{-4}$ $mol \cdot dm^{-3}$ (see Fig. 3). The decrease may indicate that a significant part of available calcium in solution is being sorbed (or precipitated) on the solid surface.

Likewise, the potential sorption of organic ligands onto the solid surface was tested. Similar to the previous results, additions of small amounts of gluconate also result in a decrease in measured gluconate concentration in solution. This observation (described in detail in [21]) would indicate that a surface gluconate species acts a precursor of the thorium hydroxide dissolution.

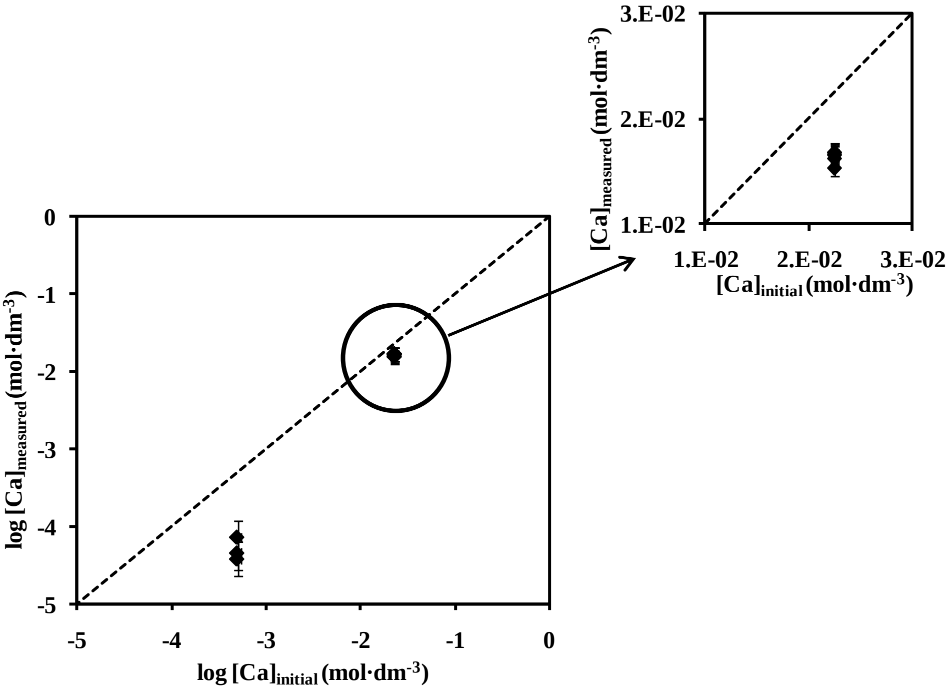

Fig. 3 Initial vs. measured calcium concentrations in thorium hydroxide solubility experiments at pH_c=12 in the presence of both calcium and gluconate. Black dotted line indicates $[Ca]_{initial}=[Ca]_{measured}$

3.2.3 EXAFS measurements

Two samples from oversaturation direction were prepared from a solution of $[Th]_0$=1 x 10^{-3} mol·dm^{-3} and $[GH_4^-]$=0.1 mol·dm^{-3} at $pH_c \approx 11.8$ for EXAFS analysis. In addition, one of the samples contained 1 x 10^{-2} mol·dm^{-3} calcium. The Fourier transform magnitude of the EXAFS spectra is shown in the appendix section. The relatively low Th concentration and the high disorder characteristic of aqueous samples result in a limited data quality. However, both spectra were very similar, which indicates a similar coordination environment for thorium in both cases. This may indicate that, in case that a Ca:Th:GH_4 complex is formed, calcium coordination in the sample does not influence significantly thorium coordination environment, neither its coordination with gluconate.

3.3 Results in the presence of EDTA and calcium

In Fig. 4, measured thorium solubilities as a function of EDTA concentration, in the presence and in the absence of calcium are compared. Measured thorium aqueous concentrations (filled symbols) show that Ca concentrations up to 2 x 10^{-3} mol·dm^{-3} do not affect thorium oxyhydroxide solubility. Hence, the results obtained in both, the presence and the absence of Ca in the system can be explained by assuming only the formation of $Th(OH)_2(EDTA)^{2-}$ complex.

EDTA experimental measurements suggest that there is no significant EDTA sorption on the thorium hydroxide solid under the conditions used in the experiments.

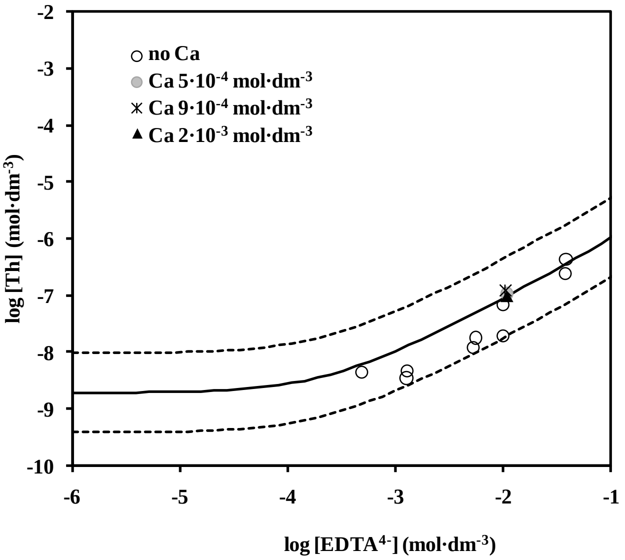

Fig. 4 Solubility of thorium oxyhydroxide from undersaturation direction as a function of measured EDTA concentration at fixed pH_c=12 (I=0.5 mol·dm^{-3}, $NaClO_4$). Open circles: in the absence of calcium, t >19 days. Grey circles: [Ca]=5.0 x 10^{-4} mol·dm^{-3}. Crosses: [Ca]=9.0 x 10^{-4} mol·dm^{-3}. Black triangles: [Ca]=2.0 x 10^{-3} mol·dm^{-3}. Solid line is thorium hydroxide solubility taking into account $Th(OH)_2(EDTA)^{2-}$ formation (with uncertainty as 2σ, dotted line)

EDTA is expected to form weak complexes with sodium. The concentration of sodium in the experiments is high, as 0.5 mol·dm^{-3} $NaClO_4$ is used as ionic media in order to kept a constant ionic strength. Thus, the formation of the $NaEDTA^{3-}$ complex was taken into account in the calculations (Table 2).

Table 2 Stability constants in the Th-EDTA-Ca-Na system

Reaction	*Log K*	*Original source*
$Ca^{2+} + EDTA^{4-} \leftrightarrows Ca(EDTA)^{2-}$	$\log_{10}K(I=0.5) = 10.19$	[1]
$Na^{+} + EDTA^{4-} \leftrightarrows NaEDTA^{3-}$	$\log_{10}K(I=0.5) = 1.6$	[1]
$ThO_2 \cdot xH_2O \leftrightarrows Th(OH)_{4(aq)} + (x\text{-}2)H_2O$	$\log_{10}K_s(I=0.5) = -8.72\pm0.6$	[21]
$ThO_2 \cdot xH_2O + EDTA^{4-} + 2H^{+} \leftrightarrows Th(OH)_2(EDTA)^{2-} + xH_2O$	$\log_{10}K_s(I=0.5) = 20.2\pm0.7$	p.w.

p.w.=present work

The possible formation of a Th-EDTA-Ca complex has not been observed under the conditions of the solubility experiments in the presence of both calcium and EDTA (see Fig. 5). This is probably due to the structure of the EDTA ligand itself, that chelates thorium without leaving free coordination sites.

Results obtained in present work are in agreement with the results of [11], which involved the study of Pu(IV) solubility in the system Pu(IV)/Fe(III)/Ca/EDTA. Those authors did not observe the formation of ternary Ca-Pu(IV)-EDTA complexes.

4 Conclusions

Both gluconate and EDTA are able to enhance thorium hydroxide solubility at alkaline pH_c values due to the formation of Th-OH-L complexes. Furthermore, complexation capacity of gluconate is higher in the alkaline pH_c range than EDTA. Additionally, thorium complexation with EDTA is significantly affected by the competitive formation of $NaEDTA^{3-}$ and $Ca(EDTA)^{2-}$ complexes.

In the presence of both gluconate and $[Ca]\approx10^{-2}$ $mol\cdot dm^{-3}$, a small solubility increase on thorium hydroxide (in comparison with the solubility encountered under the same conditions but in the absence of calcium) is observed. On the contrary, no evidences of a Ca-Th-EDTA complex have been found.

Therefore, it can be concluded that, in alkaline systems where gluconate or EDTA are present, calcium concentrations below 10^{-2} $mol\cdot dm^{-3}$ may not enhance significantly thorium hydroxide solubility.

Acknowledgements

The authors would like to thank the French National Agency for Radioactive Waste Management (ANDRA) for funding this work. E. Giffaut is acknowledged for fruitful scientific discussions. We acknowledge the European Synchrotron Radiation Facility (ESRF) for provision of synchrotron radiation facilities and we would like to thank A. Scheinost and C. Henning for help in using the Rossendorf Beamline (ROBL) and with EXAFS data elucidation. Thanks are due to the reviewers for their comments, which improved the quality of the original manuscript.

Appendix

Table 3 Solubility of thorium hydroxide as a function of gluconate concentration in the absence of calcium.

pH_c	log_{10} *gluconate (initial)*	log_{10} *gluconate (measured)*	log_{10} *Th*
11.65	-1.64	-1.64	-5.18
11.66	-1.79	-1.83	-5.42
11.93	-1.98	-2.01	-5.11
11.77	-1.98	-2.08	-5.08
11.87	-1.98	-2.05	-5.09
11.75	-2.06	-2.13	-4.99
11.73	-2.35	-2.42	-5.74
12.27	-2.35	-2.22	-5.66
11.74	-2.54	-2.69	-5.55
11.66	-2.61	-2.89	-6.22
11.68	-2.90	-3.40	-6.59

Table 4 Solubility of thorium hydroxide as a function of gluconate concentration in the presence of calcium.

pH_c	log_{10} *gluconate (initial)*	log_{10} *gluconate (measured)*	log_{10} *Th*	log_{10} *Ca (initial)*	log_{10} *Ca (measured)*
12.00	-2.04	-2.09	-5.45	-3.30	
12.00	-2.25	-2.33	-5.66	-3.30	-4.42
11.99	-2.47	-2.61	-5.91	-3.30	
12.00	-2.93	-3.43	-6.76	-3.30	-4.34
11.88	-3.16	-3.34	-6.20	-1.65	-1.79
11.87	-2.76	-2.87	-5.42	-1.65	-1.77
11.87	-2.30	-2.36	-5.05	-1.65	-1.78
11.87	-2.03	-2.05	-5.04	-1.65	-1.77

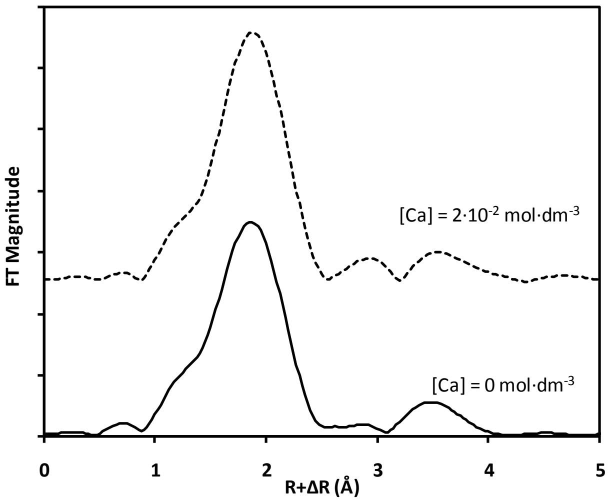

Fig. 5 Experimental data of EXAFS fourier transforms of Th L_{III} edge for Th-gluconate solutions in the absence (solid lines) and presence (dotted lines) of calcium

References

1. Hummel, W., Anderegg, G., Rao, L., Puigdomènech, I., Tochiyama, O.: Chemical Thermodynamics of Compounds and Complexes of U, Np, Pu, Am, Tc, Se, Ni and Zr with Selected Organic Ligands. Elsevier, Amsterdam (2005)

2. Baston, G. M. N., Berry, J. A., Bond, K. A., Brownsword, M., Linklater, C. M.: Effects of organic degradation products on the sorption of actinides. Radiochim. Acta **52/53,** 249–356 (1992)

3. Felmy, A. R.: Chemical speciation of Americium, Curium and selected tetravalent actinides in high level waste. EMSP Project 73749 PNNL (2004)

4. Sawyer, D.: Metal-gluconate complexes. Chem. Rev. **64,** 633–643 (1964)

5. Tits, J., Wieland, E., Bradbury, M.: The effect of isosaccharinic acid and gluconic acid on the retention of Eu(III), Am(III) and Th(IV) by calcite. Appl. Geochem. **20,** 2082–2096 (2005)

6. Warwick, P., Evans, N., Hall, T., Vines, S.: Stability constants of uranium(IV)-alpha-isosaccharinic acid and gluconic acid complexes. Radiochim. Acta **92,** 897–902 (2004)

7. Zhang, Z., Clark, S., Tian, G., Zanonato, P., Rao, L.: Protonation of D-gluconate and its complexation with Np(V) in acidic to nearly neutral solutions. Radiochim. Acta **94,** 531–536 (2006)

8. Zhang, Z., Helms, G., Clark, S., Tian, G., Zanonato, P., Rao, L.: Complexation of Uranium(VI) by gluconate in acidic solutions: a thermodynamic study with structural analysis. Inorg. Chem. **48,** 3814–3824 (2009)

9. Mathur, J. N., Thakur, P., Dodge, C. J., Francis, A. J., Choppin, G. R.: Coordination modes in the formation of the ternary Am(III), Cm(III), and Eu(III) complexes with EDTA and NTA: TRLFS, ^{13}C-NMR, EXAFS, and thermodynamics of the complexation. Inorg. Chem. **45,** 8026–8035 (2006)

10. Meyer, M., Burgat, R., Faure, S., Batifol, B., Hubinois, J., Chollet, H., Guilard, R.: Thermodynamic studies of actinide complexes. 1. A reappraisal of the solution equilibria between plutonium(IV) and ethylenediaminetetraacetic acid ($EDTAH_4$) in nitric media. C.R. Chim. **10,** 929–947 (2007)

11. Rai, D., Moore, D., Rosso, K., Felmy, A., Bolton, H. J.: Environmental mobility of Pu(IV) in the presence of ethylenediaminetetraacetic acid: Myth or reality? J. Solution Chem. **37,** 957–986 (2008)

12. Wang, Z., Felmy, A., Xia, Y. X., Mason, M. J.: A fluorescence spectroscopic study on the speciation of Cm(III) and Eu(III) in the presence of organic chelates in highly basic solutions. Radiochim. Acta **91,** 329–337 (2003)

13. Xia, Y., Felmy, A., Rao, L., Wang, Z., Hess, N.: Thermodynamic model for the solubility of ThO_2(am) in the aqueous Na^+-H^+-OH^--NO_3^--H_2O-EDTA system. Radiochim. Acta **91,** 751–760 (2003)

14. Rand, M., Fuger, J., Grenthe, I., Neck, V., Rai, D.: (2009) Chemical Thermodynamics of Thorium Elsevier, Amsterdam (2009)

15. Tits, J., Wieland, E., Bradbury, M., Eckert, P., Schaible, A.: The uptake of Eu(III) and Th(IV) by calcite under hyperalkaline conditions Paul Scherrer Institute, Villigen (2002)

16. Ochs, M. Hager, D. Helfer, S. Lothenbach, B.: Solubility of radionuclides in fresh and leached cementitious systems at 22ºC and 50ºC. Mat. Res. Soc. Symp. Proc. **506**, 773–780 (1998)

17. Ochs, M. Lothenbach, B. Giffaut, E.: Uptake of oxo-anions by cements through solid-solution formation: experimental evidence and modelling. Radiochim. Acta, **90,** 639–646 (2002)

18. Kitamura, A., Kohara, Y.: Carbonate complexation of Neptunium(IV) in highly basic solutions. Radiochim. Acta **92**, 583–588 (2004)

19. Gran, G.: Determination of the equivalence point in potentiometric titrations. Part II. The Analyst **77**, 661–671 (1952)

20. Neck, V., Müller, R., Bouby, M., Altmaier, M., Rothe, J., Denecke, M. A., Kim, J.: Solubility of amorphous Th(IV) hydroxide – application of LIBD to determine the solubility product and EXAFS for aqueous speciation. Radiochim. Acta **90,** 485–494 (2002)

21. Colàs, E., Grivé, M., Rojo, I., Duro, L.: Solubility of $ThO_2 \cdot xH_2O$(am) in the presence of gluconate. Radiochim. Acta **99,** 269-273 (2011)

22. Parkhurst, D., Appelo, C.: User’s guide to PHREEQC (version 2.4.6). A computer program for speciation, batch reaction, one dimensional transport and inverse geochemical calculations. U. S. Geological Survey (2001)

23. Rai, D., Yui, M., Moore, D., Rao, L.: Thermodynamic model for ThO_2(am) solubility in isosaccharinate solutions. J. Solution Chem. **38,** 1573–1587 (2009)

24. Altmaier, M., Neck, V., Muller, R., Fanghanel, T.: Solubility of $ThO_2 \cdot H_2O$(am) in carbonate solution and the formation of ternary Th(IV) hydroxide-carbonate complexes. Radiochim. Acta **93,** 83–92 (2005)

25. Webb, S.: SIXPack: a graphical user interface for XAS analysis using IFEFFIT. Physica Scripta, **T115,** 1011–1014 (2005)

26. Ressler, T.: WinXAS: a program for X-ray absorption spectroscopy data analysis under MS-Windows. Journal of Synchrotron Radiation **5,** 118–122 (1998)

27. Herbelin, A., Westall, J.: FITEQL 4.0: a computer program for determination of chemical equilibrium constants from experimental data. Technical report, Report 99-01. Department of Chemistry, Oregon State University, Corvallis (1999)

28. Altmaier, M., Neck, V., Fanghänel, T.: Solubility of Zr(IV), Th(IV) and Pu(IV) hydrous oxides in $CaCl_2$ solutions and the formation of ternary Ca-M(IV)-OH complexes. Radiochim. Acta, **96,** 541–550 (2008)

29. Brendebach, B., Altmaier, M., Rothe, J., Neck, V., Denecke, M. A.: EXAFS study of aqueous Zr(IV) and Th(IV) complexes in alkaline $CaCl_2$ solutions: $Ca_3[Zr(OH)_6]^{4+}$ and $Ca_4[Th(OH)_8]^{4+}$. Inorg. Chem. **46,** 6804–6810 (2007)

30. Schubert, J. Lindenbaum, A.: Stability of alkaline earth-organic acid complexes measured by ion exchange. J. Am. Chem. Soc. **74,** 3529–3532 (1952)

Paper IV

(Published)

E. Colàs, M. Grivé and I. Rojo
Complexation of uranium(VI) by gluconate in alkaline solutions
Journal of Solution Chemistry 42, 1545-1557 (2013) / DOI 10.1007/s10953-013-0048-0

Complexation of uranium(VI) by gluconate in alkaline solutions

Elisenda Colàs
Amphos 21. Pg. Garcia i Fària, 49-51, 08019 Barcelona, Spain.
T: +34 93 583 05 00
F: +34 93 307 59 28
eli.colas@amphos21.com

Mireia Grivé
Amphos 21. Pg. Garcia i Fària, 49-51, 08019 Barcelona, Spain.
T: +34 93 583 05 00
F: +34 93 307 59 28
mireia.grive@amphos21.com

Isabel Rojo
Fundació CTM Centre Tecnològic. Av. Bases de Manresa, 1, 08242 Manresa, Spain
T: +34 93 877 73 73
F: +34 93 877 73 74
isabel.rojo@ctm.com.es

Abstract

Gluconate ($C_6H_{11}O_7$) is a polyhydroxycarboxylic acid that can be assumed as a representative model-compound for a wide variety of additives in cement formulations. It can play an important role in the cementitious environments characteristic of radioactive waste disposal sites, as actinides (such as U(VI)) may form stable complexes with gluconate. As a consequence, the presence of the organic ligand can lead to an enhancement of actinide mobility. The results presented in this work show that gluconate increases significantly uranium solubility at pH_c=12, even if the study of U(VI) speciation in alkaline solutions is complex, mainly due to formation of sparingly soluble uranates of varying compositions (e.g. sodium and potassium uranates). UV-VIS measurements in the alkaline pH range have been used to determine the stability constant for the formation of a 1:1 U(VI):gluconate complex. The results obtained with spectroscopic techniques allow explaining the measurements from solubility experiments, from both over- and undersaturation conditions.

Uranium / Gluconate / Solubility / UV-VIS

1 Introduction

Concrete and cement materials are widespread in radioactive waste disposal sites. Gluconate ($C_6H_{11}O_7$, abbreviated to GH_4, see Fig. 1) is a polyhydroxycarboxylic acid that can be assumed as a representative model-compound for a wide variety of additives in cement formulations [1]. A number of investigations [2-7] indicate that actinides, including U(VI), may form stable complexes with polyhydroxy carboxylic acids such as, or similar to, gluconate, which may lead to an enhancement of their mobility.

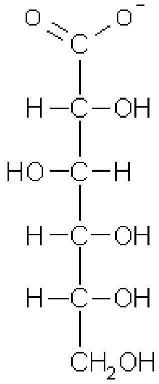

Fig. 1 GH_4^- chemical structure. H_4 refers to the hydrogens of the secondary alcohols in the molecule [8].

U(VI) forms sparingly soluble uranates of varying compositions in alkaline solutions, what makes difficult the determination of the stability of the dominant aqueous species. Formation of sodium, potassium, calcium or magnesium uranates is reported in the literature [9]. The precipitation of those uranates is expected to occur even at low concentrations of background electrolytes, what complicates the studies under controlled ionic strength conditions. Uranates may also be formed as a consequence of the presence of the counterions or impurities of the reactants used in the system (e.g. sodium gluconate, TMAOH).

The objective of this work is to study the complexation of U(VI) with gluconate under the alkaline conditions characteristic of cement environments. In order to overcome the inherent difficulties of the system, both solubility (of sodium uranates) and UV-VIS studies (using TMAOH) have been undertaken.

2 Materials and methods

2.1 Reagents

Sodium perchlorate ($NaClO_4 \cdot H_2O(s)$, p.a.), potassium chloride ($KCl(s)$, p.a.), sodium gluconate ($NaC_6H_{11}O_7$, p.a.), and tetramethylammonium hydroxide pentahydrate (TMAOH, $(CH_3)_4N(OH) \cdot 5H_2O$) were purchased from Sigma Aldrich. Sodium hydroxide ($NaOH(s)$, p.a.), potassium hydroxide ($KOH(s)$, p.a.) and uranyl nitrate hexahydrate ($UO_2(NO_3)_2 \cdot 6H_2O$, p.a.) were purchased from Panreac.

Ultrapure water from a Milli-Q Academic water purification system was degassed by boiling and cooling it in a $N_2(g)$ atmosphere and used in all experiments. Reagents and solutions were CO_2-free and were prepared and stored inside a nitrogen glove box.

2.1 Experimental procedures

pH_c was determined using an alkaline resistant combined glass electrode (Crison 52.22) where the reference electrolyte had been replaced by the background electrolyte used in the experiments ($NaClO_4$ or KCl) [10]. The electrode was calibrated using a Gran titration procedure [11].

The orange solid $Na_2U_2O_7(s)$ was obtained by mixing solutions of U(VI) and sodium hydroxide, following the procedure reported in [12]. Sodium uranate was prepared inside the glove box under $N_2(g)$ atmosphere. 11g of $UO_2(NO_3)_2 \cdot 6H_2O$ were dissolved in 400 ml of boiled water, and a large excess of 10 $mol \cdot dm^{-3}$ free-carbonate NaOH (≈12ml) was added to the solution. The solution was shaken at ambient temperature for 10 days. After removing the supernatant, the solid phase was washed with a 0.01 $mol \cdot dm^{-3}$ NaOH solution, filtered under nitrogen atmosphere, and dried for a few days inside the glove box. Then it was placed in a vacuum desiccator for a week, and afterwards crushed and homogenized before using it in the experiments. X-ray diffraction analysis (Bruker-AXS D5005 instrument) of the amorphous solid obtained identified the formation of sodium uranate; no impurities were identified within the detection limits of the technique.

The solubility experiments were done at 25±2 ºC in polypropylene tubes (20-50 ml). CO_2-free NaOH or KOH was used to adjust the solutions to the desired pH value (pH_c=12). Tubes were kept under constant stirring for different time intervals. The possible sorption of U(VI) onto the tube walls was tested by leaching them with 2%

HNO_3 after their use; the analysis of the solutions by Inductively Coupled Plasma Mass Spectrometry (ICP-MS) did not show significant sorption within detection limits.

The complexation behaviour was investigated through solubility experiments from both undersaturation and oversaturation directions. Undersaturation experiments were carried out by contacting 0.05g of uranate solid with 20 ml of a solution containing a given organic ligand concentration at the appropriate pH value. Oversaturation experiments were performed by preparing 20 ml of a solution containing a given organic ligand concentration at pH≈12 and adding a spike of acidic concentrated uranyl nitrate solution, being the total U(VI) concentration in the tubes of 1×10^{-4} $mol \cdot dm^{-3}$.

1 ml aliquots of the samples were filtered through polyether sulfone membrane filters (Microsept™ 1 kD, pore size ≈ 1.2 nm or 300 kD, pore size ≈ 20 nm) prior to uranium analysis. Uranium concentrations were determined by ICP-MS (Agilent 7500cx). Detection limit for U in the original solutions (after dilution with HNO_3 2%) was 1×10^{-9} $mol \cdot dm^{-3}$. Gluconate was measured as Total Organic Carbon (TOC) concentration using TOC equipment (Shimadzu TOC-5050A) after dilution and acidification of the samples.

UV-VIS measurements were performed with a Shimadzu UV-1603 spectrometer using quartz glass cells of optical path equal to 1 cm. Measurements were carried out in the range 400-450 nm or at 435 nm [5]. Samples were prepared inside the glove box and kept under a nitrogen atmosphere until measurements were performed. TMAOH was used to adjust the pH to 12 in UV-VIS samples. Preliminary experiments show that neither TMAOH nor gluconate absorb in the range of wavelengths under study.

3 Results

3.1 Results in the absence of organic ligands

The solubility of amorphous sodium uranate in the absence of organic ligands was measured from undersaturated solutions of $NaClO_4$ at two different ionic strengths, $I=0.5$ $mol \cdot dm^{-3}$ and $I=0.1$ $mol \cdot dm^{-3}$. Aqueous uranium concentrations, determined after filtration at different time intervals (between 34 and 118 days) are shown in Fig 2.

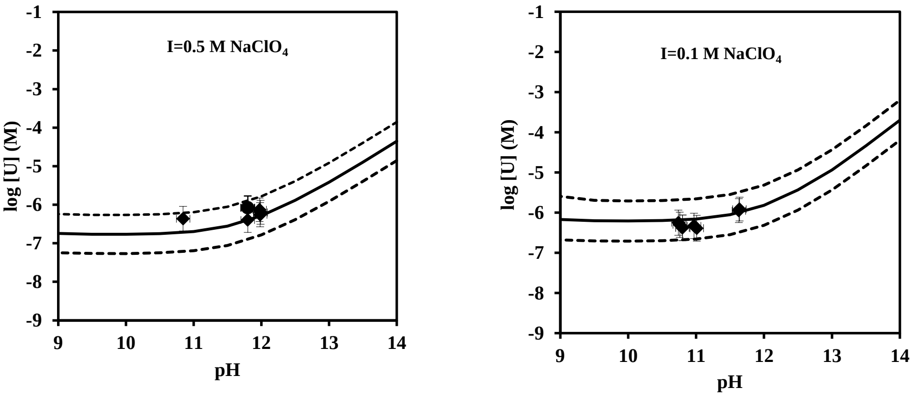

Fig. 2 Solubility of sodium uranate (left: I=0.5 mol·dm^{-3} NaClO$_4$; right: I=0.1 mol·dm^{-3} NaClO$_4$) from undersaturated solutions after filtration, solid/solution contact time>34 days. Solid line stands for calculated $Na_2U_2O_7(s)$ solubility (with uncertainty, dashed lines).

In Fig. 2 the black solid line represents the solubility calculated by considering the solubility constant shown in Eq. 1 or Eq. 2. The solubility was calculated using the software FITEQL [13]. In FITEQL, every component has one balance equation with two variables: the free concentration X and the total concentration T of the given element. A set of thermodynamic data (summarized in the appendix), must also be included in the calculations. The FITEQL code iteratively optimizes the desired parameter (*i.e.* stability constant) by minimizing the differences between calculated and experimental values using a nonlinear least squares optimization routine. Uncertainty (dotted lines in the Fig. 2) was calculated taking into account the dispersion of the experimental data obtained.

$$Na_2U_2O_7(s) + 6H^+ = 2Na^+ + 2UO_2^{2+} + 3H_2O \quad \begin{array}{ll} \log_{10}K_s(I=0.5)=27.0\pm1.0 & (1) \\ \log_{10}K_s(I=0.1)=26.6\pm1.0 & (2) \end{array}$$

Values in Eq. 1 and Eq. 2 were corrected to I=0 using Specific Interaction Theory (SIT), with the interaction coefficients reported in the NEA reviews [14-17] (see the appendix section). The corrected stability constants are shown in Eq. 3 and Eq. 4 respectively.

$$Na_2U_2O_7(s) + 6H^+ = 2Na^+ + 2UO_2^{2+} + 3H_2O \quad \begin{array}{ll} \log_{10}K^o_s=26.3\pm1.0 & (3) \\ \log_{10}K^o_s=26.1\pm1.0 & (4) \end{array}$$

The average value at I=0 is $\log_{10}K^o_s=26.2\pm1.0$. This value is in agreement with $Na_2U_2O_7(s)$ solubility reported by Yamamura and co-workers [12], which was $\log_{10}K^o_s = 25.1\pm1.04$, and with the value reported by Warwick et al. [18], ($\log_{10}K^o_s = 26.5$).

Additionally, $Na_2U_2O_7$(s) solubility was also measured from undersaturated KCl (I=0.5 mol·dm^{-3}) media. The dissolution of sodium uranate under relatively high concentrations of K^+ from the ionic media causes the formation of potassium uranate ($K_2U_2O_7$) in the system.

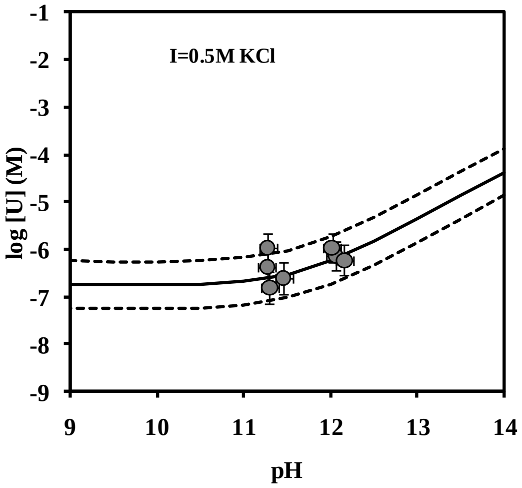

Fig. 3 Solubility of sodium uranate in 0.5 mol·dm^{-3} KCl from undersaturation direction after filtration, contact solid/solution time>27 days. Solid black line stands for calculated $K_2U_2O_7$(s) solubility (with uncertainty, dashed lines), as explained in the text.

Measured uranium concentrations shown in Fig. 3 have been modelled by considering the precipitation of $K_2U_2O_7$(s). Black solid line in Fig. 3 represents the theoretical solubility constant of $K_2U_2O_7$(s) fitted using FITEQL. The calculated value is shown in Eq. 5 and corrected to I=0 using SIT in Eq. 6.

$$K_2U_2O_7(s) + 6H^+ = 2K^+ + 2UO_2^{2+} + 3H_2O \qquad \log_{10}K_s(I=0.5)=27.2\pm1.0 \quad (5)$$

$$\log_{10}K^o_s=26.3\pm1.0 \quad (6)$$

Sutton and co-workers [19] studied the formation of solid uranium precipitates in alkaline solutions. In KOH at pH=12, $K_2U_2O_7$(s) was identified as the main solid formed in solution (>98%), by XRD measurements and model calculations. The value obtained in present work ($\log_{10}K^o s$ = 26.3±1.0) is in good agreement with data for $K_2U_2O_7$(s) solubility reported by Sutton and co-workers ($\log_{10}K^o s$ = 25.8).

3.2 Results in the presence of organic ligands

3.2.1 Solubility measurements

Initial solubility tests were performed from oversaturation direction in 1 mol·dm^{-3} $NaClO_4$ media at pH_c=12, by spiking gluconate solutions with uranyl nitrate solution, so that the total U(VI) concentration was 1 x 10^{-4} mol·dm^{-3}. Solutions were filtered and measured after 5 days of equilibration; results are shown in Fig. 4.

Thermodynamic calculations indicate that, in the absence of any complexing agent, sodium uranate solid should precipitate, and therefore U(VI) concentration in the aqueous phase should be close to 1 x 10^{-6} mol·dm^{-3} (grey zone in Fig. 4). However, the measurements indicate that all uranium added is maintained in solution, suggesting a solubility enhancement due to the presence of the gluconate ligand.

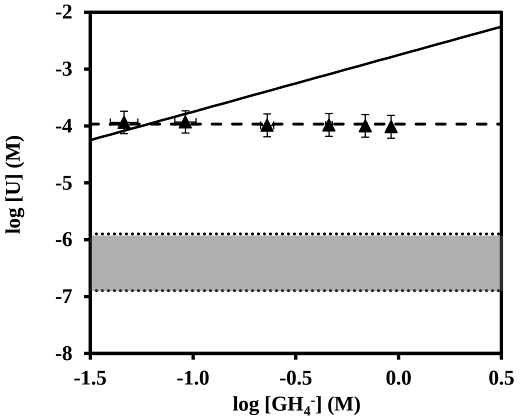

Fig. 4 Results from solubility (oversaturation) experiments. Triangles: Measured uranium concentrations in solution as a function of gluconate concentration at fixed pH_c=12 (I=1 mol·dm^{-3} $NaClO_4$), after filtration. Dashed line: total uranium concentration added (1 x 10^{-4} mol·dm^{-3}). Grey zone: expected $Na_2U_2O_7$ solubility under those conditions in the absence of organic ligands. Black solid line: calculated solubility taking into account the formation of a 1:1 U(VI):gluconate complex (see text).

Additional undersaturation solubility tests were performed by contacting sodium uranate with KCl=0.5 mol·dm^{-3} solutions and different gluconate concentrations (ranging between 10^{-3} and 10^{-1} mol·dm^{-3}) at pH_c=12. Uranium concentrations measured in solution after 27 days are presented in Fig. 5. At low gluconate concentrations, the results are in the range of solubility expected for uranates (grey zone in the figure). At [GLU]>5 x 10^{-3} mol·dm^{-3}, measured uranium concentrations are significantly higher in comparison with the uranium solubility expected under those conditions in the absence of organic ligands.

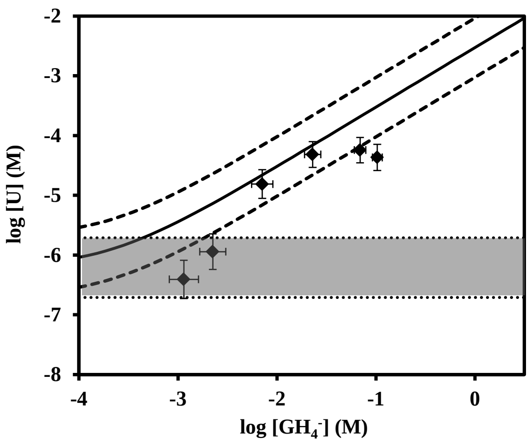

Fig. 5 Results from solubility (undersaturation) experiments. Diamonds: Measured uranium concentrations in solution as a function of gluconate concentration at fixed pH_c=12 (I=0.5 mol·dm^{-3}, KCl), after filtration. Grey zone: expected $K_2U_2O_7$ solubility under those conditions in the absence of organic ligands. Black solid line: calculated solubility taking into account the formation of a 1:1 U(VI):gluconate complex (see text), with uncertainty (dotted lines).

The uranium solubility enhancement observed in both oversaturation and undersaturation experiments suggests the formation of U(VI):gluconate complexes. For this reason, the U(VI) complexation to gluconate in the alkaline range was further investigated by UV-VIS spectrophotometry.

3.2.2 UV-VIS

UV-VIS spectra shown in Fig. 6 were recorded in alkaline solutions with a constant uranium concentration (5 x 10^{-3} mol·dm^{-3}) and a variable gluconate concentration (ranging from 2 x 10^{-4} to 4 x 10^{-3} mol·dm^{-3}). Samples were measured immediately after preparation, without filtration. The measured absorbance increases with the gluconate concentration in the system, compared with the absorbance in the absence of organic ligand (dashed black line). Furthermore, a displacement on the wavelength that shows the maximum absorbance signal is also noticed. This indicates the formation of U(VI)-gluconate complexes.

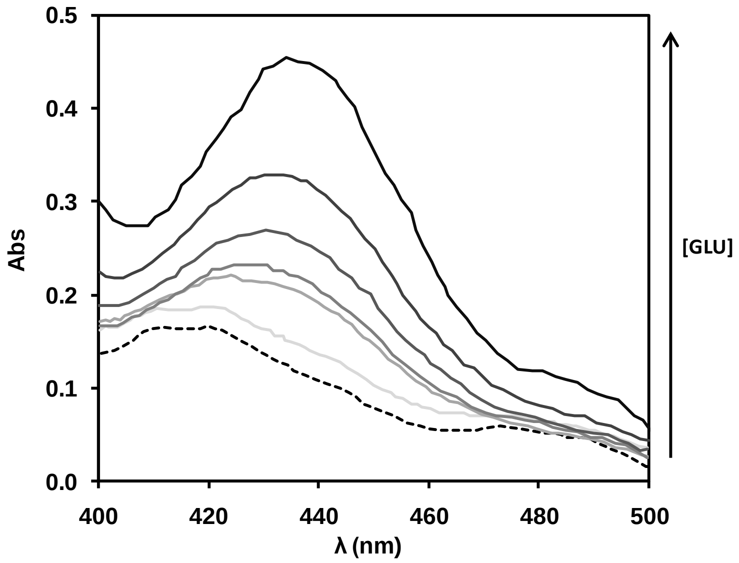

Fig. 6 Spectra recorded for solutions with a constant uranium concentration (5 x 10^{-3} mol·dm^{-3}) and increasing gluconate concentrations (from 2 x 10^{-4} to 4 x 10^{-3} mol·dm^{-3}) at pH=12. Dashed black line indicates the absorbance in the absence of organic ligand.

Measurements were also performed using the continuous variation method [5, 20-21] at λ=435nm, which is expected to be the absorbance maximum of the uranium-gluconate complex [5]. The sum of metal and ligand concentrations was kept constant in all the samples at [U]+[L]=1 x 10^{-2} mol·dm^{-3}. The measured absorbance versus the uranium mole fraction is shown in Fig. 7. The inflection at mole fraction 0.5 (vertical dotted line) indicates a metal:ligand stoichiometry of 1:1, therefore suggesting the formation of a 1:1 U(VI):gluconate complex.

It should be mentioned that after 1 week of sample preparation, a yellow precipitate appeared in tubes with uranium molar fractions higher than 0.75 (open symbols in Fig. 7). TMAOH (with a final concentration of 0.1 mol·dm^{-3}) was used to adjust the pH to 12 in UV-VIS samples. The tetramethylammonium counterion was expected to suppress formation of uranate salts, as reported by Clark et al. [22]. However, other solids may limit U(VI) solubility under alkaline conditions. In the absence of any complexing agent, schoepite ($UO_2(OH)_2(s)$) may precipitate if uranium concentrations of 10^{-4} mol·dm^{-3} or higher are present in solution [14, 23]. Thus, the formation of schoepite in the samples with low gluconate concentrations seems likely.

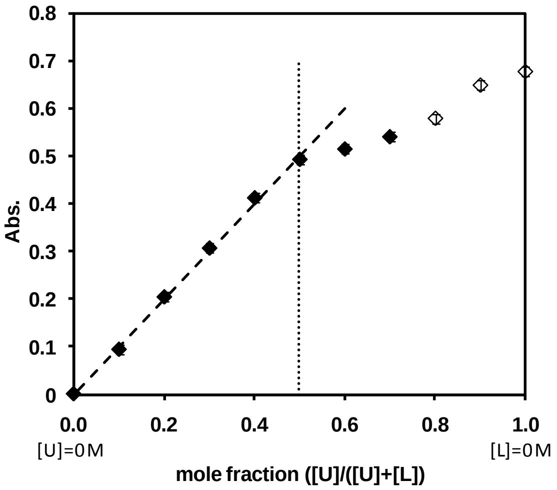

Fig. 7 UV-VIS results in the continuous variation method for uranium-gluconate samples at pH≈12; $[U]+[L]=1 \times 10^{-2}$ mol·dm^{-3}. The plot shows absorbance at λ=435nm *vs.* the mole fraction for uranium. Open symbols indicate the samples where a yellow precipitate was observed.

In order to determine the stability constant of the U(VI)-gluconate complex, further UV-VIS experiments were performed using the molar variation method [21, 24-25]. The ligand concentration in sample solutions was varied from 0 to 7×10^{-3} mol·dm^{-3}. Uranium concentration in each sample was kept constant at $[U(VI)]_{total}=1 \times 10^{-3}$ mol·dm^{-3}.

8 days after its preparation, a yellow precipitate was present in those samples with no gluconate present or with gluconate concentrations below 5×10^{-4} mol·dm^{-3}. As discussed above, this may be due to the formation of schoepite in the solutions. Preliminary tests with lower uranium concentration (which would have avoided the formation of schoepite in the samples) did not provide useful results, as measured absorbance was very small.

Samples were filtered before absorbance measurements. Results are shown in Fig. 8.

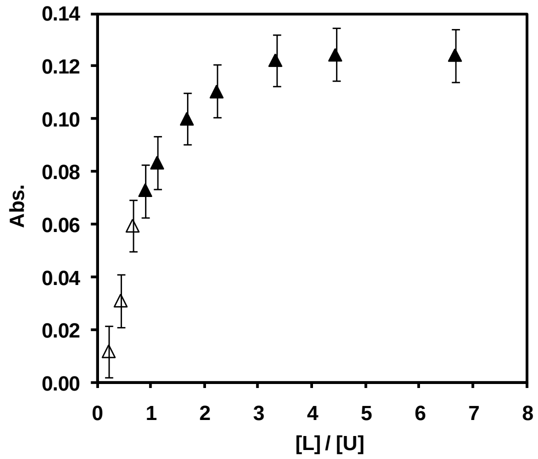

Fig. 8 UV-VIS results in the molar variation method for uranium-gluconate samples at pH≈12; $[U]_{total}=1 \times 10^{-3}$ mol·dm^{-3}. The graph shows absorbance at $\lambda=435$nm vs. the ratio [L]/[U], after sample filtration. Open symbols: samples were precipitation was observed before filtration.

The molar absorptivity $\varepsilon=119$ for the 1:1 U:gluconate complex was estimated from the samples where [L]/[U]>3 by using the Beer's law [21]. Under those conditions, uranium-gluconate complex is expected to be the main species in solution, and the contribution of the non-complexed uranium species ($UO_2(OH)_3^-$ and $UO_2(OH)_4^{2-}$) to the total signal should be less than 10%.

The amount of free gluconate ligand "$[L]_{free}$" was calculated in samples with [L]/[U]>1 by considering that all the measured absorbance was due to the formation of an uranium-gluconate complex. Table 1 summarises the calculated data.

Table 1 Experimental total uranium and gluconate concentrations and calculated free gluconate concentrations used as initial input parameters for iterative FITEQL calculations.

$[U]_T$ (mol·dm^{-3})	$[L]_T$ (mol·dm^{-3})	$[L]_{free}$ (mol·dm^{-3})
1.04×10^{-3}	1.16×10^{-3}	4.56×10^{-4}
1.04×10^{-3}	1.74×10^{-3}	8.94×10^{-4}
1.04×10^{-3}	2.32×10^{-3}	1.38×10^{-3}
1.04×10^{-3}	3.47×10^{-3}	2.44×10^{-3}
1.04×10^{-3}	4.63×10^{-3}	3.58×10^{-3}
1.04×10^{-3}	6.95×10^{-3}	5.90×10^{-3}

Data from Table 1 was used as input data in FITEQL iterative calculations [13] in order to obtain stability constant for the U(VI)-gluconate complex, taking into account the U(VI) hydrolysis species.

The estimated stability constant for the formation of the uranium-gluconate complex is shown in Eq. 7.

$$UO_2(OH)_3^- + GH_4^- = UO_2(OH)_2(GH_3)^{2-} + H_2O \quad \log_{10}K^\circ = 3.9 \pm 1 \quad (7)$$

A difficult aspect of establishing a reaction stoichiometry is to know the proton composition of the species. Further data at varying pH values would be necessary in order to confirm the number of protons involved in the reaction. However, taking into account the studies by Zhang et al. [7], were the α-hydroxyl group was demonstrated to deprotonate and coordinate to U(VI) even in the acidic pH range, it is expected that the hydroxyl groups of gluconate should also play a role on U(VI) complexation under alkaline conditions.

The geometries of gluconate complexes of uranyl(VI) were also studied using density functional theory by Birjkumar and co-workers [26]. The authors suggested the formation of different complexes depending on the pH of the solution. The species reported in present work, $UO_2(OH)_2(GH_3)^{2-}$, is in agreement with the $UO_2Glu_{-H}(HO)_2^{2-}$ complex suggested to be formed at high pH values by Birjkumar et al (notice that the gluconate nomenclature used in [26] is different from the one used in present work).

4 Comparison with literature data

The complexation of U(VI) with gluconate (or isosaccharinate) in the alkaline pH range has been studied in previous works [5, 18].

Sawyer and Kula [5] studied the complexation of U(VI) with gluconate under alkaline conditions characteristic of cement environments. On the basis of the results obtained from spectrophotometry, polarography, polarimetry, and pH measurements the authors reported the formation of an $(UO_2)(GH_4)(OH)_2^-$ complex and proposed the reaction shown in Eq. 8 for its formation.

$$UO_2(OH)^+ + OH^- + GH_4^- = (UO_2)(GH_4)(OH)_2^- \quad \log_{10}K = 6.3 \qquad (8)$$

According to the currently accepted uranium thermodynamic data [14], the speciation of U(VI) in solution under alkaline pH values (pH≈11 and higher) in the absence of organic ligands is dominated by $UO_2(OH)_3^-$ and $UO_2(OH)_4^{2-}$, and not by $UO_2(OH)^+$. This implies that the stability constant suggested by Sawyer and Kula is not in agreement with the expected U(VI) chemical speciation in the absence of organic ligands.

Warwick and co-workers [18] studied the U(VI)-isosaccharinate system using as a basis the solubility of sodium uranate at different pH values in the presence of the organic ligand. At pH=13.3 the authors reported a value of $\log_{10}\beta = 18.8 \pm 1.6$ for the formation of a $UO_2ISA(OH)_4$ complex, as seen in Eq. 9 (the charge of the species formed was omitted by the authors).

$$UO_2^{2+} + ISA + 4OH^- = UO_2ISA(OH)_4 \quad \log_{10}\beta = 18.8 \pm 1.6 \qquad (9)$$

The uranium hydrolysis constants used in the calculations by Warwick and co-workers were those in the NIST database ($\log_{10}\beta(UO_2(OH)_4^{2-})$=22.2 and $\log_{10}\beta(UO_2(OH)_3^-)$=22.2), which are slightly different from the ones used in present work. Furthermore, although both isosaccharinate and gluconate are polyhydroxycarboxylic acids with a similar chemical structure, the analogy between both ligands should be used with caution [27]. Thus, the comparison between the results by Warwick and co-workers and the ones obtained in present work may not be straightforward.

5 Conclusions

The formation of a U(VI)–gluconate complex was investigated by UV-VIS absorbance measurements. The analysis of UV-VIS data (using the continuous variation method and the molar variation method) allowed the calculation of a stability constant for the formation of a $UO_2(OH)_2(GH_3)^{2-}$ complex in alkaline solution (pH≈12).

The stability constant determined by UV-VIS (Eq. 7) was used to explain the results obtained from solubility experiments, from both over- and undersaturation conditions. The observed results in experiments from oversaturation direction can be explained by the formation of the U-gluconate complex. According to the calculations, even higher uranium concentrations could be maintained in solution with $[GLU]>10^{-2}$ $mol\cdot dm^{-3}$, if these data were available.

The undersaturation results can be partially explained taking into account the formation of the U-gluconate with the stability constant shown in Eq. 7. However, the high uncertainty observed for both the uranate solubility and the U-gluconate complex complicates the interpretation of the data. At high gluconate concentrations ($\approx 10^{-1}$ $mol\cdot dm^{-3}$) the dissolution of the solid seems to be limited. This could be explained by the gluconate sorption or precipitation onto the solid; a similar behaviour was observed in thorium hydroxide solubility experiments in the presence of gluconate [28].

The formation of $UO_2(OH)_2(GH_3)^{2-}$ increases significantly sodium and potassium uranates solubility at gluconate concentrations higher than 10^{-2} $mol\cdot dm^{-3}$, thus affecting the mobility of U(VI) under alkaline conditions. However, gluconate has been previously reported to strongly sorb on cement phases [29-30]. If we consider this sorption effect, the uptake on the organic ligand on the cement phase would then reduce the aqueous gluconate concentration below 10^{-7} mol·dm^{-3}. According to the results obtained in present work, those concentrations would not entail a significant increase in U(VI) solubility. Additionally, U(VI) could also be immobilized by cement sorption [31]. A competition between gluconate and U(VI) sorption onto cement might be disregarded according to the high amount of cement sites available.

It can be concluded that, although gluconate has been shown to significantly increase U(VI) solubility, sorption of the organic ligand onto cement would reduce the ligand availability and its capacity to from complexes with U(VI) under repository conditions.

Acknowledgements

The authors would like to thank the French National Agency for Radioactive Waste Management (ANDRA) for funding this work through the ThermoChimie project. E. Giffaut and L. Duro are acknowledged for fruitful scientific discussions. Thanks are due to the reviewers for their comments, which significantly improved the quality of the original manuscript.

Appendix

Table 2 Stability constants for U(VI) used in FITEQL calculations.

Species	$\log_{10} K^o$	*Ref.*
$UO_2(OH)^+$	-5.25±0.24	[14,16]
$UO_2(OH)_2$	-12.15±0.07	[14]
$UO_2(OH)_3$-	-20.25±0.42	[14]
$UO_2(OH)_4^{2-}$	-32.4±0.68	[14]
$(UO_2)_2(OH)^{3+}$	-2.7±1.0	[16]
$(UO_2)_2(OH)_2^{2+}$	-5.62±0.04	[16-17]
$(UO_2)_3(OH)_4^{2+}$	-11.9±0.3	[16-17]
$(UO_2)_3(OH)_5^+$	-15.55±0.12	[16-17]
$(UO_2)_3(OH)_7^-$	-32.2±0.8	[23]
$(UO_2)_4(OH)_7^+$	-21.9±1.0	[16]

Table 3 Ion interaction coefficients used in the calculations for ionic strength corrections with the SIT approach.

Species	$\varepsilon(Na^+,Anion)$ $\varepsilon(K^+,Anion)$	$\varepsilon(Cation,Cl^-)$	$\varepsilon(Cation, ClO_4^-)$	*Reference*
H^+		0.12±0.01	0.14±0.02	[15]
UO_2^{2+}		0.46±0.03	0.46±0.03	[15]
$UO_2(OH)^+$		0±0.23	-0.1±0.4	[14]
OH^-	0.04±0.01			[15]
Cl^-	0.03±0.01			[15]
ClO_4^-	0.01±0.01			[15]
$UO_2(OH)_3^-$	-0.1±0.05			[16]
$UO_2(OH)_2(GH_3)^{2-}$	-0.08			By analogy with the interaction coefficient with oxalate reported in [4]

References

[1] Bradbury, M.H., Van Loon, L.R.: Cementitious near-field sorption databases for performance assessment of a L/ILW repository in a Palfris Marl host rock. CEM-94: Update I, June 1997. Technical Report 98-01, PSI (1998)

[2] Baston, G. M. N., Berry, J. A., Bond, K. A., Brownsword, M., Linklater, C. M.: Effects of organic degradation products on the sorption of actinides. Radiochim. Acta **52/53**, 249–356 (1992)

[3] Felmy, A.R.: Chemical speciation of Americium, Curium and selected tetravalent actinides in high level waste. Technical Report EMSP Project 73749, PNNL (2004)

[4] Hummel, W., Anderegg, G., Puigdomenech, I., Rao, L., Tochiyama, O.: Chemical Thermodynamics of Compounds and Complexes of U, Np, Pu, Am, Tc, Se, Ni, and Zr with Selected Organic Ligands. Elsevier, Amsterdam (2005)

[5] Sawyer, D. T., Kula, R.: Uranium(VI) gluconate complexes. Inorg. Chem. **1**, 303–309, (1962)

[6] Tits, J., Wieland, E., Bradbury, M. The effect of isosaccharinic acid and gluconic acid on the retention of Eu(III), Am(III) and Th(IV) by calcite. Appl. Geochem. **20**, 2082–2096 (2005)

[7] Zhang, Z., Helms, G., Clark, S., Tian, G., Zanonato, P., Rao, L.: Complexation of Uranium(VI) by gluconate in acidic solutions: a thermodynamic study with structural analysis. Inorg. Chem. **48**, 3814–3824 (2009)

[8] Sawyer, D.T.: Metal-gluconate complexes. Chem. Rev. **64**, 633–643 (1964)

[9] Meinrath, G.: Aquatic chemistry of uranium. Geoscience **1**, 1–101 (1998)

[10] Kitamura, A., Kohara, Y.: Carbonate complexation of Neptunium(IV) in highly basic solutions. Radiochim. Acta **92**, 583–588 (2004)

[11] Gran, G.: Determination of the equivalence point in potentiometric titrations. Part II. The Analyst **77**, 661–671 (1952)

[12] Yamamura, T., Kitamura, A., Fukui, A., Nishikawa, S., Yamamoto, T., Moriyama, H.: Solubility of U(VI) in highly basic solutions. Radiochim. Acta **83**, 139–146 (1998)

[13] Herbelin, A., Westall, J. FITEQL 4.0: a computer program for determination of chemical equilibrium constants from experimental data. Technical report, Report 99-01. Department of Chemistry, Oregon State University, Corvallis (1999)

[14] Guillaumont, R., Fanghänel, J., Neck, V., Fuger, J., Palmer, D., Grenthe, I., Rand, M.: Update on the Chemical Thermodynamics of Uranium, Neptunium, Plutonium, Americium and Technetium. Elsevier, Amsterdam (2003)

[15] Rand, M., Fuger, J., Grenthe, I., Neck, V., Rai, D.: Chemical Thermodynamics of Thorium. Elsevier, Amsterdam (2009)

[16] Grenthe, I., Fuger, J., Konings, R., Lemire, R., Muller, A., Nguyen-Trung, C., Wanner, H.: Chemical Thermodynamics 1: Chemical Thermodynamics of Uranium. Elsevier, Amsterdam (1992)

[17] Lemire, R. J., Fuger, J., Nitsche, H., Potter, P., Rand, M. H., Rydberg, J., Spahiu, K., Sullivan, J. C., Ullman, W. J., Vitorge, P., Wanner, H.: Chemical Thermodynamics of Neptunium and Plutonium. Elsevier, Amsterdam (2001)

[18] Warwick, P., Evans, N., Vines, S.: Studies on some divalent metal alpha-isosaccharinic acid complexes. Radiochim. Acta **94**, 363–368 (2006)

[19] Sutton, M., Warwick, P., Hall, A., Jones, C.: Carbonate induced dissolution of uranium containing precipitates under cement leachate conditions. J. Environ. Monit. **1**, 177–182 (1999)

[20] Bruneau, E., Lavabre, D., Levy, G., Micheau, J. C.: Quantitative analysis of continuous-variation plots with a comparison of several methods: Spectrophotometric study of organic and inorganic 1: 1 stoichiometry complexes. J. Chem. Educ. **69**, 833–837 (1992)

[21] Rossotti, F. J. C., Rossotti, H.: The Determination of Stability Constants and Other Equilibrium Constants in Solution. McGraw-Hill Book Company, Inc., New York, Toronto, London (1961)

[22] Clark, D.L., Conradson, S. D., Donohoe, R. J., Keogh, D. W., Morris, D. E., Palmer, P. D., Rogers, R. D., Tait, C. D.: Chemical speciation of the uranyl ion under highly alkaline conditions. Synthesis, structures, and oxo ligand exchange dynamics. Inorg. Chem. **38**, 1456–1466 (1999)

[23] Sandino, A., Bruno, J.: The solubility of $(UO_2)_3(PO_4)_2{:}4H_2O(s)$ and the formation of U(VI) phosphate complexes: Their influence in uranium speciation in natural waters. Geochim. Cosmochim. Acta **56**, 4135–4145 (1992)

[24] Havel, J., Soto-Guerrero, J., Lubal, P.: Spectrophotometric study of uranyl-oxalate complexation in solution. Polyhedron **21**, 1411–1420 (2002)

[25] Meyer Jr, A., Ayres, G.: The mole ratio method for spectrophotometric determination of complexes in solution. J. Am. Chem. Soc. **79**, 49–53 (1957)

[26] Birjkumar, K. H., Bryan, N. D., Kaltsoyannis, N.: Computational investigation of the speciation of uranyl gluconate complexes in aqueous solution. Dalton Trans. **40**, 11248–11257 (2012)

[27] Birjkumar, K. H., Bryan, N. D., Kaltsoyannis, N.: Is gluconate a good model for isosaccharinate in uranyl(VI) chemistry? a DFT study. Dalton Trans. **41**, 5542–5552 (2012)

[28] Colàs, E., Grivé, M., Rojo, I., Duro, L.: Solubility of $ThO_2{\cdot}xH_2O(am)$ in the presence of gluconate. Radiochim. Acta **99**, 269–273 (2011)

[29] Glaus M.A., Van Loon, L. R.: A generic procedure for the assessment of the effect of concrete admixtures on the retention behaviour of cement for radionuclides: concept and case studies. Technical Report 04-02, PSI (2004)

[30] Glaus, M. A., Laube, A., Van Loon, L. R.: Solid–liquid distribution of selected concrete admixtures in hardened cement pastes. Waste Manag. **26**, 741–751 (2006)

[31] Wieland E., Van Loon, L. R.: Cementitious near-field sorption database for performance assessment of an ilw repository in opalinus clay. Technical Report 03-06, PSI (2003)

12 Appendix A: Application on performance assessment calculations

The influence of organic ligands on enhancing the solubility of radionuclides in alkaline conditions has been shown in this work. However, this influence under repository conditions may be affected by other phenomena:

-the competition with other metals such as Na or Ca, especially in the case of EDTA, as studied in this work.

-sorption of organic ligands in the solid materials (e.g. cement) present in the repository, as described below.

Concrete and cement materials used in radioactive waste disposal must fulfil several requirements to ensure mechanical stability and durability of the structures. Different types of cement formulations can be used in a radioactive waste repository. One of the most common cement types is CEM I, a general purpose cement with a Portland clinker content of over 95%.

A large number of different types of organic compounds, such as superplasticizers (polycarboxylate ethers, PCEs), are added to cement in order to influence its properties. Typical dosage range for superplasticizers is usually between 0.5 to 2.2 % by weight of cement (Dransfield 2005). Admixtures are usually sold diluted in water, with a concentration less than 40% (Dransfield 2005). Hence, the real concentration of superplasticizers on cement will be below 0.9% on weight.

Structure, molecular weight or the number of carboxylic or alcohol groups in each polymer chain of the superplasticizer is not exactly know; however, gluconate can be used as a simple molecule representative of the worst effect (very conservative estimate) that superplasticizers can have on radionuclide mobility. By considering the gluconate structure and its molecular weight, a concentration of 0.04 mols of “gluconate” (used as superplasticizer analogue) per kg of cement could be calculated.

In the case of CEM I formulations, an approximate concentration of 0.04 mols of "gluconate" (using gluconate as a direct analogue for superplasticizer) per kg of cement material may be expected. Then, from a conservative point of view, the maximum concentration of "gluconate" in cement would be $\approx 4 \cdot 10^{-5}$ mol/g.

If all this admixture could be leached from cement, and using the parameters of a highly compact concrete in the calculations (within the range of 300 to 550 kg/m^3, with a low porosity between 10-20 %, (ANDRA 2005a), the maximum "gluconate" concentration in cement pore water can be estimated to be in the range $6 \cdot 10^{-2}$ to $2 \cdot 10^{-1}$ M. Such a high concentration of gluconate could increase thorium mobility, increasing thorium hydroxide solubility some orders of magnitude according to the results obtained in present work.

Nevertheless, both superplasticizers and gluconate are expected to sorb strongly on cement. Superplasticizers are expected to sorb onto the surface of the cement particles at a very early stage in the hydration process and produce an electrostatic repulsion that disperses cement particles. Lateral chains are also expected to play a key role, generating a steric hindrance which also separates and disperses the particles[7]. As a consequence, the superplasticizer will be sorbed on cement, and its free concentration on the system will be reduced, decreasing its influence on thorium mobility.

Gluconate has also been shown to be strongly sorbed onto fresh cement materials (Glaus et al. 2006, Glaus & Van Loon 2004). According to Glaus et al., the sorption of gluconate onto cement can be fitted by a two-site Langmuir isotherm. Using the parameters reported for this isotherm (Glaus et al. 2006) it is possible to calculate that most of the gluconate would be sorbed onto the cement phase. Uptake on the cement phase would then reduce the aqueous gluconate concentration to approximately 10^{-7} M; this concentration would not produce a significant increase in thorium hydroxide solubility according to the results obtained in present work.

Solubility is not the only mechanism that could reduce radionuclide mobility under repository conditions. Sorption of radionuclides (as Th) on cement are also a key mechanism to slow down or even avoid the release of the metals from their confinement. It could then be argued that the organic ligands could compete with thorium for sorption sites on cement materials, thus increasing the mobility of this radionuclide. Nevertheless, data provided by Glaus et al. seem to indicate that cement would be undersaturated with respect to sorption of gluconate; part of the sites may still be available to radionuclide sorption and immobilization.

---

[7] Information from Glenium 27 Technical data sheet. Glenium 27 is polycarboxylic ether superplasticizer from BASF company.

It can be concluded that, although gluconate could significantly enhance thorium mobility, sorption of the organic ligand onto cement would reduce the ligand free availability and its capacity to form complexes with Th, at least on non-degraded cement materials.

A similar conclusion could be reached in the case of isosaccharinate. The total isosaccharinate content in the repository will depend on the initial cellulose amount present in the waste. The degradation of cellulose will result in the formation of isosaccharinate (Glaus & Van Loon 2008, Pavasars et al. 2003, Van Loon & Glaus 1997). In any case, isosaccharinate is also strongly sorbed on cement (Glaus et al. 2006); an initial concentration of 0.1-0.01 M in cement porewater could be reduced to $10^{-4} – 10^{-5}$ M due to sorption (Van Loon & Glaus 1998).

13 Appendix B: Thermodynamic database

Thermodynamic data selected in ThermoChimie were used in the calculations.

ThermoChimie is Andra (the French National Radioactive Waste Management Agency) thermodynamic database (Duro et al. 2010, Duro et al. 2012). ThermoChimie has been issued together with PhreeqC code (Parkhurst & Appelo 2001). The database contains all the parameters relevant for the calculations performed in present work, including SIT interaction coefficients and data valid in the pH range of 5 to 14.

13.1 Thorium

Thermodynamic data for thorium are based in the NEA selection (Rand et al. 2009), with minimum modifications.

The stability constant for the thorium hydroxide solid used in the calculations was determined experimentally (section 4.2).

The stability constants for thorium are summarized in Table 13-1.

Table 13-1. Summary of stability constants for thorium used in present work.

Species	LogK°	Reference
Th^{4+}	master species	(Rand et al. 2009)
$Th(OH)^{3+}$	-2.5±0.5	(Rand et al. 2009)
$Th(OH)_2^{2+}$	-6.2±0.5	(Rand et al. 2009)
$Th(OH)_3^{+}$	-11	(Rand et al. 2009) as discussed in ThermoChimie database
$Th(OH)_4$	-17.4±0.7	(Rand et al. 2009)
$Th_2(OH)_2^{6+}$	-5.9±0.5	(Rand et al. 2009)
$Th_2(OH)_3^{5+}$	-6.8±0.2	(Rand et al. 2009)
$Th_4(OH)_{12}^{4+}$	-26.6±0.2	(Rand et al. 2009)
$Th_4(OH)_8^{8+}$	-20.4±0.4	(Rand et al. 2009)
$Th_6(OH)_{14}^{10+}$	-36.8±1.2	(Rand et al. 2009)
$Th_6(OH)_{15}^{9+}$	-36.8±1.5	(Rand et al. 2009)
$Ca_4Th(OH)_8^{4+}$	-63.1±1.0	(Altmaier et al. 2008)
Th-gluconate	p.w.	see present work
Th-isosaccharinate	p.w.	see present work
Ca-Th-gluconate	p.w.	see present work
Th-EDTA	p.w.	see present work
Ca-Th-EDTA	p.w.	see present work
$ThO_2 \cdot xH_2O$	p.w.	see present work

13.2 Uranium

Thermodynamic data for U(VI) are based in the NEA selection (Grenthe et al. 1992, Guillaumont et al. 2003), with minimum modifications.

Several solid species can limit U(VI) solubility under alkaline conditions. Formation of uranates such as Na^+, K^+, Ca^{2+}, Mg^{2+} and other cations is reported in the literature (Meinrath 1998). Solubility constants for $Na_2U_2O_7{\cdot}xH_2O$ and $K_2U_2O_7{\cdot}xH_2O$ were determined experimentally in present work.

The stability constants for U(VI) are summarized in Table 13-2.

Table 13-2. Summary of stability constants for U(VI) used in present work.

Species	LogK°	Reference
UO_2^{2+}	master species	(Rand et al. 2009)
$UO_2(OH)^+$	-5.25±0.24	(Grenthe et al. 1992)
$UO_2(OH)_2$	-12.15±0.07	(Guillaumont et al. 2003)
$UO_2(OH)_3^-$	-20.3±0.4	(Guillaumont et al. 2003)
$UO_2(OH)_4^{2-}$	-32.4±0.7	(Guillaumont et al. 2003)
$(UO_2)_2(OH)^{3+}$	-2.7±1.0	(Grenthe et al. 1992)
$(UO_2)_2(OH)_2^{2+}$	-5.62±0.04	(Grenthe et al. 1992)
$(UO_2)_3(OH)_4^{2+}$	-11.9±0.3	(Grenthe et al. 1992)
$(UO_2)_3(OH)_5^+$	-15.6±0.1	(Grenthe et al. 1992)
$(UO_2)_3(OH)_7^-$	-32.2±0.8	(Sandino & Bruno 1992)
$(UO_2)_4(OH)_7^+$	-21.9±1.0	(Grenthe et al. 1992)
U(VI)-gluconate	p.w.	see present work
U(VI)-EDTA	p.w.	see present work
$Na_2U_2O_7 \cdot xH_2O$	p.w.	see present work
$K_2U_2O_7 \cdot xH_2O$	p.w.	see present work

13.3 Organic ligands

Stability constants for acid/base, sodium and calcium complexes with the organic ligands like gluconate, isosaccharinate and EDTA are summarized in Table 13-3 and were taken into account in the calculations.

Table 13-3. Summary of stability constants for acid/base, sodium and calcium complexes with organic ligands used in present work.

Species	$\mathrm{LogK^o}$	Reference
GH_4^-	master species	
$HGH_4(aq)$	3.9±0.1	(Zubiaur et al. 1998)
$Ca(GH_4)^+$	1.73±0.05	(Schubert & Lindenbaum 1952)
$Ca(GH_3)(aq)$ or $Ca(OH)(GH_4)(aq)$	-10.4±0.5	(Tits et al. 2002)
$Ca(GH_4)_2(s)$	4.19±0.05	(Van Loon et al. 1999)
$ISAH_2^-$	master species	
$HISAH_2$	4.0±0.5	(Hummel et al. 2005)
$Ca(ISAH)(aq)$ or $Ca(OH)(ISAH_2)(aq)$	-10.4±0.5	(Hummel et al. 2005)
$Ca(HISAH_2)^+$	1.7±0.3	(Hummel et al. 2005)
$Ca(ISAH_2)_2(s)$	6.4±0.2	(Hummel et al. 2005)
$EDTA^{4-}$	master species	
$HEDTA^{3-}$	11.24±0.03	(Hummel et al. 2005)
$NaEDTA^{3-}$	2.8±0.2	(Hummel et al. 2005)
$Ca(EDTA)^{2-}$	12.69±0.06	(Hummel et al. 2005)

13.4 Ionic strength calculations

13.4.1 SIT approach

In order to deduce the stoichiometry and equilibrium constants in experimental systems, it is always necessary to vary the concentrations of reactants and products over concentration ranges under conditions where the activity coefficients of the species are either known or constant. Only in this way is it possible to use the mass balance equations for the various components together with the measurement of one or more free concentrations to obtain the information desired. The activity coefficient γ_i of the species i is the factor that accounts for the difference of the behaviour of the solute from ideality, defined as the ratio between activity and concentration.

To subtract the effect of the ionic strength and obtain the value at infinite dilution several models, that allow the estimation of the activity coefficients of solutes, have been established. One of these models is the Specific Interaction Theory, SIT (Grenthe et al. 1997).

$$\log(\gamma_i) = -z_i^2\left(\frac{A\sqrt{I_m}}{1+Ba_i\sqrt{I_m}}\right) + \sum_k \varepsilon(i,k,I_m)m_k \qquad \text{eq. 13-1}$$

In the SIT approach, the activity coefficient γ_i of the species $_i$ of charge z_i in the solution of ionic strength I_m may be described by eq. 13-1. A and B are constants which are temperature and pressure dependent, and a_i is an ion size parameter for the hydrated ion. The Debye-Hückel limiting slope, A, has a value of (0.509 ± 0.001) $kg^{1/2}\cdot mol^{-1/2}$. The term Ba_i has been assigned a value of 1.5 $kg^{1/2}\cdot mol^{-1/2}$ at 25ºC and 1 bar (Grenthe et al. 1997). The ion interaction coefficients ε(j,k)($kg\cdot mol^{-1}$) depends on each species and each ionic medium.

$$mM + qL + nH_2O(l) = M_mL_q(OH)_n + nH^+ \qquad \text{r. 13-1}$$

For a model reaction (r. 13-1), and taking into account the calculated activity coefficient γ_i obtained with eq. 13-1 and the log β value determined in an ionic medium ($I\neq0$), the log βº value at standard state (infinite dilution) can be calculated by using eq. 13-2.

$$\begin{aligned} log_{10}\beta_{q,n,m} &= log_{10}\beta^0_{q,n,m} + mlog_{10}\gamma_M + qlog_{10}\gamma_L + nlog_{10}a_{H2O} - log_{10}\gamma_{q,n,m} \\ &\quad + nlog_{10}\gamma_{H+} \end{aligned} \qquad \text{eq. 13-2}$$

The ion interaction coefficients ε(j,k)($kg\cdot mol^{-1}$) used in present work are summarized in Table 13-4.

Table 13-4. Ion interaction coefficients used in present work.

Species	ε(Na^+, Anion)	ε(Cation, Cl^-)	ε(Cation, ClO_4^-)	Reference
H^+		0.12±0.01	0.14±0.02	(Rand et al. 2009)
K^+		0.00±0.01		(Rand et al. 2009)
OH^-	0.04±0.01			(Rand et al. 2009)
Cl^-	0.03±0.01			(Rand et al. 2009)
ClO_4^-	0.01±0.01			(Rand et al. 2009)
$EDTA^{4-}$	0.32±0.14			(Rand et al. 2009)
Th^{4+}			0.7±0.1	(Rand et al. 2009)
$Th(OH)^{3+}$			0.48±0.08	(Rand et al. 2009)
$Th(OH)_2^{2+}$			0.33±0.1	(Rand et al. 2009)
$Th(OH)_3^+$			0.15±0.1	(Rand et al. 2009) as discussed in ThermoChimie database
$Th_2(OH)_2^{6+}$			1.22±0.24	(Rand et al. 2009)
$Th_2(OH)_3^{5+}$			0.91±0.21	(Rand et al. 2009)
$Th_4(OH)_{12}^{4+}$			0.56±0.42	(Rand et al. 2009)
$Th_4(OH)_8^{8+}$			1.69±0.42	(Rand et al. 2009)
$Th_6(OH)_{14}^{10+}$			2.2±0.3	(Rand et al. 2009)
$Th_6(OH)_{15}^{9+}$			1.85±0.74	(Rand et al. 2009)
$Ca_4Th(OH)_8^{4+}$			0.21±0.17	(Altmaier et al. 2008)
UO_2^{2+}		0.46±0.03	0.46±0.03	(Rand et al. 2009)
$UO_2(OH)^+$		0±0.23	-0.1±0.4	(Guillaumont et al. 2003) (Grenthe et al. 1992)
$UO_2(OH)_3$-	-0.1±0.05			(Guillaumont et al. 2003)
$(UO_2)_2(OH)_2^{2+}$		0.69±0.07	0.57±0.07	(Grenthe et al. 1992) (Lemire et al. 2001)
$(UO_2)_3(OH)_4^{2+}$		0.5±0.18		(Grenthe et al. 1992) (Lemire et al. 2001)
$(UO_2)_3(OH)_5^+$		0.81±0.17		(Grenthe et al. 1992) (Lemire et al. 2001)

Not all the interaction coefficients needed to perform ionic strength corrections in present work are available in the literature. The value of ε for these complexes have been obtained by estimations based on the analogy to similar compounds, given that ions of the same charge type have similar ion interaction coefficients with a given counter ion (Silva et al. 1995). Analogies between species with identical charge z_i have been as done to estimate the interaction coefficients for GH_4^-, $ISAH_2^-$, Th-gluconate, Th-isosaccharinate complexes (see section 5 and 6) and Th-EDTA complexes (see section 7). Oxalate (Ox^{2-} and HOx^-) and H_2EDTA^{2-} have been used as a model (Table

13-5). Oxalate had previously been used to estimate isosaccharinate interaction coefficients by Rai and co-workers (Rai et al. 2009).

Table 13-5. Ion interaction coefficients used in present work in order to perform analogies.

Species	ε(Na^+, Anion)	Reference	used to estimate the interaction coefficients for:
HOx^-	-0.07±0.01	(Rand et al. 2009)	GH_4^-, $ISAH_2^-$, $Th(OH)_n(GH_x)^-$, $Th(OH)_n(ISAH_x)^-$
Ox^{2-}	-0.08±0.01	(Rand et al. 2009)	$Th(OH)_n(GH_x)_2^{2-}$, $Th(OH)_n(ISAH_x)_2^{2-}$
H_2EDTA^{2-}	-0.37±0.14	(Rand et al. 2009)	$Th(OH)_2(EDTA)^{2-}$

13.4.2 Comparison with Davies corrections

As explained in the previous section, the ε values for GH_4^-, $ISAH_2^-$, Th-gluconate and Th-isosaccharinate complexes have been estimated using an analogy with oxalate. In order to verify the influence of the estimated ε values in the stability constants after the correction to I=0, the values corrected using SIT have been compared with the values corrected using the Davies approach.

$$\log(\gamma_i) = -Az_i^2\left(\frac{\sqrt{I_m}}{1+\sqrt{I_m}} - 0.3I_m\right) \qquad \text{eq. 13-3}$$

In the Davies approach, the activity coefficient γ_i of the species $_i$ of charge z_i in the solution of ionic strength I_m may be described by eq. 13-3 (Grenthe et al. 1997). The Debye-Hückel limiting slope, A, has a value of 0.51 $kg^{1/2}\cdot mol^{-1/2}$. Ion interaction coefficients are not used in this approach.

Table 13-6. Comparison of Th-gluconate and Th-isosaccharinate constants obtained in present work (I=0.5) and after correction to I=0 with SIT or Davies approaches. Two significant figures are provided for the values at log K° in order to facilitate the comparison.

	log K (I=0.5)	log K° (SIT)	log K° (Davies)
$Th(OH)_4 + GH_4^- = Th(OH)_n(GH_x)^-$	5.6±0.6	5.61	5.61
$Th(OH)_4 + 2GH_4^- = Th(OH)_n(GH_x)_2^{2-}$	≈ 7.8	≈ 7.49	≈ 7.54
$Th(OH)_4 + ISAH_2^- = Th(OH)_n(ISAH_x)^-$	≈ 4.2	≈ 4.21	≈ 4.21
$Th(OH)_4 + 2ISAH_2^- = Th(OH)_n(ISAH_x)_2^{2-}$	7.3±1.0	6.99	7.04

The comparison indicates that the major effects on activity corrections result from the Debye-Hückel term rather than being related to the estimated ion-interaction parameters.

14 Appendix C: Analytical techniques

14.1 pH determination

Determination of H^+ concentration (pH_c measurement) was conducted using the approach described in the literature (Kitamura & Kohara 2004, Yamamura et al. 1998). A Crison 52.22 electrode (an alkaline-resistant glass electrode with high tolerance to suspended solids) was used. The internal electrolyte was replaced by a mixture of the original electrolyte and the background electrolyte used in the experiments (usually $NaClO_4$).

$$\text{Test solution (I M), } NaClO_4 \text{ (I M)} \parallel NaCl \mid AgCl, Ag$$

The electrode is calibrated by a Gran titration procedure (Gran 1952) using a solution with the same background electrolyte. An example of a calibration is provided below.

Example:

The glass electrode equation (eq. 14-1) provides a relationship between the potential measured with the electrode E and the proton concentration H. The E_0 value is determined in the calibration procedure.

$$E=E_0 + g \log (H) \qquad \text{eq. 14-1}$$

To obtain the E_0 value, 0.05ml of concentrated $HClO_4$ (9.17 M) were added to 50 ml (V_0) of the ionic media (50 ml of $NaClO_4$ 0.5 M). This solution was titrated with a NaOH solution of a 0.0534 M concentration (C_b). Results are shown in Figure 14-1.

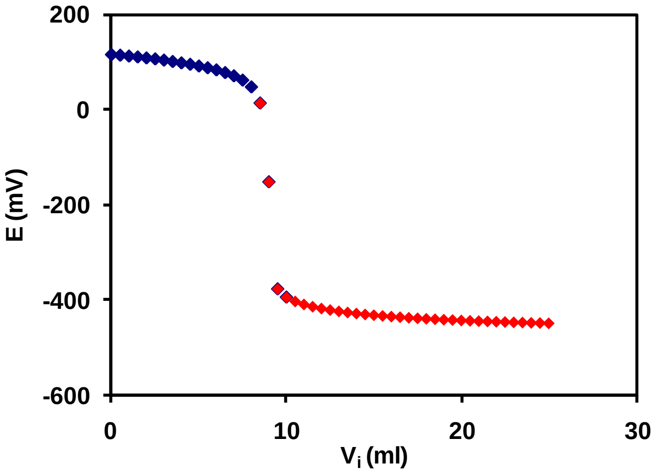

Figure 14-1. Electrode calibration titration plot. The graph shows the potential measured *vs*. the volume of NaOH added (V_i).

Results of the titration procedure are plotted in a graph (Figure 14-2) were x is the total volume ($V_0 + V_i$) and y is the Gran function (eq. 14-2 and eq. 14-3).

$$y = 10^{\frac{E}{g}}\, x\, (V_0 + V_i) \qquad \text{acid region} \qquad \text{eq. 14-2}$$

$$y = 10^{\frac{-E}{g}}\, x\, (V_0 + V_i) \qquad \text{basic region} \qquad \text{eq. 14-3}$$

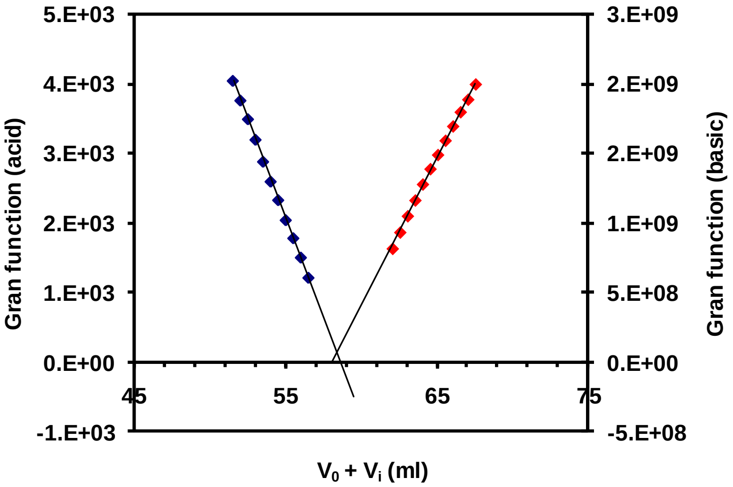

Figure 14-2. Plot of the Gran function in front of the total volume of solution.

The E_0 value can be obtained from eq. 14-4, using the slope calculated from the Gran function in Figure 14-2 and the concentration of the NaOH solution (C_b) used in the titration.

$$E_0 = g\ x\ log\left(\frac{-slope}{C_b}\right) \qquad \text{eq. 14-4}$$

14.2 ICP-MS and ICP-OES

Thorium or uranium concentrations were determined by ICP-MS (Perkin Elmer Elan 6000 or Agilent 7500cx). An example of a typical calibration is shown in Figure 14-3. Quantification limit for the metals in the original solutions (after dilution with HNO_3 2%) was $1\cdot10^{-9}$mol/l, and the typical error was 5%.

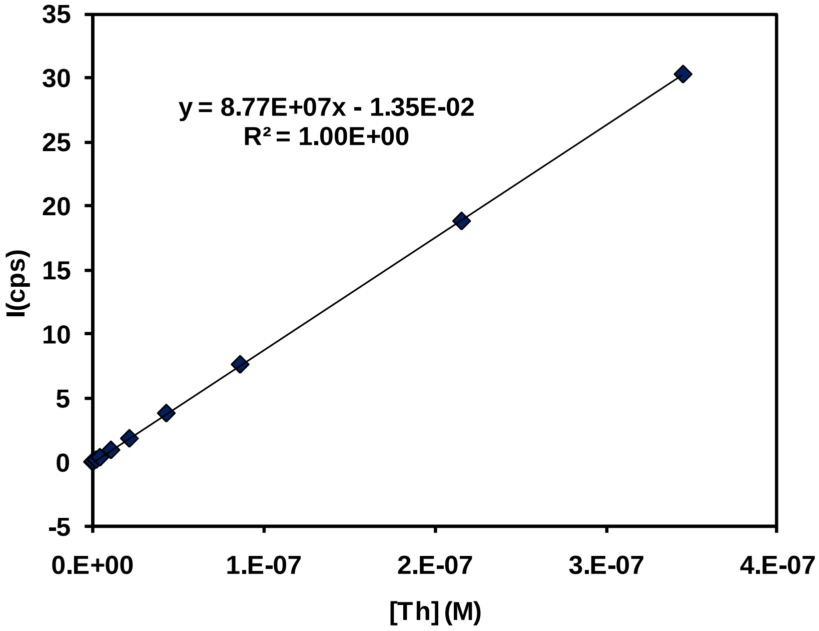

Figure 14-3. Example of an ICP-MS calibration for thorium.

Calcium was measured using ICP-OES (Thermo ICAP 6300MCF DUO). Quantification limit for calcium in the original solutions was $2.5\cdot10^{-5}$ M, and the typical error was 5%.

14.3 TOC

Gluconate, isosaccharinate and EDTA were measured as total organic carbon concentrations using TOC equipment (Shimadzu TOC-5050A) after dilution and acidification of the samples. Detection limit after dilution was $1\cdot10^{-4}$ M and typical error was 10%.

14.4 EXAFS

Thorium L_{III}-edge EXAFS spectra were collected at the ROssendorf Beam Line (ROBL) at the European Synchrotron Radiation Facility (ESRF) located in Grenoble (France). Spectra were collected in fluorescence mode at room temperature. A minimum of five and a maximum of twelve scans were collected for each sample. Spectra were pre-treated and averaged using Sixpack (Webb 2005). Data analysis was performed using the WinXAS software (Ressler 1998). Theoretical scattering amplitudes for each absorber and backscattered pair were calculated with the FEFF 8.20 code (Rehr & Albers 2000). The amplitude reduction factor, S_0^2, was defined as 1.0 and a single value of the shift in threshold energy, ΔE_0, was allowed to vary for all coordination shells of a given sample.

The EXAFS spectra were fitted using as a reference different crystal structures published in the open literature, such as calcium gluconate (Wieczorek et al. 1996), manganese citrate (Felmy et al. 2006, Matzapetakis et al. 2000) or guanidinium pentacarbonato thorate (Felmy et al. 1997, Voliotis & Rimsky 1975). The atomic positions for the calcium gluconate and manganese citrate crystal structures were modified prior to FEFF calculation of the scattering paths to compensate for the difference in atomic radii between Ca(II), Mn(III) and Th(IV).

14.5 XRD

X-ray diffraction (XRD) involves the interaction of electromagnetic radiation with the atoms of a solid. As the distances between the atoms in a crystal structure are comparable with the wavelength of the radiation, crystals diffract X-rays, providing a characteristic pattern. It is a non-destructive and fast method widely used to characterise solid phases, although in the case of very amorphous samples the broadening of the signals is large.

XRD analysis were performed in the X-ray laboratory of Institut de Ciències de la Terra Jaume Almera (CSIC).

14.6 NMR

Nuclear magnetic resonance (NMR) spectroscopy takes advantage of the response of the atom nuclei when exposed to a magnetic field. This response provides information about the chemical environment of the nuclei and can be used to identify an unknown substance; the lines for the bound atoms may shift or be broadened when coordinated with the metal.

In the present work, this technique was used to characterise the isosaccharinate solids synthesised in the laboratory (see section 15).

^{13}C-NMR spectra were recorded with a Bruker ARX 300 instrument from D_2O solutions at 25ºC in the NMR laboratory of Institut de Ciència de Materials de Barcelona (CSIC).

14.7 SEM-EDX

SEM (scanning electron microscopy) uses a focused beam of high-energy electrons to generate a variety of signals at the surface of solid specimens. Emission products from the interaction between the electrons and the sample (X-rays from inner shell excitation or inelastically scattered electrons) are detected from above, allowing the analysis of thick substrates and giving a three-dimensional impression of objects. Moreover, it is also possible to detect the X-rays energy-resolved by energy-dispersive spectrometry (EDS) and gain qualitative and quantitative information on the elemental composition of the sample from the characteristic spectral patterns (Walther 2003).

Field-emission SEM (Ultra Plus, ZEISS, operating at 2.5-3 kV) and EDS (X-Max, Oxford instruments, operating at 20 kV) were used in present work.

14.8 ESI-MS

Electrospray-ionization mass spectrometry (ESI-MS) is based on a gentle ionization process that keeps complexes largely intact, and generates a mass spectrum from which complexes can be identified by the mass-to-charge ratio of the parent complexion. It has been used, for example, to study uranyl-citrate and thorium-EDTA complexes (Cartwright et al. 2007, Pasilis & Pemberton 2003).

A preliminary study of the thorium-gluconate samples at pH=12 using ESI-MS was done in the Servei d'Anàlisi Química (SAQ) at Unversitat Autònoma de Barcelona (UAB). Mass spectra were recorded in the negative ion mode.

Some experimental handicaps were encountered:

-In the initial tests, tetramethylammonium hydroxide (TMAOH) was used to adjust pH value instead of sodium hydroxide, to avoid an excess of sodium in the samples that could interfere electrospray ionization process. However, the presence of TMAOH resulted in precipitation of solids on the introduction system of the equipment, leading to poor sensibility and a noisy background.

-The test was repeated using NH_3(aq) instead of TMAOH, to avoid problems in the introduction system concentration. In this case the background was lower. However, all the peaks identified were related to gluconate adducts, and no peaks related with Th-Glu complexes were identified. The absence of Th-GLU signals in the ESI-MS spectrum may be related to the relatively high detection limit of this technique in the case of metal-organic ligand complexes.

15 Appendix D: Solid synthesis and characterization

15.1 Thorium hydroxide

$ThO_2 \cdot xH_2O$ was prepared by slow titration of a thorium nitrate solution up to pH=10 using free-carbonate NaOH under nitrogen atmosphere (Altmaier et al. 2006, Neck et al. 2002).

The solid was filtered under nitrogen atmosphere, washed several times with carbonate-free water, and dried for a few days inside the glove box. Then it was placed in a vacuum desiccator for a week.

X-ray diffraction analysis of the solid (Figure 15-1) obtained showed broad bands, indicating low degree of cristallinity in the precipitated material. Minor quantities of $NaNO_3$(s) were identified in the spectra due to the high HNO_3 amount present in the initial reactants.

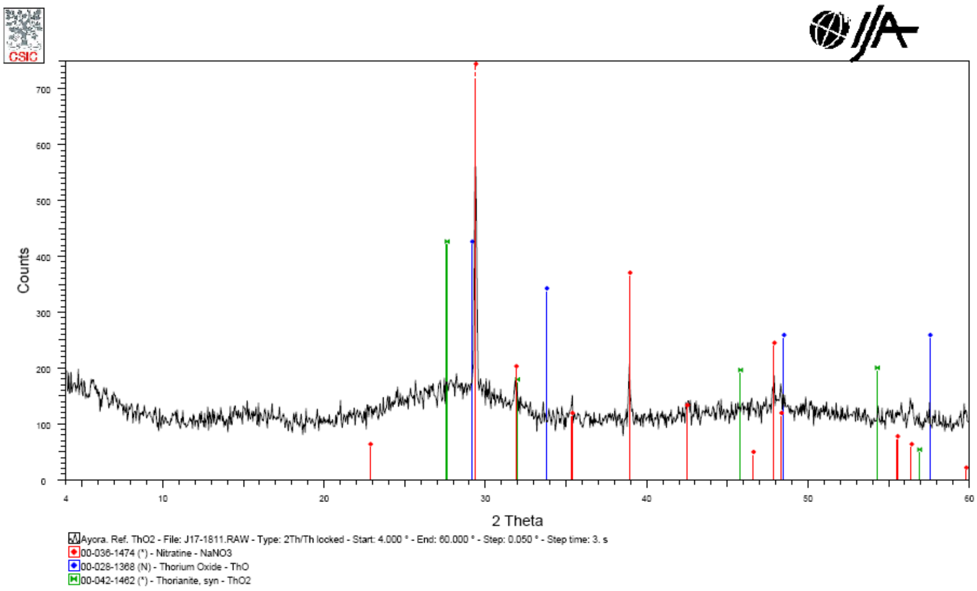

Figure 15-1. X-ray powder diffractogram for the $ThO_2 \cdot xH_2O$ solid. Blue and green lines indicate characteristic patterns of thorium oxide. Red lines are due to minor $NaNO_3$ impurities.

15.2 Sodium uranate

Sodium uranate was prepared inside the glove box under nitrogen atmosphere, following the procedure reported by Yamamura et al. (Yamamura et al. 1998). 11g of $UO_2(NO_3)_2 \cdot 6H_2O$ (Panreac) were dissolved in 400 ml of boiled water, and a large excess of 10 M free-carbonate NaOH (≈12ml) was added to the solution. The solution was shaken at ambient temperature for 10 days. After removing the supernatant, the solid phase was washed with a 0.01 M NaOH solution, filtered under nitrogen atmosphere, and dried for a few days inside the glove box. Then it was placed in a vacuum desiccator for a week, and afterwards crushed and homogenized before using it in the experiments.

X-ray diffraction analysis of the orange amorphous solid (Figure 15-2) did not identify any impurities within the detection limits of the technique.

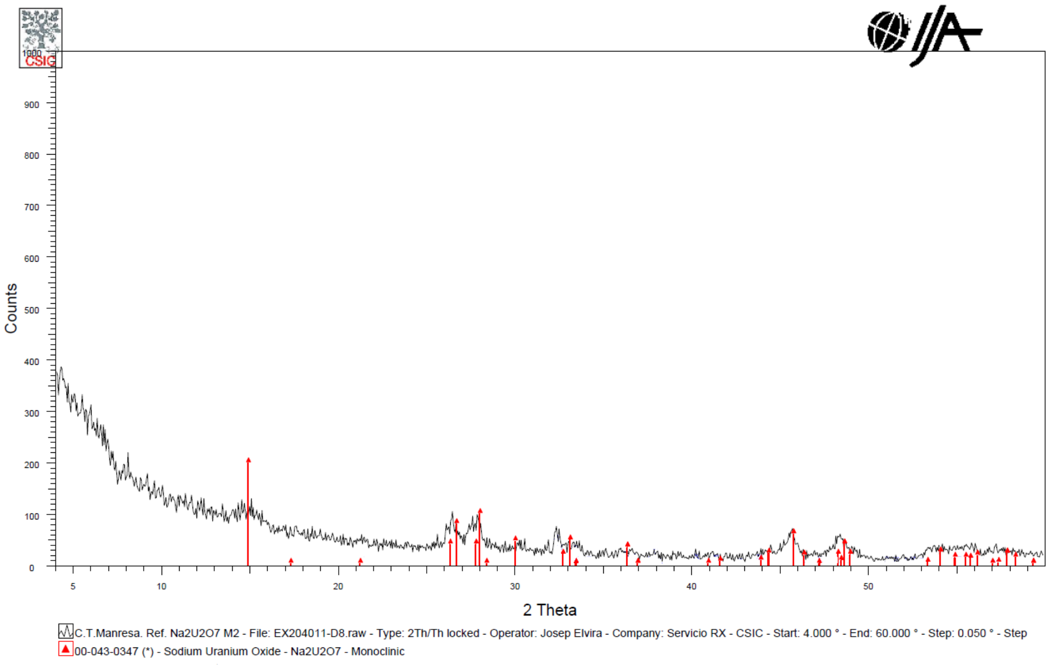

Figure 15-2. X-ray powder diffractogram for sodium uranate.

15.3 Sodium isosaccharinate

Na(ISA)(s) is not commercially available. In order to obtain this solid, it is necessary to synthesize the calcium salt of isosaccharinic acid, and use an ionic exchange resin in order to obtain the sodium salt, as shown in Figure 15-3.

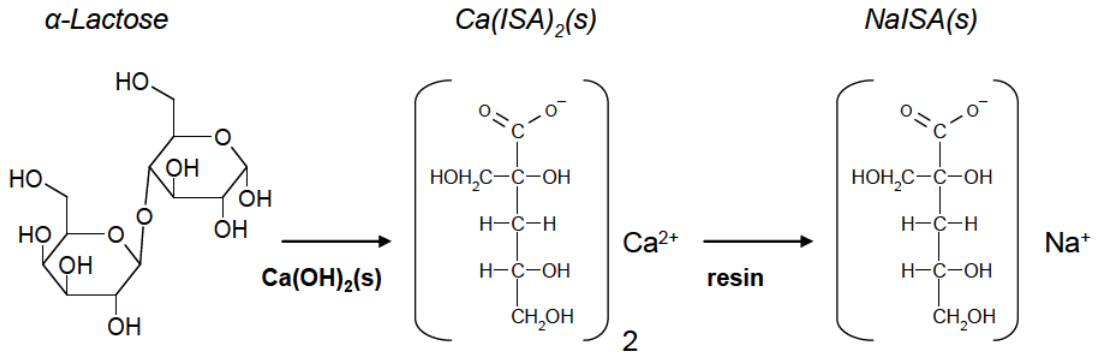

Figure 15-3. Scheme for the synthesis of the sodium isosaccharinate salt.

The calcium salt of isosaccharinic acid was obtained by the alkaline degradation of α-lactose hydrate (Sigma Aldrich) in an aqueous solution saturated with calcium hydroxide. The procedure followed was the one reported by Whistler and BeMiller (Whistler & BeMiller 1961) with some modifications (Evans 2003, Vercammen 2000). The X-ray diffraction pattern of the solid obtained (Figure 15-4) was in agreement with the spectra reported in the literature for crystalline calcium isosaccharinate (Rai et al. 1998).

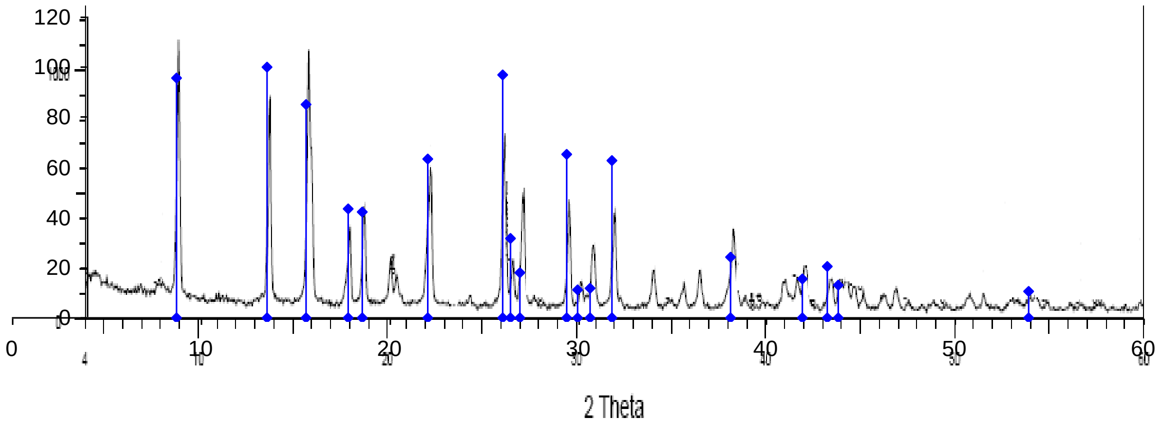

Figure 15-4. X-ray powder diffractogram for solid calcium isosaccharinate (black) and comparison with the spectra reported in (Rai et al. 1998) (blue lines).

ISA sodium salt was obtained exchanging calcium against sodium with a cation exchange resin (Chelex 100, Fluka) in the sodium form (Glaus et al. 1999, Pointeau et al. 2006, Rai et al. 2004).

The sodium salt was characterized using nuclear magnetic resonance spectroscopy. ^{13}C spectra obtained was in agreement with the one reported in the literature (Cho et al. 2003). The signals obtained were assigned to different carbon atoms in the isosaccharinate structure, as shown in Figure 15-5.

Bontchev and Moore (Bontchev & Moore 2004) suggested that sodium isosaccharinate contains one water molecule in the structure ($NaC_6H_{11}O_6 \cdot H_2O$). Total organic carbon analysis of solutions with different isosaccharinate concentrations confirmed this formula for the solid salt prepared in present work.

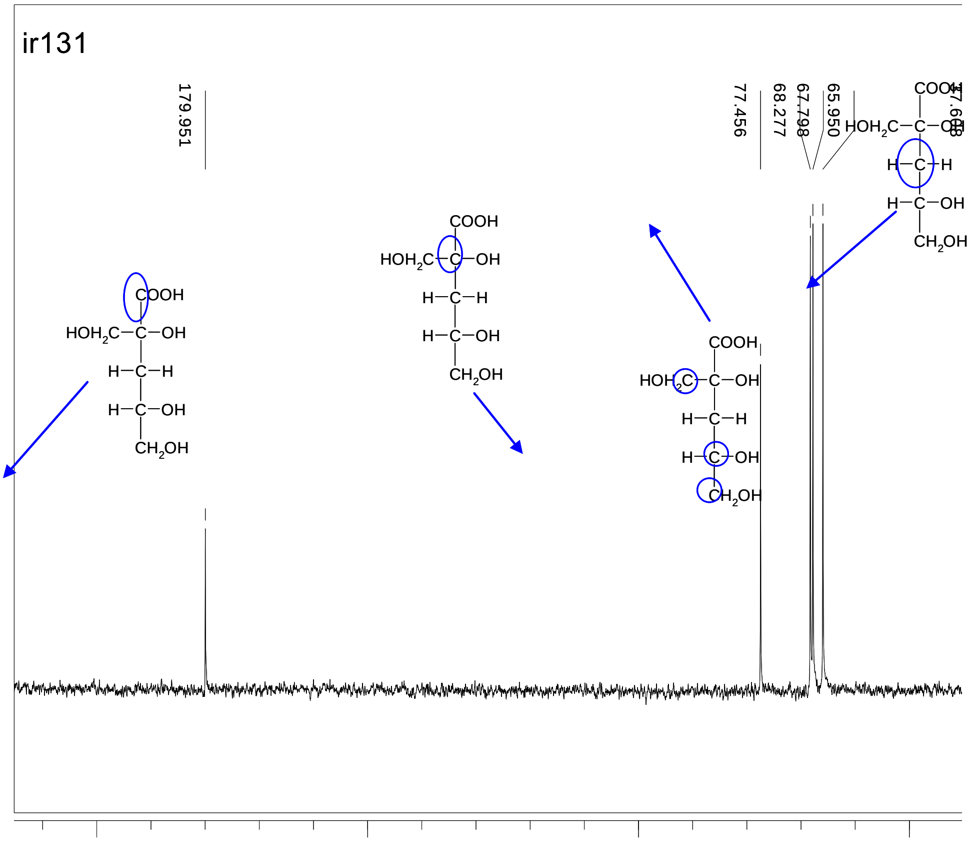

Figure 15-5. $^{13}C\{^1H\}$ NMR spectra of solid sodium isosaccharinate.

16 References

Allard, S. & Ekberg, C. (2006*a*), 'Complexing properties of alpha-isosaccharinate: Stability constants, enthalpies and entropies of Th-complexation with uncertainty analysis', *Journal of Solution Chemistry* **35**, 1173–1186.

Allard, S. & Ekberg, C. (2006*b*), 'Complexing properties of alpha-isosaccharinate: thorium', *Radiochimica Acta* **94**, 537–540.

Allen, P., Shuh, D. K., Bucher, J., Edelstein, N., Reich, T., Denecke, M. & Nitsche, H. (1996), 'EXAFS determinations of uranium structures: The uranyl ion complexed with tartaric, citric, and malic acids', *Inorganic Chemistry* **35**, 784–787.

Altmaier, M., Metz, V., Neck, V., Muller, R. & Fanghanel, T. (2003), 'Solid-liquid equilibria of $Mg(OH)_2$(cr) and $Mg_2(OH)_3Cl\cdot4H_2O$(cr) in the system Mg-Na-H-OH-Cl-H_2O at 25ºC', *Geochimica et Cosmochimica Acta* **67**(19), 3595–3601.

Altmaier, M., Neck, V., Denecke, M., Yin, R. & Fanghanel, T. (2006), 'Solubility of ThO_2 •xH_2O(am) and the formation of ternary Th(IV) hydroxide-carbonate complexes in $NaHCO_3$-Na_2CO_3 solutions containing 0–4M NaCl', *Radiochimica Acta* **94**, 495–500.

Altmaier, M., Neck, V. & Fanghanel, T. (2004), 'Solubility and colloid formation of Th(IV) in concentrated NaCl and $MgCl_2$ solution', *Radiochimica Acta* **92**, 537–543.

Altmaier, M., Neck, V. & Fanghänel, T. (2008), 'Solubility of Zr(IV), Th(IV) and Pu(IV) hydrous oxides in $CaCl_2$ solutions and the formation of ternary Ca-M(IV)-OH complexes', *Radiochimica Acta* **96**, 541–550.

Altmaier, M., Neck, V., Muller, R. & Fanghanel, T. (2005*a*), 'Solubility of $ThO_2\cdot H_2O$(am) in carbonate solution and the formation of ternary Th(IV) hydroxide-carbonate complexes', *Radiochimica Acta* **93**, 83–92.

Altmaier, M., Neck, V., Muller, R. & Fanghanel, T. (2005*b*), Solubility of U(VI) and formation of CaU_2O_7•$3H_2O$(cr) in alkaline $CaCl_2$ solutions, *in* 'Abstracts of Migration Conference, Avignon 2004'.

Andersson, M., Ervanne, H., Glaus, M., Holgersson, S., Karttunen, P., Laine, H., Lothenbach, B., Puigdomenech, I., Schwyn, B., Snellman, M., Ueda, H., Vuorio, M., Wieland, E. & Yamamoto, T. (2008), Development of methodology for evaluation of long-term safety aspects of organic cement paste components, Technical Report 2008-28, Posiva.

ANDRA (2005*a*), Dossier 2005 argile - architecture and management of a geological disposal system, Technical report, ANDRA.

ANDRA (2005*b*), Dossier 2005 Argile. Référentiel de comportement des radionucléides et des toxiques chimiques d'un stockage dans le Callovo-Oxfordien jusqu'à l'homme. Site de Meuse/Haute-Marne, Technical Report C.RP.ASTR.04.0032, ANDRA.

ANDRA (2009), Inventaire national des matières et déchets radioactifs 2009, Technical report, ANDRA.

Baraniak, L., Bernhard, G. & Nitsche, H. (2002), ‘Influence of hydrothermal wood degradation products on the uranium adsorption onto metamorphic rocks and sediments’, *Journal of Radioanalytical and Nuclear Chemistry* **253**, 185–190.

Baston, G. M. N., Berry, J. A., Bond, K. A., Brownsword, M. & Linklater, C. M. (1992), ‘Effects of organic degradation products on the sorption of actinides.’, *Radiochimica Acta* **52/53**, 249–356.

Bechtold, T., Burtscher, E. & Turcanu, A. (2002), ‘Ca^{2+}-Fe^{3+}-D-gluconate-complexes in alkaline solution. complex stabilities and electrochemical properties’, *J. Chem. Soc., Dalton Trans.* (13), 2683–2688.

Birjkumar, K. H., Bryan, N. D. & Kaltsoyannis, N. (2012*a*), ‘Computational investigation of the speciation of uranyl gluconate complexes in aqueous solution’, *Dalton Transactions* **40**, 11248–11257.

Birjkumar, K. H., Bryan, N. & Kaltsoyannis, N. (2012*b*), ‘Is gluconate a good model for isosaccharinate in uranyl(VI) chemistry? a DFT study’, *Dalton Transactions* **41**, 5542–5552.

Bogucki, R. & Martell, A. (1958), ‘Hydrolysis and olation of Th(IV) chelates of polyaminopolycarboxylic acids’, *Journal of the American Chemical Society* **80**(16), 4170–4174.

Bontchev, R. & Moore, R. (2004), ‘Crystal structure of sodium isosaccharate, $NaC_6H_11O_6{\cdot}H_2O$’, *Carbohydrate Research* **339**, 801–805.

Bradbury, M. & Van Loon, L. (1998), Cementitious near-field sorption databases for performance assessment of a L/ILW repository in a Palfris Marl host rock. CEM-94: Update I, June 1997, Technical Report 98-01, PSI.

Brendebach, B., Altmaier, M., Rothe, J., Neck, V. & Denecke, M. A. (2007), ‘EXAFS study of aqueous Zr(IV) and Th(IV) complexes in alkaline $CaCl_2$ solutions: $Ca_3[Zr(OH)_6]^{4+}$ and $Ca_4[Th(OH)_8]^{4+}$’, *Inorganic Chemistry* **46**(16), 6804–6810.

Brown, P., Sylva, R. N. & Ellis, J. (1985), ‘An equation for predicting the formation constants of hydroxo-metal complexes’, *Chemical Society of Dalton Transactions* **4**, 723–730.

Bruneau, E., Lavabre, D., Levy, G. & Micheau, J. C. (1992), ‘Quantitative analysis of continuous-variation plots with a comparison of several methods: Spectrophotometric study of organic and inorganic 1: 1 stoichiometry complexes’, *Journal of chemical education* **69**(10), 833–837.

Cartwright, A. J., May, C. C., Worsfold, P. J. & Keith-Roach, M. J. (2007), ‘Characterisation of Thorium–Ethylenediaminetetraacetic acid and Thorium–Nitrilotriacetic acid species by electrospray ionisation-mass spectrometry’, *Analytica Chimica Acta* **590**, 125–131.

Chapman, N. & McKinley, I. (1987), *The geological disposal of nuclear waste*, John Wiley and Sons Ltd.

Cho, H., Rai, D., Hess, N., Xia, Y. & Rao, L. (2003), 'Acidity and structure of isosaccharinate in aqueous solution: a nuclear magnetic resonance study', *Journal of Solution Chemistry* **32**(8), 691–702.

Choppin, G. R., Thakur, P. & Mathur, J. N. (2006), 'Complexation thermodynamics and structural aspects of actinide-aminopolycarboxylates', *Coordination Chemistry Reviews* **250**, 936–947.

Clark, D. L., Conradson, S. D., Donohoe, R. J., Keogh, D. W., Morris, D. E., Palmer, P. D., Rogers, R. D. & Tait, C. D. (1999), 'Chemical speciation of the uranyl ion under highly alkaline conditions. Synthesis, structures, and oxo ligand exchange dynamics', *Inorganic Chemistry* **38**, 1456–1466.

Cross, J. E., Ewart, F. T. & Greenfield, B. F. (1989), 'Modelling the behaviour of organic degradation products', *Mater. Res. Soc. Symp. Proc.* **127**, 715.

Dransfield, J. (2005), 'Leaching of organic admixtures from concrete', Cement Admixtures Association Homepage.

Duro, L., Grivé, M. & Giffaut, E. (2010), ThermoChimie, the ANDRA thermodynamic database, *in* 'Proceddings of the 2nd anual workshop of the 7th EC FP CP Recosy'.

Duro, L., Grivé, M. & Giffaut, E. (2012), ThermoChimie, the ANDRA thermodynamic database, *in* 'Scientific Basis for Nuclear Waste Management XXXV, MRS Proceedings', Vol. 1475.

Ekberg, C., Albinsson, Y., Comarmond, M. & Brown, P. (2000), 'Studies on the complexation behavior of Thorium(IV). 1. Hydrolysis equilibria', *Journal of Solution Chemistry* **29**(1), 63–86.

Evans, N. D. M. (2003), Studies on Metal alpha-Isosaccharinic Acid Complexes, PhD thesis, Loughborough University.

Fanger, G., Skagius, K. & Wiborgh, M. (2001), Project SAFE. Complexing agents in SFR, Technical Report R-01-04, SKB.

Felmy, A., Cho, H., Dixon, D., Xia, Y., Hess, N. & Wang, Z. (2006), 'The aqueous complexation of thorium with citrate under neutral to basic conditions', *Radiochimica Acta* **94**, 205–212.

Felmy, A. R. (2004), Chemical speciation of Americium, Curium and selected tetravalent actinides in high level waste., Technical Report EMSP Project 73749, PNNL.

Felmy, A., Rai, D., Sterner, S., Mason, M., Hess, N. & Conradson, S. (1997), 'Thermodynamic models for highly charged aqueous species: Solubility of th(IV) hydrous oxide in concentrated $nahco_3$ and na_2co_3 solutions', *Journal of solution chemistry* **26**(3), 233–248.

Gaona, X., Montoya, V., Colàs, E., Grivé, M. & Duro, L. (2008), 'Review of the complexation of tetravalent actinides by ISA and gluconate under alkaline to hyperalkaline conditions.', *Journal of Contaminant Hydrology* **102(3-4)**, 217–227.

Glaus, M. A., Laube, A. & Van Loon, L. R. (2006), ‘Solid–liquid distribution of selected concrete admixtures in hardened cement pastes’, *Waste Management* **26**, 741–751.

Glaus, M., Hummel, W. & Van Loon, L. (2000), ‘Trace metal-humate interactions. I. Experimental determination of conditional stability constants’, *Applied geochemistry* **15**(7), 953–973.

Glaus, M. & Van Loon, L. (2008), ‘Degradation of cellulose under alkaline conditions: New insights from a 12 years degradation study’, *Environmental Science and Technology* **42**(8), 2906–2911.

Glaus, M., Van Loon, L., Achatz, S., Chodura, A. & Fischer, K. (1999), ‘Degradation of cellulosic materials under the alkaline conditions of a cementitious repository for low and intermediate level radioactive waste: Part I: Identification of degradation products’, *Analytica Chimica Acta* **398**(1), 111–122.

Glaus, M. & Van Loon, L. R. (2004), A generic procedure for the assessment of the effect of concrete admixtures on the retention behaviour of cement for radionuclides: concept and case studies, Technical Report 04-02, PSI.

Gran, G. (1952), ‘Determination of the equivalence point in potentiometric titrations. Part II.’, *The Analyst* **77**, 661–671.

Greenfield, B., Hurdus, M., Spindler, M. & Thomason, H. (1997), The effect of the products from the anaerobic degradation of cellulose on the solubility and sorption of radioelements in the near field, Technical Report NSS/R376, NIREX.

Grenthe, I., Fuger, J., Konings, R., Lemire, R., Muller, A., Nguyen-Trung, C. & Wanner, H. (1992), *Chemical Thermodynamics 1: Chemical Thermodynamics of Uranium*, OECD Publishing.

Grenthe, I., Puigdomenech, I. & Allard, B. (1997), *Modelling In Aquatic Chemistry*, Nuclear Energy Agency.

Guillaumont, R., Fanghänel, J., Neck, V., Fuger, J., Palmer, D., Grenthe, I. & Rand, M. (2003), *Chemical Thermodynamics 5. Update on the Chemical Thermodynamics of Uranium, Neptunium, Plutonium, Americium and Technetium*, OECD Publishing.

Gyurcsik, B. & Nagy, L. (2000), ‘Carbohydrates as ligands: coordination equilibria and structure of the metal complexes’, *Coordination Chemistry Reviews* **203**, 81–149.

Hakanen, M. & Ervanne, H. (2006), The influence of organic cement additives on radionuclide mobility. A literature survey, Technical Report 2006-06, Posiva.

Hallbeck, L. (2010), Principal organic materials in a repository for spent nuclear fuel, Technical Report TR-10-19, SKB.

Hayes, M., Angus, M. & Garland, R. (2012), Current status paper on the potential use of superplasticisers in a geological disposal facility, Technical Report NNL (12) 11905 Issue 4, NNL.

Herbelin, A. & Westall, J. (1999), FITEQL 4.0: a computer program for determination of chemical equilibrium constants from experimental data, Technical report, Report 99-01. Department of Chemistry, Oregon State University, Corvallis.

Hummel, W. (1993), Organic complexation of radionuclides in cement pore water: A case study, Technical Report 93-617, PSI.

Hummel, W., Anderegg, G., Rao, L., Puigdomènech, I. & Tochiyama, O. (2005), *Chemical Thermodynamics 9: Chemical Thermodynamics of Compounds and Complexes of U, Np, Pu, Am, Tc, Se, Ni and Zr with Selected Organic Ligands.*, OECD Publishing.

Keith-Roach, M. J. (2008), 'The speciation, stability, solubility and biodegradation of organic co-contaminat radionuclide complexes: a review', *Science of the total environment* **396**, 1–11.

Kitamura, A. & Kohara, Y. (2004), 'Carbonate complexation of Neptunium(IV) in highly basic solutions.', *Radiochimica Acta* **92**, 583–588.

Koningsberger, D. & Prins, R. (1988), *X-Ray Absorption. Principles, Applications, Techniques of EXAFS, SEXAFS and XANES*, John Wiley and Sons Ltd.

Lemire, R. J., Fuger, J., Nitsche, H., Potter, P., Rand, M. H., Rydberg, J., Spahiu, K., Sullivan, J. C., Ullman, W. J., Vitorge, P. & Wanner, H. (2001), *Chemical Thermodynamics 4: Chemical Thermodynamics of Neptunium and Plutonium*, OECD Publishing.

Matzapetakis, M., Karligiano, N., Bino, A., Dakanali, M., Raptopoulou, C., Tangoulis, V., Terzis, A., Giapintzakis, J. & Salifoglou, A. (2000), 'Manganese citrate chemistry: Syntheses, spectroscopic studies, and structural characterizations of novel mononuclear, water-soluble manganese citrate complexes', *Inorganic Chemistry* **39**(18), 4044–4051.

Meinrath, G. (1997), 'Uranium(VI) speciation by spectroscopy', *Journal of Radioanalytical and Nuclear Chemistry* **224**, 119–126.

Meinrath, G. (1998*a*), 'Aquatic chemistry of uranium', *Geoscience* **1**, 1–101.

Meinrath, G. (1998*b*), 'Direct spectroscopic speciation of schoepite-aqueous phase equilibria', *Journal of Radioanalytical and Nuclear Chemistry* **232**, 179–188.

Meyer, M., Burgat, R., Faure, S., Batifol, B., Hubinois, J., Chollet, H. & Guilard, R. (2007), 'Thermodynamic studies of actinide complexes. 1. A reappraisal of the solution equilibria between plutonium(IV) and ethylenediaminetetraacetic acid ($EDTAH_4$) in nitric media', *Comptes Rendus Chimie* **10**, 929–947.

Miller, W., Alexander, R., Chapman, N., McKinley, I. & Smellie, J. (2000), *Geological disposal of radioactive wastes and natural analogues. Waste Management series Vol. 2.*, Elsevier Science Limited.

Moreton, A. D. (1993), 'Thermodynamic modelling of the effect of hydroxycarboxylic acids on the solubility of plutonium at high ph', *Mater. Res. Soc. Symp. Proc.* **294**, 753.

Neck, V., Müller, R., Bouby, M., Altmaier, M., Rothe, J., Denecke, M. A. & Kim, J. (2002), 'Solubility of amorphous Th(IV) hydroxide – application of LIBD to determine the solubility product and EXAFS for aqueous speciation', *Radiochimica Acta* **90**, 485–494.

Newville, M. (2004), Fundamentals of XAFS, Technical report, Consortium for Advanced Radiation Sources. University of Chicago, Chicago, IL.

Nirex (2001), Why a cementitious repository?, Technical Report N/034, Nirex.

Ochs, M., Hager, D., Helfer, S. & Lothenbach, B. (1998), ‘Solubility of radionuclides in fresh and leached cementitious systems at 22ºc and 50ºc’, *Materials Research Society Symposium Procedures* **506**, 773–780.

Ochs, M., Lothenbach, B. & Giffaut, E. (2002), ‘Uptake of oxo-anions by cements through solid-solution formation: experimental evidence and modelling’, *Radiochimica Acta* **90**, 639–646.

Osthols, E., Bruno, J. & Grenthe, I. (1994), ‘On the influence of carbonate on mineral dissolution. III. the solubility of microcrystalline ThO2 in CO2-H2O media.’, *Geochimica et Cosmochimica Acta* **58**, 613–623.

Parkhurst, D. & Appelo, C. (2001), User’s guide to PHREEQC (version 2.4.6). A computer program for speciation, batch reaction, one dimensional transport and inverse geochemical calculations., Technical report, U. S. Geological Survey.

Pasilis, S. & Pemberton, J. (2003), ‘Speciation and coordination chemistry of uranyl-citrate complexes in aqueous solution’, *Inorganic Chemistry* **42**, 6793–6800.

Pavasars, I., Hagberg, J., Boren, H. & Allard, B. (2003), ‘Alkaline degradation of cellulose: Mechanism and kinetics’, *Journal of Polymers and the Environment* **11**, 39–47.

Pointeau, I., Hainos, D., Coreau, N. & Reiller, P. (2006), ‘Effect of organics on selenite uptake by cementitious materials’, *Waste Management* **26**, 733–740.

Puigdomènech, I. (2009), ‘Medusa: Make equilibrium diagrams using sophisticated algorithms. chemical equilibrium software. http://www.kemi.kth.se/medusa’, Chemical Equilibrium Software. http://www.kemi.kth.se/medusa.

Rai, D., Moore, D., Rosso, K., Felmy, A. & Bolton, H. J. (2008), ‘Environmental mobility of Pu(IV) in the presence of ethylenediaminetetraacetic acid: Myth or reality?’, *Journal of Solution Chemistry* **37**, 957–986.

Rai, D., Rao, L. & Moore, A. (1998), ‘The influence of isosaccharinic acid on the solubility of Np(IV) hydrous oxide.’, *Radiochimica Acta* **83**, 9–13.

Rai, D., Rao, L., Moore, R., Bontchev, R. & Holt, K. (2004), Development of biodegradable isosaccharinate-containing foams for decontamination of actinides: Thermodynamic and kinetic reactions between isosaccharinate and actinides on metal and concrete surfaces, Technical Report EMSP-82715-2004, USDOE.

Rai, D., Yui, M., Moore, D. & Rao, L. (2009), ‘Thermodynamic model for ThO_2(am) solubility in isosaccharinate solutions’, *Journal of Solution Chemistry* **38**, 1573–1587.

Rand, M., Fuger, J., Grenthe, I., Neck, V. & Rai, D. (2009), *Chemical Thermodynamics 11: Chemical Thermodynamics of Thorium*, OECD Publishing.

Rehr, J. J. & Albers, R. C. (2000), ‘Theoretical approaches to X-ray absorption fine structure’, *Reviews of Modern Physics* **72**, 621–654.

Reich, T., Bernhard, G., Geipel, G., Funke, H., Hennig, C., Rossberg, A., Matz, W., Schell, N. & Nitsche, H. (2000), ‘The ROssendorf Beam Line ROBL-a dedicated experimental station for XAFS measurements of actinides and other radionuclides', *Radiochimica Acta* **88**(9-11), 633.

Rendleman, J. (1978), 'Metal-polysaccharide complexes: Part I.', *Food Chemistry* **3**, 47–79.

Ressler, T. (1998), 'WinXAS: a program for X-ray absorption spectroscopy data analysis under MS-Windows', *Journal of Synchrotron Radiation* **5**, 118–122.

Rihs, S., Sturchio, N., Orlandini, K., Cheng, L., Teng, H., Fenter, P. & Bedzyk, M. (2004), 'Interaction of uranyl with calcite in the presence of edta', *Environmental Science and Technology* **38**, 5078–5086.

Rojo, H., Tits, J., Gaona, X., Garcia-Gutierrez, M., Missana, T. & Wieland, E. (2013), 'Thermodynamics of Np(IV) complexes with gluconic acid under alkaline conditions: sorption studies', *Radiochimica Acta* **101**, 133–138.

Rossotti, F. J. C. & Rossotti, H. (1961), *The Determination of Stability Constants and Other Equilibrium Constants in Solution*, McGraw-Hill Book Company, Inc., New York, Toronto, London.

Rothe, J., Denecke, M., Neck, V., Muller, R. & Kim, J. (2002), 'XAFS investigation of the structure of aqueous thorium (IV) species, colloids, and solid thorium (IV) oxide/hydroxide', *Inorganic Chemistry* **41**(2), 249–258.

Sandino, A. & Bruno, J. (1992), 'The solubility of $(UO_2)_3(PO_4)_2{:}4H_2O(s)$ and the formation of U(VI) phosphate complexes: Their influence in uranium speciation in natural waters', *Geochimica et Cosmochimica Acta* **56**(12), 4135–4145.

Sawyer, D. (1964), 'Metal-gluconate complexes', *Chemical Reviews* **64**(6), 633–643.

Sawyer, D. T. & Kula, R. (1962), 'Uranium(VI) gluconate complexes', *Inorganic Chemistry* **1**, 303–309.

Scheinost, A. C. (2010), 'EXAFS shell fitting for beginners', Personal communication.

Schubert, J. & Lindenbaum, A. (1952), 'Stability of alkaline earth-organic acid complexes measured by ion exchange', *Journal of the American Chemical Society* **74**, 3529–3532.

Sillen, L. (1959), Some laboratory methods, Technical report, KTH oorg kemi, Royal Institute of technology, Stockolm, Sweden.

Silva, J. F. D. & Simoes, M. L. S. (1968), 'Studies on uranyl complexes—III: Uranyl complexes of EDTA', *Talanta* **15**(7), 609–622.

Silva, R., Bidoglio, G., Rand, M., Robouch, P., Wanner, H. & Puigdomenech, I. (1995), *Chemical Thermodynamics 2; Chemical Thermodynamics of Americium*, OECD Publishing.

Stankovic, J., Milonjic, S., Kopecni, M. & Ceranic, T. (1990), 'Sorption of alkaline-earth cations on amorphous zirconium oxide', *Colloids and surfaces* **46**(2), 283–296.

Sutton, J. (1955), 'Hydrolyse de l'ion uranyle et formationd'uranates de sodium', *Journal of Inorganic and Nuclear Chemistry* **1**(1-2), 68–74.

Sutton, M., Warwick, P., Hall, A. & Jones, C. (1999), ‘Carbonate induced dissolution of uranium containing precipitates under cement leachate conditions’, *Journal of Environmental Monitoring* **1**, 177–182.

Szabo, Z., Toraishi, T., Vallet, V. & Grenthe, I. (2006), ‘Solution coordination chemistry of actinides: Thermodynamics, structure and reaction mechanisms’, *Coordination Chemistry Reviews* **250**, 784–815.

Tits, J., Wieland, E. & Bradbury, M. (2005), ‘The effect of isosaccharinic acid and gluconic acid on the retention of Eu(III), Am(III) and Th(IV) by calcite.’, *Applied Geochemistry* **20**, 2082–2096.

Tits, J., Wieland, E., Bradbury, M., Eckert, P. & Schaible, A. (2002), The uptake of Eu(III) and Th(IV) by calcite under hyperalkaline conditions, Technical Report PSI Bericht 02-03, PSI.

Toraishi, T., Farkas, I., Szabo, Z. & Grenthe, I. (2002), ‘Complexation of Th (IV) and various lanthanides (III) by glycolic acid; potentiometric, ^{13}C-NMR and EXAFS studies’, *J. Chem. Soc., Dalton Trans.* (20), 3805–3812.

Van Duin, M., Peters, J., Kieboom, A. & van Bekkum, H. (1989), ‘A general coordination-ionization scheme for polyhydroxy carboxylic acid in water’, *Recueil des Travaux Chimiques des Pays-Bas* **108**, 57–60.

Van Loon, L. & Glaus, M. A. (1998), Experimental and theoretical studies on alkaline degradation of cellulose and its impact on the sorption of radionuclides, Technical Report 98-07, PSI.

Van Loon, L., Glaus, M., Laube, A. & Stallone, S. (1999), ‘Degradation of cellulosic materials under the alkaline conditions of a cementitious repository for low-and intermediate-level radioactive waste. II. Degradation kinetics’, *Journal of Polymers and the Environment* **7**(1), 41–51.

Van Loon, L. R. & Glaus, M. A. (1997), ‘Review of the kinetics of alkaline degradation of cellulose in view of its relevance for safety assessment of radioactive waste repositories’, *Journal of Environmental Polymer Degradation* **5**, 97–1069.

Venema, F. (1992), Coordination of aluminium(III) with hydroxycarboxylates in water, PhD thesis, TU Delft, Delft University of Technology.

Vercammen, K. (2000), Complexation of Calcium, Thorium and Europium by alpha-Isosaccharinic Acid under Alkaline Conditions, PhD thesis, Swiss Federal Institute of Technology Zurich.

Vercammen, K., Glaus, M. & Van Loon, L. (1999), ‘Evidences for the existence of complexes between Th(IV) and alpha-isosaccharinic acid under alkaline conditions’, *Radiochimica Acta* **84**, 221–224.

Vercammen, K., Glaus, M. & Van Loon, L. R. (2001), ‘Complexation of Th(IV) and Eu(III) by alpha-isosaccharinic acid under alkaline conditions’, *Radiochimica Acta* **89**, 393–401.

Voliotis, S. & Rimsky, A. (1975), ‘Etude structurale des carbonates complexes de cerium et de thorium. II. Structure cristalline et moleculaire du pentacarbonatothorate de guanidine tetrahydrate.’, *Acta Crystallographica Section B: Structural Crystallography and Crystal Chemistry* **31**(11), 2612–2615.

Walther, C. (2003), ‘Comparison of colloid investigations by single—particle analytical techniques-a case study on thorium oxyhydroxydes’, *Colloids and Surfaces A: Physicochemical and Engineering Aspects* **217**, 81–92.

Warwick, P., Evans, N., Hall, T. & Vines, S. (2004), ‘Stability constants of uranium(IV)-alpha-isosaccharinic acid and gluconic acid complexes.’, *Radiochimica Acta* **92**, 897–902.

Warwick, P., Evans, N. & Vines, S. (2006), ‘Studies on some divalent metal alpha-isosaccharinic acid complexes’, *Radiochimica Acta* **94**, 363–368.

Webb, S. (2005), ‘SIXPack: a graphical user interface for XAS analysis using IFEFFIT’, *Physica Scripta* **T115**, 1011–1014.

Whistler, R. & BeMiller, J. (1961), *Methods in Carbohydrate Chemistry, vol. 2, Reactions of Carbohydrates*, Academic Press, New York., chapter Alpha-D-Isossacharino-1,4-lactone. Action of lime water on lactose, pp. 477–479.

Wieczorek, M., Blaszczyk, J. & Krol, B. (1996), ‘Effects of cation interactions on sugar anion conformation in complexes of lactobionate and gluconate with calcium, sodium or potassium’, *Acta Crystallographica Section C: Crystal Structure Communications* **52**(5), 1193–1198.

Xia, Y., Felmy, A., Rao, L., Wang, Z. & Hess, N. (2003), ‘Thermodynamic model for the solubility of ThO_2(am) in the aqueous Na^+-H^+-OH^--NO_3^--H_2O-EDTA system’, *Radiochimica Acta* **91(12)**, 751–760.

Yamamura, T., Kitamura, A., Fukui, A., Nishikawa, S., Yamamoto, T. & Moriyama, H. (1998), ‘Solubility of U(VI) in highly basic solutions.’, *Radiochimica Acta* **83**, 139–146.

Zubiaur, J., Castaño, R., Etxebarria, N., Fernandez, L. & Madariaga, J. (1998), ‘Potentiometric study of the protonation and distribution equilibria of d-gluconic-delta-lactone acid in sodium perchlorate solutions at 25°C and construction of a thermodynamic model’, *Talanta* **45**(5), 1007–1014.